Dextran hydrogel preparation and applications in biomedical engineering

Zhang, Rongsheng

Award date:
2004

Awarding institution:
University of Bath

Dextran Hydrogel Preparation and Applications in Biomedical Engineering

submitted by Rongsheng Zhang

for the degree of PhD

of the University of Bath

2004

ProQuest LLC
789 East Eisenhower Parkway
P.O. Box 1346
Ann Arbor, MI 48106-1346

Acknowledgements

My profound thanks are due to my supervisors, Dr. John Hubble, Dr. Adrian Bowyer, Professor Robert Eisenthal who allowed me freedom to roam but were always invaluable help, professional advice, support and guidance throughout my time in Bath, and for their countless suggestions and constructive criticism as the work proceeded.

My thanks are also due to the department of Chemical Engineering as a whole, administrative and technical staff; in particular Mrs. Suzanne Barkley, Mrs. Anne O'Reilly and Mr. Fernando Acosta for their constant support, as well as all my fellow students and friends I met during the time spent in Bath.

I am very grateful to Dr. Mingguo Tang whom I worked with in the first part of this research, and discussed interesting aspects of the project. I am also particularly grateful towards Dr Julian B Chaudhuri and Dr Marcus Jarman-Smith, whom I worked with cell culture research.

I wish to thank the following people for conducting experiments of some related projects, Miss. Isobel Morten, Miss Sally Howells, (University of Bath, BSc Biochemistry), Miss. Yiru Hao (University of Bath, Chemical Engineering, exchange student) and Mr. John Gavin (University of Bath, Chemical Engineering, M.Eng. student).

Finally, my biggest thanks are reserved for my wife, Yu Gan, for her love and my family in China for their supports.

The generous financial supports, provided by the project, under BBSRC Grant No 86/E12129, the University of Bath and an ORS award, are also gratefully acknowledged.

Abstract

This project investigates dextran hydrogel fabrication for various practical applications in biomedical engineering, based on a number of cross-linking reactions.

D-glucose sensitive dextran/Con-A hydrogel membranes can be synthesized via a nucleophilic replacement reaction in a triazine ring. The resultant hydrogels are capable of releasing insulin in a dose-dependent response to changes in D-glucose concentrations. An alternative procedure for the synthesis of D-glucose responsive hydrogels based on carbodiimide chemistry allows production of gels with varying and controllable levels of protein and carboxylic group substitution.

Final a CM-dextran with 5 COOH/CM-dextran (10^{-4} Mol/g) and a proportion of cross-linking agents at 7 EDC/NHS (W/W), a weight ratio of 0.10 CM-dextran / hydrogel (W/W) was the optimum for forming cross-linkages. pH-sensitive hydrogels were also formed by the intermolecular cross-linking of CM-dextran dextran with a high level of carboxylic group substitution using EDC and NHS. Preliminary studies with primary human dermal fibroblast cultures showed that these gels are capable of supporting cell growth.

A proof of concept study was conducted to assess the potential of these gels to act as sensing elements by cast a diffraction grating into the gel surface. Test experiments showed the size of diffraction and reflection spots from an incident laser beam changed in size as the gel changed dimensions in response to changes in environmental. A further application of affinity material was the fabrication of membranes containing protein and CB. Results proved that intristic competitive binding existed and effectively shield the ligand from extern weak effects interactions.

The D-glucose sensitive hydrogel was also fabricated into bead. Size exclusion chromatography (SEC) was employed to detect the effect of D-glucose on throughout of protein across these beads. This serves both to confirm the effect of glucose on pore size and offer the possibility of a novel adaptive size exclusive resin.

Contents

Acknowledgements *2*

Abstract *3*

Contents *4*

Table of Symbols *8*

Table of definitions of some terms in hydrogel applications *9*

Table of Abbreviations *11*

Chapter 1. General Introduction and Project objectives *12*

1.1 General introduction to hydrogels **12**

1.2 Specific objectives **16**

1.3 Thesis outline **17**

Chapter 2. Review of Hydrogel Applications in Biomedical Engineering *18*

2.1 Introduction **18**

2.2 Review articles **19**

2.3 Hydrogel applications **23**

2.3.1 pH-sensitive hydrogels 23

2.3.2 D-glucose sensitive hydrogels 27

2.3.3 Hydrogel applications in cell culture or tissue engineering 29

2.3.4 Hydrogels based on biosensors 33

2.3.5 Hydrogels in bioseparation 37

2.4 Dextran hydrogels **40**

2.4.1 Dextran hydrogels for drug-delivery application 41

2.4.2 Dextran-hydrogels in cell culture and tissue engineering 43

2.4.3 Dextran-hydrogels in biosensors 45

2.5 Hydrogels from carbodiimide chemistry **46**

2.6 Conclusion **50**

Chapter 3. A Triazine based reversible hydrogel membrane for controlling the delivery of macromolecules *52*

3.1 Background **52**

3.2 Materials and methods **55**

3.2.1 Materials 55

3.2.2 Gel synthesis 55

3.2.3 Protein diffusion experiments 56

3.3 Results **59**

3.3.1 Specificity assessment 59

3.3.2 Effect of D-glucose concentration 61

3.3.3 Reversibility of D-glucose effects 62

3.3.4 Temperature, pH and membrane thickness effects 66

3.4 Discussion **66**

3.5 Conclusions **68**

Chapter 4. A CM-dextran based Reversible Hydrogel Membrane for Controlling the Delivery of Macromolecules ***70***

4.1 Introduction **70**

4.2 Materials and methods **72**
4.2.1 Materials 72
4.2.2 Hydrogel preparation 72
4.2.3 physicochemical properties of the hydrogel 75
4.2.4 Hydrogel morphology 75
4.2.5 Characterisation of binding interactions 76
4.2.6 Protein diffusion experiments 77

4.3 Results **77**
4.3.1 Hydrogel characterization 77
4.3.2 Morphology of hydrogels by SEM 79
4.3.3 Binding capacity comparison of different sugars with Con A by ITC 80
4.3.4 Diffusion of lysozyme through the hydrogel 84

4.4 Discussion **89**

4.5 Conclusion **91**

Chapter 5. Synthesis and Characterization of pH-sensitive carboxymethyl -dextran hydrogel for protein loading and release ***93***

5.1 Introduction **93**

5.2 Materials and method **94**
5.2.1 Materials 94
5.2.2 Preparation of CM-dextran hydrogel 94
5.2.3 Experimental set-up 95
5.2.4 Preparation and detection of cyctochrome C solutions for mass transfer analysis via protein studies 96
5.2.5 Preparation of dextranase solution for biodegradability analysis 96

5.3 Equilibrium swelling studies **96**
5.3.1 Determination of swelling ratio 96
5.3.2 Determination of $\overline{M_c}$ 97
5.3.3 Determination of ρx 98
5.3.4 Determination of k' in protein loading studies 98
5.3.5 Determination of n in protein release studies 99
5.3.6 Determination of rate of enzyme degradation 100

5.4 Results and discussion **101**
5.4.1 Network structure analysis – determination of SRE, $\overline{M_c}$ and ρ_x 101
5.4.2 Mass Transfer and Releasing Properties via Protein Studies 109
5.4.3 Biodegradability Studies 116

5.5 Conclusions **121**

Chapter 6. A Novel pH- and Ionic-strength-sensitive Carboxyl Methyl Dextran Hydrogel ***124***

6.1 Background **124**

6.2 Materials and methods **127**
6.2.1 Materials 127
6.2.2 Hydrogel membrane synthesis 128
6.2.3 Lysozyme diffusion experiments 129
6.2.4 Morphology of the pH-sensitive hydrogel membrane in different pH environments 130
6.2.5 Physicochemical properties of the hydrogel 130

6.3 Results **130**
6.3.1 Hydrogel characterization 130
6.3.2 Reversibility of the pH response 133
6.3.3 Effect of pH on diffusion rate 134
6.3.4 The effect of ionic strength on diffusion rate 135
6.3.5 Osmotic pressure effects 137
6.3.6 pH and ionic strength effects on control hydrogels 137

6.4 Discussion **138**

Chapter 7. The evaluation of Carboxyl Methyl Dextran as a Potential Tissue Engineering Extracellular Matrix for Human Cell Culture ***140***

7.1 Introduction **140**

7.2 Materials and methods **142**
7.2.1 Materials 142
7.2.2 Tissue culture 142
7.2.3 Hydrogel membrane synthesis for tissue culture 142
7.2.4 Analysis of samples 143

7.3 Results **143**

7.4 Discussion **145**

Chapter 8. An Intelligent hydrogel with diffraction grating structure: Novel Biosensor Materials ***148***

8.1 Background **148**

8.2 Materials and method **151**
8.2.1 Materials 151
8.2.2 Method 151

8.3 Results **158**
8.3.1 Hydrogel characterization 158
8.3.2 Images from of intelligent hydrogel with a diffraction grating 161
8.3.3 Morphology of the IHDG 163
8.3.4 Testing diffraction gratings on the hydrogels 167

8.4 Discussion **168**

8.5 Conclusion **170**

Chapter 9. Intrinsic shielding effects in ligand-receptor substituted affinity membranes ***171***

9.1 Introduction **171**

9.2 Materials and methods **175**
9.2.1 Materials 175

9.2.2 Hydrogel preparation 175
9.2.3 Physicochemcal properties of the hydrogel 177
9.2.4 Hydrogel morphology 177
9.2.5 Characterization of binding interactions 178
9.2.6 Protein diffusion and adsorption experiments 178

9.3 Results 179
9.3.1 Hydrogel characterization 179
9.3.2 Morphology of hydrogel SEM 180
9.3.3 ITC characterization of protein binding 182
9.3.4 Diffusion and elution of proteins through the hydrogel membrane coupled with different ligands 185

9.4 Discussion and conclusion 192

Chapter 10. Chromatographic elution characteristics of protein using D-glucose sensitive hydrogel beads 194

10.1 Introduction 194

10.2 Materials 195

10.3 Methods 195
10.3.1 Bead Preparation 195
10.3.2 Packing the beads into the column 200
10.3.3 Running samples 200
10.3.4 Characterisation of binding interactions between Con A with alginate. 201

10.4 Results 202
10.4.1 Binding capacity comparison of alginate with concanavalin A by ITC. 202
10.4.2 CM-dextran Con A alginate beads using the first detector system 203
10.4.3 Experiments of alginate beads using the second detector system 208

10.5 Discussion 214

10.6 Conclusion 218

Chapter 11. Conclusions and Future Work 220

11.1 Conclusions 220

11.2 Future work 224

References 225

Appendix 247

Table of Symbols

Symbol	Definition	Dimension
C_e	Equilibrium concentration of protein in solution	mg/ml
C_i	Initial concentration of protein in solution	mg/ml
$\frac{dc}{Adt}$	rate of solute diffusion per unit time per unit surface area	$Mol/cm^{-2}s^{-1}$
D_{im}	solute diffusion coefficient	$cm^{-2}s^{-1}$
k'	Hydrogel permeability coefficient	
K	Proportionality constants	
K_i	solute partition coefficient	
$\overline{M_c}$	Number average molecular weight between cross-links	g/mol
$\overline{M_n}$	Number average molecular weight of dextran 482,000 Da	g/mol
M_t	the amounts of protein released at time, t	mg/minute
M_∞	the amounts of protein released at equilibrium,	mg/minute
$\frac{M_t}{M_\infty}$	Fraction of protein released at time t	
n	diffusional exponent	
ρ_x	Cross-linking density	mol/cm^3
R	Ratio of amount of protein loaded to amount of CM-dextran in gel	
$v_{2,r}$	Polymer fraction of the gel after gel formation	
$v_{2,s}$	Polymer fraction of the gel at equilibrium swelling	
v_1	Partial specific volume of dextran	$0.62\ cm^3/g$
V_1	Molar volume of water	$18\ cm^3/mol$
W_d	Weight of dried gel	g
$W_{CM-dextran}$	Weight of CM-dextran used for gel formation	g
W_p	Weight of protein loaded into gel	g
W_{water}	Weight of water used in gel formation	g
W_s	Weight of swollen gel at equilibrium	g
x_1	Flory polymer-solvent interaction parameter	0.473 for dextran-water
V	Volume of protein solution added	ml

Table of Definitions of Some Terms in Hydrogel Applications

Definition	Reference
Biocompatibility: Acceptance of an implant by surrounding tissues and by the body as a whole, and compatibility with tissues in the terms of mechanical, chemical, surface, and pharmacological properties.	Ramakrishna *et al.*, 2001
Biodegradable polymers: macromolecular materials capable of conversion into less complex products through chemical reactions, such as simple or enzyme catalyzed hydrolysis over a reasonable period of time.	Park, 1993
Biomaterials: materials derived from biological sources or materials used for therapies in the human body.	Griffith, 2000
Biosensor: a self-contained integrated device which is capable of providing specific quantitative or semi-quantitative analytical information using a biological recognition element (biochemical receptor) which is in direct spatial contact with a transducer element.	Theenot, *et al.*, 1999
Cell culture: cells growing outside the organism in nutrient medium in the laboratory.	Lawrence, 1995
Controlled drug delivery systems: intended to deliver drugs at predetermined rates for predefined periods of time	Qiu *et al.*, 2001

Extracellular matrix (ECM): the gel of proteins, proteoglycans, and charged polysaccharides which provides a physical scaffolding for cells and tissues, helps provide a permeability barrier between tissue compartments, and enables polarization of tissue structures such as skin.	Griffith, 2000
Gels: semi-solid systems comprising small amounts of solid, dispersed in relatively large amounts of liquid, yet possessing more solid-like than liquid-like character.	Klech, 1990
Hydrogels: a cross-linked network of hydrophilic polymers which possess the ability to absorb large amounts of water and swell, while maintaining their three-dimensional 3D) structure.	Gehrke *et al.*, 1990
Intelligent gels or Smart hydrogels: gels with the ability to receive, transmit or process a stimulus, and respond by producing a useful effect such as: changes in phase, shape, optics, mechanics, electric fields, surface energy, recognition, reaction rate and permeation rates.	Dagani, 1997 Harvey, 1995 Kost, 1999
Tissue engineering: creating living, three-dimensional tissues and organs using cells obtained from readily available sources such as biopsy of the patient's own (autologous) tissue or foreign tissue which would be discarded after surgical procedures such as circumcision.	Griffith, 2000

Table of Abbreviations

3D	Three dimensions
BSA	Bovine serum albumin
CB	Cibacron blue
CM-dextran	Carboxymethyl-dextran
Con A	Concanavalin A
EDC	N-(3-dimethylaminopropyl)-N'-ethylcarbodiimide
EDX	Energy dispersive X-ray
FT-IR	Fourier transform infrared
GAGs	glycosaminoglycans
HA	Hyaluronic acid
IHDG	Interrlgent hydrogel with diffraction grating
ITC	Isothermal titration calorimeter
MA-dextran	Methacrylated-dextran
MW	Moleular weight
NaCl	Sodium chlorate
NAD	Nicotinamide adenine dinucleotide
NHS	N-hydroxysuccinimide
NIPAAm	N-isopropylacrylamide
PBS	Phosphate buffer saline
SEC	Size exclusion chromatography
SEM	Scanning electron microscope
SPR	Surface plasmon resonance

Chapter 1. General Introduction and Project Objectives

1.1 General introduction to hydrogels

Hydrogels have emerged as promising materials in various biomedical (Hoffman, 2002) and pharmaceutical (Peppas, 2000) applications. Recently, hydrogels have been explored in tissue engineering, drug delivery, biosensors, biosepapration and a variety of other potential uses. This results from the ease with which physicochemical properties of the hydrogel can be modified by changing monomer structure, the degree of crosslinking, and the fabrication method (Piyush *et al*, 2002, Kytai *et al*, 2002, Olgun *et al.*, 1999, Mark *et al.*, 2002).

In comparison to other biomaterials used in the biomedical field, hydrogels have the following advantages: they resemble living tissues, they can be controlled, ther are chemically stable or biodegrade, and they are biocompatible. These properties suggest that they will have many new biomedical applications. As our understanding of the structures and functions of hydrogels improves this will lead to the development of novel hydrogels for these target applications and others.

pH-sensitive hydrogels have been most frequently studied and used to develop controlled release formulations for oral drug administration. The functional mechanism of pH-sensitivity is that small changes in pH can result in significant change in the mesh size of the gels' polymeric networks. pH-sensitive hydrogels are often fabricated using monomers from natural or synthetic sources. The crosslinking methods used to produce pH-sensitive hydrogels can be either physical or chemical. Physical methods include high-energy radiation, UV-irradiation (Chen *et al.*, 2001). Alternatively emulsification methods (Soppimath *et al.*, 2001) and free radical polymerisation (Chiu *et al.*, 2001) are also often employed to chemically fabricate pH-sensitive hydrogels. The force of the volume collapse arising from the pH-response can easily be detected allowing these hydrogels to be used to make biosensors and permeation switches (Qiu *et al.*, 2001, Hoffman, *et al.*, 1999).

D-glucose-sensitive hydrogels have been proposed for the development of self-regulated insulin delivery systems to act as an artificial pancreas that can administer

the necessary amount of insulin in response to the blood glucose concentration (Miyata *et al.*, 2002). In order to develop D-glucose-sensitive hydrogels, three approaches have been devised. The earlier method is a system consisting of immobilized glucose oxidase in a pH-responsive hydrogel. The second approach is based on competitive binding. Concanavalin A (Con A) is frequently used in binding systems for modulated insulin delivery. In one approach, insulin was chemically modified to introduce a glucose moiety, which binds specifically to Con A (Lee *et al.*, 2000). The glycosylated insulin–Con A system exploits the complementary and competitive binding behaviour of Con A with glucose and glycosylated insulin.

The most attractive method for making delivery systems including competitive binding is to use a sol-gel phase transformation. Hydrogels fabricated from Con A with glucose-containing polymer chains can be made to undergo sol–gel phase transformations depending on the glucose concentration in the environment (Taylor *et al.*, 1995). A non-biological route to fabricate glucose-sensitive hydrogels has been developed using polymers having phenylboronic groups and polyol polymers which form a gel through complex formation between the pendant phenylboronic and hydroxyl groups. Glucose can compete with polyol polymers for the borate crosslinkages, thus the crosslinking density of the gel decreases and the gel swells or transforms from the gel phase to release more drugs as the glucose concentration increases (Kitano *et al.*, 1992, Kataoka *et al.*, 1994, Shiino, *et al.*, 1994, 1995, Aoki, *et al.*, 1996, Hisamitsu, *et al*, 1997, Kataoka, *et al.*, 1998).

Owing to structural similarity to the macromolecular-based components in the body (and their biocompatibility, permeability, and physical characteristics), hydrogels can serve as a synthetic extracellular matrix (ECM) to organize cultural cells into a three-dimensional architecture and to present stimuli; there direct the growth and formation of a desired tissue (Yang *et al.*, 2001). To design hydrogels for use as an ECM, the morphology of the hydrogel should contain pores large enough to accommodate living cells, and should controllably dissolve or degrade, releasing growth factors and creating pores into which living cells may penetrate and proliferate. The balance between mechanical properties and controlled degradation of hydrogels mainly depends on the original rigidity of the polymer chains, the types of crosslinking

molecules and the cross-linking density, and swelling as a result of hydrophilic/hydrophobic balance (Lee *et al.*, 2000).

The development of responsive hydrogels as biosensor materials has been limited by the lack of accurate techniques to gauge their volume change in response to any stimulus. Recently, with the advent of the sophistication of advanced microfabrication facilities and new material technologies, diffractive and miniaturized optical gratings have been widely used in hydrogel fabrication for biosensors (Dennis *et al.,* 2001). Using hydrogels in biosensors allows a combination of biological receptor compounds (antibody, enzyme, nucleic acid, etc.) and the physical or physico-chemical signal transduction required, (e.g. optical, mass, electrochemical and thermal). Ideally, these biosensors permit "real-time" observation of a specific biological event (e.g. antibody–antigen interaction) and allow the detection of a broad spectrum of analytes in complex sample mixtures.

Since inert and hydrophilic hydrogels were developed, hydrogels have been used as an important matrix support of chromatography columns (Nishikawa *et al.*, 1976). The intrinsic macroporous structure in the hydrogel allows modification for ligand attachment, so the main application is as a matrix support for affinity chromatography. In addition to a microporous structure to accommodate the internal interaction of large-molecular-weight biomolecules with ligands, an ideal hydrogel support for in chromatography should be hydrophilic and neutral to prevent non-specific interactions with the hydrogel itself, contain functional groups to allow activation using a wide variety of reactions, be chemically stable to withstand harsh conditions during adsorption, elution and regeneration, be physically stable to withstand transmembrane or drop pressure where applicable, be able to withstand sterilization by autoclaving, and be readily available at low cost to facilitate scale up for industrial applications(Charcosset, 1998).

Furthermore, additional applications using immobilizing biocatalysts have been expected to act as biomimetic actuators giving surfaces with switchable hydrophobic–hydrophilic properties (Galaev *et al.,* 1999).

Dextrans, which are produced from sucrose by numerous lactic acid bacteria, are polymers composed exclusively of D-glucose with a predominance of alpha-1, 6-linkages and a small percentage of a-1, 3 linked side chains. Unlike similar polysaccharides such as starch and cellulose, dextrans are soluble in cold water at 10 ^{o}C. The availability of dextran with different molecular weights, its solubility in polar organic solvents (which enables chemical modification) and its biocompatibility make this natural polysaccharide synthetically useful. Dextrans have a variety of uses in pharmaceuticals, cosmetics, photographic industries, etc. Dextran has a number of features including high molecular weight, water solubility, neutral charge, good stability at room temperature between pH 4 and 10, and is readily biodegradable.

Because of these properties, dextrans have been used for many years as blood expanders to maintain or replace blood volume, and studied for use as a carrier system for a variety of therapeutic agents including antidiabetics, antibiotics, anticancer drugs, peptides and enzymes (Molteni, 1979, Poznansky *et al.,* 1980). Dextrans can be degraded in the gut by dextranase present in the colon (Sery *et al.,* 1956). Taking advantage of these enzymes, polymeric prodrugs for colonic drug delivery based on dextran have been designed (Larsen *et al.,* 1989). It was concluded that the dextran molecule in the prodrug conjugate was degraded by microbial dextranases in the gut making the ester bond accessible to hydrolysis, releasing the drug.

Dextran hydrogels have recently received increased attention due to their variety of biotechnological and biomedical applications. Owing to their low tissue toxicity and high enzymatic degradability at desired sites, dextran hydrogels have been frequently considered as a potential matrix system for drug delivery and/or controlled release of bioactive agents, cell cultures and biosensors (Vandamme *et al.,* 2002). Several approaches to preparing dextran hydrogels have been adopted.

For dextran hydrogels targeted at colon-specific drug delivery, the colon-specific drug is loaded into the hydrogel which undergoes no or little release in the stomach and small intestine and is protected against digestion by enzymes. (Hovgaard *et al.,* 1995). For a dextran-based hydrogel aimed cell culture or tissue engineering, other polymers required for cell growth and proliferation, such as gelatin, hyaluronan, or glycosaminoglycans (GAGs), often need to be incorporated. Interest in dexran

hydrogels in tissue engineering results from two reasons: the first is data available on the cytotoxicity and biodegradation of dextran-based hydrogels or polymers used in drug-delivery in vitro; the second is an ability to produce three-dimensional (3D) porous scaffolds for artificial tissue.

Dextran hydrogel has been successfully applied in biosensors based on surface plasmon resonance. Carboxymethyl-dextran (CM-Dextran) hydrogel is the original sensor surface for biomolecular interaction analysis and hence the most extensively studied and versatile. It has been used in a very wide range of interaction analyses including those between proteins, nucleic acids and carbohydrates (Ballerstadt *et al.,* 1994, Ehwald *et al.,* 1996).

Recently, attention has been paid to new syntheses and applications of carbodiimides in hydrogels, and also to bioconjugation based on amide formation under very mild conditions between carboxylic acids and amines in aqueous and organic systems in the presence of carbodiimides (Hennink *et al.,* 2002). When using EDC as the crosslinking agent for hydrogel preparation, two advantages were found: one is the reaction condition was mild, easily controlled by the level of COOH group substitution, the other is that EDC is not incorporated into the cross-linked structure, but is simply changed to a water-soluble easily washed away urea derivative for which cytotoxity has been found to be quite low compared with that of EDC (Benslimane *et al,* 1988). Carbodiimide chemistry will become a more attractive method to fabricate the hydrogel as a matrix used in drug-delivery or tissue engineering because of these potential merits.

In brief, hydrogels are frequently used, or will potentially be useful, as biomaterials in many medical applications, including tissue engineering, drug-delivery, biosensors and bioseparation.

1.2 Specific objectives

The aim of the studies presented in this thesis was to develop dextran hydrogels crosslinked using N-(3-dimethylaminopropyl)-N'-ethylcarbodiimide (EDC) in

combination with N-hydroxysuccinimide (NHS) and study its potential application in smart hydrogel fabrication, tissue engineering, biosensors and bioseparation.

1.3 Thesis outline

In Chapter 2 a literature survey is given reviewing hydrogel preparation and applications. Dextran hydrogel is described in detail. Various aspects concerning carbodiimide chemistry are addressed, and an overview of the use of hydrogel in biomedical applications is given. Chapter 3 describe glucose-sensitive hydrogel membranes that have been synthesized and characterized for their rate-of-delivery of macromolecules. The D-glucose sensitive properties of a hydrogel fabricated using EDC and NHS is described in Chapter 4. In Chapter 5, the effect of compositions on hydrogel properties is investigated and tested. A hydrogel with extra COOH response to pH is described in Chapter 6. Possible cytotoxicity and cell reactions of EDC/NHS crosslinked CM-dextran was determined as described in Chapter 7. To confirm hydrogel applications in biosensors, a hydrogel with an inbuilt diffraction grating was fabricated and tested as described in Chapter 8. In the affinity membrane presented in Chapter 9, the effect of protein competitive binding onto diffusion is investigated. SEC is used to examine the beads made from D-glucose sensitive hydrogel in Chapter 10. Finally, the conclusions and possible future experiments are summarized in Chapter 11.

Chapter 2. Review of Hydrogel Applications in Biomedical Engineering

2.1 Introduction

Since Wichterle and Lim first proposed the use of hydrophilic networks of poly (2-hydroxyethyl methacrylate) (PHEMA) in contact lenses in 1960 (Wichterle *et al.*, 1960), hydrogels have emerged as promising materials in various biomedical (Hoffman, 2002) and pharmaceutical (Peppas *et al.*, 2000) applications. Hydrogels preformed by chemical or physical crosslinking are a special class of hydrophilic polymer that may absorb up to thousands of times their dry weight in water while maintaining much of their structure (Byeongmoon *et al.*, 2002, Peppas *et al*, 1986, Ratner *et al*, 1976). Recently, hydrogels have been explored in tissue engineering, drug delivery, biosensors, biosepapration and a variety of other related and potential uses because various physicochemical properties required of hydrogels can be met with by changes in monomer structure, the degree of crosslinking, and the fabrication method (Piyush *et al.*, 2002, Nguyen *et al.*, 2002, Olgun *et al.*, 1999, Byrne *et al.*, 2002).

In comparison to other biomaterials used in the biomedical field, hydrogels have the following advantags:

(1) They resemble living tissues closely in their physical properties because of their relatively high water content and soft and rubbery consistency.

(2) Their stability can be chemically controlled such that they are biodegradable and eventually disintegrate and dissolve.

(3) They are biocompatible

Not surprisingly, research reports and reviews in this area have dramatically increased in the past three decades, so a large number of reviews about hydrogels describing application, composition, and properties have been found in the literature. Accompanying the development and application of new hydrogels, more novel terms

were coined in different reviews and papers. The generally accepted definitions used in this study are summarized in the preface.

In this chapter the topics are separated as follows: first there is a discussion of other reviews which have appeared in the last 3 years. This discussion covers reviews of hydrogel application and preparation since 2000 but does not claim to be comprehensive. This is followed by the latest studies on applications of hydrogels in drug-delivery that are D-glucose or pH–sensitive, and further applications in tissue engineering, biosensors and affinity membranes. Then, there is a review of hydrogels formed from dextran. Finally there is a review of applying carbodiimide chemistry in hydrogel fabrication.

2.2 Review articles

As the main biomaterials application is drug delivery, reports about hydrogels in drug delivery accounted for the most papers. Table 2.1 indicates the categories of publications in this field in recent years (2000-2003).

For example, 261 papers focus on drug delivery, 83 on tissue engineering, and 49 on biosensors. Obviously 'hydrogels' especially in responsive forms have found more applications in controlled drug delivery because they can perceive the prevailing stimuli and respond by exhibiting changes in their physical or chemical behaviour, resulting in the release of entrapped drugs in a controlled manner (Kost, 1999). Two excellent reviews help to explain the functional mechanisms of smart hydrogels. One was presented by Qiu and Park to summarize various environment-sensitive hydrogels and identified the limitations and improvements of current smart hydrogels in practical applications (Qiu *et al.,* 2001). Another review from Miyata and Uragami focuses on biomolecule-sensitive hydrogels and provides an overview of the important and historical research regarding the synthesis and applications of hydrogels sensitive to stimulus from D-glucose, antigen and protein (Miyata *et al.,* 2002).

Search terms	Found in	Number of documents
Hydrogel	Title/Keywords/Abstract	2001
Hydrogel, drug-delivery	Title/Keywords/Abstract	261
Hydrogel , glucose	Title/Keywords/Abstract	92
Hydrogel, dextran	Title/Keywords/Abstract	88
Hydrogel, tissue engineering	Title/Keywords/Abstract	83
Hydrogel, pH-sensitive	Title/Keywords/Abstract	63
Hydrogel, biosensor	Title/Keywords/Abstract	49
Hydrogel AND carbodiimide	Title/Keywords/Abstract	9
Hydrogel, affinity membrane	Title/Keywords/Abstract	2

Table 2.1: Categories of published paper in the field of hydrogel preparation and application 2000-2003. This table has been complied from searches in the ISI web of Science (expanded Science Citation Index) conducted during July 2003. The database contains a total of 3,530,076 documents. No attempt has been made to distinguish original research papers and review articles. Patent documents have not been surveyed. The categories above may not be mutually exclusive. (The method used in here was adapted from Ciarán ÓFágáin, 2003)

Peppas, one pioneer in hydrogel research, presents a concise review on the applications of hydrogels in the pharmaceutical field, hydrogel characterization and analysis of drug release from such devices. This review addresses the use of hydrogels as carriers for the development of novel pharmaceutical formulations and for the delivery of drugs, peptides and proteins, as targeting agents for site-specific delivery, or as components for the preparation of protein or enzyme conjugates. (Peppas *et al.*,

2000). Gupta *et al.* review highlights the use of hydrogels in controlled drug delivery, and their application in stimuli-responsive, especially pH-responsive, drug release. They make a clear distinction between gels and hydrogels (see Table 2.1) and list some hydrogel-based products on the market (Gupta *et al.*, 2002). Kikuchi and Okano discuss several types of drug delivery systems using hydrogels for pulsing and/or pulsatile drug delivery, and special attention has been given to thermally responsive hydrogels made from poly(N-isopropylacrylamide) and its derivatives (Kikuchi *et al.*, 2002).

The review by Nguyen and West emphasizes photopolymerized hydrogel preparation and application in tissue engineering (Nguyen *et al.*, 2002). There is an extensive discussion of the photoinitiators and materials in current use. They also illustrated photopolymerized hydrogels that have a wider potential application in tissue engineering as barriers, drug delivery systems, and cell encapsulation and scaffold materials. Suh and Matthew's review presents not only some of those biomaterials to promote chondrogenesis and that have potential for tissue engineering of articular cartilage, but also introduce a chitosan-based polysaccharide hydrogel with an application in chondrocyte culture (Suh *et al.*, 2000). Lee and David have summarized a wide range of hydrogels that are frequently used in tissue engineering and list polymers from natural resources and synthetically created ones (Lee *et al.*, 2001). As an important extracellular matrix, the later review by Drury and Mooney focuses on the use of hydrogels as scaffolds for tissues engineering and builds the relationship between hydrogel properties with specific applications as scaffolds in space filling agents, bioactive molecule delivery, and cell/tissue delivery (Drury *et al.*, 2003).

Byrne *et al.* focused on reviewing molecular imprinting within hydrogels and discuss analyte-responsive intelligent hydrogels, specifically suggesting the possibility of utilizing molecular imprinting strategies to impart analyte specificity and responsiveness within these systems (Byrne *et al.*, 2002). As far as thermosensitive hydrogels are concerned, Jeong *et al.* stress the sol-to-gel transition of aqueous polymer solutions primarily induced by temperature, and cover the natural or seminatural polymeric systems, N-isopropylacrylamide (NiPAAM) copolymers, poly (ethylene glycol-b-provides pylene glycol-b-ethylene glycol) (Poloxamer) and its analogs, and poly (ethylene glycol) / poly (D, L-lactic acid-co-glycolic acid) block

copolymers (Jeong *et al.,* 2002). Another short review of thermosensitive hydrogels is described by Martina who demonstrated the current developments in different laboratories around the world in this area and also showed applications from tissue engineering to drug delivery (Martina, 2001).

One comprehensive review by Hoffman, another pioneer who is dedicated to biomaterials study, contains the composition and synthesis of hydrogels, and the characteristics of their absorbed water and permeation of solutes within their swollen matrices. The most important properties of hydrogels relevant to their biomedical applications are also identified, especially in the use of hydrogels as drug and cell carriers, and as tissue engineering matrices (Hoffman, 2002). Another interesting review by Hennink *et al.* contributed to novel crosslinking methods for the design of hydrogels and described the relationship between characteristics and some potential applications of the gels with their preparation methods (Hennink *et al.,* 2002).

Owing to hydrogels' hydrophilic properties and their high compatibility with commonly used ligands, they have often acted as a matrix in an affinity membrane to couple ligand-like antigens and antibodies, dye, amino acid, other biological ligand. Review on hydrogel membranes as affinity matrices were hardly evident in the recent literature, but a review by Zeng and Ruckenstein particularly emphasises on preparation of chitin and chitosan hydrogel as membranes and the application of these novel hydrogels in membrane chromatography (Zeng *et al.,* 2000). Here was pointed out that many affinity membranes or beads were in fact hydrogel structures. The detailed research reports in recent years will be discussed in the next section.

As seen in Figure 2.1, smart or intelligent hydrogels show a discontinuous volumetric change above a certain threshold of an external stimulus and rochemical luminescence or optoelectronic devices using them are easily detected or controlled reversibly. Thus a novel biosensor may combine detection and response together. Few specialist reviews talk about smart hydrogel applications in biosensors. However, Dong and Chen present the immobilization materials based on sol-gel organic-inorganic hybrid materials, cryohydrogel or organohydrogel and bilayer lipid membranes, all as biosensors materials and highlight applications of the biosensors in extreme environments (Dong *et al.,* 2002).

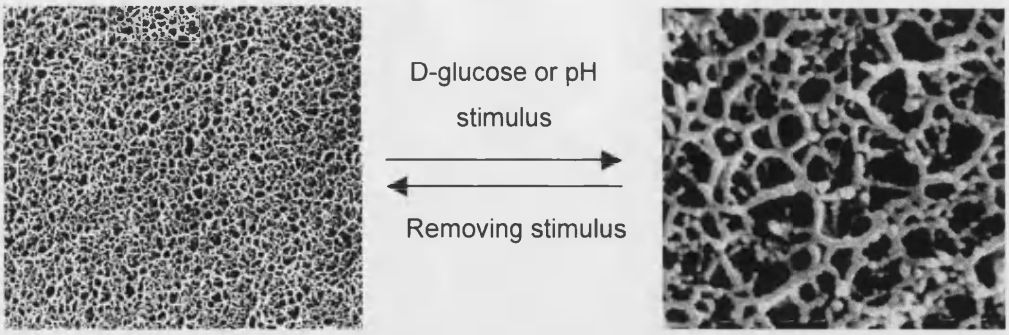

Figure 2.1 Structural framework change of smart hydrogel in response to pH or D-glucose stimulus (the photos was taken in house of a CM-dextran gel).

There are various reviews that talk of the general application of hydrogels or biomaterials which take account of hydrogels as a subsidiary category (Kissel *et al.,* 2002, Kumar *et al.,* 2001, Griffith, 2000, Tabata *et al.,* 1998, Gombotz *et al.,* 1998, Peppas *et al.,* 1996, Langer, 2000).

The fascinating properties of hydrogels suggest that they will have many future uses as the next generation of materials for biological and biomedical applications. Furthermore, a better understanding of the structures and functions of hydrogels will lead to the development of novel hydrogels for meeting practical needs. For example, hydrogels for affinity membranes need higher mechanical strength than those for controlled drug delivery. This aim can be attained by controlling crosslinkage degree or the properties of the polymer.

2.3 Hydrogel Applications

2.3.1 pH-sensitive hydrogels

pH-sensitive hydrogels have been most frequently studied and used to develop controlled release formulations for oral administration. The functional mechanism of this is that small changes in pH can result in significant change in the mesh size of the polymeric networks. As shown in Figure 2.2, two types of such a hydrogel can be fabricated based on pendant groups that are acidic or basic. Differential swelling of ionic hydrogels in acidic or alkaline buffers exhibit different pH-dependent swelling behavior generating swollen networks as seen in Figure 2.2. Ionic hydrogels are swollen polymer networks containing pendent groups, such as carboxylic or sulfuric acid, which show sudden or gradual changes in their dynamic and equilibrium

swelling behavior when the pH of the environment is above the pKa of the ionizable group. A novel pH-sensitive gel described in Chapter 5 and 6 was fabricated using a similar method. Conversely, cationic hydrogels contain pendent groups, such as amines, and will swell to an increased level resulting from increased electrostatic repulsions at a pH below the pKb of the ionizable species (Peppas *et al.,* 2000, Gupta *et al.*, 2002, Qiu *et al.,* 2001).

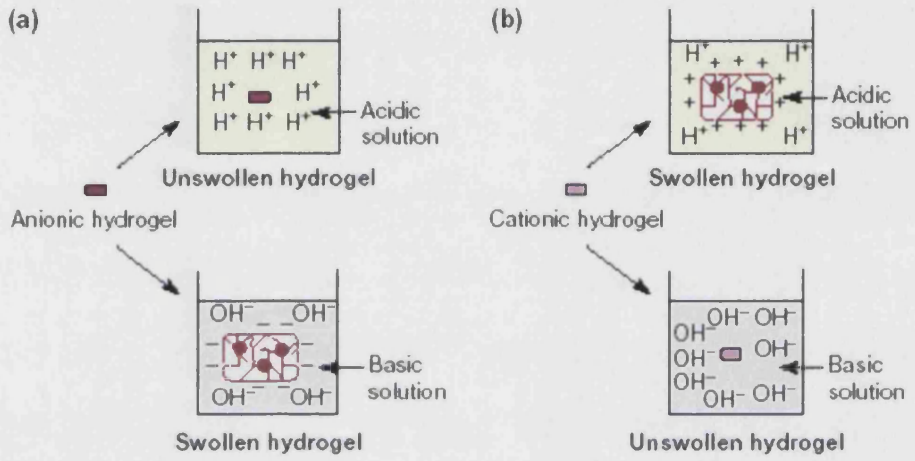

Figure 2.2 The pH-responsive swelling of (a) anionic and (b) cationic hydrogels (from Gupta *et al.*, 2002)

pH-sensitive hydrogels are often fabricated using monomers from natural sources or from synthetic polymers. Table 2.2 summarizes the many varied compositions which can be crosslinked. Hydrogels based on the nature of the side groups, such as dextran or chitosan, and the pendent groups can be precisely controlled by the choice of the chemical entities used in the polymer synthesis (Zhao *et al.*, 2003, Chiu *et al.,* 2002, 2001). However, the hydrogel properties, like the cross-linking density, can also be adjusted by the reactant ratio of the monomer forming the hydrogel when a synthesized polymer is used to prepare the hydrogel (Soppimath *et al.*, 2001, Murat, *et al.,* 2000).

The crosslinking methods used to design pH-sensitive hydrogels can be either physical or chemical. The physical methods include high-energy using a radiation electronic accelerator in vacuum (Zhao *et al.*, 2002), γ- ray irradiation (Murat *et al.*, 2000, 2001), UV-irradiation (Chen *et al.,* 2001), emulsification (Soppimath *et al.*,

2001) and free radical polymerization (Chiu *et al.*, 2001). All have been often employed to chemically fabricate pH-sensitive hydrogels.

Natural resource
Carboxymethylchitin (CM-chitin) carboxymethylchitosan (CM-chitosan)
methacrylated dextran (MA-dextran)
alginate
chitosan
chitosan grafted lactic acid (LA) and/or glycolic acid (GA)
hyaluronic acid (HA)
Synthesized
poly(vinyl alcohol) (PVA)
2-hydroxyethyl methacrylate (HEMA).
dimethylaminoethyl methacrylate (DMAEMA)
N-aminopropylmethacrylamide(NAPA)
acrylic acid (AAc)
N-iso(propylacrylamide) (NIPAAm)
N-*t*-butylacrylamide (NBAA)
Acrylamide (Aam)
maleic acid (MA)
polyvinyl pyrrolidone (PVP)
N-isopropyl acrylamide (NIPAAm)
acrylic acid (AAc).
polypeptide
methacrylic acid (MAA)
polyethylene glycol (PEG)
[*N*-vinyl pyrrolidone-acrylic acid] [NVP-AA]
methyl methacrylate (MMA)
N,*N*-dimethylaminoethyl methacrylamide (DMAA)
hydroxyethyl methacrylate-coacrylic acid(HEMA-AC)
acrylamide-co-acrylic acid (AA-AC)

Table 2.2: Some polymers used to synthesize hydrogel matrices

The widest application of pH-sensitive hydrogels lies in controlled release formulations for oral administration. Drug delivery for colon-specificity is achieved by the means of pH-sensitive monomers and azo cross-linking agents in the hydrogel structure. During the transit through the gastrointestinal tract, the swelling capacity of the hydrogels increases as the pH increases as they move further and further beyond the low pH of the stomach. Upon arrival in the colon, the hydrogels have reached a degree of swelling that makes the cross-links accessible to the enzymes (azoreductase) or mediators. Subsequently, the hydrogel network is progressively degraded via the cleavage of the cross-links, and the drug entrapped is thus released. The swelling characteristics of the hydrogels can be further controlled by incorporating the hydrolyzable moieties in the hydrogel structure (Akala *et al.,* 1998, Yang *et al.*, 2002). Another example is for stomach-specific drug delivery. The pH in the stomach is much lower than the neutral pH in the intestine, and such a difference is suitable for polycationic hydrogels where swelling is minimal at neutral pH and reaches a maximum to release drug at pH 3 to 5 (Ravichandran, *et al.,* 1997, Patel *et al.,* 1996).

The volume collapse from pH-sensitivity can easily give a detectable signal, so hydrogels have also been used to make biosensors and permeation switches (Qiu *et al.*, 2001, Hoffman *et al.,* 1999). pH-dependent hydrogels loaded with glucose oxidase will change the pH of their internal microenvironment in response to environmental glucose, thus glucose concentration can be determined from this phase change. The same approach worked when a pH-sensitive hydrogel was formed by copolymerizing N-isopropylacrylamide with acrylic acid containing immobilized glucose dehydrogenase (Kokufuta *et al.*, 1994).

The introduction of stimuli-responsive hydrogels has further strengthened the link between therapeutic need and drug delivery. When applying stimuli-responsive hydrogels as drug delivery systems for marketed products, the essential requirements for patient care are biocompatibility, biodegradability, and the coordinated relationship of the gel's mechanical strength with their response-time in a physiological environment.

2.3.2 D-glucose sensitive hydrogels

D-glucose-sensitive hydrogels have been proposed for the development of self-regulated insulin delivery systems and may enable an artificial pancreas that can administer the necessary amount of insulin in response to blood glucose concentration (Miyata *et al.*, 2002).

In order to develop D-glucose-sensitive hydrogels, three approaches have often been used. The earliest are based on immobilized glucose oxidase in a pH-responsive hydrogel as mentioned above. As glucose diffuses into the hydrogel, glucose oxidase catalyzes its conversion to gluconic acid reducing local pH, thus pH-sensitive swelling of the hydrogels can be controlled by D-glucose concentration. Two mechanisms exist with different pH-sensitive method: in the first the stimulus of glucose results in swelling of the membranes and an enhanced permeation of insulin from a reservoir via diffusion through the swollen hydrogel (Albin *et al.*, 1985, 1987, Ishihara *et al.*, 1986, Cartier *et al.*, 2003, Podual *et al.*, 2000). In the second mechanism, insulin is loaded inside a hydrogel matrix which shrinks as a result of lowering of the pH; therefore insulin release is enhanced due to the 'squeezing' action of the hydrogel (Hassan *et al.*, 1997, Parker *et al.*, 1999, Heller *et al.*, 1990).

The second approach is based on competitive binding. Concanavalin A (Con A) has also been frequently used in modulated insulin delivery. Con A is a glucose-binding protein obtained from the jack bean plant, *Canavalia ensiformis*. In this type of system, insulin molecules are attached to a support or carrier through specific interactions which can be interrupted by glucose itself. This generally requires the introduction of functional groups onto insulin molecules. In one approach, insulin was chemically modified to introduce glucose, which itself binds especially to Con A (Lee *et al.*, 2000). The glycosylated insulin–Con A system exploits the complementary and competitive binding behavior of Con A with glucose and glycosylated insulin. The free glucose molecules compete with glucose–insulin conjugates bound to Con A and thus the glycosylated insulin is desorbed from the Con A host in the presence of free glucose. The desorbed glucose–insulin conjugates are released within the surrounding tissue, where studies have shown that they are bioactive. Various glycosylated insulins having different binding affinities to Con A have been synthesized in an effort to manipulate the displacement of immobilized insulin from Con A at different

glucose levels (Lee *et al.*, 2001, Park *et al.,* 2002, Schoof *et al.*, 2001, Alberts *et al.*, 1994).

The basic principle of competitive binding provided new concepts with regard to the competitive and complementary binding properties of glucose derivatives and glucose to Con A, as well as their suitability for the fabrication of glucose-sensitive hydrogels. Brownlee and Cerami first suggested glycosylated insulins complementary to Con A which they immobilized on sepharose beads. The glycosylated insulin is displaced from the Con A by glucose in response to, and proportional to, the amount of glucose present which competes for the same binding sites (Brownlee *et al.,* 1979, 1983). The same strategy was further explored by Kim *et al.*. (Seminoff *et al.*, 1989, Kim *et al.*, 1990).

Another attractive method using competitive binding is to generate a sol-gel phase transformation. Hydrogels fabricated from Con A with glucose-containing polymer chains can be made to undergo sol–gel phase transformations depending on the glucose concentration in the environment. Because of the non-covalent crosslinking between glucose-containing polymer and Con A, individual free glucose molecules can compete with the polymer-attached glucose molecules and exchange with them as the external glucose molecules diffuse into the hydrogel. It has been shown that diffusion of insulin through the solution (Sol) phase is faster than that through the hydrogel (gel) phase, and that insulin release can be controlled as a function of the glucose concentration in the environment (Nakamae *et al.*, 1994, Miyata *et al.,* 1996, Tanna *et al.,* 1994, 1999, 2002, Taylor *et al.*, 1994, 1995, Kim *et al.,* 2001).

The third approach used to fabricate glucose-sensitive hydrogels employs polymers having phenylboronic groups and polyol polymers which form a gel through complex formation between the pendant phenylboronic and hydroxyl groups. Glucose can compete with polyol polymers for the borate crosslinkages, thus the crosslinking density of the gel decreases and the gel swells or transforms gel phase to release more drugs as the glucose concentration increases (Kitano *et al.*, 1992, Kataoka *et al.*, 1994, Shiino *et al.*, 1994, 1995, Aoki *et al.*, 1996, Hisamitsu *et al*, 1997, Kataoka *et al.*, 1998).

The application of glucose–sensitive hydrogels lies in the development of self-regulated insulin delivery systems eliminating the need for separate detection. There are still some drawbacks with current glucose-hydrogels which preventing them from being clinically useful. (1) The response time of existing hydrogels or systems may be too slow for therapeutic applications (Qiu *et al.,* 2001). (2) Differences in the diffusion rate of insulin and glucose through the porous membrane can make control difficult. (3) A problem encountered in the sol-gel method was the significant leakage of concanavalin A during the low viscosity phases, which could lead to an undesirable immune response. The ideal hydrogel should have rapid response, reproducibility, and biocompatibility without requiring a phase change. In chapter 3 and 4, two types of D-glucose sensitive hydrogel membrane were developed and investigated for the contolled delivery of macromolecules.

2.3.3 Hydrogel applications in cell culture or tissue engineering

Hydrogels have found numerous applications in tissue engineering as well as in drug delivery owing to their structural similarity to the macromolecular-based components in the body and their biocompatibility, permeability, and physical characteristics. Hydrogels serve as a synthetic extracellular matrix (ECM) to organize cells into a three-dimensional architecture and to present stimuli, which direct the growth and formation of a desired tissue (Yang *et al.,* 2001). To design hydrogels for use as ECM, the morphology of the hydrogel may contain pores large enough to accommodate living cells, the easily controlled to dissolve or degrade away, and release growth factors and create pores into which living cells may penetrate and proliferate as shown in Figure 2.3.

To design a suitable hydrogel for tissue engineering, critical parameters to be met include: degradation rate, mechanical properties, cell adhesion, biocompatibility, and good transport of nutrient. It should be mentioned that the mechanical properties of hydrogels are important design parameters in tissue engineering which provide the ability to create and maintain a space for tissue development and have a significant effect on the adhesion and gene expression of cells (Huang *et al.*, 1999). The balance between mechanical properties and controlled degradation of hydrogels mainly depends on the original rigidity of polymer chains, types of crosslinking molecules

and the cross-linking density, and swelling as a result of hydrophilic/hydrophobic balance (Lee *et al.*, 2000).

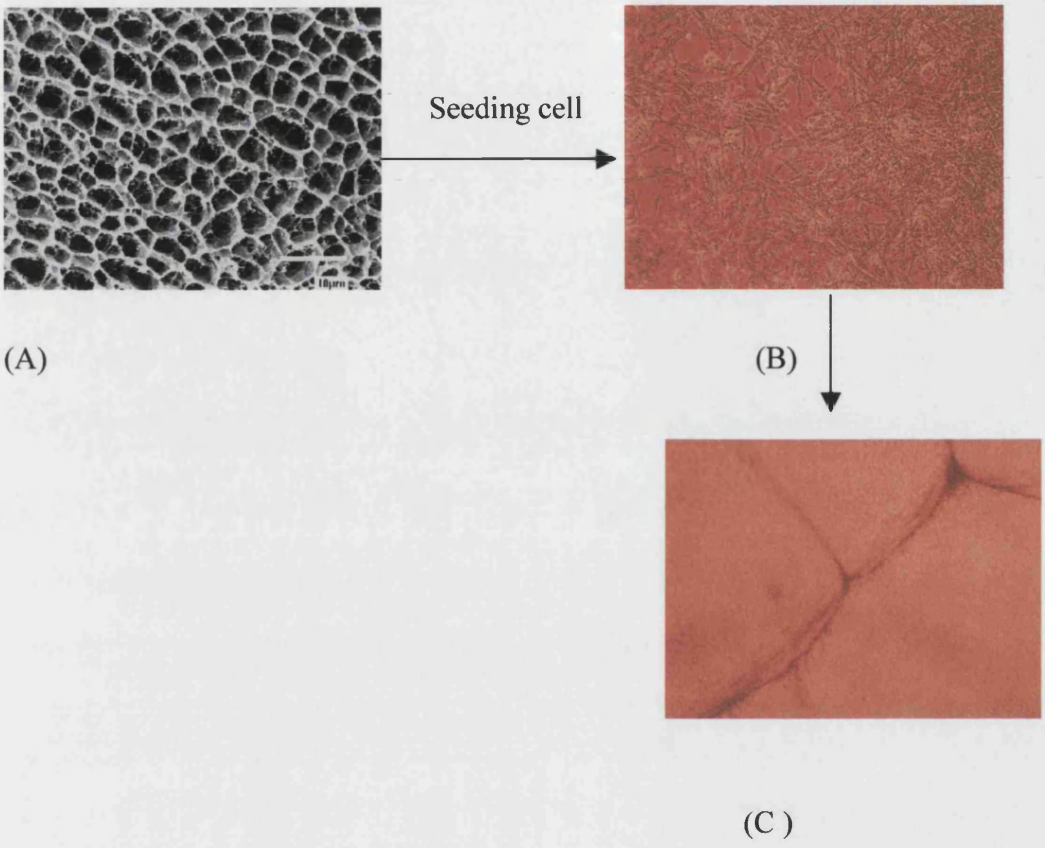

Figure 2.3 Hydrogel applications in tissue engineering. (A) SEM of the gel structure, (B) human dermal fibroblast cells seeded on the hydrogel surface and attached (C) the confluent sheets of primary human dermal fibroblasts formed on the surface of the hydrogel.

The polymer used to fabricate the hydrogel can originate from natural sources or be synthetically created. Natural polymers used in hydrogels include collagen, gelatin, hyaluronate, fibrin, alginate, chitosan, and dextran.

Collagen is the most widely used tissue-derived natural polymer as it is the most abundant protein in mammalian tissues and is the main component of natural ECM (Lee *et al.,* 2001). A hydrogel formed by collagen meets many design parameters. In addition, collagen hydrogel ECM's can be created and their mechanical properties enhanced by introducing various chemical crosslinkers with physical treatments (Lee, *et al.*, 2001, Park *et al.*, 2002, Schoof *et al.*, 2001, Tan *et al.*, 2001). Collagen is

naturally degraded by metalloproteases, specifically collagenase, and serine proteases, allowing for its degradation to be locally controlled by cells present in the engineered tissue (Alberts *et al.,* 1994). As a derivative of collagen, gelatin easily forms hydrogels when changes are made to the temperature of its solution. However, the mechanical weakness of hydrogels from both collagen or gelatin has been a drawback, thus a number of chemical modification methods have to be used to improve the mechanical properties of gelatin gels (Kuijpers *et al.*, 1999, Choi *et al.*, 1999).

Hydrogel formed from hyaluronate, one of the glycosaminoglycan (GAG) components in natural ECM plays a significant role in wound healing. It is easily crosslinked with other natural or synthesized polymers and also degraded by hyaluronidase in ECM (Oerther *et al.,* 2000, Borzacchiello *et al.,* 2001, Gamini *et al.*, 2002, Afify *et al.*, 1993).

Because alginate hydrogels are formed under gentle conditions, have low toxicity, and are readily available, they have been used in a variety of medical applications including cell encapsulation and drug stabilization and delivery. To enhance its effective application in cell culture, alginate has been modified with receptors e.g. lectin, and been covalently crosslinked with other polymer such as PEG (Eiselt *et al.*, 1999, LeRoux *et al.,* 1999).

Chitosan based hydrogel has been widely investigated for tissue engineering applications because it is structurally similar to naturally occurring GAGs, has low toxicity and is degradable by enzymes in humans (Suh *et al.*, 2000). Owing to chitosan's cationic nature and high charge density in solution, chitosan gelation can be generated with a wide variety of water-soluble anionic polymers. In addition, chitosan derivatives and blends have also been gelled via glutaraldehyde crosslinking, UV irradiation, and thermal variations (Mi *et al.*, 2000, Shen *et al.,* 2000, Ono *et al.,* 2000, Chenite *et al.,* 2000).

Fibrin hydrogels can be produced from the patient's own blood and can be used as an autologous scaffold for tissue engineering, thereby giving no toxic degradation nor inflammatory reactions. Another advantage of this hydrogel is that it favors cell migration, proliferation, and matrix synthesis through the incorporation of platelet-derived growth factors and transforming growth factor β (Sierra *et al.,* 1996). The

gelation can be conducted by the enzymatic polymerisation of fibrinogen at room temperature in the presence of thrombin (Perka *et al.*, 2000).

Dextran is a relatively inexpensive polysaccharide. After grafting with polyacrylic acid (Thermes *et al.*, 1992) or bioactive carboxylic acids (Sanchez *et al.*, 1997), derivatives of dextran can be fabricated into a hydrogel through photopolymerization (Pitarresi *et al.*, 2003, Trudel *et al.*, 2002). A more detailed discussion of dextran hydrogels will be present in chapter 7.

The hydrogel's natural biocompatibility and biodegradation mentioned above are of benefit in tissue engineering, but weak mechanical strength is a limitation. In practical applications, combining them with synthetic materials improves the balance between mechanical strength and biodegradation.

Because synthetic polymers can be reproducibly made with specific molecular weights, block structures, degradable linkages, and crosslinking modes, the properties of the resulting hydrogel, such as formation dynamics, cross-linking density, mechanical strength and degradability, become easily controlled.

Synthetic polymers often used in hydrogels include poly(acrylic acid) and its derivatives, poly(ethylene oxide)(PEO), poly(vinyl alcohol) (PVA), polyphosphazene, and polypeptides. Among these polymers, PEO has been approved by the FDA for several medical applications due to its biocompatibility and low toxicity and is the most commonly applied synthetic hydrogel polymer for tissue engineering. PEO hydrogels can be prepared by UV photopolymerization and have also been formed from block copolymers of PEO and poly(l-lactic acid) (PLLA) (Bryant *et al.,* 2001, Jeong *et al.*, 1997).

Poly(N-isopropylacrylamide) (PNIPAAm) is another attractive polymer for tissue engineering applications as it exhibits phase transition behavior above the lower critical solution temperature (LCST) (Heskins *et al.*, 1968). Poly(N-isopropylacrylamide, NIPAAm) hydrogels exhibit a thermally reversible volume transition behavior in aqueous solution: reversible swelling and deswelling behaviour below and above the LCST respectively, which is approximately 32 °C and can be matched to body temperature by copolymerisation (Schild, 1992). Hydrogel grafted with PNIPAAm has been copolymerized with acrylic acid, methacrylic acid, or

butylmethacrylic acid, depending on the desired final applications (Guilherme *et al.*, 2003, Ozmen *et al.*, 2003, Kim *et al.*, 2003). The preparation method includes free-radical polymerisation, γ-radiation and redox copolymerisation (Masci *et al.*, 2002, Mun *et al.*, 2002, Yildiz *et al.*, 2002).

To conclude, further hydrogel development is likely to have a great impact on tissue engineering when understanding and information on the biological process of tissue development and healing expand. Novel methods are expected to engineer new hydrogels with biocompatibility, cell-controlled degradability, and intrinsic cellular interaction, therefore enhancing the development of more natural and functional tissues.

2.3.4 Hydrogels based on biosensors

A biosensor definition proposed by IUPAC (Theenot *et. al.*, 1999) is that of a self-contained integrated device capable of providing specific quantitative or semi-quantitative analytical information using a biological recognition element (biochemical receptor) which is in direct spatial contact with a transducer element.

A biosensor should be clearly distinguished either from a bioanalytical system, which requires additional processing steps, or from a bioprobe which is either disposable after one measurement or unable to continuously monitor the analyte concentration. Biosensors are chemical sensors in which the recognition system utilizes a biochemical mechanism (Turner, 2002).

According to the biological specificity-conferring mechanism, the mode of signal transduction, or a combination of biological recognition element and signal transduction, biosensors can be based on amperometric, potentiometric, field-effect or conductivity effects. More recently, researchers have used ion channels, membrane receptors or binding proteins as molecular recognition systems in conductometric, and optical sensors (Brahim *et al.*, 2002). Hydrogels may be able to mimic biological membranes by incorporating coupled special enzymes or proteins. Using the optical or mechanical properties, a hydrogel can be made into a biosensor to recognize signals generated from an environmental stimulus.

The successful commercialisation of real-time optical biosensors based on surface plasmon resonance (SPR) using CM-dextran hydrogel relies on detecting alterations in the optical evanescent waves that result from small changes in refractive index at the interface between the sample and the device. There are caused by, for example, an antibody binding to an antigen. The advantage of these label-free biosensors is that they detect a binding event directly by monitoring a change in a physical property (Turner, 2000).

Electroactive dimethylaminoethyl methacrylate hydrogels physically-entraped glucose oxidase, cholesterol oxidase or galactose oxidase have been fabricated for glucose, cholesterol or galactose amperometric biosensors (Brahim *et al.,* 2002). According to the authors, these biosensors displayed extended linear response ranges, rapid response times, retained storage stabilities, and excellent screening of the physiological interferents ascorbic acid, uric acid, and acetaminophen. When insulin was co-loaded with glucose oxidase into these `bio-smart' devices, there was a twofold increase in insulin release rate when the devices were immersed in glucose solutions. This demonstrates the potential of such systems to function as a chemically synthesized artificial pancreas.

Redox hydrogels consisting of a poly (vinyl pyridine), poly(vinyl imidazole), poly(acrylic acid) or a poly(allyl amine) backbone with covalently bound osmiumcomplexes or poly(siloxane) backbones with covalently bound ferrocene units were all proposed by Schuhmann (2002) for the development of biosensors. Miniaturised biosensors have been developed on the basis of these redox hydrogels, as in, for example, a horseradish peroxidase micro-sensor for the local detection of photoelectrochemically produced hydrogen peroxide. Also produced were needle-type implantable glucose sensors and disk-type glutamate micro-sensors for the detection of glutamate release from cells

The use of intelligent hydrogels as sensor materials has been limited by the lack of accurate techniques to gauge volume changes in response to stimulus. Recently, with the advent of the sophistication of advanced microfabrication facilities and new material technologies, diffractive and miniaturized optical gratings have been widely used in hydrogel fabrication for biosensors.

Grier (1997) fabricated a hydrogel by encapsulating a mesoscopically periodic crystalline colloidal array (CCA) within a gel or as an engineered surface pattern on the surface of the gel. Thereby, the optical prosperities of this hydrogel responsed immediately to a small environmental stimulus. Intelligent hydrogel with CCA incorporates chemical molecular recognition agents that cause the gel to swell in response to the concentration of particular analytes; the gel volume is a function of the analyte concentration. The color diffracted from the hydrogel film is, thus, a function of analyte concentration: the swelling of the gel changes the periodicity of the CCA, which results in a shift in the diffracted wavelength (Holtz *et al.,* 1997).

Another method of making hydrogel biosensors was proposed by Hu *et al,* (1998, 2000). They imprint the surface of a hydrogel with a square array of gold thin films using sputter deposition as showen in Figure 2.4. The periodicity of the array can be continuously varied as a function of temperature or electric field, and thus can alter the gel's volume. So such an array might serve as an optical grating for sensor applications.

Future application of hydrogel in biosensors is anticipated in a combination with biological receptor compounds (antibody, enzyme, nucleic acid, etc.) and physical or physico-chemical signal transduction. Examples are: optical, mass, electrochemical and thermal properties. In most cases, a biosensor can make "real-time" observations of a specific biological event e.g. an antibody–antigen interaction (Figure 2.5) and allow the detection of a broad spectrum of analytes in complex sample matrices. Current studies focusing on optically-based transduction methods aim to achieve a more robust, easy to use, portable, and inexpensive analytical system (Leonard *et al.,* 2003, Purohit, 2003). Optical transducers are particularly attractive as they can allow direct "label-free" and "real-time" detection of bacteria. Biosensors show great promise in areas such as clinical diagnostics, food analysis, and bioprocess and environmental monitoring (Invitski *et al.*, 1999, Fitzpatrick *et al.,* 2000). In chapter 8, a novel biosensor material is described and evaluated.

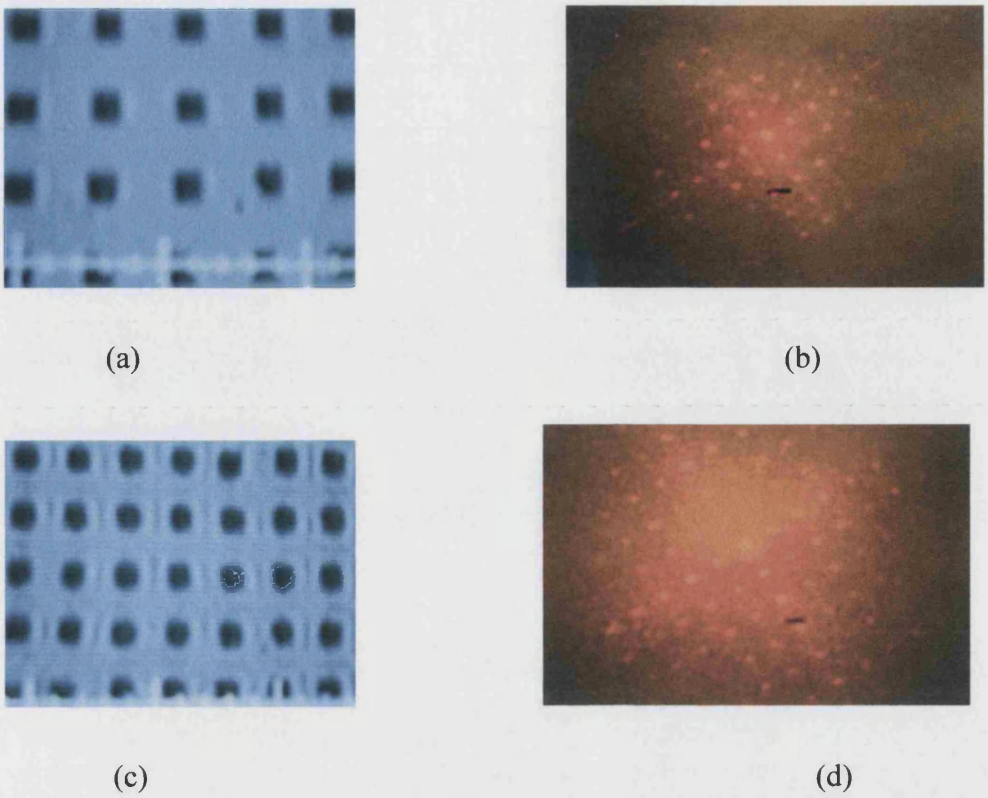

Figure 2.4. The periodic square surface array on the NIPA hydrogel and its diffraction pattern, at various temperatures. At 30°C: a, the surface array; b, the diffraction pattern. At 33.6 °C: c, the surface array; d, the diffraction pattern. In the diffraction experiment, the distance between the screen and the sample was 95 cm. In a and c, each small division in the white scale at the bottom of the image is 0.0193 mm; in b and c, the black bar is 1cm long (Hu *et al.*, 1998).

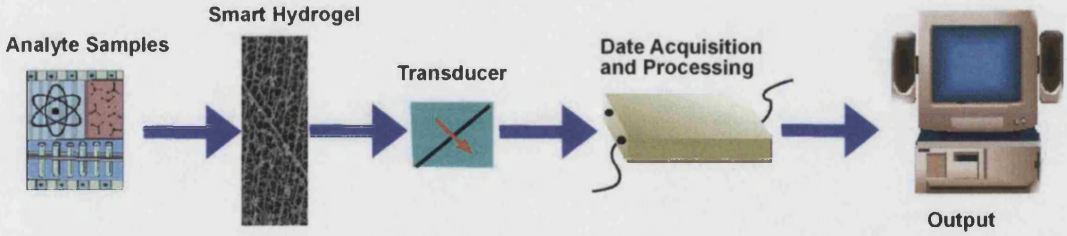

Figure 2.5 Schematic diagrams showing the main components of a biosensor using a smart hydrogel. The biological event, e.g. an antibody–antigen interaction, elicits a volume change of the hydrogel, which is converted by the transducer to an electrical signal. The output from the transducer is then amplified, processed and finally, displayed as a measurable signal (Leonard *et al.*, 2003).

2.3.5 Hydrogels in bioseparation

Since inert and hydrophilic hydrogels were recognized as early as 1950's, hydrogels have been used as an important matrix support of chromatography columns (Nishikawa *et al.*, 1976). A hydrogel matrix can be fabricated into membranes or beads depending on the practical need. The existing macroporous structure of hydrogels allows modification for ligand attachment, so the main application of hydrogels as matrix supports lie in affinity chromatography or membranes. In chapter 9 and 10, membrane and beads produced from dextran hydrogel were investigated.

Conventionally, affinity chromatography uses a porous beaded hydrogel particles which have a ligand or receptor molecule covalently and stably attached to them; the ligand guarantees continued selective association with a biospecific interactant. The most efficient means of contact of such an assembly with feedstock solutions rich in that product has been a fixed bed contactor wherein specifically interacting products can be separated chromatographyically from non-reacting impurities. An expanded bed is a low back-mixing liquid fluidized bed with a solid phase of a defined size and/or density distribution (Matejtschuk, 1997). Due to its high bed voidage and good column efficiency, expanded bed adsorption (EBA) can be employed to directly recover target bioproducts from cell culture broths, cell disruptates and other unclarified feedstocks. Hence, this technique offers the advantages of decreasing the costs and time of biological production and the number of operation steps, and increasing the process yield and product quality (Tong *et al.*, 2002).

Membrane-based chromatography generally can be distinguished from particle-based chromatography by the fact that the interaction between a solute (say a protein) and a matrix (say an immobilized ligand) does not take place in the dead-ended pores of a particle, but mainly in the through-pores of a membrane. While the mass transport in dead-ended pores necessarily takes place by diffusion, the liquid moves through the pores of a membrane by convective flow. In new particulate materials with "through"-pores or convective pores, the liquid has the choice of flowing through the particles or around them; in a stacked membrane there is no choice but to flow through the pores, thus simplifying the analysis. The main difference between the two chromatographic methods is hydrodynamic in nature: the use of membranes reduces the mass transport resistance for the solute by the matrix by reducing pore diffusion, leaving film

diffusion from the core of the liquid to the membrane surface in the interior of a through-pore as the only transport resistance (Thommes *et al.,* 1995).

Except for its microporous structure required to accommodate the free interaction of large molecular weight biomolecules with ligands, an ideal hydrogel support for successful application in chromatography should also show the following properties (Charcosset, 1998):

- It should be hydrophilic and neutral to prevent the biomolecules from interacting non-specifically with the hydrogel itself ;
- It should contain functional groups to allow activation by a wide variety of reactions ;
- It should be chemically stable so as to withstand harsh conditions during adsorption, elution and regeneration,
- It should be physically stable to withstand transmembrane or drop pressure and, when applicable, sterilization by autoclaving, and be readily available at low cost to facilitate industrial applications.

To fabricate the hydrogel matrices used in chromatography, natural or synthesized macromolecular materials, such as agarose, dextrin, chitosan, cellulose, polyacrylamide, poly(hydroxyethyl methacrylate) poly(vinyl alcohol), are employed because they are compatible with commonly used ligands.

Agarose is the traditional, and still the most popular, matrix used for affinity chromatography because of its large beads, macroporous nature, and accessible pore structure suited for used with large target molecules. More important, it has high-capacity, the presence of functional groups, and a good chemical stability (especially at high pH), low non-specific binding, and good reproducibility. Its main drawbacks are that it is easily degraded at high temperature and by microbial contamination and its lack of rigidity. There is a range of marketed products derived from agarose. In addition, some of the beads available for affinity chromatography can be prepared from agarose / polyacrylamide (trade name: Ultrogel), cross-linked dextran (trade

name: sephadex), dextran/poluacrylamide (trade name: sephacryl), ployacrylamide (trade name: Bio-Gel-P), and methacrylate (trade name: Separon).

Cellulose has long been used in membrane preparation and is a good matrix for affinity ligand coupling. Regenerated acetate cellulose or cellulose nitrate membranes can be obtained through the phase-inversion method, and ion exchange groups or affinity ligands can be coupled to the crosslinked regenerated membranes (Kubota, *et al.*, 1996). These membranes have, however, a low porosity, small pore sizes, and a nonrigid structure. These are inherited from the initial acetate or nitrate moieties of the cellulose materials, and the membranes are not suitable for affinity chromatography because of the high-pressure drop through them. Therefore, a new type cellulose micro filtration membrane has been prepared and used as an affinity matrix which is cross-linked by epoxypropane chloride prior to immobilization of triazine dyes, therefore enhancing the mechanical and chemical stabilities (Guo *et. al.*, 1994). Composite macroporous cellulose membranes can be obtained by grafting an acrylic polymer on a cellulose backbone, and can be used for the purification of immunoglobulins and the removal of endotoxins (Hou *et al.*, 1991). Synthetic hydrogel membranes made from poly(hydroxyethyl methacrylate) possesses a high mechanical strength and resistance to many chemicals and to microbial degradation (Aryca, 2000). Macroporous chitosan membranes with controlled, reproducible porosity and good mechanical properties have high selectivity and high adsorption capacity for lysozyme due to their high porosity (Ruckenstein *et al.*, 1997). Some novel affinity membranes can be attained by combining different polymers; such as pHEMA -chitosan via UV initiated photo-polymerization (Bayramoglu *et al.*, 2003), and chitosan–cellulose composite membranes via the phase inversion process (Yang, *et al.*, 2002).

A promising application of hydrogels is to expand their use to cell affinity chromatography. Affinity chromagrophy of grafted cells on a supermacro-porous cryogel was used selectively to separate target cells and showed potential recovery of cells from fermentation media and crude cell homogenates (Arvidsson *et al.*, 2002, 2003).

In summary, hydrogels, especially intelligent hydrogel, can find a wide application in biosensors or drug–delivery because their easily undergo conformational changes

caused by only small changes in the environment. They also have uses in bioseparation or tissue engineering owing to their macroporous and hydrophilic structure. Furthermore, they have been explored for more applications in immobilizing biocatalysts, as biomimetic actuators, and as surfaces with switchable hydrophobic–hydrophilic properties.

2.4 Dextran hydrogels

Dextrans, which are produced from sucrose by numerous lactic acid bacteria, are polymers composed exclusively of D-glucose with a predominance of alpha-1,6-linkages and a small percentage of α-1,3 linked side chains. Commercial dextran preparations are manufactured through partial hydrolysis, fractionation and purification of native dextran produced by a strain of *Leuconostoc mesenteroides*. Unlike similar polysaccharides such as starch and cellulose, dextrans are very soluble in cold water. The availability of dextran with different molecular weights, its solubility in polar organic solvents which enables chemical modification and its biocompatibility make this natural polysaccharide synthetically useful. Dextrans have a variety of uses for pharmaceuticals, cosmetics, and in photographic industries, etc. Their molecular weight (Mr) from commercial manufacture has been estimated to be between 10–30 million.

Dextran has the following features:

• It is a high molecular weight polymer

• It is a water soluble, neutral polymer

• It has good stability at room temperature between pH 4 and 10

• It is readily biodegradable

• It is easily derivatised

Because of these properties, dextrans have been used for many years as blood expanders to maintain or replace blood volume, and studied for use as a carrier system for a variety of therapeutic agents including antidiabetics, antibiotics, anticancer drugs, peptides and enzymes (Molteni, 1979, Poznansky *et al.,* 1980). Dextrans can be

degraded by dextranases which are found to be present in the colon (Sery *et al.*, 1956). Taking advantage of these enzymes, polymeric prodrugs for colonic drug delivery based on dextran have been designed (Larsen, *et al.*, 1989). It was concluded that the dextran molecule was degraded by microbial dextranases making the ester bond accessible to hydrolysis, releasing drugs. Numerous dextran derivatives, such as Carboxymethyl-dextran, cationic-dextran, dextran-sulfates, and dextran-methyl methacrylate, have been prepared and studied to find commercial uses. Those derivatives serve a variety of purposes in pharmaceuticals, cosmetics, veterinary use, animal feed, etc.

Dextran hydrogels have received increased attention due to their variety of biotechnological and biomedical applications. Owing to their low tissue toxicity and high enzymatic degradability at desired sites, dextran hydrogels have been frequently considered as a potential matrix system for drug delivery and/or controlled release of bioactive agents, cell cultures and biosensors. Several approaches for preparing dextran hydrogels have been adopted.

2.4.1 Dextran hydrogels for drug-delivery application

Because dextranases are able to degrade dextran, the application of dextran hydrogel focuses on colon-specific drug delivery. The general method is that a colon-specific drug is loaded into the hydrogel and undergoes no or little release in the stomach and small intestine and is protected against digestion by other enzymes. In the colon the dextran hydrogel is degraded by dextranases resulting in disintegration of the hydrogel matrix and the release of the drug specifically in the colon (Hovgaard *et al.*, 1995).

There are two principles to loading the drug in this hydrogel for colon-delivery. Firstly, a pH-sensitive dextran hydrogel was fabricated from dextran derivatives. By exploiting the pH change along the gastrointestinal tract, pH-responsive dextran hydrogels may enhance the efficiency of drug delivery, especially the targeting of bioactive peptides/proteins to the colon where the content of proteolytic enzymes is low and of dextranase is high (Chiu *et al.*, 2002). Many attempts to synthesize pH-responsive dextran hydrogels have been made. Dextran hydrogels capable of undergoing pH-responsive swelling can be obtained by the activation of dextran with

4-nitrophenyl chloroformate, followed by conjugation with 4-aminobutyric acid and cross-linking with 1,10-diam inodecane (Chiu *et al.*, 1999). Hydrogels were also obtained by polymerization of maleic acid-carrying dextrans (Kim, 1999). Copolymerization of methacrylated -dextran (MA-dextran) with acrylic acid (AAc) was performed and the pH-dependent swelling properties were characterized. (Chiu, *et al.*, 2002, Chiu *et al.*, 2001).

In the application of pH-sensitive coatings for colon-specific drug delivery it is assumed that the coating is stable in the low pH of the stomach and the neutral pH of the small intestine, and dissolves at the pH of the colon. The drawback of these principles is that they are not very reliable in terms of site-specific drug release to the colon due to large variations in transit times and pH depending on diet, food intake, intestinal motility and disease status (Haeberlin *et al.*, 1992). In addition, the pH of the colon can be lower than 7, and the pH of the small intestine can be as high as 8 (Evans, *et al.*, 1988); thus a pH-sensitive hydrogel coated does not always target the drug specifically to the colon (Hovgaard *et al.*, 1995).

The specific characteristic of the second system is that the hydrogel maxtrix is made of dextran or modified dextran and a crosslinking agent providing network linkage between the polymer chains. The colon-specific drug is loaded in the swelled phase of the hydrogel and dried in vitro. Owing to the fact that dextranase are only present in the colon, the hydrogel matrix can only be degraded by dextranase once the dosage forms reach the colon (Vandamme *et al.*, 2002).

Recent dextran hydrogel for drug-delivery is mainly originated from Methyl Acrylate -dextran, because it is less harmful to the human body than other reagents commonly used for the incorporation of vinyl groups, such as acryloyl chloride. The anhydride linkage of methacrylic anhydride is unstable enough to be broken by a nucleophilic attack of the hydroxyl groups in dextran (Vollhardt *et al.*, 1987). Therefore, dextran–methacrylate could be easily synthesized as a hydrogel precursor by taking advantage of the functionality of hydroxyl groups in dextran and the instability of anhydride linkage in methacrylic anhydride. One of the most important properties of hydrogels, swelling ratio, then could be easily manipulated by controlling the degree of substitution of the methacrylate group (Kim *et al.*, 2000). Photocrosslinking of a dextran derivative containing glycidyl methacrylate in the side chain represents a

simple and reproducible procedure to obtain networks able to swell in aqueous medium and to dissolve in the presence of dextranases (G. Pitarresi *et al.*, 2003). Hydrogels were obtained by radical polymerization of methacrylated dextran (MA-dextran) in aqueous solution, using ammonium peroxydisulfate (APS) and N,N,N',N'-tetramethylethylenediamine (TMEDA) as the initiator system (Van *et al.*, 1995, 1997). Kim *et al.* also reported the syntheses of methacrylated and acrylated dextrans by reacting dextran with methacrylic anhydride, and with bromoacetyl bromide and sodium acrylate, respectively (Kim *et al.*, 2000). Preparation of dextran hydrogels was then carried out by UV irradiation of MA-dextrans. Hovgaard *et al.* obtained hydrogels directly by cross-linking dextran with either 1,6-hexanediisocyanate or glutaraldehyde (Hovgaard *et al.*, 1995, Brondsted *et al.*, 1998). Sequential reactions of dextran with glycidyl acrylate, followed by polymerization of acrylated dextran also led to the formation of the polymer network (Edman *et al.,* 1980).

Azo-dextran gels were obtained from N,N'-bis(methacryloylamino)azobenzene (B(MA)AB) and methacrylated dextran having low degree of substitution; thus this gel became more swollen in water. The degradation of azo-dextran gels by dextranase seemed to be more pronounced. The potential for colon delivery was evaluated (Barbara *et al.*, 2001). Hennink, a pioneer in dextran-hydrogel research, also presented a range novel hydrogels from dextran for colon-special drug or protein delivery (Cadee *et al.*, 2002, Stenekes *et al.*, 1999, 2001, Jong *et al.*, 2001, Franssen *et al.*, 1997, 1999, Franssen *et al.*, 1998, Hennink *et al.*, 1997).

2.4.2 Dextran-hydrogels in cell culture and tissue engineering

To apply dextran-based hydrogels in cell culture or tissue engineering, other polymers favoured for cell growth and proliferation, such as gelatin, hyaluronan, and glycosaminoglycans (GAGs), need often be incorporated into the hydrogel's network. Studying dexran hydrogels in tissue engineering is done for two reasons. One is evaluating the cytotoxicity and biodegradation of dextran-based hydrogels or polymers used in drug-delivery *in vitro*, and another is to produce three-dimensional (3D) porous scaffolds or cartilage for artificial tissue.

Hydrogels made of dextran with glycidyl methacrylate and/or hyaluronan are created through photopolymerization. An evaluation of the cellular response to these materials

demonstrated that most of these hydrogels are highly compatible with vascular smooth muscle cells. And it was hoped that future studies would determine the *in vivo* biocompatibility of these gels to be used as drug delivery matrices for cardiovascular implants (Trudela *et al.*, 2002).

A biodegradable material was developed by blending polylactide with dextran, and a novel sponge-like scaffold made of it was fabricated thereof using solvent-casting and particle-leaching techniques. The attained scaffold has higher porosity and an open-porous structure and the hydrophilicity of this materials was significantly improved. Therefore good cell affinity and biocompatibility enhanced cell-attaching efficiency, facilitated cells penetrating into the scaffold and cell proliferation (Cai *et al.,* 2002).

The biosafety of a new dextran dialdehyde cross-linked gelatin hydrogel for use as a wound dressing was evaluated *in vitro* in cultures of dermal fibroblasts, epidermal keratinocytes, and endothelial cells. The study showed that this hydrogel displayed an acceptable cytotoxicity using very sensitive *in vitro* tests and had good *in vivo* biocompatibility because the foreign-body reaction induced by the implanted hydrogel samples was characterised by only a weak and gradually fading inflammatory reaction without cell degeneration or deviant morphologies (Draye *et al.,* 1998).

To evaluate the cytotoxicity of dextran, methacrylate dextrans, and dextran-based hydrogel discs and microspheres, as well as of their degradation products, the proliferation, morphological deviancies, or cell death were determined as human fibroblasts incubated with these materials. The results demonstrated that methacrylate-derivatized dextran hydrogels show good biocompatibility *in vitro* making these degradable biomaterials promising systems for drug delivery purposes (Groot *et al.*, 2001).

The modification of dextran hydrogel with bioactive molecules has been useful for designing scaffolds or drug–delivery systems that can provide effective patient-care and direct new tissue formation. The surface and bulk modification of hydrogels can allow for the modulation of cellular functions such as adhesion, proliferation and migration through alterations of bioactive molecule concentrations or their spatial distribution. Despite the recent advances toward the development of dextran hydrogels for tissue engineering applications, several challenges still remain,

including the design of adhesion molecules for specific cell types as needed for guided tissue regeneration and the synthesis of hydrogels exhibiting the mechanical responsiveness of living tissues.

2.4.3 Dextran-hydrogels in biosensors

Dextran hydrogel has been successfully applied in biosensors based on surface plasmon resonance. Carboxymethyl-dextran (CM-Dextran) hydrogel is the original sensor surface for biomolecular interaction analysis and hence the most extensively studied and versatile. It has been used in a very wide range of interaction analyses including those between proteins, nucleic acids and carbohydrates. As shown in Figure 2.6, it is a hydrophilic, three-dimensional, high-surface-area matrix bearing charged derivatizable carboxylate groups. This allows the unique feature of efficient electrostatic binding prior to covalent immobilization. This can be vital when the ligand is only available at low concentrations. Ligands containing primary amines are coupled directly to carboxylates using EDC/NHS chemistry (http://www.affinity-sensors.co.uk).

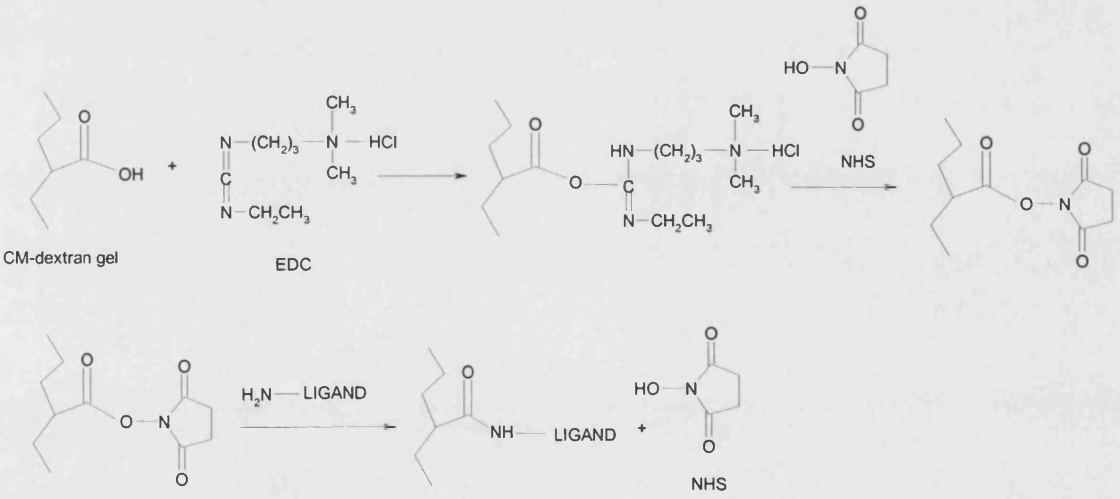

Figure 2.6 Chemistry for immobilization of biomolecules to a CM-dextran surface on SPR via EDC/NHS chemistry.

Aldehyde dextran sulfonate (ADS), a modified oligosaccharide polymer, was also used to prepare a new hydrogel matrix structure for affinity biosensors. The aldehyde group is responsible for covalent bonding in biomaterials, and the negatively charged sulfonate group provides electrostatic attraction of the positively charged biomolecules. By varying the ratio between the aldehyde and sulfonate groups in the

matrix, one can control contributions from the two binding modes (covalent and electrostatic) (Chegel *et al.*, 2002).

A glucose affinity sensor was proposed base on the sol-gel transformation of aqueous dispersions of dextran and Concanavalin A. Both glucose-dependent Con A distribution and glucose-dependent sol-gel changes of the dextran/Con A solution showed a sufficiently fast response (<2 min) to a change in the glucose concentration. The long term stability of the lectin, with respect to binding to dextran and its influence on the viscosity of a concentrated solution of high molecular weight dextran, was obvious (Ballerstadt *et al.*, 1994, Ehwald *et al.*, 1996).

In all, dextran hydrogels play an important matrix role when used in biosensors. Recently, new hydrogels from derivatized dextran or novel polymerisation methods were developed for functional matrices.

In addition, as far as dextran hydrogel application in bioseparation is concerned, few reports could be found, possibly because hydrogel from dextran has weak mechanical strength. Generally, dextran can be made into beads with other polymers for chromatography and they are available as market products (http://www.sigmaaldrich.com/).

2.5 Hydrogels from carbodiimide chemistry

Carbodiimides (RN=C=NR') are unsaturated compounds with an allene structure. Since their first synthesis from thioureas, carbodiimides have been widely used in organic synthesis and biotechnology. Extensive studies have been also devoted to reactions of carbodiimides such as isomerization of themselves, addition reactions with water, alcohols, amines, phenols, and carboxylic acids, peptide synthesis, modification of polysaccharides and reactions with proteins in aqueous systems. Recently, attention has been paid to new synthese and applications of carbodiimides in hydrogels and bioconjugation. Carbodiimides are very effective in modifying and crosslinking proteins because no residues remain in the crosslinked protein (zero-length crosslinker)(Grabarek *et al.*, 1990).

Most of the above-mentioned studies are based on amide formation under very mild conditions between carboxylic acids and amines in aqueous solution and organic

systems in the presence of carbodiimides. Ikada elucidated the reaction mechanism of carbodiimide chemistry (Nakajima *et al.*, 1995). EDC rapidly loses its activity in aqueous media of low pH, producing the corresponding urea derivative, but is very stable at neutral and higher pH regions. EDC could react with carboxyl groups at a relatively narrow low pH range such as 3.5-4.5. If carboxyl groups were cyclizable, they would react quickly with EDC producing carboxylic anhydrides, which formed the corresponding amides when amine compounds were present. On the other hand, a trace of amide was formed in the case of noncyclizable carboxylic acids. In addition, an excess of EDC caused an undesired side reaction to form stable N-acylurea, regardless of the special location of carboxylic acids.

N-Hydroxysuccinimide (NHS) is often used to assist carbodiimide coupling in the presence of EDC (Sehgal *et al.*, 1994). The reaction includes formation of the intermediate active ester (the product of condensation of the carboxylic group and N-hydroxysuccinimide) that further reacts with the amine function finally to yield the amide bond. The stable, active esters hydrolyze slowly in aqueous media compared with their rates of reaction with amino groups and can enhance coupling efficiencies with primary amines. So when using EDC to prepare a hydrogel or for bioconjugation, NHS is used to promote the efficiency of reaction.

Because the hydrogel is prepared between hydroxyl groups or amines with carboxylic acids or derivatives by carbodiimide chemistry, this is also called condensation reaction. This is frequently applied for the synthesis of polymers to yield polyesters and polyamides (Hennink *et al.*, 2002).

When using EDC as the crosslinking agent for hydrogel preparation, two advantages were found: one is that the reaction conditions were mild, easily controlled by COOH group number provided by the polymer; another is that EDC is not incorporated into the cross-linked structure, but is simply changed to a water-soluble urea derivative which has been found to have quite low cytotoxity compared with that of EDC and is easily washed away (Benslimane *et al,* 1988).

Earlier application of EDC/NHS in hydrogels was based on collagen hydrogel for growing spinal axons implanted between the stumps of a transected spinal cord. Collagen was coprecipitated with chondroitin-6-sulfate (C-6-S) or chemically cross-

linked with EDC. Thus cross-linking treatments with EDC improved the stability of collagen implants which withstood implantation for at least 6 months. Collagen hydrogel has improved the mechanical properties of the matrix, modified the normal scarring process, and favored axonal regeneration (Marchand *et al.*, 1993).

Porous collagen matrices crosslinked with various amounts of hyaluronic acid (HA) by EDC were developed as scaffolds with mean diameters of 150–250 mm for dermal tissue regeneration. The effect of HA on cells with HA concentrations in the collagenous matrices was investigated using cultures of fetal human dermal fibroblasts and it was shown that the proliferation of fibroblasts was enhanced on a 9.6% HA-containing collagen matrix. No significant difference was found fibroblast migration into the various types of scaffolds as HA content was increased (Park *et al,* 2003).

Hydrogels from collagen and chitosan may be created by EDC/NHS. Platelet deposition and hepatocyte culture experiments show this hydrogel has moderate mechanical strength and good hepatocyte compatibility as well as excellent blood compatibility. These properties indicate that this hydrogel can be a promising biomaterial for implantable bioartificial livers with microchannels(Wang *et al.*, 2003).

Feijen and his research group, who have done lots of studies in hydrogel preparation by EDC/NHS, fabricated hydrogels by the cross-linking of dermal sheep collagen (DSC) with 1,4-butanediol diglycidyl ether by EDC/NHS. They described the relationship of the material properties, such as the denaturation temperature, swelling, *in vitro* degradation, and tensile properties with the presence of interhelical, intrahelical and intermicrofibrillar cross-links. Cross-links between and in the helices will affect the denaturation temperature and resistance against collagenase, while the mechanical properties and degradation by pronase are apparently dependent on the degree and nature of intermicrofibrillar cross-links and the type of groups available at the outer surface of (micro) fibrils and fibers (Zeeman *et al.,* 1999). Immobilization of heparin to EDC/NHS crosslinked collagen results in increased basic fibroblast growth factor (bFGF) binding and in a prolonged release of bFGF compared to the non-heparinized substrate. This leads to improved proliferation of seeded human umbilical vein endothelial cells (HUVECs) (Wissink *et al.*, 2000). In the further study, HUVECs were seeded on (heparinized) EDC/NHS-crosslinked collagen, pre-loaded

with bFGF. Proliferation of HUVECs on (heparinized) crosslinked collagen increased with increasing amounts of pre-loaded bFGF. It was concluded that heparinized, EDC/NHS-crosslinked collagen pre-loaded with bFGF is a candidate matrix for in vivo endothelial cell seeding of synthetic vascular graft materials (Wissink *et al.*, 2001).

A study on heparin immobilization to this collagen hydrogel suggests that heparin immobilization to EDC/NHS-crosslinked collagen may improve the *in vivo* blood compatibility of this material (Wissink *et al.*, 2001).

Feijen and coworkers also described the preparation of gelatin hydrogels using this chemistry (Kuijpers *et al.*, 2000). These hydrogels were designed as a delivery device for the release of antibacterial proteins and were incorporated in a Dacron prosthetic valve. Lysozyme was loaded in the gels after their formation and released both in vitro and in vivo for a period of 2 days. To improve loading capacity, a negatively charged-polysaccharide, (chrondroitin sulfate) was incorporated in the hydrogels' network (Kuijpers *et al.*, 2000). The loading capacity indeed substantially increased and the release was retarded with increasing chrondroitin content of the gels. This was mostly due to electrostatic interactions between the cationic protein and anionic polysaccharide.

In order to obtain alginate gels with better mechanical properties than ionically crosslinked gels, Mooney et al. developed a method to covalently crosslink this polymer. Alginate and PEG-diamines were crosslinked-using EDC. The mechanical properties could be controlled by the amount of PEG-diamine in the gel and the molecular weight of PEG (Eisel *et al.*, 1999). When covalently modified, alginate polysaccharides with RGD-containing cell adhesion ligands utilizing EDC/NHS may prove to be an ideal material with which to confer specific cellular interactive properties, potentially allowing for the control of long-term gene expression of cells within these matrices (Jon *et al.*, 1999).

EDC/NHS is also applicable for attachment of GAGs to collagen. Modulation of crosslinking conditions provides matrices with well-defined GAG contents, and biodegradabilities (Pieper *et al.*, 2000).

When Ikada et al. studied crosslinking between HA and pectin with the use of EDC, the detailed reaction mechanism was discussed (Tomihata *et al.*, 1997). The result suggests that the intermolecular formation of ester bonds between the hydroxyl and the carboxyl groups in different polysaccharide molecules must have led to crosslinking.

Carbodiimide chemistry will become a more attractive method for fabricating the hydrogels as a matrix for use in drug-delivery or tissue engineering because of its potential merit.

2.6 Conclusion

This section summarized a wide range of hydrogels, especially from dextran, that have been frequently used, or will potentially be useful as biomaterials. Owing to their biocompatibility, permeability, and physical characteristics, hydrogels are good candidates as biomaterials for use in many medical applications, including tissue engineering, drug-delivery, biosensors or bioseparation.

(1) Hydrogels may be useful for the manipulation of tissue function or for scaffolds for tissue regeneration or replacement. Regardless of whether they originate from natural sources or are synthetically created, hydrogels used in this area should meet certain design parameters, such as biocompatibility, cell-controlled degradability, and intrinsic cellular interaction, and precisely controlled structures and functions.

(2) The success of hydrogels as delivery systems can be judged by their mechanical strength and response-time in a physiological environment. Fast-responding hydrogels releasing maximal drug in less time while maintaining the structural integrity in a biological system will be the most appreciated delivery systems. Thus, new synthetic methods have been proposed to prepare homo- and co-polymeric hydrogels, especially when they contain temperature- or pH-sensitive pendent groups. These will be used for a wide range of drug, peptide, and protein delivery applications. Either pH-sensitive and/or temperature and specific-molecules (such as glucose or antigens) sensitive hydrogels can be used for site-specific controlled drug delivery.

(3) Biosensors offer an exciting alternative to more traditional methods, allowing rapid "real-time" detection and multiple bimolecular depending on the transducer's properties. On line, real time and *in vivo* measurement is the ultimate application goal of biosensors. There is a huge challenge in applying hydrogels to create biosensors with superior performance for reliable and continuous use. New immobilization schemes and advanced sensing hydrogels are highly desired for improving the analytical capabilities of biosensing devices, and for meeting the challenges posed by complex environmental and clinical samples. In particular, the application of hydrogels in biosensors will bring extraordinary results if the use of novel and promising transducers such as electrochemical luminescence or optoelectronic devices open new scope for the sensitive detection of trace substrates. Miniaturization, microfabrication and multi-sensor arrays are becoming trends in the development of biosensors. In particular, the idea of the biochip has attracted much attention at present.

(4) The use of carbodiimide chemistry in the preparation of hydrogels is advantageous in comparison with conventional crosslinking methods because liquid hydrogel precursors can be delivered and crosslinked to form hydrogels *in situ* in a minimally invasive manner. This process also gives one spatial and temporal control over the conversion of a liquid to a gel, so that complex shapes can be fabricated.

Chapter 3. A Triazine Based Reversible Hydrogel Membrane for Controlling the Delivery of Macromolecules

3.1 Background

In many clinical situations, controlled drug delivery systems - which deliver drugs at a predetermined rate - are replacing conventional drug formulations. However, in the case of diabetes mellitus, there is currently no entirely effectively system for continuously controlling blood glucose levels. The treatment of insulin-dependent diabetes requires the provision of insulin in response to increases in blood glucose concentration. Although a conventional oral route would be preferred, this is not practical for the systemic delivery of peptide and protein drugs, including insulin because the digestive systems destroys them (Hinchcliffe *et al.*, 1999). The consequent required daily injection of insulin may cause discomfort, and can lead to a number of the long-term complications associated with diabetes mellitus such as retinal damage and cardiovascular disease. Therefore, an insulin-delivery system capable of mimicking the pancreas and delivering insulin in response to increases in blood glucose would be highly attractive (Pitt, 1990).

The specific interactions between plant lectins with carbohydrates have been used to study the molecular basis of a range of biological recognition events (Loris *et al.*, 1998, Singh *et al.*, 1999). Such mechanisms have also been evaluated for use in drug delivery systems based on response to chemical and biochemical stimuli, including pH, changes in specific ion concentration and specific molecular recognition events (Qiu *et al.*, 2001). One approach is the development of a self-regulated insulin delivery system based on glucose-sensitive hydrogels capable of regulating the delivery of insulin in response to changes in blood glucose levels. Several such systems have been developed (Galaev *et al.*, 1999; Qiu *et al.*, 2001), including pH-sensitive membrane systems, and two Con A based systems.

In the first approach immobilized Con A is used to control the delivery of a glycosylated insulin, which is initially bound by the Con A. Interaction of environmental glucose with the glycosylated insulin-Con A complex leads to the

displacement of glycosylated insulin (Brownlee *et al.,* 1979). A more recent approach has been the use of Con A/dextran mixtures to form a reversible sol-gel system (Obaidat *et al.,* 1997; Taylor *et al.,* 1995; Tanna *et al.,* 1999). In this system, a glucose-based polymer is mixed with con A to form a sol-gel, which is sandwiched between two porous membranes (Taylor *et al.,* 1995; Obaidat *et al.,* 1997, Tanna *et al.,* 1999). Gelation is reversible in response to changes in environmental glucose concentration such that the diffusion coefficient for insulin changes with degree of gelation. In earlier work, the gels were based solely on soluble components. However, leakage of Con A which is toxic through the membrane during gel-sol transition led to revised systems with Con A coupled to the polymer.

While reducing leakage, coupling of Con A to the polymer still results in a system that is in a soluble form in the presence of glucose (Tanna *et al.,* 1999, Kim *et al.,* 2001). Thus, support membranes are still required, leading to increased complexity and slow diffusion rates. To overcome these problems this chapter investigates the synthesis of a mechanically stable, glucose responsive hydrogel membrane, which can be cast in a number of mechanical forms.

The polymer is produced by crosslinking two dextrans with different molecular weights. The smaller dextran is functionalized with covalently grafted Con A. This material is mixed with the larger, nonfunctionalized dextran, allowing easy control of the overall concentration of grafted Con A in the material. The affinity of Con A for dextran provides additional affinity crosslinks which are competitively inhibited by free glucose, resulting in a decrease in total cross-link density and increase in permeability to protein.

This is conceptually similar to the work of Miyata *et al.,* (1999), who describe an antibody/antigen based gel that swells in response to the free antigen. However, the use of the two dextran species allows greater control over the gel structure such that property changes can be restricted to changes in internal porosity. In this case the porosity increases because of the displacement of con A/dextran interactions by the stimulus of soluble D-glucose. The principle of operation can be summarized using a simple schematic diagram (Figure 3.1).

To achieve this goal, gels were formed via a nucleophilic displacement reaction with a triazine ring, such that both gel formation and Con A fixation occur in the same step of synthesis. A specific requirement of gel synthesis was to maintain the reaction pH below 9 to minimize Con A inactivation during coupling. The results presented here, demonstrate a material that is mechanically stable, changes permeability in response to changes in glucose concentration, and that shows negligible Con A leakage over extended periods.

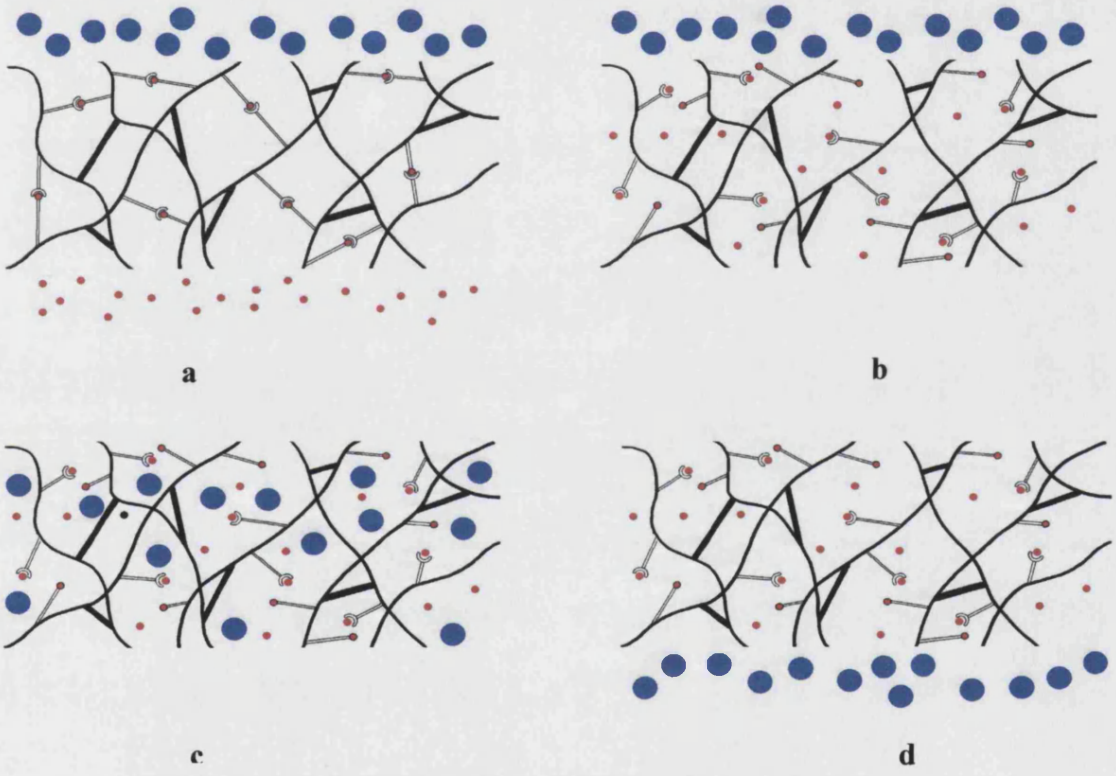

Figure 3.1 Schematic of the composite hydrogel (bold lines denote covalent links)

a) Gel porosity reduced by affinity cross-links that exclude large molecules, e.g. insulin. ●

b) Glucose • diffuses in and competitively displaces affinity cross-links.

c) Insulin is able to diffuse into the more highly porous gel.

d) Insulin diffuses through the gel providing that the concentration gradient and the glucose concentration is maintained.

3.2 Materials and methods

3.2.1 Materials

Dextran 40,000(MW), dextran 500,000(MW), divinyl sulfone, ethylenediamine.2HCl, cyanuric chloride, concanavalin A (type IV from the jack bean), insulin, lysozyme and BSA were obtained from from Sigma-Aldrich, UK. All other chemicals were of reagent grade and obtained from BDH chemicals Ltd., UK.

3.2.2 Gel synthesis

The chemistry of hydrogel synthesis is shown in Figure 3.2.

The procedure was as follows:

1) 10 g dextran was dissolved in 150 ml water, 0.795 g Na_2CO_3 was added, followed by the addition of 1.2 ml 97% divinyl sulfone. This was allowed to react at 18°C for 60 minutes, prior to the addition of 2.74 g ethylenediamine.2HCl. The reaction was then allowed to proceed for 48 hours after which the reaction mixture was dialyzed extensively against distilled water. The final dextran derivative solution was freeze-dried and then redisolved in distilled water to give a 14% dextran solution.

2) 20 ml solution of the dextran derivative was mixed with 0.17 g cyanuric chloride and allowed to react at room temperature for 24 hours. The solution was centrifuged for 20 minutes at 4000 rpm at 4°C, and the supernatant was recovered.

(The dextran derivative made using the procedure above with a 40,000 MW dextran will be referred to as Solution A; the dextran derivative made using 500,000 MW dextran will be referred to as Solution B.)

3) 0.8 g of Solution A, 0.8 g of Solution B, 0.5 ml 0.8M $NaHCO_3$ and 40 mg Con A (in 1.2 ml water) containing 1 mg $CaCl_2$ and 1.2 mg $MnCl_2$ were added and mixed fully. After mixing for 10 minutes, the solution was de-gassed and cast on a nylon gauze support (pore size 0.1 mm, thickness of 0.05 mm) between two glass plates using spacers to give the required total membrane thickness.

Gelation was allowed to proceed at 25°C for 16 hours before the membrane was removed from the casting plates. The membrane was washed twice in distilled water and immersed overnight in 10 mM glycine solution in 20 mM acetate buffer, pH 6.0, containing 50 mM NaCl and 0.1% NaN_3 at 4°C. Finally the gel was washed with distilled water twice and stored in 20 mM Tris buffer, pH 7.4, containing 1 mM $CaCl_2$, 1mM $MnCl_2$, 50 mM NaCl and 0.1% NaN_3, until it was used.

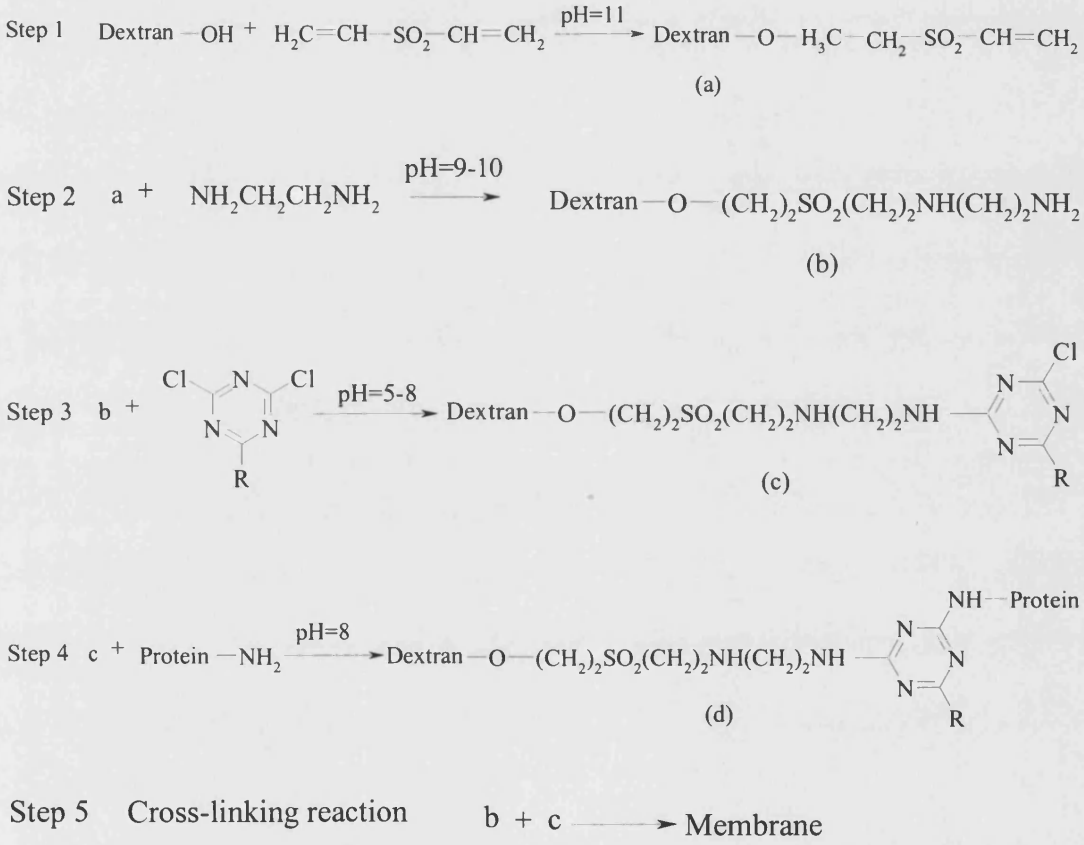

Figure 3.2: The principle of smart membrane synthesis

3.2.3 Protein diffusion experiments

The diffusion of model proteins (including insulin: mw 5800, lysozyme: mw 12400, and BSA: mw 66000) through the gel membranes was examined in a diffusion cell consisting of donor and receptor chambers with equal volume (4.4 ml), and with a surface area of 4.6 cm^2 available for diffusion. The gel membrane was mounted between the two chambers of the diffusion cell as shown in Figure 3.3, and

equilibrated with 20 mM Tris storage buffer as above. The donor chamber was connected to a protein reservoir through a pump. The receptor chamber was connected via a closed loop recycle through a flow cell mounted in the spectrophotometer (Shimadzu, UV-1601). The diffusion of the protein was continuously measured from absorbance changes at 280nm logged to a computer. The effect of putative transport-enhancing agents was investigated by varying the composition of the donor buffer such that protein concentration remained constant.

For the experiments with insulin, the protein (from Bovine Pancreas, Sigma) was dissolved in a small amount of 0.05 N HCl and then adjusted at pH 7.4 with 0.05 N NaOH, and finally diluted with Tris buffer to give an insulin concentration of 2.0 mg/ml. In all experiments using insulin, urea was added to a final concentration of 2.0mg/ml to inhibit insulin aggregation (Sato *et al.,* 1983). Concentration-time courses were determined from absorbance changes using a conversion factor determined from a standard curve constructed using known insulin concentrations. For experiments with lysozyme and BSA, the proteins were dissolved directly in Tris buffer to a concentration of 2.0 mg/ml. In each case the concentrations observed in the diffusion experiments were determined using calibration data from standard curves prepared using the specific protein. To evalute the diffusivity of protein across membrane, the following equation was employed:

$$D = \frac{V \times \delta}{A \times C} \times J$$

D	$diffusivity(cm^2 s^{-1})$
V	$chamber\ \ volumer(ml)$
δ	$membrane\ \ thickness\ \ (cm)$
A	$membrane\ \ area\ \ (cm^2)$
C	$concentration\ of\ donor\ chamber\ (mg/ml)$
J	$diffusion\ \ rate\ (mg/ml.\mathrm{sec}ond)$

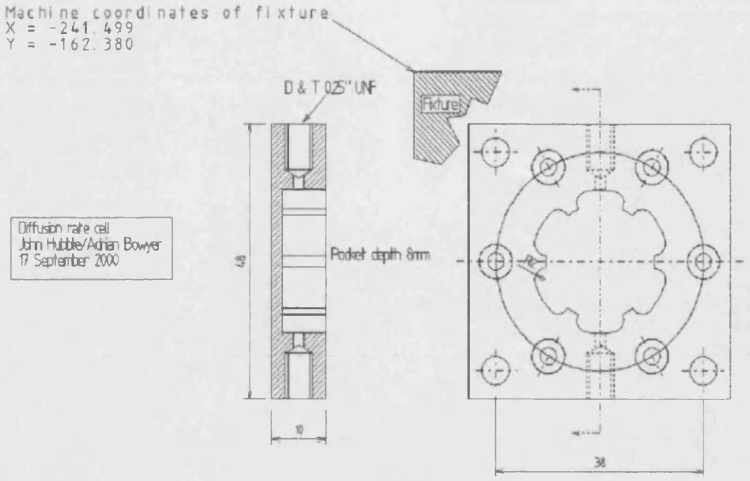

(A)

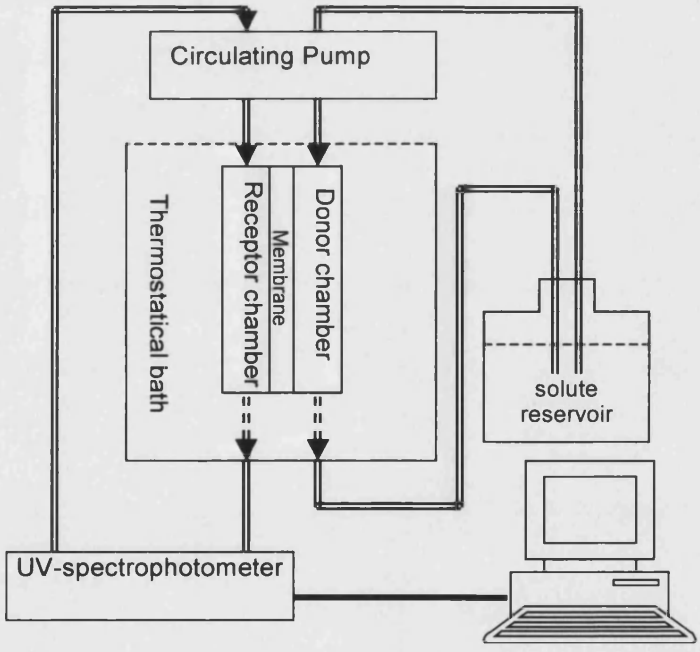

(B)

Figure 3.3: Diffusion test rig. (A) Geometry of the chambers (B) Experimental set-ups for diffusion studies with pump speed at 2mg/min, membrane surface as 4.6 cm^2, chambers' volume as 4.4 ml, and the volume of solute reservoir as 50 ml.

3.3 Results

3.3.1 Specificity assessment

The specificity of the hydrogel membrane was determined using D-glucose, L-glucose, and glycerol. While D-glucose is specifically bound by Con A, L-glucose and glycerol are not. Hence membrane permeability changes would be expected in response to D-glucose, but not L-glucose or glycerol. Figure 3.4 shows the diffusion curves of insulin in response to glucose, L-glucose and glycerol through a 0.4mm membrane. In control experiments, where insulin solution without carbohydrate a glycerol was used, little diffusion was observed. When L-glucose or glycerol was added to the protein reservoir of the donor side (final concentration 0.1 M), there was a small increase in the diffusion rate in the initial stages, after which the profile mirrored that observed for the control. After a stabilizing period of 42 minutes D-glucose (0.1 M) was added. Then, after a lag of about a further 18 minutes, there was a substantial increase in diffusion rate which was maintained for an extended period. The lag between addition and response matches the residence time in the donor cell such that diffusion limitations will be partially masked by the time course of D-glucose increase in the liquid phase.

The results show that the hydrogel membrane allows protein transport at a rate that is controllable using a soluble effector molecule, and that this effect is limited to molecules recognized by the Con A receptor. This suggests that, as anticipated, changes in porosity of the membrane where dextran serves as both a ligand for Con A affinity and a structural matrix results from a reduction of internal affinity cross links when a soluble competitor is introduced. It is also implicit in this result that a significant fraction of the total Con A is not inactivated during membrane synthesis.

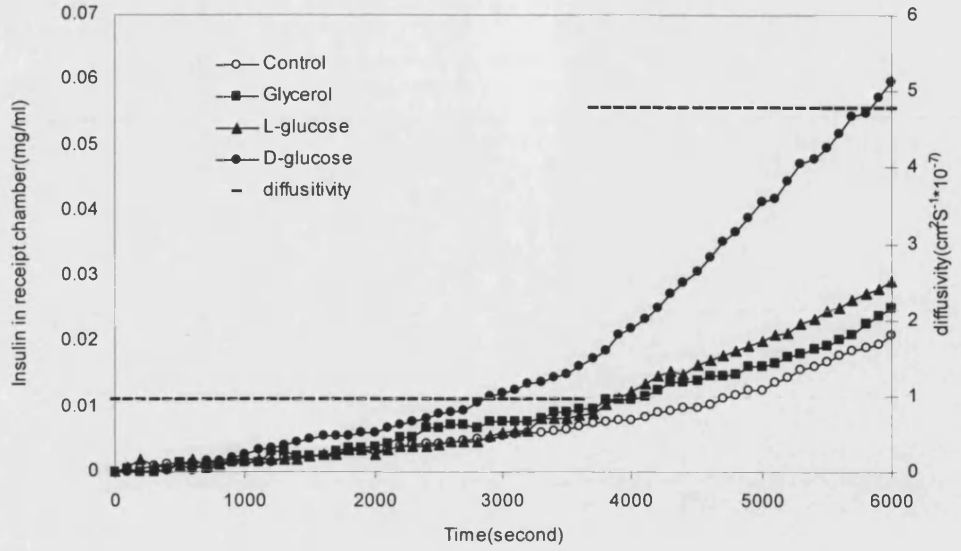

Figure. 3.4: Diffusion curves in response to 0.1M D-glucose (•), glycerol (■), and L-glucose (▲) with respect to the diffusion of Insulin (2 mg/ml). The control was carried out with insulin only (○). Putative activators were added at 2500s. The assay was conducted at 20°C.

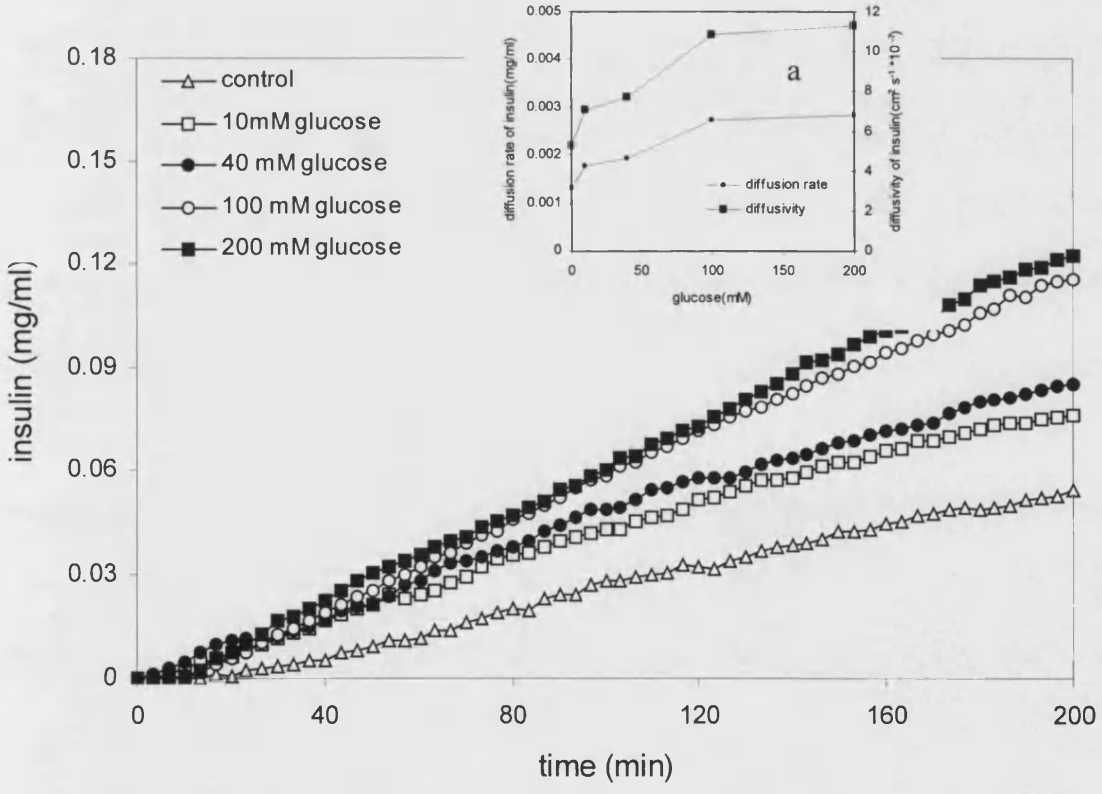

Figure. 3.5: Diffusion curves for insulin with respect to D-glucose concentration: 0 mM (control, Δ), 10 mM (□), 40 mM (•), 100 mM (○) and 200 mM (■). Insulin concentration was 2.0 mg/ml; insulin and/or glucose solution was added in the donor reservoir. Temperature at 25°C. Fig. 3.5a (inset) shows the rate of diffusion as a function of D-glucose concentration.

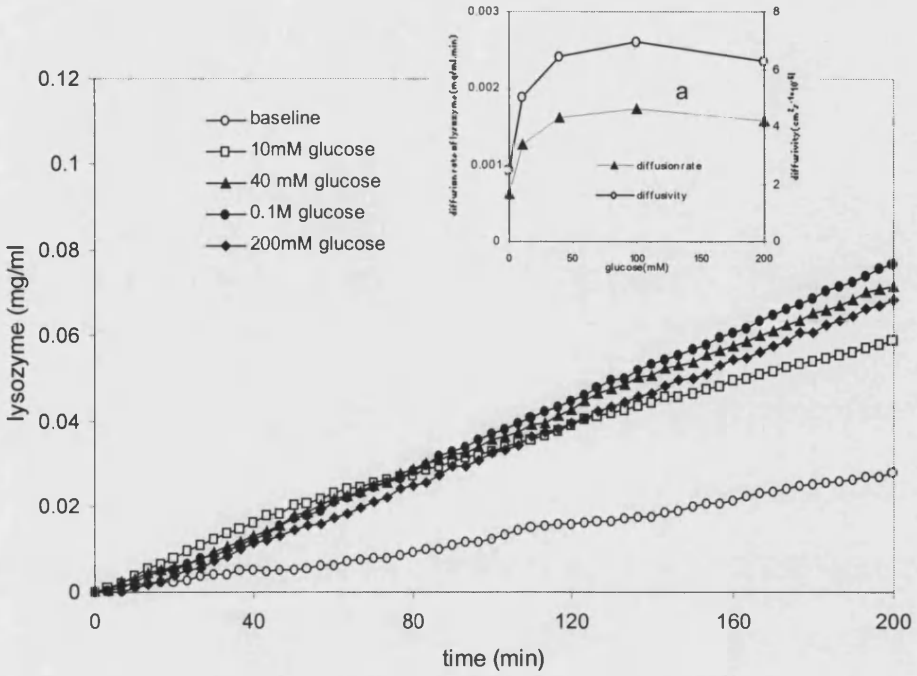

Figure. 3.6: Diffusion of lysozyme (conditions as for Figure 3.5). Fig. 3.6a (inset) shows the rate of diffusion as a function of D-glucose concentration. Temperature at 25°C.

3.3.2 Effect of D-glucose concentration

Three proteins of different molecular sizes, insulin, lysozyme and BSA, were used to examine the effect of glucose concentration on diffusion rates. Figure 3.5 shows the diffusion of insulin in response to changes in glucose concentrations over the range 0-200mM. In these experiments, membranes were pre-incubated with protein (2mg/ml with or without glucose) in the donor side of the cell to minimize subsequent lag times. The diffusion rates obtained as a function of glucose concentration are shown in Figure 3.5a.

These experiments were repeated with two progressively larger proteins. Studies with lysozyme gave essentially similar results (Figure 3.6). As might be expected from the higher molecular weight the diffusion in the absence of glucose was lower than that observed for insulin. However, glucose has a more pronounced effect on diffusion rates at low concentrations and shows a lower saturation value than that observed with insulin (Figure 3.6a). Results obtained with BSA are shown in Figure 3.7. Again diffusion is sensitive to changes in glucose concentration, with 100 mM glucose leading to a 3.5-fold increase in the rate of BSA diffusion. BSA diffusion in response to glucose is shown in Figure 3.7a.

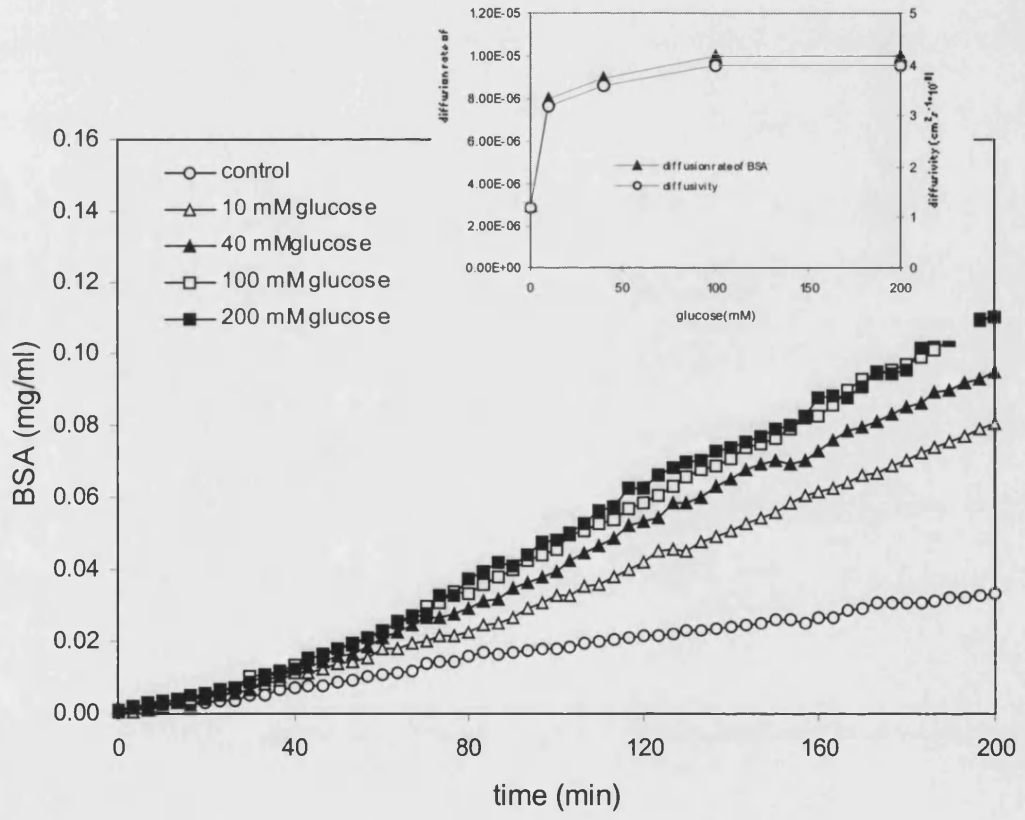

Figure. 3.7: Diffusion of bovine serum albumin (conditions as for Figure 3.5) Fig. 3.7a (inset) shows the rate of diffusion as a function of D-glucose concentration. Temperature at 25°C.

3.3.3 Reversibility of D-glucose effects

A series of experiments was conducted with each of the test proteins in which two reservoir solutions were used alternately: protein, and then protein containing 0.1 M

glucose. Results for insulin are shown in Figure 3.8. The donor solution was sequentially switched between glucose-containing and non-glucose-containing solutions as indicated by arrows on the plot. The response shows that, while there is a diffusion time lag between each solution change, the introduction and removal of glucose causes a reversible switch between lower and higher diffusion rates. Similar results obtained for lysozyme are shown in Figure 3.9, and for BSA in Figure 3.10. Again, the reversibility of the glucose effect on diffusion rate is clearly demonstrated.

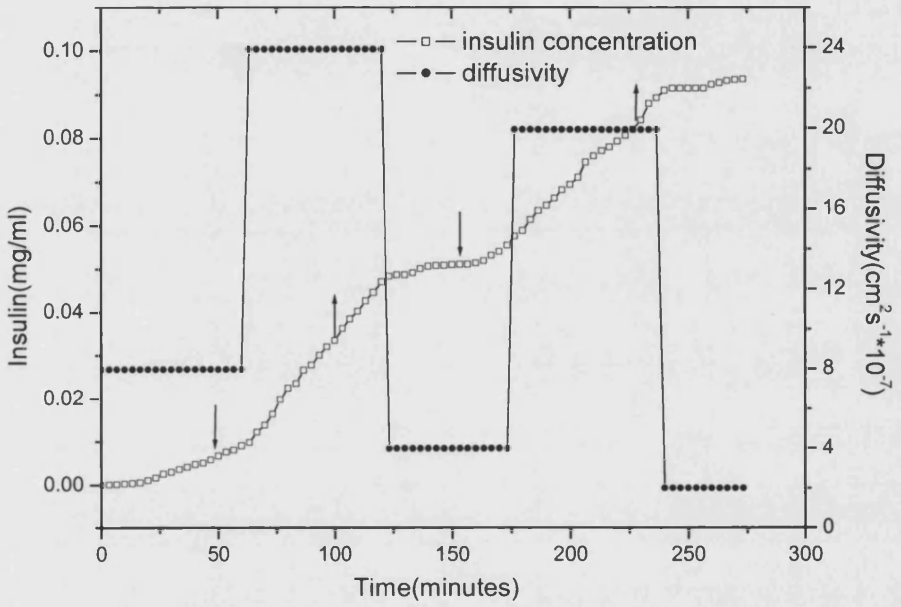

Figure. 3.8: Reversibility of insulin diffusion in response to changes in D-glucose. 0.1 M D-glucose plus insulin (2.0 mg/ml) buffer was added at the down-arrows. Insulin solution without glucose was restored at the up-arrows. Diffusivity calculation was described in Chapter 3 (page 57). Temperature is 25°C.

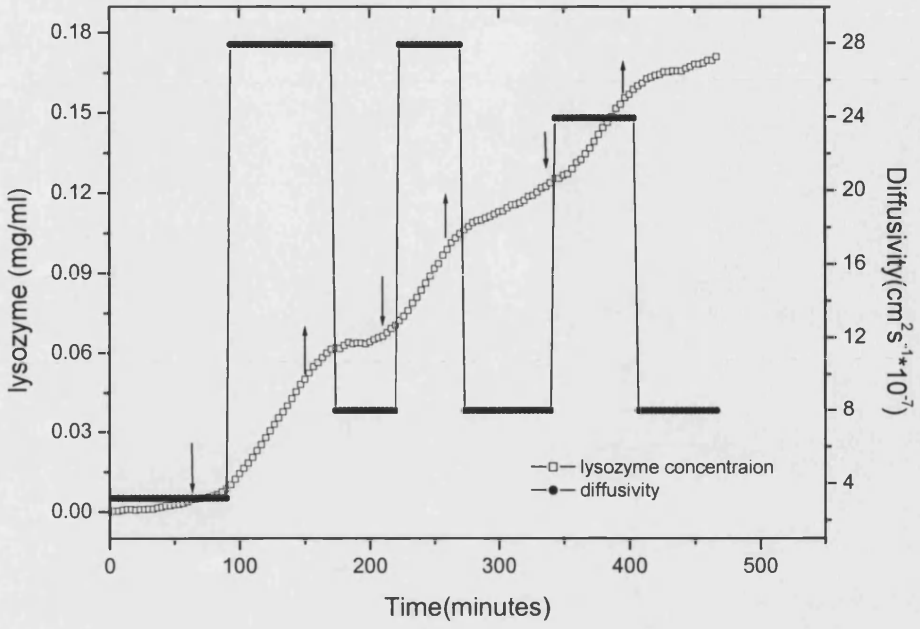

Figure. 3.9: Reversibility of lysozyme diffusion in response to changes in D-glucose. 0.1 M D-glucose plus lysozyme (2.0 mg/ml) buffer was added at the down-arrows. Lysozyme solution without glucose was restored at the up-arrows. . Diffusivity calculation was described in Chapter 3 (page 57). Temperature 25°C.

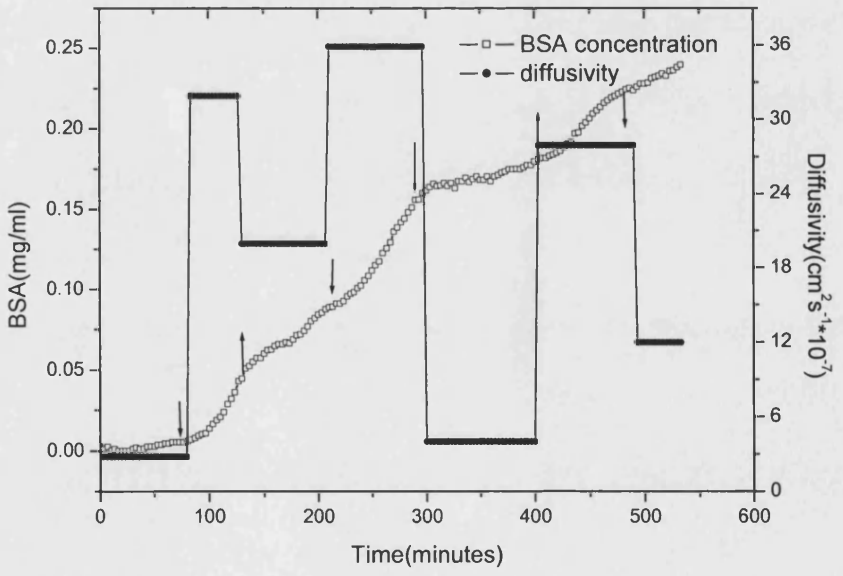

Figure. 3.10: Reversibility of bovine serum albumin diffusion in response to changes in D-glucose. 0.1 M D-glucose plus BSA (2.0 mg/ml) buffer was added at the down-arrows. BSA solution without glucose was restored at the up-arrows. Diffusivity calculation was described in Chapter 3 (page 57). Temperature 25°C.

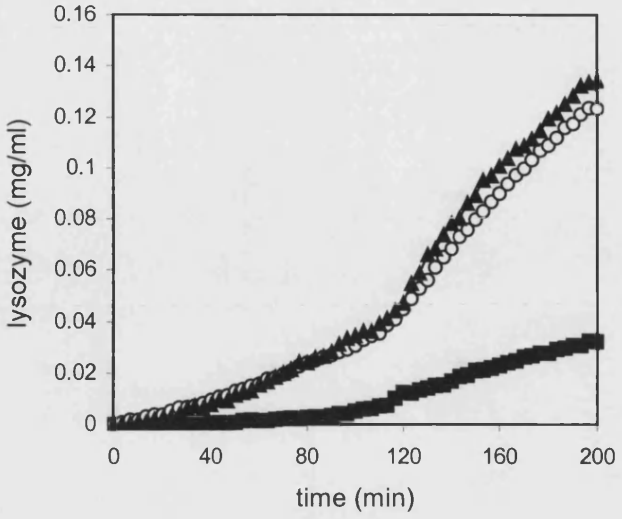

Figure. 3.11a: Effects of temperature on the diffusion of lysozyme (2.0 mg/ml). 0.1 M D-glucose was added to the donor reservoir at 100 min. Temperatures 5°C (■), 25°C (○), and 37°C (▲).

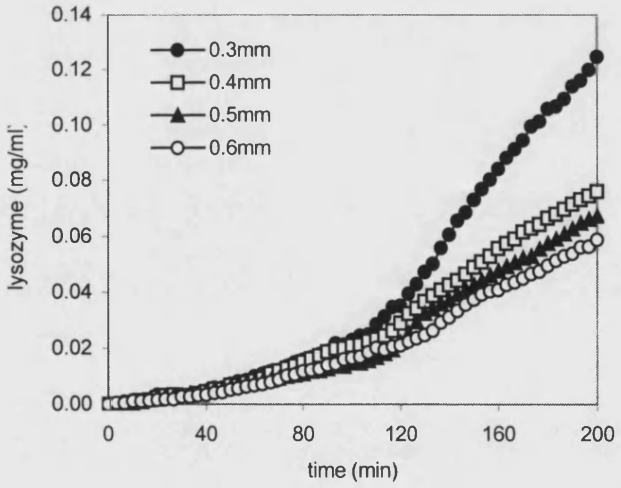

Figure. 3.11b: Effects of membrane thickness on the diffusion rate of lysozyme (2 mg/ml). D-glucose (0.1 M) was added to the donor reservoir at 100min. Temperature 25°C.

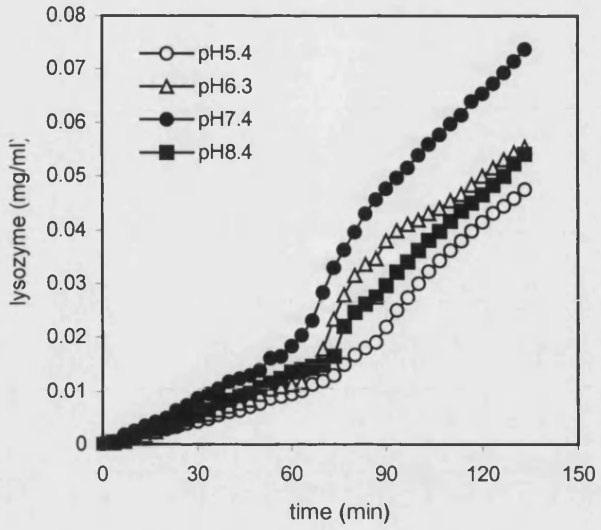

Figure. 3.11c: Effects of pH on the diffusion rate of lysozyme (2 mg/ml). D-glucose (0.1 M) was added to the donor reservoir at 50 min. Temperature 25°C.

3.3.4 Temperature, pH and membrane thickness effects

Diffusion experiments were conducted using a 0.4mm membrane at 5 °C, 25 °C and 37°C using lysozyme as the test protein. Glucose was introduced after 100 minutes. Results shown in Figure 3.11a confirm that diffusion rates increase with temperature between 5 °C and 25 °C, but that little additional increase is observed between 25-37 °C. It would appear that there is a slightly greater effect on specific transport compared with the non-specific component.

Experiments with different gel thickness (Figure 3.11b) show that diffusion rate decreases with increasing membrane thickness, as expected from Fick's law. More importantly, the fractional increase in diffusion rate obtained when glucose is introduced appears inversely proportional to membrane thickness.

Figure 3.11c shows pH effects over the range 5.4-8.4. This shows an optimum response at pH 7.4.

3.4 Discussion

In undertaking this project, the goal was to produce a chemically and mechanically stable membrane capable of specific permeability changes in response to concentration changes in external metabolites. While generic in scope, the initial

application envisaged was the controlled release of insulin in response to D-glucose concentration.

Experiments to assess the mechanical stability of pre-cast membranes showed no evidence of dissolution over a 1-week incubation period in storage buffer. Assays of buffer composition showed no evidence of Con A leakage during this period.

The first phase of characterization studies aimed to establish (i) that permeability as evidence by protein diffusion could change in response to concentration changes in D-glucose concentration and (ii) that this effect was specific. The results presented in Figure 3.4 confirm that this is the case. While it is apparent that the porosity of the gel does not totally exclude insulin, the addition of D-glucose results in a 3-fold increase in diffusion rate. While there is a very slight increase observed with the addition of L-glucose and glycerol this probably results from a non-specific chemical effect modifying the degree of gel swelling.

Similar experiments with a hydrogel membrane synthesized with BSA instead of Con A failed to show any significant increase in diffusion when glucose was applied. This confirms that changes in the porosity of the gel membrane resulting from the dissociation of affinity crosslinks lead to changes in protein diffusion. Previous reports (Ballerstadt *et al.,* 1998; Miyata *et al.,* 1999), suggest the diffusion of glucose through hydrogels will be slower than the dissociation of Con A/dextran affinity crosslinks. As proteins have lower diffusivities than sugars, the response will be determined by the diffusivity of the protein in the dissociated gel membrane. Similar specific increases in diffusion rate were observed with mannose, which is also known to bind to Con A.

The effect of D-glucose concentration on the diffusion of three different sized proteins is shown in Figures 3.5, 3.6 and 3.7. The inset figures show transport rate as a function of D-glucose concentration, and indicate a half-saturation constant between 40-60mM. This is consistent with the displacement of a weak affinity interaction. As the size of the protein increases, the ratio of competitor induced to background diffusion also increases. This suggests that, in addition to optimising the base level of

affinity plus covalent crosslinks to ensure zero background diffusion, porosity should also be optimised with respect to maximizing competitor-induced transport.

As the goal was to make a responsive material suitable for drug delivery applications, reversibility of the selective response is an essential requirement. The results reported in Figures 3.8, 3.9 and 3.10, where D-glucose was sequentially added and removed, clearly show that the con-A/dextran membrane meets this requirement. Reversible responses were found with all three proteins tested.

The affinity displacement of an interaction between Con A and an immobilized ligand is clearly attractive for an insulin delivery application, but it also has the specific advantage that the displaced ligand also forms part of the gel matrix. However, in the two-component synthesis protocol described here, the larger dextran might be regarded as acting as the matrix and the smaller, pendant, dextran as the ligand. In an analogous system, Miyata *et al.,* (1999) report the synthesis of an antigen-antibody hydrogel membrane where goat anti-rabbit IgG and rabbit IgG were coupled to N-succinimidylacrylate separately, and then co-polymerised with acrylamide to form a hydrogel. This gel also showed a reversible response to the environmental addition of rabbit IgG, suggesting that it should be possible to develop responsive polymers for a range of solute delivery applications.

3.5 Conclusions

Dextran/Con A hydrogel membranes can be synthesized that are capable of releasing insulin in a dose-dependent response to changes in D-glucose concentrations. The response observed is selective to sugars that are bound by Con A and is repeatable and reversible. Figures 3.6, 3.7 and 3.8 suggest a lag time of approximately 40 minutes between point of insulin introduction and increase in transport rate. While this could be improved if thinner membranes were used it compares favourably with the figure 30-120 minutes reported by Lembert et al. (2001) for insulin release by free-floating islets. Unlike sol-gel systems, the membrane described here retains structural integrity in the presence of elevated D-glucose concentrations and needs no additional external membrane containment. The synthesis protocol I report can be extended to

allow the attachment of ligands as well as receptors to an inert support. This would allow the formation of responsive gels based on a range of ligand-receptor interactions.

Chapter 4. A CM-dextran based Reversible Hydrogel Membrane for Controlling the Delivery of Macromolecules

4.1 Introduction

An ideal drug delivery system should be capable of adjusting delivery rate to match a time-varying level of demand. To meet this ideal, closed-loop delivery systems have been developed that are self-regulating i.e. they respond to changes in the local environment, such as the presence or absence of a specific molecule (Sershen *et al.*, 2002). A prominent application of this approach is development of systems that can autonomously release insulin in response to changes in monitored blood glucose levels.

An alternative approach for controlling the delivery of insulin is based on competitive binding (Miyata *et al.*, 2002). Mixtures of the plant lectin concanavalin A with specific polysaccharides can biospecifically interact in a reversible gelation process that can be used to control the release process (Goldstein *et al.*, 1965, 1973, 1976). There have been two separate approaches to utilizing this effect.

The first involves the preparation of glycosylated insulin, which can bind to concanavalin A and be competitively displaced by free glucose (Brownlee *et al.*, 1979). The displacement of glycosylated insulin from Con A was found to be proportional to the external glucose concentration. A similar approach was development by Kim and coworkers, using a polymeric membrane permeable to glucose and glycosylated insulin and nonpermeable to Con A (Kim *et al.*, 1994, Liu *et al.*, 1997). Control of the binding constants of glycosylated insulin derivatives to concanavalin A allowed control of the response to external glucose levels. While this approach is highly elegant, the requirement for chemically-modified insulin increases cost and could potentially modify the therapeutic response.

The alternative approach uses a glucose-containing polymer and glucose receptor molecules to prepare glucose-sensitive hydrogel systems. Taylor (Taylor, 1993) proposed a system where the concanavalin-A is mixed with polysaccharides such as polysucrose (Taylor *et al.*, 1994, 1995), dextran (Tanna *et al.*, 1994, 1997, 1998), and

glycogen (Tanna *et al.*, 1998, 1999). Biospecific binding between Con A and polysaccharide lead to the formation of a gel which changes its viscosity in response to free glucose concentration, thus providing the switch for controlling the insulin diffusion rate. The release mechanism is thus repeatable, releasing insulin in response to a number of free glucose fluctuations, in a manner that mimics the in vivo feedback mechanism of pancreatic cells. A problem encountered in these studies was the significant leakage of concanavalin A during the low viscosity phases. In a more recent refinement to reduce leakage, concanavalin A was first covalently bonded to carboxylic moieties on Carbopol 934P NF and 941P NF using carbodiimide chemistry before mixing these with dextran to produce a glucose-sensitive formulation that still shows a transformation from gel to sol in the presence of free glucose (Tanna *et al.*, 2002).

Park and coworkers (Lee *et al.*, 1994, Obaidat *et al.*, 1996, 1997) used a similar approach to show that polymer-bound glucose and Con A could form a gel capable of reversible gel-sol transition for the regulation of insulin release. In this case, mixing glucose-containing polymers with Con A formed the gel. Glucose containing polymer chains were synthesized by co-polymerizing allyl glucose and acrylamide or vinylpyrrolidone. The glucose-sensitive hydrogel layer was sandwiched between porous poly[hydroxyethyl methacrylate] membranes. Although this system controlled the release of insulin in response glucose concentration, its response time may be too slow for therapeutic applications. In addition differences in the diffusion rate of insulin and glucose through the porous membrane can make control difficult.

To overcome these problems we have developed the synthesis of a mechanically stable, glucose responsive hydrogel membrane (chapter3), based on copolymerising Con A with two dextrans of different molecular weights (Tang *et al.*, 2003). The larger species was used to provide structural support, while the second smaller species, to which the Con A was coupled, provided the necessary internal flexibility. This is conceptually similar to the work of Miyata *et al.* (1999), who describe an antibody/antigen based gel that swells in response to free antigen.

This hydrogel demonstrated mechanical stability, changed permeability in response to changes in glucose concentration, and showed negligible Con A leakage over

extended periods. However, its major drawback for use in biomedical application is the presence of the cytotoxic triazine moiety.

To overcome these problems a novel synthesis has been developed for the fabrication of a pH-responsive dextran hydrogel. This is based on the intermolecular cross-linking of carboxymethyl dextran (CM-dextran) using 1-Ethyl-(3-3-dimethylaminopropyl) carbodiimide hydrochloride (EDC) and N-hydroxysuccinimide (NHS). EDC was used as it is not incorporated into the cross-linked structure, but is simply changed to a water-soluble urea derivative as the reaction proceeds. The cytotoxity of the urea derivative has been found to be quite low compared with that of EDC (Benslimane *et al.,* 1988) as shown by the work of Ikada et al (Tomihata *et al.,* 1997) who synthesised an uncharged hydrogel for tissue engineering applications using EDC crosslinking of hyaluronic acid. We also demonstrated that the CM-dextran hydrogel from this method could be used as a support for the attachment and maintenance of primary human dermal fibroblast cultures as study in Chapter 7 described later.

The main aim of this chapter is to demonstrate that a novel D-glucose sensitive hydrogel membrane can be produced using this approach i.e. by incorporated concanavalin A into a CM-dextran hydrogel network using carbodiimide chemistry such that the protein, distributed throughout the hydrogel, can reversibly modify its permeability in response to changes in environmental D-glucose.

4.2 Materials and methods

4.2.1 Materials

Dextran and lysozyme were obtained from Sigma-Aldrich, UK. All other chemicals were of reagent grade and obtained from Lancaster Synthesis Ltd., UK.

4.2.2 Hydrogel preparation

The reaction, utilizing carbodiimide chemistry, catalyses the formation of amide bonds between carboxylic acids or phosphates and amines by activating carboxyl to form an O-urea derivative. This derivative reacts readily with nucleophiles (Figure 4.1). The reagent can be used to make ether links from alcohol groups, ester links

from acids and alcohols or phenols, and peptide bonds from acids and amines (Tedder *et al.,* 1972). The water-soluble derivative EDC can then be used to synthesise peptide bonds using NHS (Grabarek *et al.,* 1990). The reaction includes formation of the intermediate active ester (the product of condensation of the carboxylic group and N-hydroxysuccinimide) that further reacts with the amine function finally to yield the amide bond.

Various degrees of carboxylic substitution in CM-dextran were obtained by adjusting the reaction time. 5 g 480KD dextran was dissolved in 75ml distilled water, followed by the addition of 5-g sodium chloroacetate. The carboxymethylation reaction was initiated by the addition of 25 ml of 8 M NaOH. The reaction mixture was diluted to a total volume of 100-ml. Carboxymethylation was allowed to proceed for different times at 50°C with stirring. At the required time, the reaction was terminated by lowering the solution pH to 7 with 6 M HCl. The products were then precipitated with 300 ml absolute ethanol and allowed to stand overnight. The sediments was dissolved using distilled water solution and then dialysed extensively for two days. The dialysed solution was rapidly frozen using liquid nitrogen and then lyophilized to give a white power.

The carboxymethylation reactions were run for 15 minutes. The degree of COOH substitution in the CM-dextrans was calculated by acid titration. The target ratio of COOH groups per dextran was 1-COOH:65glucose residues.

An unknown concentration of CM-dextran is neutralized and quantified with a known volume and concentration of NaOH determine the concentration of CM-dextran with a indicator which changes colour.

Equation 1 can produce the molar amount of COOH in 1 g CM-dextran, and equation 2 transfer the unit to COOH/Glucose assuming the glucose' MW in CM-dextran is 180.

(1) $$C = COOH\ Mol \Big/ (CM - dextran)g = \frac{(NaOH\ amount) \times (NaOH\ concentration)}{(sample\ volume) \times (sample\ concentration)}$$

(2) $$one\ COOH/glucose\ amount = 180 \times C : 1$$

Example:

Sample amount	10 mM NaOH amount	COOH Mol/g(CM-Dextran)	Each COOH/glucose amount
25ml 2.602mg/ml	2.1ml	3.228e-4	1COOH/17
25ml 2.602mg/ml	3.2ml	4.919e-4	1COOH/11

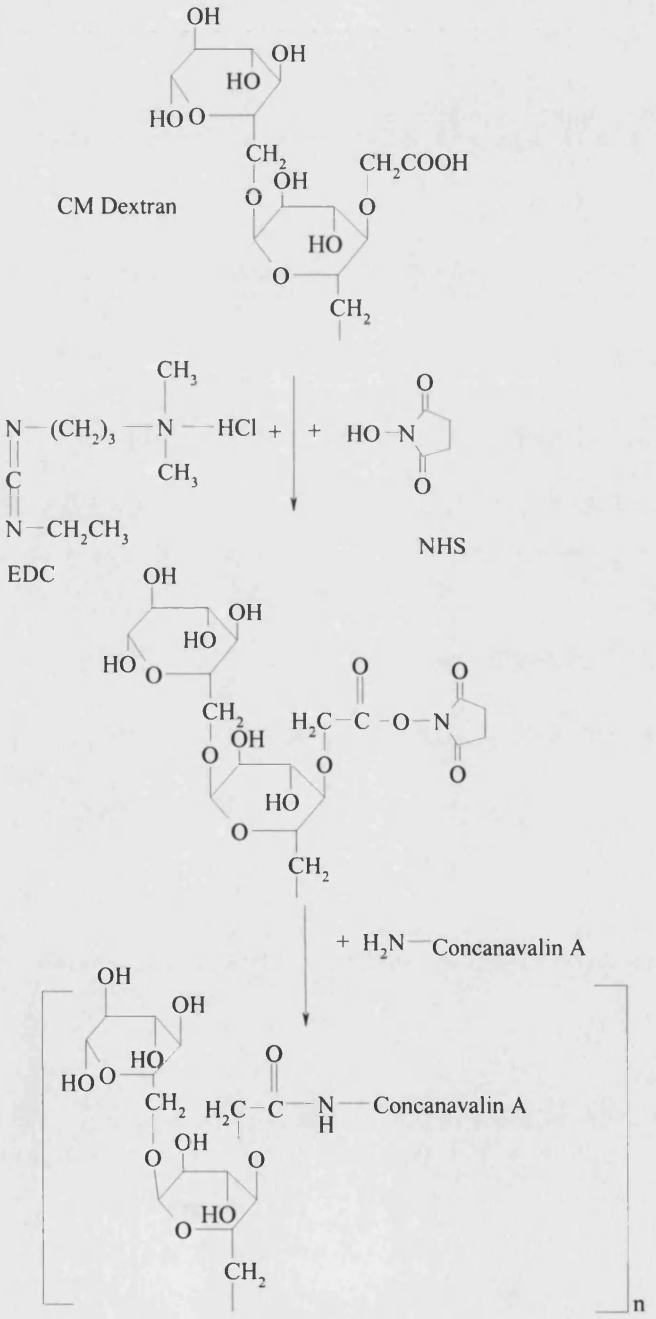

(a)

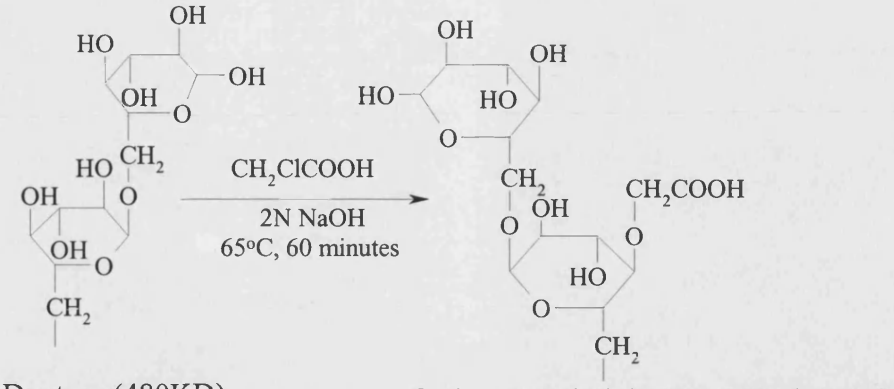

(b)

Figure 4.1: The chemistry of Concanavalin A hydrogel preparation based on carbodiimide chemistry (a) or CM-dextran (b)

To fabricate the Con A hydrogel, 1 g CM-dextran was dissolved using 4.2ml distilled water, with stirring causing the resulting solution to be degassed. 210mg EDC and 30mg NHS were dissolved in 1.5 ml distilled water, added to the CM-dextran solution, and stirred for 10 minutes. 130mg Con A dissolved in 3.0ml distilled water containing trace ions was then added. The solution started to gel after 30 minutes at which point it could be cast as required (in this case onto a nylon gauze support, pore size 0.1 mm, thickness of 0.5 mm mounted between two glass plates using spacers to give the required total membrane thickness).

4.2.3 physicochemical properties of the hydrogel

Infrared spectroscopy samples taken at different stages of the reaction sequence were performed using a Bruker-equinox 55 FT-IR spectrometer. Freeze-dried samples were mixed with potassium bromide powder and pressed into tablets under vacuum. For each sample 100 scans were recorded from 4000 to 400 cm^{-1} at a resolution of 2 cm^{-1}.

4.2.4 Hydrogel morphology

The morphology of the hydrogel under different conditions was examined using a Jeol 6310 scanning electron microscope (SEM) equipped with a cryo-stage and energy-dispersive X-ray (EDX). Samples of hydrogel were clamped between two pieces of metal sheet, rapidly frozen in liquid nitrogen and then introduced into the SEM

chamber pre-cooled to a temperature of ca. –160 °C. The stage was then heated to a temperature of ca-80 °C to sublime the surface water. After cooling to –160 °C, the sample was gold-sputtered for 3 minutes. Samples were scanned at a magnification of 10000.

4.2.5 Characterisation of binding interactions

The binding properties of Con A towards glucose, dextran and derivativised dextran were studied using Isothermal Titration Calorimetry (ITC) in an OMEGA ITC (Microcal Ltd). The instrument was calibrated and experiments conducted in accordance with the manufacturer's operating instructions.

Before use, Con A was dissolved in and dialysed against 20 mM Tris buffer pH 7.4 containing 0.5mM $CaCl_2$, 0.5 mM $MnCl_2$, 0.5 mM $MgCl_2$, 150 mM NaCl, and 0.02% NaN_3 at 4 °C, filtered with PVD/PE syringe filters and the monomer concentration (MW:27 KD) adjusted to 0.092 mM. Titrant sugar samples of D-glucose, dextran (MW: 15KD), and L-glucose were diluted to a final concentration of 27.8 mM (dextran concentration expressed in terms of glucose monomer). Titrations were run at 20 °C and all the samples degassed at 15°C prior to use. In each case 54 injections of 5 µl of sugar solution were automatically added at 2 minute intervals into the lectin solution stirred at 300 rpm. The heat evolved after each injection was measured by the cell's feedback network as differential heat effects between the sample and reference cells.

In the case of Con A grafted CM-dextran(12KD), prepared as described above, the conjugation concentration of Con A-CM-dextran was determined using optical density measurements against a Con A standard curve.

In addition to direct binding measurements, the competitive displacement of bound dextran using monosaccharides was also studied. Con A or Con A in conjugation with CM-dextran was firstly mixed with dextran (MW: 15KD) and then titrated with D-glucose of 27.8 mM. The concentration of Con A, Con A conjugation with CM-dextran, and dextran was 0.092, 0.146, and 0.139 mM respectively in the finial samples used in the ITC experiments.

In all cases control experiments were carried out using identical sugar injections into a cell containing buffer without protein, and relative heats of dilution and mixing were subtracted from the heats of binding relative to the real titration experiment.

Final experimental results, represented by heat developed versus cell ligand/lectin ratio, were fitted to one-binding-site-per-monomer models using Origin ITC Data Analysis Software (Microcal Ltd).

4.2.6 Protein diffusion experiments

Trans-membrane protein diffusion was investigated using lysozyme as the test molecule. Experiments were conducted in a diffusion cell consisting of donor and receptor chambers of equal volumes of 4.4 ml. Hydrogel membranes with a surface area of 4.58 cm^2 were mounted between the two chambers. Once the membranes were mounted, both chambers were filled with 20 mM Tris buffer. The donor chamber was connected to the lysozyme reservoir via a peristaltic pump. The receptor chamber was connected to a UV-Visible spectrophotometer (Shimadzu 1601), to allow lysozyme diffusion across the membrane to be automatically monitored and logged from optical density changes. The amount of lysozyme diffusing across to the receptor chamber was calculated using calibration data for lysozyme at 280 nm. The effect of pH and ionic strength was investigated by varying the pH of the phosphate buffer and ionic strength levels in the lysozyme solution fed to the donor chamber, and following the resultant changes in transport rate. All experiments were conducted at 20°C.

4.3 Results

4.3.1 Hydrogel characterization

In this study, carbodiimide chemistry was employed to cross-link carboxylic and hydroxyl groups in CM-dextran. According to the expected cross-linking mechanism, when Con A is included the activated ester bond will react with amino acid groups on the protein. In the case of the D-glucose-sensitive hydrogel, concanavalin A was to a certain extent covalently bound with CM-dextran and affinity bound with the D-glucose residues of the dextran. Control hydrogels were made using ovalbumin as the coupled protein.

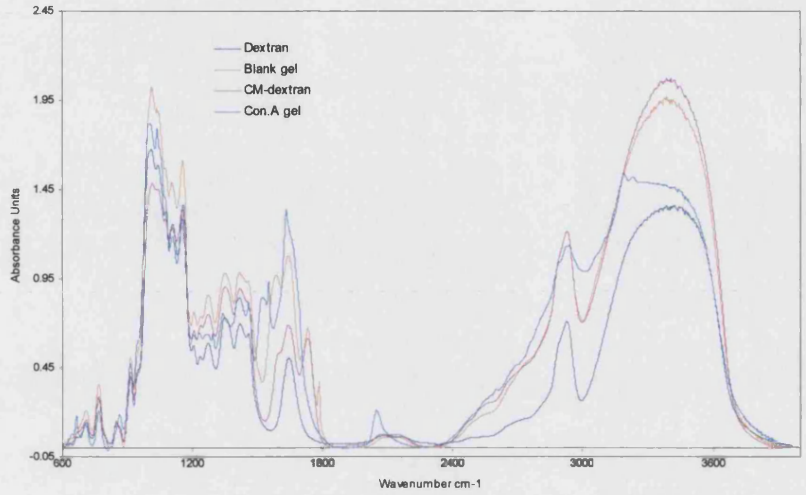

(a)

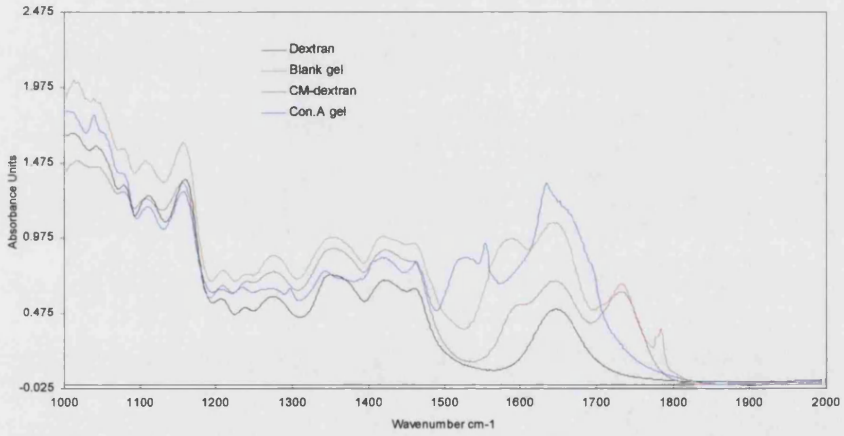

(b)

Figure 4.2: Dextran hydrogel and hydrogel grafted Con A were characterized by Fourier Transform Infrared Spectroscopy (FT-IR). Peaks from the carbonyl (C=O) stretching in the CM-dextran and the gel appeared at wavenumber 1734 cm^{-1} and 1580 cm^{-1}. The peak of the carbonyl of gel ester bond appeared at wavenumber as 1775 cm^{-1}. The peak of 1570-1515cm^{-1} in Con A gel was due to the characteristic absorption of secondary amides in this hydrogel.

The successful incorporation of the COOH group into the dextran is demonstrated by the presence of a carboxylic FT-IR band from the carbonyl (C=O) stretching of CM-dextran at ca1734 cm^{-1} and 1580 cm^{-1} as shown in Figure 4.2. Activated carboxyl groups by EDC/NHS can react with hydroxyl groups in CM-dextran to form ester linkages without protein. Furthermore, in the solid phase, primary amides in Con A

hydrogel have a weak-to-medium intensity band at 1650-1620cm^{-1} which is generally too close to the strong carbonyl band to be resolved. The amide II band from protein bound to dextran as seen at 1570-1515cm^{-1}is due to a motion combining both the N-H bending and the C-N stretching vibrations of the group –CO-NH- in its *trans*- form.

4.3.2 Morphology of hydrogels by SEM

Four samples of the Con A gel were prepared for SEM analysis. (A) incubated in buffer, (B) incubated in buffer + D-glucose, (C) incubated in buffer + L-glucose, (D) incubated in buffer + D-glucose followed by incubation in buffer only for 2 days. As a control, a gel (E) was made with an inert protein (ovalbumin).

Results presented in Figure 4.3 show that the Con A (A) and ovalbumin (E) gels show a small pore structure when incubated in buffer. Addition of D-glucose to the Con A gel leads to significant swelling. The response of the Con A hydrogel to D-glucose is proposed to result from changes in the pore walls such that a relatively compact structure in the buffer expands, resulting in a larger internal pore volume.

The control test with L-glucose as a non-competitive ligand at a similar concentration (C) shows little evidence of expansion confirming that the effect is the result of a specific displacement rather than an osmotic pressure effect. Examination of a Con A gel incubated with D-glucose and then extensively washed (D) shows clear evidence of reversibility with the internal pore structure partly returning to that seen for the native gel.

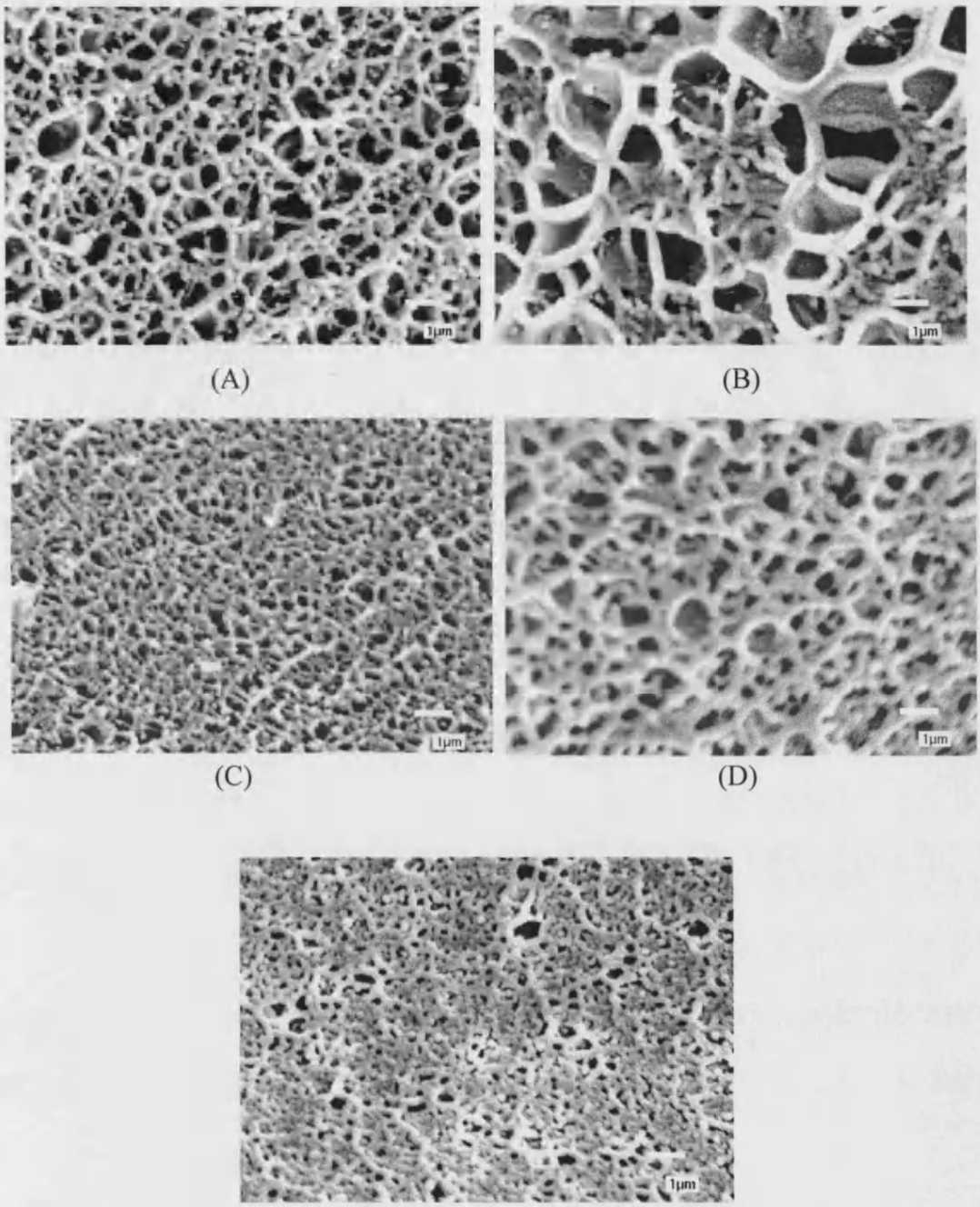

Figure 4.3: (A) Con A hydrogel in 20 mM Tris buffer. (B) Con A hydrogel in 0.1 M D-glucose with 20 mM Tris buffer. (C) Con A hydrogel in 0.1 M L-glucose with 20 mM Tris buffer. (D) Con A hydrogel washed in buffer after incubation in 0.1 m D-glucose with 20 mM Tris buffer for 2 days. (E) Ovalbumin hydrogel. All SEMs were with a magnification as 10000.

4.3.3 Binding capacity comparison of different sugars with Con A by ITC

Isothermal titration microcalorimetry (ITC) has found extensive use in ligand-binding studies. A ligand is titrated into a solution containing the binding protein (here

concanavalin A), and the heat evolved or absorbed during binding is measured. Deconvolution of data obtained from a sequence of additions yields the binding constant, enthalpy and enthalpy of binding, and the stoichiometry of the interaction. Figure 4.4 (panel 1) shows the raw calorimetric data for titration of native con A with D-glucose, denoting heat evolved (negative exothermic peaks). Panel 2 shows the plot of heat evolved per injection as a function of the molar ratio of ligand to the Con A. The smooth solid line represents the best fit of the experimental data using a single binding site model. The binding constants of different ligands to Con A and CM-dextran-Con A conjugates are shown in Table 4.1. Comparison of the binding constants obtained for free Con A and CM-dextran-Con A conjugates with D-glucose show a reduction in the association constant from 166.3 to 94.68 M^{-1} indicating a reduced affinity. A similar decrease is seen for the interaction with dextran (34.95 to 12.24 M^{-1}). When D-glucose is used to competitively displace pre-bound dextran the binding constant decreases from 56.5 M^{-1} for Con A conjugated dextran to 22.1M^{-1} for the displacement of dextran from native Con A. This is consistent with the lower association constant values obtained in direct binding titrations.

Titrations with L-glucose show no evidence of binding to free Con A. However, weak binding is observed with CM-dextran-Con A suggesting that the immobilization has reduced the binding specificity of the Con A.

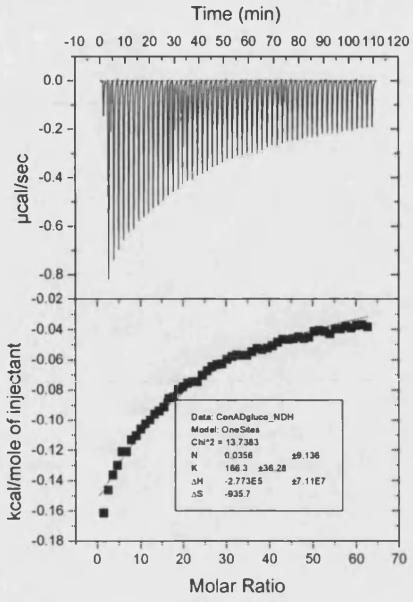

2.5mg/ml Concanavalin A was titrated by 5mg/ml D-glucose

(1)

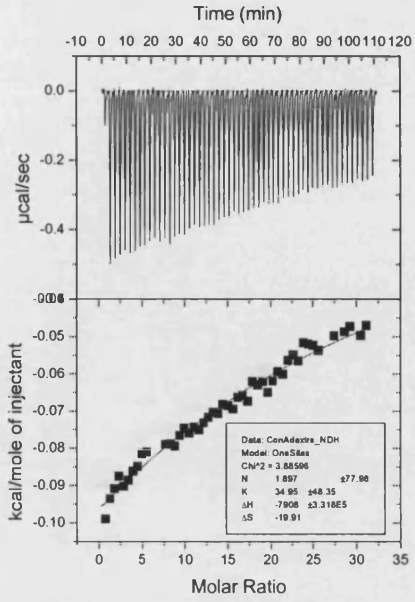

2.5mg/ml Concanavalin A was titrated by 5mg/ml 12 KD dextran.

(2)

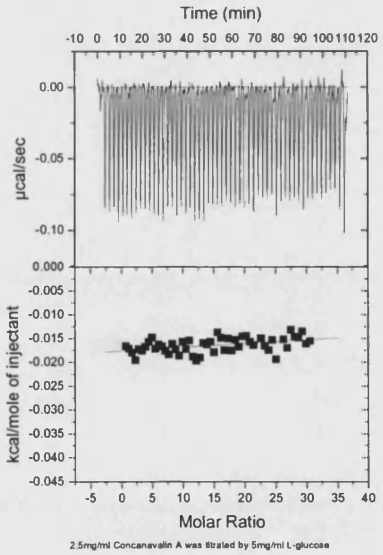

2.5mg/ml Concanavalin A was titrated by 5mg/ml L-glucose

(3)

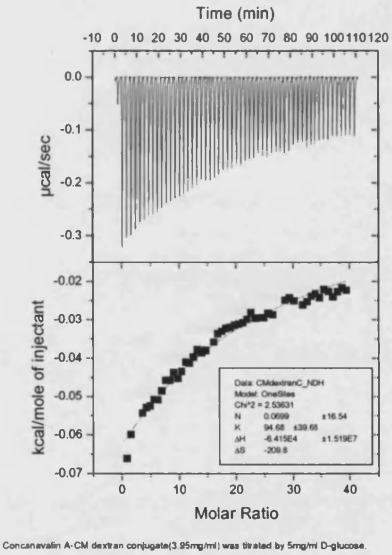

Concanavalin A-CM dextran conjugate(3.95mg/ml) was titrated by 5mg/ml D-glucose.

(4)

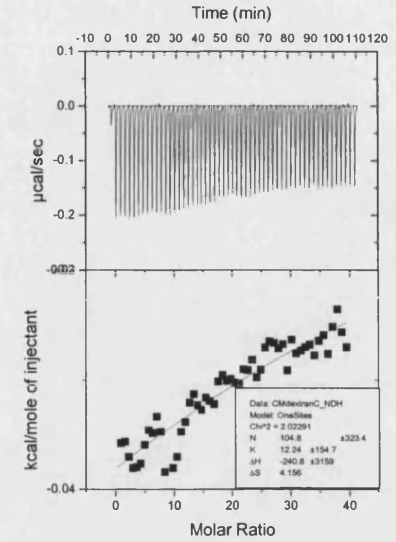

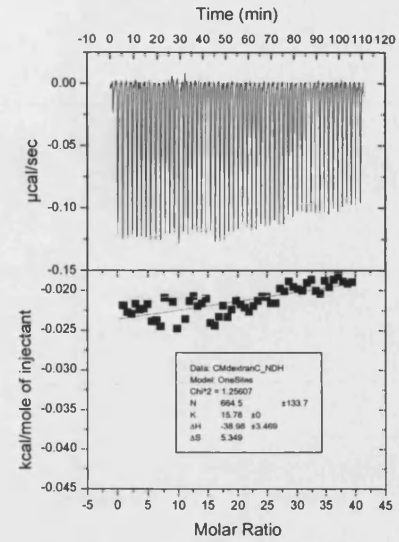

(5) (6)

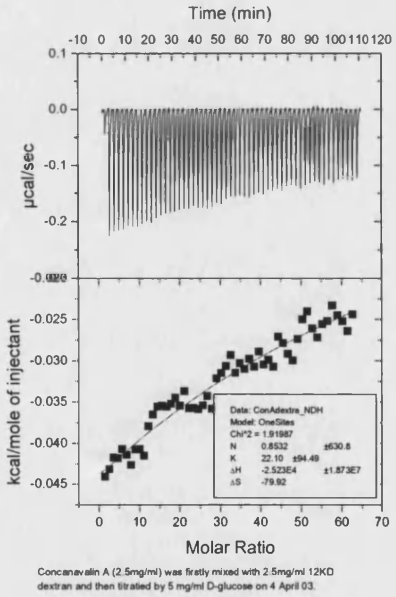

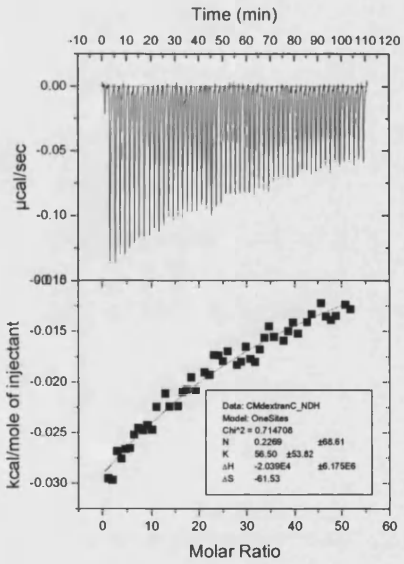

(7) (8)

Figure 4.3: ITC results of Con A titrated against sugar under different conditions, with one binding site model and parameter results (N - Stoichiometry, K- Association constant [M^{-1}], H – Enthalpy [cal mol^{-1}], S - Entropy of [cal mol^{-1} K^{-1}]). 0.092 mM of Con A titrated with 27.8mM of D-glucose (1), dextran (2), L-glucose(3) at 20 °C. 0.146 mM conjugate of CM-dextran with Con A titrated with 27.8 mM of D-glucose (4), dextran (5), L-glucose (6) at 20 °C. (7) and (8) showed the D-glucose (27.8 mM) completive bind the mixture of dextran with Con A (0.092mM) or CM-dextran-Con A (0.111mM) conjugation respectively.

Figure	1	2	3	4
Reaction	Con A with D-glucose	Con A with dextran	Con A with L-glucose	Con A-dextran with D-glucose
$K_a(M^{-1})$	166.3	34.95		22.10
Figure	5	6	7	8
Reaction	CM-dextran-Con A with D-glucose	CM-dextran-Con A with dextran	CM-dextran-Con A with L-glucose	CM-dextran –Con A –dextran with D-glucose
$K_a(M^{-1})$	94.68	12.24	15.78	56.5

Table 4.1. Summary of association constants in the different reactions.

4.3.4 Diffusion of lysozyme through the hydrogel

The proposed response mechanism of the D-glucose-sensitive hydrogel membrane is based on the competitive displacement of biospecific interactions between Con A leading to an increase in permeability. Results from both SEM and ITC experiments show D-glucose is an effective competitor and that displacement of Con A/dextran interactions within the gel lead to clearly observable changes in morphology.

For an effective delivery system it is necessary to show that these morphological changes lead to changes in gel permeability and that these changes are both specific and reversible. Figure 4.5 compares the permeability of membranes produced using both Con A and ovalbumin as an inert control. Both gels show negligible transport of the protein lysozyme (molecular weight 13KD) for the first 100 minutes. After the addition of 0.1 M glucose as a competitive displacer the difference is marked, with the Con A gel showing a clearly enhanced permeability.

In addition to specific permeability changes in response to competitor concentration changes in both pH and ionic strength are also likely to influence response. In Figure 4.6 lysozyme concentration/time curves are shown as a function of pH over the range 2-9 (ionic strength was to 0.1M using NaCl for each value). The inset gives rate as a function of pH showing a curve with 2 maximal.

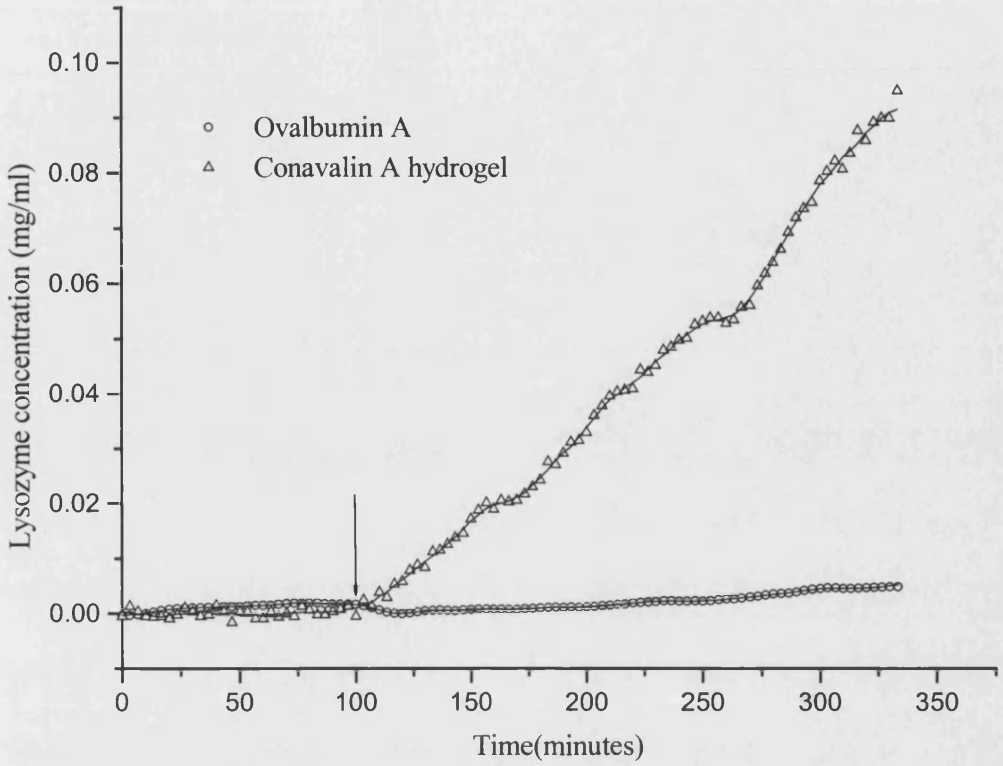

Figure 4.5: Lysozyme diffusion through the Ovalbumin gel and the Con A hydrogel at room temperature 0.1 mol glucose was added at 100 minutes.

Figure 4.7 shows the effect of ionic strength on lysozyme transport at a fixed pH of 7.4. In this case transport rate increases between 0.05-0.35M and then decreases over the range 0.35-0.5M.

The specificity of permeability changes in the membrane was determined using a number of solute molecules (D-glucose, L-glucose, glycerol and dextran). Figure 4.8 shows that, as expected from the ITC results, D-glucose had the most pronounced effect L-glucose, glycerol and dextran show a similar less pronounced effect. In the case of L-glucose and dextran this would be anticipated from the ITC results. In control experiments, where lysozyme solution without carbohydrate/glycerol was used little diffusion was observed. The response lag observed between addition of competitor and the change in transport rate was approximately 20 minutes, which matches the residence time in the donor cell diffusion limitations were partially masked by the time course of D-glucose build up.

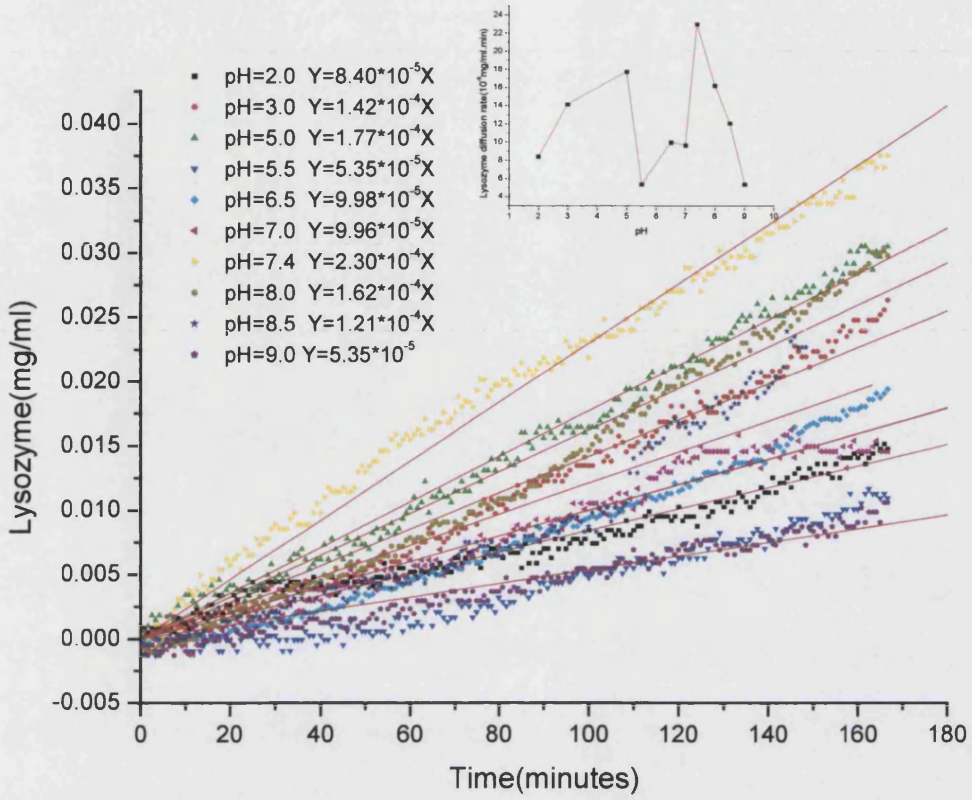

Figure 4.6: Diffusion curves of lysozyme through the Con A hydrogel in response to pH change. The lysozyme concentration was 2.0 mg/ml, and the temperature was 25°C. A phosphate buffer of 20 mM was employed with constant ionic strength of 0.1 M using NaCl to adjust it.

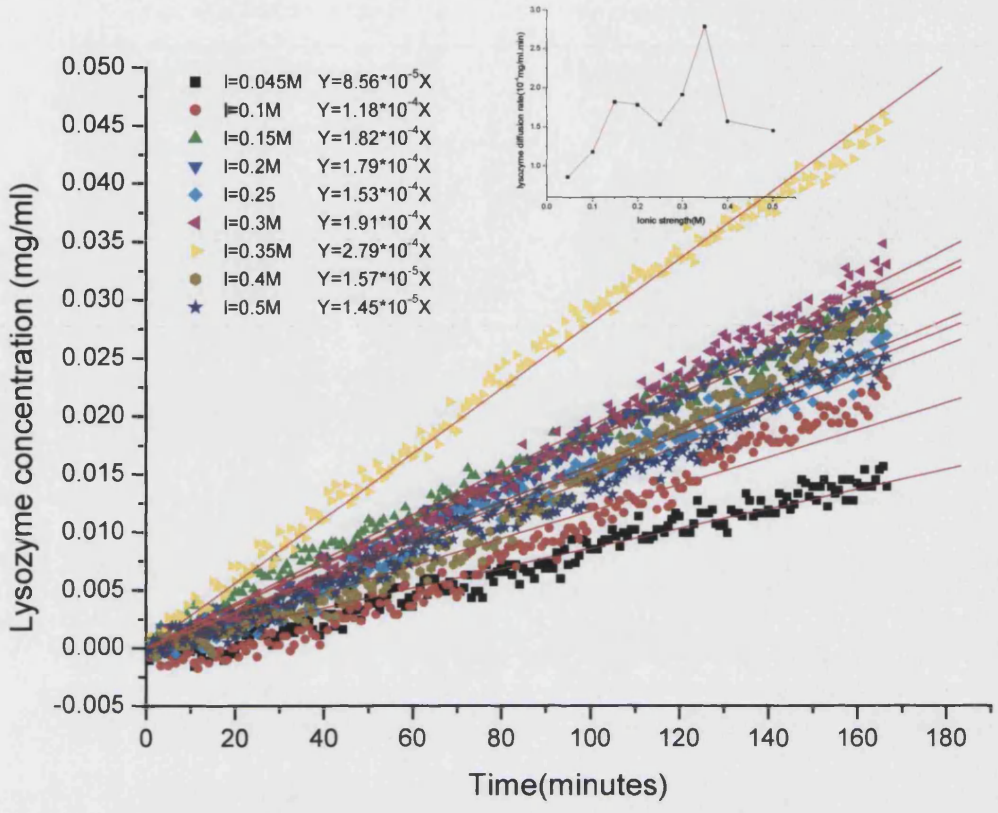

Figure 4.7: The effect of different ionic strengths on 2mg/ml lysozyme diffusion through the Con A hydrogel membrane at room temperature. In the experiment, the pH was kept at 7.4 using a phosphate buffer of 20 mM containing different concentrations of NaCl.

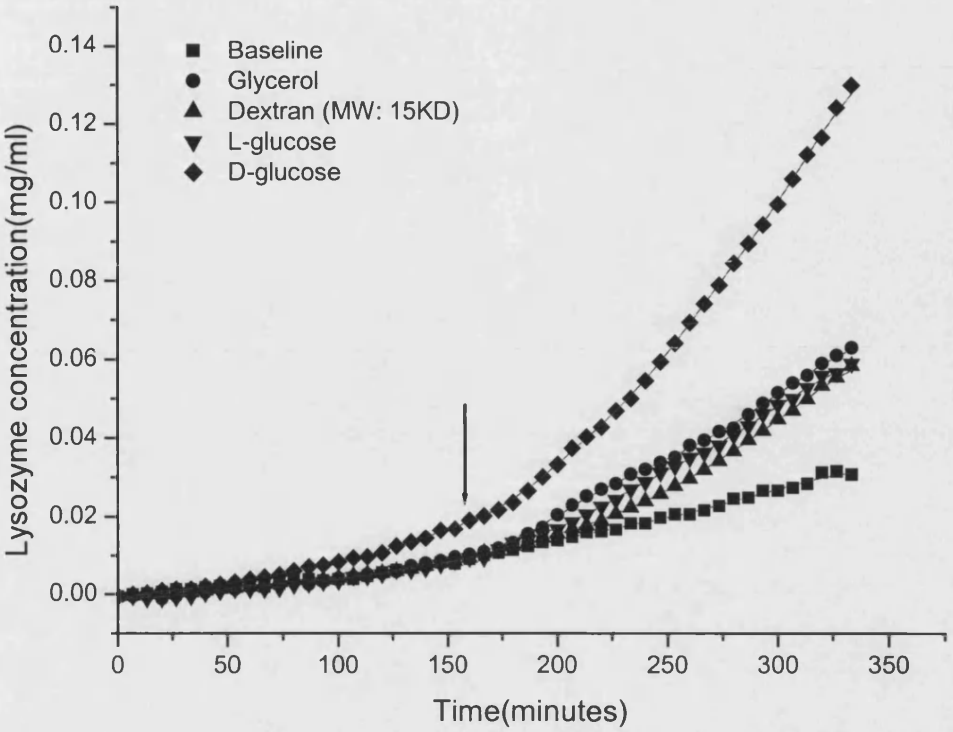

Figure 4.8: Diffusion curves in response to 0.1M D-glucose, L-glucose, dextran (12KD) and glycerol with respect to the diffusion of insulin (2 mg/ml). The baseline control was carried out with lysozyme only. Putative activators were added at 166 minutes. The assay was conducted at room temperature (25°C).

The results show that the hydrogel membrane allows lysozyme transport at a rate that is controllable using a soluble competitor molecule, and that this effect is specific to molecules recognized by the Con A receptor. This suggests that, as anticipated, changes in porosity of the membrane where dextran serves as both a ligand for Con A affinity and a structural matrix result from a reduction of internal affinity cross links when a soluble competitor is introduced. It is also implicit in these results that a significant fraction of the total Con A is not inactivated during membrane synthesis.

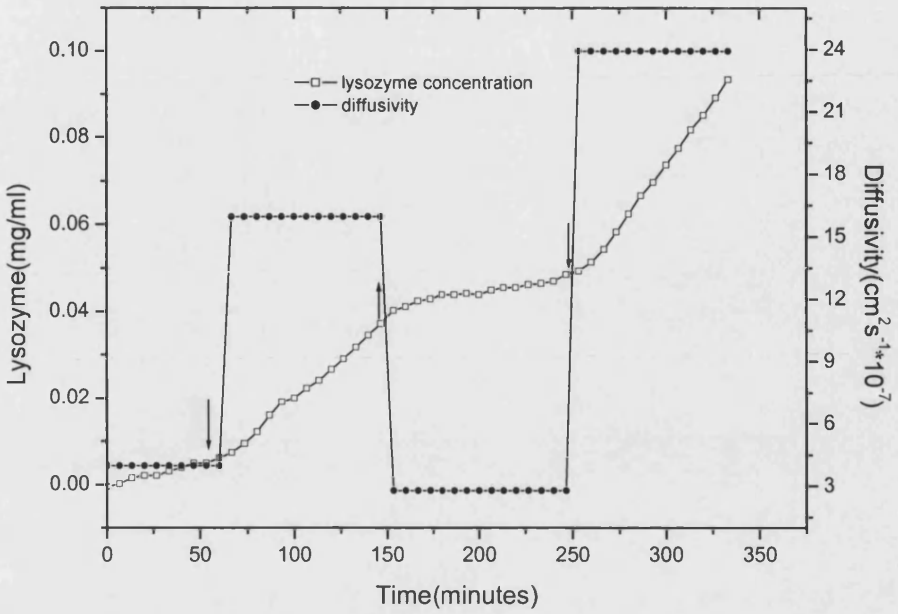

Fig. 4.9: Reversibility of lysozyme diffusion in response to changes in D-glucose. 0.1 M D-glucose plus insulin (2.0 mg/ml) buffer was added at the down-arrow. Lysozyme solution without glucose was restored at the up-arrows. Diffusivity calculation was described in Chapter 3 (page 57). Temperature 25°C.

An essential property of responsive gels of the type described here is the reversibility of the response generated. SEM results suggest that structural changes generated by the addition of the competitor (D-glucose) are largely reversed when this is removed. In Figure 4.9 the effect of sequential addition and removal of D-glucose on lysozyme transport is shown. As expected the reversible changes in physical properties are clearly mirrored by permeability changes in response to competitor concentration. The response shows that, while there is a diffusion time lag between each solution change, the introduction and removal of D-glucose causes a reversible switch between lower and higher diffusion rates.

4.4 Discussion

Grafting carboxylic groups on dextran using sodium chloroacetate while controlling reaction temperature and time allows the formation of polymers with varying degrees of carboxylic substitution. These carboxylic groups can then be cross-linked in the scheme shown in Figure 4.1 to produce hydrogels. Variation of the degree of

substitution allows control of the residual number of non-cross-linked carboxylic groups and hence the charge properties of the gels. Incorporation of functional proteins into gels based on these carboxylated dextrans allows the formation of bio-responsive hydrogels with controlled charged properties (Figure 4.1). Here, CM-dextran containing one COOH per 65 glucose residues was used to prepare gels incorporating protein. FTIR results (Figure 4.2) support the proposed reaction scheme, but of greater significance is the evidence provided by the SEM results presented in Figure 4.3 that show that the gels prepared via this route exhibit reversible, biospecific structural changes.

From the SEM results in Figure 4.3, it is apparent that hydrogel porosity changes in response to exposure to different stimuli. The effects are as might be expected from the specificity of Con A. While both D-glucose and dextran lead to morphology changes that correlate with increases in gel permeability, L-glucose has little observable effect. These results show that at a structural level the effect of a competitor is both specific and reversible.

To achieve a functional gel it is essential that the protein is not inactivated during the coupling process. While SEM results in Figure 4.3 provide indirect evidence that this is the case, they do not eliminate the possibility that structural changes are an artefact resulting from effects unrelated to biospecific interactions. However, the fundamental investigation of the binding interactions anticipated using ITC (Figure 4.4 and Table 4.1) confirm that the Con A coupled gel precursors maintain their ability to bind D-glucose and glucose based polymers (dextran). It is interesting to note that the binding affinity of CM-dextran-Con A for dextran is lower than that observed for native Con A, possibly as a result of the carboxylic groups complexing the divalent cations required for Con A binding (Ca^{2+} and Mn^{2+}). For some applications (e.g. affinity adsorption) this might cause a problem; however, for use in a responsive polymer, weaker binding-indicative of a faster dissociation rate is likely to have a beneficial effect in reducing response times.

In addition to changes in the concentration of specific competitors, responsive gels are also likely to experience changes caused by both pH and ionic strength. These effects are shown in Figure 4.6. Previous studies have shown that the carboxylic groups in these gels have a dissociation constant of 6.1 while lysozyme has an isoelectric point

of 11. This suggests that at pH values below 5 the gel will be carry a small positive charge and the lysozyme will be positively charged; this will lead to charge repulsion effects limiting transport. As the pH is increased towards 5 the positive charge on the gel will decrease and transport rate increases. Above 5 and the concentration of negative charges on the gel start to increase leading to ion exchange interactions between protein and gel, again limiting transport. In this region transport properties might also be influenced if the immobilised Con A switches between a dimer and tetramer conformation as would be expected in free solution. As pH is further increased the ion exchange effect is lost as the positive charge on the lysozyme starts to decrease leading to the second transport maximum. Also, as the carboxylic groups dissociate and the net negative charge in the gel increases, charge repulsion effects will cause the gel to swell, increasing permeability. Further increases in pH lead to an increase in the negative charge on the lysozyme, again leading to charge repulsion limitations with the negatively charged gel.

The effect of ionic strength was measured at pH 7.4 (Figure 4.7) where it is likely that transport will be limited by ion exchange interactions between gel and lysozyme. Therefore as ionic strength is increased swamping these effects, transport rate increases. Further increases in ionic strength result in a degree of gel shrinkage leading to a subsequent decrease in transport rate.

The key requirements of the gel are specific and reversible changes in transport properties in response to changes in competitor concentration. The results reported in Figures 4.8, and 4.9 confirm that, as expected from the SEM results, increases in permeability are observed in response to changes in D-glucose concentration (Figure 4.8), and that these effects are reversible over a number of addition/removal cycles (Figure 4.9).

4.5 Conclusion

A simple procedure is reported for the synthesis of D-glucose responsive hydrogels. This allows production of gels with varying levels of protein substitution and with a controllable degree of carboxylic group substitution.

There are two major advantages of the materials described here compared with the glucose-responsive gel we have described previously (Tang *et al.*, 2003). (i) The gel no longer requires the use of a potentially cytotoxic triazine group, and hence is more likely to be biocompatible. (ii) The use of CM dextran allows the intrinsic charge properties of the gel to be easily controlled such that gels can be tailored for use in environments of different pH and ionic strength.

In the course of these studies it was found that the gelation time and the mechanical strength of the final gel produced are dictated by the initial degree of substitution of carboxylic groups and subsequently by the concentration of coupled protein e.g. the gelation time for hydrogel-grafted Con A is far shorter than that of gels without protein produced using the same procedure. This suggest that mechanical properties can be modified independently of response levels by including inert proteins or other amine containing compounds to increase the degree of covalent cross-linking.

The gels described have obvious potential for the control of insulin delivery *in vivo*. However, toxicity risks associated with insulin overdose coupled with the limited aqueous solubility of insulin suggest that bio-responsive gels of this type where both ligand and receptor are immobilized may find more immediate application in non-medicinal applications such as analysis or responsive packaging.

Chapter 5. Synthesis and Characterization of pH-Sensitive Carboxymethyl -Dextran Hydrogel for Protein Loading and Release

5.1 Introduction

The response properties of stimuli-sensitive hydrogels suggest that they will find many new applications in the biological and biomedical fields (Miyata *et al.,* 2002). To date, pH-sensitive hydrogels are most frequently used to develop controlled release formulations for oral administration or tissue engineering applications (Qiu *et al.,* 2001).

There are two types of pH-sensitive hydrogel classified according to the presence of either pendant acidic or basic groups, which either accept or release protons in response to changes in the environmental pH (Peppas *et al.*, 1993). pH-sensitive hydrogels with grafted acidic groups can undergo fast reversible changes in microstructure, going from a swollen to shrunken state when pH is changed from basic to acidic (Peppasa *et al.,* 2000). Such gels have many possible applications including: biosensors and microfluidic channels (Beebe *et al.,* 2000, Yu *et al.,* 2001), controlled release protein or drug (Franssen *et al.,* 1999, Baldwin *et al.*, 1998, A. M. Lowman *et al.,* 1999), cell culture and tissue engineering (Lee *et al.,* 2001, Hoffman, 2002).

A wide and diverse range of polymer compositions have been used to fabricate pH-sensitive hydrogels, including Poly(acrylic acid) (PAA), poly(methacrylic acid) (PMA) grafted with poly(ethylene glycol) (PEG), alginate, and dextran(Kou *et al.,* 1988, Peppas *et al.,* 1990, 1991, Khare *et al.,* 1993, Siegel *et al.,* 1988).

For hydrogels intended for use in biomedical and pharmaceutical application, it is essential that they are both biocompatible and biodegradable. In recent years, there has been considerable interest in developing hydrogels from dextran, (Kim *et al.,* 2000, Stubbe *et al.,* 2001, Wolthuis *et al.,* 1997). Dextran is broken down by dextranase - an enzyme found in many parts of the body, such as the intestinal

mucosa, spleen, liver and kidney. The biodegradability and high biocompatibility of dextran thus favours its usage over other natural polypeptides/proteins/polysaccharides.

Chapter 4 described the synthesis of Carboxyl Methyl -dextran hydrogel membranes for drug-delivery and tissue engineering applications using carbodiimide chemistry. Here CM-dextrans with a high degree of carboxylic groups substitution were used to allow fabrication of pH-sensitive gels. Since the resultant hydrogel is made up of crosslinked CM-dextran containing pendant acidic groups, carboxylic (COOH) groups (which either accept or release protons in response to changes in the environmental pH) it shows pH sensitivity.

In order to be able to design hydrogels with a desired characteristic for drug delivery, cell culture, or coupled protein, it is necessary to evaluate the influence of the chemical composition of hydrogels on equilibrium degree of swelling, mechanical strength, degradability and release properties. The objectives of this chapter were to analyze the effects of different reactant mixtures on the properties of the hydrogels. This was achieved by investigating the network structure, its mass transfer coefficients and biodegradability.

5.2 Materials and method

5.2.1 Materials

Dextran, dextranase and cytochrome C were obtained from Sigma-Aldrich, UK. All other chemicals were of reagent grade and obtained from Lancaster Synthesis Ltd., UK.

5.2.2 Preparation of CM-dextran hydrogel

Various degrees of carboxylic substitution in CM-dextran were obtained by adjusting the reaction time and prepared as described as Chapter 4 (Page 72). The carboxymethylation reactions were run for 15 minutes, 30minutes, 1.5 hours, 2 hours, and 3 hours in order to vary the degree of COOH substitution. The longer the reaction duration, the more COOH groups were introduced. The final COOH concentration was then calculated by the means of acid titration as Chapter 4 (Page 73).

An unknown concentration of CM-dextran is neutralized and quantified with a known volume and concentration of NaOH determine the concentration of CM-dextran with a indicator which changes colour.

5.2.3 Experimental set-up

Two sets of characterisation experiments were carried out.

At first, the objective was to carry out network analysis of the polymer structure. To ensure that equilibrium swelling of the hydrogels was achieved in a short timeframe, 1 ml of solution containing CM-dextran and EDC/NHS, subsequently adjusted to 0.5 ml, was placed in spectrophotometer cuvettes (total volume 4ml) for gelation.

In the second series of experiments, the objective was to assess mass transfer properties via different protein size diffusing through the membrane, and biodegradability analysis using dextranase. In order to increase the accuracy of the results, a larger volume of solutions - 2 ml of solution containing CM-dextran and EDC/NHS, and 10 ml of protein solution - was involved. Petri dishes were used instead of the curettes.

In both experiments, the effects of the following variations were examined:

- Variation in the number of monomers by changing the weight ratio of CM-dextran;
- Variation in the number of COOH groups attached to dextran; and
- Variation in the proportion of the cross-linking reagents in the formation of cross-linkages (or the ratio of EDC to NHS).

In addition, in the first set of experiments, the effect of variation in CM-dextran molecular weight was also analyzed.

In the both experiments, the CM-dextran hydrogels were prepared such that the above-mentioned variations on the properties of the hydrogel could be examined. All

the CM-dextran with 1-COOH: 12 -glucose was used under the condition EDC/NHS ratio of 7:1 unless otherwise stated.

5.2.4 Preparation and detection of cyctochrome C solutions for mass transfer analysis via protein studies

A calibration curve was prepared to correlate the concentration of Cytrochrome C solution and absorbency at 410 nm using a UV spectrometer. Cytochrome C solutions of concentration 0.047 mg/ml, 0.100 mg/ml, 0.197 mg/ml and 0.410 mg/ml were prepared for the protein studies. The protein concentrations were prepared such that they were kept well within the linear range of concentration against absorbance.

5.2.5 Preparation of dextranase solution for biodegradability analysis

186mg of dextranase was dissolved in 160ml pH 7.4 phosphate buffer solution to give a resultant dextranase solution concentration of 15 dextranase units (DU)/ml (1 DU corresponds to the amount of enzyme which liberates 1μmol of isomaltose per minute at pH 5.5 and 50°C, using dextran).

5.3 Equilibrium swelling studies

5.3.1 Determination of swelling ratio

CM-dextran hydrogels were soaked in phosphate buffer solutions of pH 3 and 7.4 at 25^0C. The buffer solution was changed daily and the hydrogels were weighed at intervals. Before weighing, the surface water on the hydrogel was gently removed by blotting with a filter paper, and the hydrogel weighed until no further weight change detected. The gels were soaked in the buffer solutions until the equilibrium weight of the hydrogel was obtained. The swollen rate at equilibrium (SRE) of the hydrogels was calculated according to Equation 1 and 2 (Mark, *et. al.*, 1987):

$$W_d = W_{CM\text{-}dextran} + W_{water} \qquad (1)$$

$$SRE = \frac{W_s}{W_d} \qquad (2)$$

Equations 1 and 2 were calculated based on the volume additions of CM-dextran and water.

5.3.2 Determination of $\overline{M_c}$

Equilibrium swelling theory (Peppas, 1986) and rubber elasticity theories (Peppas et al., 2000) are the two main theories used to determine cross-linking density of a hydrogel. The structure of hydrogels that do not contain ionic moieties can be analyzed by the Flory-Rehner theory (Flory *et al.*, 1943). This thermodynamic theory states that a crosslinked polymer gel, which is immersed in fluid and allowed to reach equilibrium with its surroundings, is subject only to two opposing forces, the thermodynamic force of mixing and the retractive force of the polymer chains. At equilibrium, these two forces are equal. Peppas and Merrill (Peppas, 1986) modified the original Flory-Rehner theory for hydrogels prepared in the presence of water. The presence of water effectively modifies the change of chemical potential due to the elastic forces. This term must now account for the volume fraction density of the chains during crosslinking. Equilibrium swelling theory predicts the molecular weight between crosslinks in a neutral hydrogel prepared in the presence of water.

In this calculation of the cross-linking theory, two different models – the Gaussian model (which assumes a Gaussian distribution of the cross-linked polymer chains) developed by Flory – Rehner later edited Peppas – Merrill (Peppas *et al.*, 1976) for cases in which the cross-links were introduced in a solution, and the non-Gaussian model. Based on the equilibrium swelling theory of Flory and Rehner, modified by Peppas *et al.* for the case where the cross-links were introduced in a solution, $\overline{M_c}$ was calculated according to Equation 5 (note: the polymer fractions were calculated based on the addition of water and CM-dextran)(See the preface for various definitions):

$$v_{2,r} = \frac{W_{CM-dextran}}{W_d} \tag{3}$$

$$v_{2,s} = \frac{W_{CM-dextran}}{W_s} \tag{4}$$

$$\frac{1}{\overline{M_c}} = \frac{2}{\overline{M_n}} - \frac{(\bar{v}/V_1)\left[\ln(1-v_{2,s}) + v_{2,s} + x_1(v_{2,s})^2\right]}{v_{2,r}[(v_{2,s}/v_{2,r})^{1/3} - 0.5(v_{2,s}/v_{2,r})]} \tag{5}$$

5.3.3 Determination of ρx

Based on Peppas-Barr-Howell (Peppas, 1986), ρ_x was calculated according to Equation 6:

$$\rho_x = \frac{1}{v_1 \overline{M}_c} \qquad (6)$$

5.3.4 Determination of k' in protein loading studies

To conduct protein loading experiments, 10 ml of cytochrome C solution at four different concentrations – 0.047 mg/ml, 0.100 mg/ml, 0.197 mg/ml and 0.410 mg/ml in pH 7.4 phosphate buffer were placed in petri dishes containing 2ml of the hydrogel each. The experiment was carried out at 25^0C and the samples were gently agitated every 15 minutes. At half hourly intervals up to five hours, the concentration of the cytochrome C solutions were measured using spectrometer (λ = 410 nm). The samples were then allowed to stand overnight and readings taken at 24, 28 and 48 hours to determine the equilibrium protein concentration in the solution.

For the loading of protein into the hydrogels, convection and diffusion are the main transport mechanisms where the predominant will depend on the structure of the hydrogel. The overall permeability of the protein within the hydrogels depends on two main factors - the solute diffusion coefficient, which is highly affected by the polymer structure, and the solute partition coefficient, which is a measure of the solute's preference for the polymer relative to the surrounding diffusion medium (Peppas, 1986).

The ratio of protein loaded into CM-dextran in the hydrogel was calculated using the following equations:

$$W_p = (C_e - C_i)V \qquad (7)$$

$$R = \frac{W_p}{W_{CM-dextran}} \qquad (8)$$

For nonporous, homogeneous, polymeric hydrogels, according to Fick's law, the system can be described using Equation 9:

$$\frac{1}{A}\frac{dC}{dt} = \frac{D_{im}K_i}{\delta}(C_{eqm} - C_t) = k'(C_{eqm} - C_t) \qquad (9)$$

where $\frac{dc}{Adt}$ - rate of solute diffusion per unit time per unit surface area ($cm^{-2}s^{-1}$)

The amount of solutes in the hydrogel was normalized with the amount of CM-dextran in the hydrogel by Equation 8.

The experimental data were then fitted using the computer program 'Scientist' to find *k'*. This is given in Equation 10:

$$C_{calc} = \frac{C_{eqm}(e^{(k' t)} - 1)}{e^{(k' t)}} \qquad (10)$$

k' is adjusted until the error between the calculated equilibrium concentration, C_{calc}, and the measured equilibrium concentration, C_{eqm}, is minimized.

5.3.5 Determination of n in protein release studies

The diffusion process is highly dependent on the network structure of the polymer. As such, it would be useful to look at how the overall *k'* values changes as the structure of the polymer changes.

Numerous theories are also available to treat the experimental results for the mechanisms of solute release from dynamically swelling hydrogels, with most based on diffusion equations. Most release mechanisms can be classified into the following categories – diffusion-controlled, chemically-controlled, or swelling controlled (Peppas *et al.*, 1991). Swelling-controlled systems refer to hydrophilic matrixes in which the inward flux of solvent molecules and the subsequent swelling of the polymer matrix control the rate of protein release.

For release studies hydrogels were loaded with a high concentration of protein solution to ensure that the amount of protein in the hydrogel would be approximately constant giving a constant driving force for protein release.

Release was measured after maximum loading in pH 7.4 buffer at 25^0C. Loaded hydrogels were then kept in different phosphate buffer solutions of pH 3.0, 5.5 and 7.4. The samples were gently agitated every 15 minutes. At half hourly intervals up to five hours, the concentration of the cytochrome C protein solutions was measured using the spectrometer (λ = 410 nm). The samples were then allowed to stand overnight and readings taken at 24, 44 and 52 hours to determine the equilibrium protein concentration in the solution. Each release profile can be estimated by linear regression to fit Equation 11:

$$\frac{M_t}{M_\infty} = K t^n \qquad (11)$$

5.3.6 Determination of rate of enzyme degradation

The effect of crosslinkage on enzymic degradation of gels was studied. 2 ml of each gel were placed in a petri dish and immersed in pH 7.4 phosphate buffer containing a concentration of 12.9 dextranase units / ml. 1 sample of gel was immersed in pH 7.4 phosphate buffer without any dextranase. The samples were incubated at 37°C, and gently swayed before the detection of the amount of reducing sugar present in the solution. Detection of the reducing sugar was carried out every half an hour until the gels degraded. Readout of glucose concentration was attained using a Bioprofile 400 Analyser (Nova Biomedical, Waltham, MA 02254, USA).

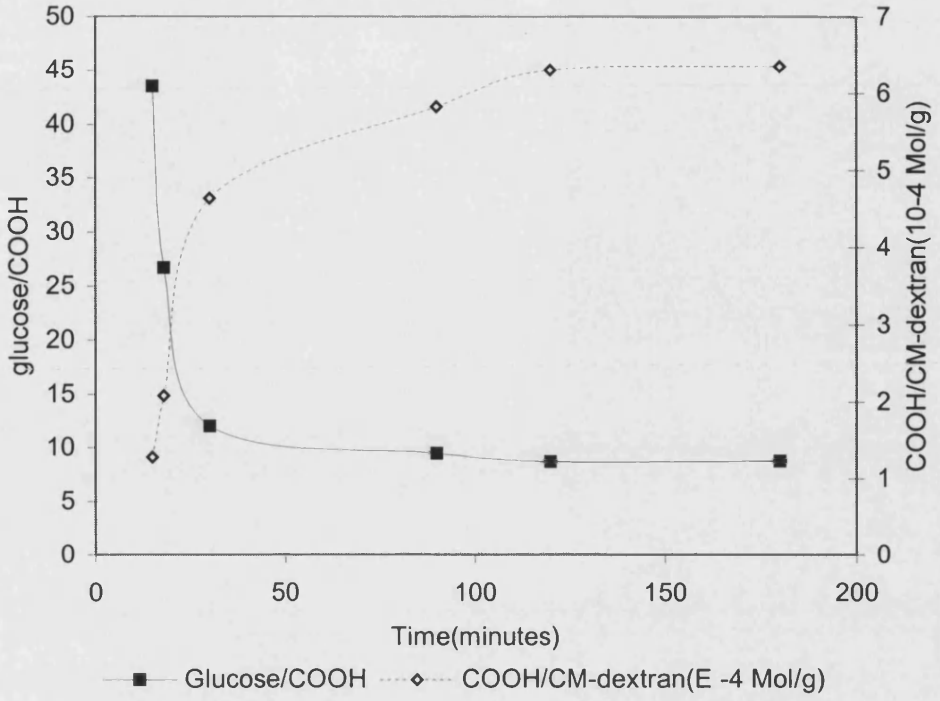

Figure 5.1: The relationship of COOH amounts in CM-dextran against reaction time during dextran carboxymethylation reaction at 50 °C.

5.4 Results and discussion

To attain different COOH substitution in the CM-dextran used for hydrogel preparation, the time was varied. As shown in Figure 5.1, COOH substitution increases with time at 50 °C, with a maximum reached after 90 minutes. Similar results are also seen at with reaction temperatures.

5.4.1 Network structure analysis – determination of SRE, $\overline{M_c}$ and ρ_x

In the evaluation of the parameters needed to describe the structural properties of the cross-linked CM-dextran hydrogels, equilibrium swelling theory (Peppas, 1896) was used. The model developed by Flory and Rehner (Flory *et al.,* 1943) for the calculation $\overline{M_c}$ assumes that the number of repeat units between the cross-links are large enough to be represented by a Gaussian distribution and that the cross-links are, on the average, tetrafunctional. This was later modified by Peppas - Merrill (Peppas *et al.,* 1976) for cases where the cross-links were introduced in a solution, as given by Equation 5.

Average SRE, $\overline{M_c}$ and ρ_x at pH 3 are tabulated in Table 5.1 while those at pH 7.4 are tabulated in Table 5.2. Since the $\overline{M_c}$ values calculated are greater than 1.6214 x 10^{-5} $gmol^{-1}$ (more than 100 repeat units with the molecular weight of each unit to be 162.14 $gmol^{-1}$), Equation 5 was assumed to be valid in this case.

The values for average SRE, $\overline{M_c}$ and ρ_x for a hydrogel with a CM-dextran weight ratio of 0.15 at pH 7.4 shows a larger degree of error as the hydrogels were damaged during the experiment. This was probably due to a reduction in mechanical strength of the gel as swelling increased.

pH 3						
Variation		Average SRE	Average polymer fraction of gel, $v_{2,r}$	Average polymer fraction of swollen gel, $v_{2,s}$	Number average molecular weight between crosslinks, $\overline{M_c}$ (10^4) g/mol	Cross-linking density,ρ_x (10^{-5}) mol/cm^3
CM-dextran weight ratio (w/g)	0.07	1.1911	1.1911	0.0589	5.5336	2.9147
	0.1	1.1645	1.1645	0.0857	2.7149	5.9410
	0.12	1.1737	1.1737	0.1025	1.8681	8.6341
	0.15	1.3349	1.3349	0.1138	1.6192	9.9610
glucose number/ COOH	43.5	1.5404	0.1003	0.0184	8.1786	1.9721
	12	1.3390	0.1003	0.0191	7.7750	2.0745
	9.5	1.2672	0.1007	0.0194	7.6420	2.1106
	8.8	1.8075	0.1000	0.0175	8.6936	1.8553
EDC/NHS ratio	6	1.3768	0.1008	0.0190	7.8609	2.0518
	7	1.2672	0.1007	0.0194	7.6420	2.1106
	10	1.3321	0.1005	0.0191	7.7680	2.0763
Molecular weight	480	1.5047	0.0999	0.0185	8.1011	1.9910
	2000	1.3730	0.1003	0.0190	7.8478	2.0552

Table 5.1: Tabulated values of SRE, $\overline{M_c}$ and ρ_x for network analysis of CM-dextran hydrogels at pH 3

All the hydrogels demonstrated an average SRE in the range of 1.2 to 1.8 in solutions of pH 3 and a range of 1.4 to 2.6 in buffer solutions of pH 7.4. Since the SREs of

conventional hydrogels range from 1.5 to over 1000 (Martin *et al.*, 1998) the comparatively low swelling ratios indicate that the CM-dextran hydrogels do not have superior hydrophilicity. Such a characteristic would be disadvantageous in applications where quick release or separations of materials is needed. However, this characteristic could be advantageous in applications whereby low water uptake is necessary.

pH 7.4						
Variation		Average swelling ratio	Average polymer fraction of gel, $v_{2,r}$	Average polymer fraction of swollen gel, $v_{2,s}$	Number average molecular weight between crosslinks, $\overline{M_c}$ (10^4) g/mol	Cross-linking density,ρ_x (10^{-5}) mol/cm^3
CM-dextran weight ratio	0.07	1.4502	1.4502	0.0474	8.4776	1.9025
	0.1	1.4224	1.4224	0.0702	4.5051	3.5802
	0.12	1.5190	1.5190	0.0798	3.6921	4.3685
	0.15	1.8387	1.8387	0.0768	4.4395	3.6331
glucose number/ COOH	43.5	1.8412	0.0996	0.0174	8.7512	1.8431
	12	1.5027	0.1000	0.0185	8.0976	1.9918
	9.5	1.7300	0.0991	0.0177	8.5284	1.8912
	8.8	2.5920	0.0996	0.0154	10.1338	1.5916
EDC/NHS ratio	6	1.9047	0.1007	0.0172	8.8804	1.8163
	7	1.7300	0.0991	0.0177	8.5284	1.8912
	10	1.8325	0.1009	0.0175	8.7459	1.8442
Molecular weight	480	1.7194	0.0999	0.0178	8.5198	1.8931
	2000	1.4855	0.1003	0.0186	8.0726	1.9980

Table 5.2: Tabulated values of SRE, $\overline{M_c}$ and ρ_x for network analysis of CM-dextran hydrogels at pH 7.4

The significantly larger swelling ratios demonstrated when immersed in pH 7.4 phosphate buffer solution are in accordance with the expected pH sensitivity of the hydrogels. When the environmental pH is above the pKa (5.6-6.0) of the ionizable group (carboxylic acid), the group loses its proton. The formation of negative charges on the polymer backbone results in an increase in hydrophilicity of the polymer

chains. Increased electrostatic repulsion and counterion diffusion into the hydrogel to maintain gel electroneutrality further increases the driving force for water diffusion into the gel.

The inverse relationship between $\overline{M_c}$ and ρ_x is calculated according to Equation 6 and illustrated in Figure 5.2.

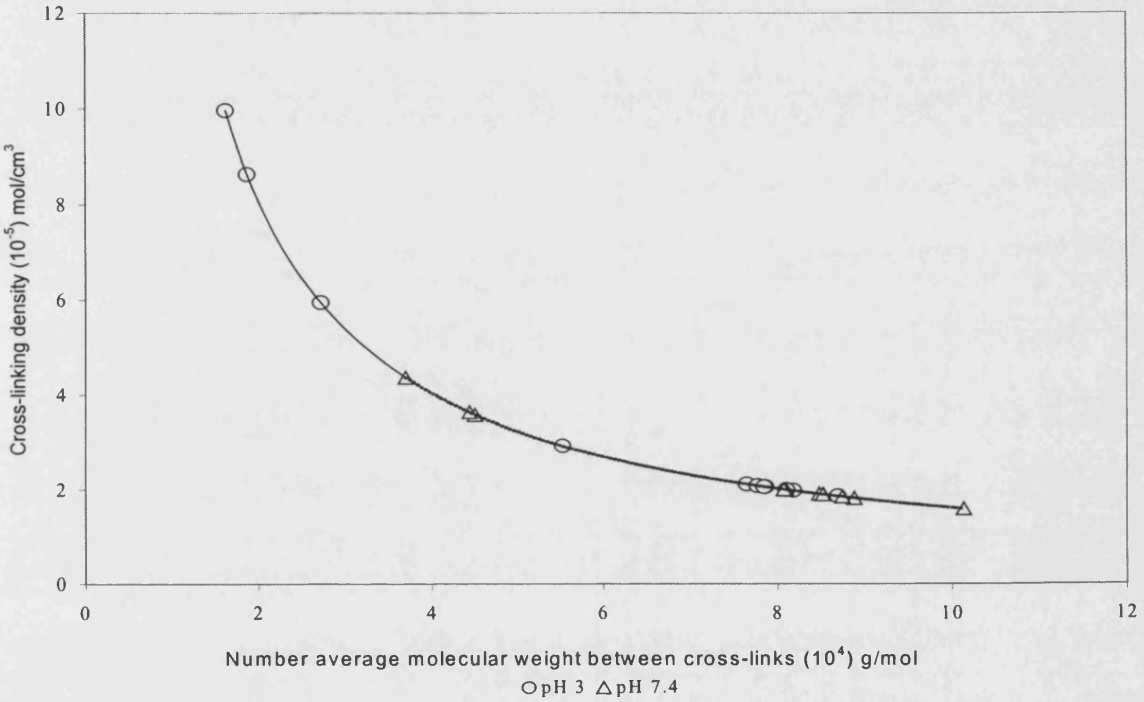

Figure 5.2: Dependence of ρ_x on $\overline{M_c}$.

This relationship is non-linear and approaches an asymptote value. This could be explained by the fact that for gel formation, a huge macromolecular network needs to permeate the whole system. This could only be achieved if sufficient cross-linkages were formed between the polymers.

In addition, the cross-linking density is affected by pH changes, with higher values and larger ranges when exposed to a higher pH (i.e. pH 7.4). This is again in accordance with the expected pH sensitivity of the hydrogels.

The dependence of SRE and $\overline{M_c}$ on CM-dextran weight ratio is illustrated in Figure 3. The CM-dextran weight ratio increases (or the concentration of monomers present during hydrogel formation) while the length of carboxymethylation reaction and amount of EDC/NHS cross-linking agent remained constant.

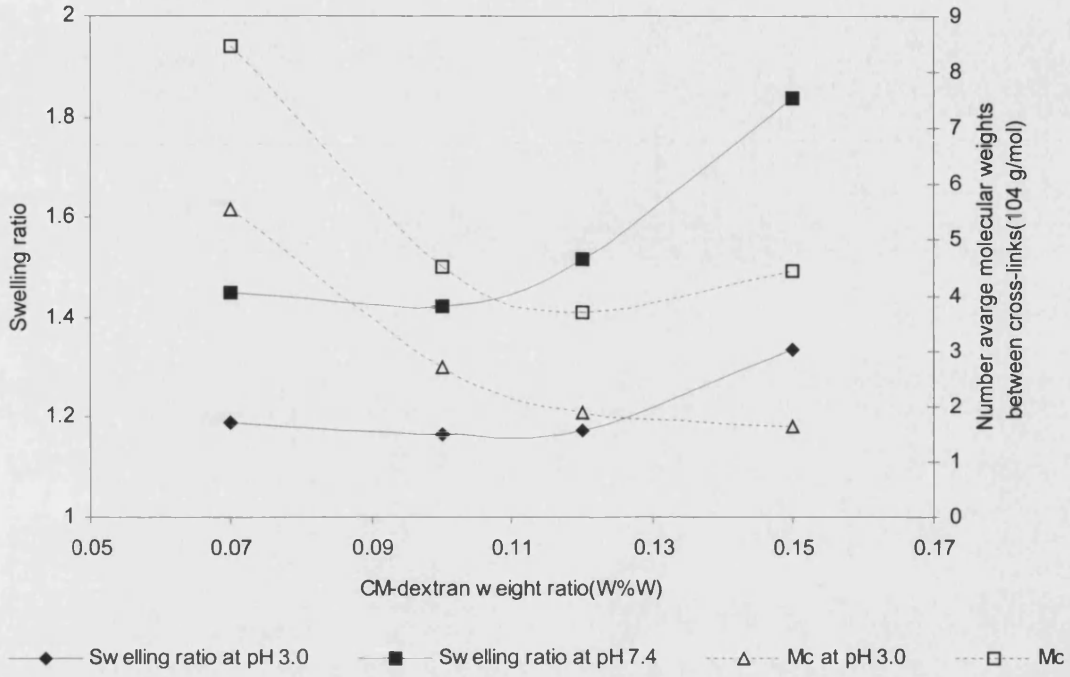

Figure 5.3: Dependence of SRE and $\overline{M_c}$ on the number of CM-dextran monomers present for the formation of the CM-dextran hydrogels.

The increased opportunity for formation of intermolecular cross-linkages as the concentration of monomers increased resulted in the decrease of $\overline{M_c}$ as the CM-dextran weight ratio increased. This trend is similar for both pH values investigated. (Note that the values for CM-dextran weight ratio of 0.15 at pH 7.4 are subject to a larger degree of error due to damage to the gels when compared to the rest of the readings.)

As $\overline{M_c}$ decreased, it was expected that the formation of a highly cross-linked network structure would experience a larger elastic restrictive force of the polymer network and hence show less swelling. However, results from the experiment indicated otherwise.

Increased intermolecular bonding results in closer proximity of neighbouring polymer chains. As a result of increased proximity, electrostatic repulsion between neighbouring carboxylic groups increased. This causes the polymer chain to further uncoil, creating additional osmotic pressure difference across the gel that increases water uptake.

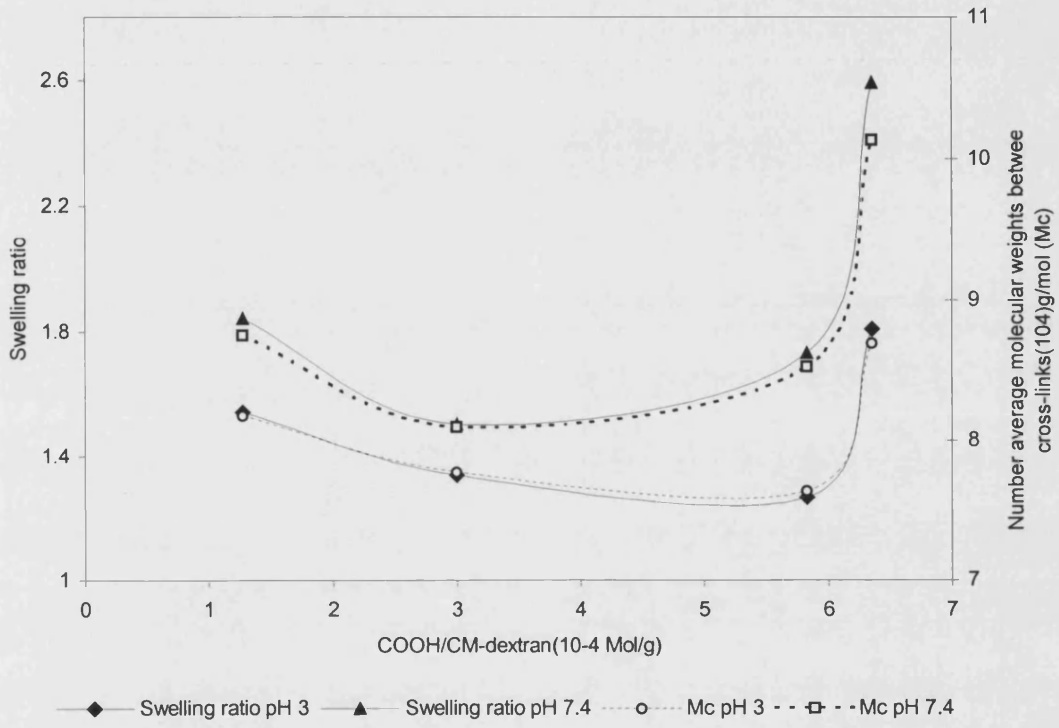

Figure 5.4: Dependence of SRE and $\overline{M_c}$ on COOH number in CM-dextran used in the formation of the CM-dextran hydrogels

It is noted that when the weight ratio was increased from 0.07 to 0.1, $\overline{M_c}$ dropped by about 3000 g/mol while the swelling ratio of the hydrogels remained constant. When the weight ratio of CM-dextran was increased to 0.12, $\overline{M_c}$ decreased by 1000g/mol and further increase in weight ratio reduced $\overline{M_c}$ by about 200g/mol. Over the same region, an increase in the rate of swelling ratio increase is observed. This indicated that a weight ratio of 0.1 might be the optimum proportion for the formation of cross-linkages. Beyond this ratio, the rate of cross-linkage formation is reduced. As more free COOH groups are present to interact with the medium, a greater swelling ratio is observed.

The dependence of SRE and $\overline{M_c}$ on COOH numbers in CM-dextran is illustrated in Figure 5.4. When CM-dextrans with a different number of COOH groups were used to form CM-dextran hydrogels, the concentration of the monomers and cross-linking agents used remained constant. The results indicated that there is an optimum COOH number in CM-dextran for cross-linkages formation. This conclusion is based on observing the change in $\overline{M_c}$ and SRE. At pH 7.4, the driving forces for water diffusion into the hydrogels were more significant than the effect of increased elastic restrictive force due to increased cross-linkages. This resulted in increased swelling. However, at pH 3, the opposite effect dominated and thus less swelling was observed. Therefore, at a weight ratio of 0.1 and ratio of 7 EDC/NHS, the optimum COOH numbers for maximum cross-linkage formation lies between 2-5 COOH/CM-dextran (10^{-4} Mol/g).

The dependence of SRE and $\overline{M_c}$ on the proportion of EDC to NHS cross-linking reagents is illustrated in Figure 5.5. The co-polymerization/cross-linking mechanism consists of four steps: initiation, propagation and cross-linking, termination by combination and disproportionate, and chain transfer to monomer (Peppas, 1986). EDC is required in the initiation of the polymerization reaction while NHS is required in the formation of a more stable intermediate for the propagation step. NHS is eliminated when the intermediate forms an ester bond with other carboxymethyl groups or when hydrolysis occurs. Thus the ratio of EDC/NHS is critical to the formation of the hydrogel.

When the EDC/NHS ratio is low (EDC: NHS 1:1 or 1:2), gelation does not take place. This implies that formation of an infinite network was not possible. At pH 7.4, the carboxymethyl groups are ionized, increasing the kinetics of the ester reaction. However, competitive hydrolysis of the EDC and NHS complexes is also enhanced (Nakajima *et al.*, 1995). The failure to form an infinite network might be due to a lack of carboxymethyl groups to form ester linkages before hydrolysis of the EDC/NHS complex take place. At higher EDC/NHS ratios, the optimum number of cross-linkages formed is highly dependent on the ratio of the cross-linking agents. For the proportion and type of CM-dextran used in this experiment (weight ratio of 0.1 and

CM-dextran with 5-COOH/CM-dextran (10^{-4} Mol/g)), the optimum proportion of weight is 7 EDC to 1 NHS.

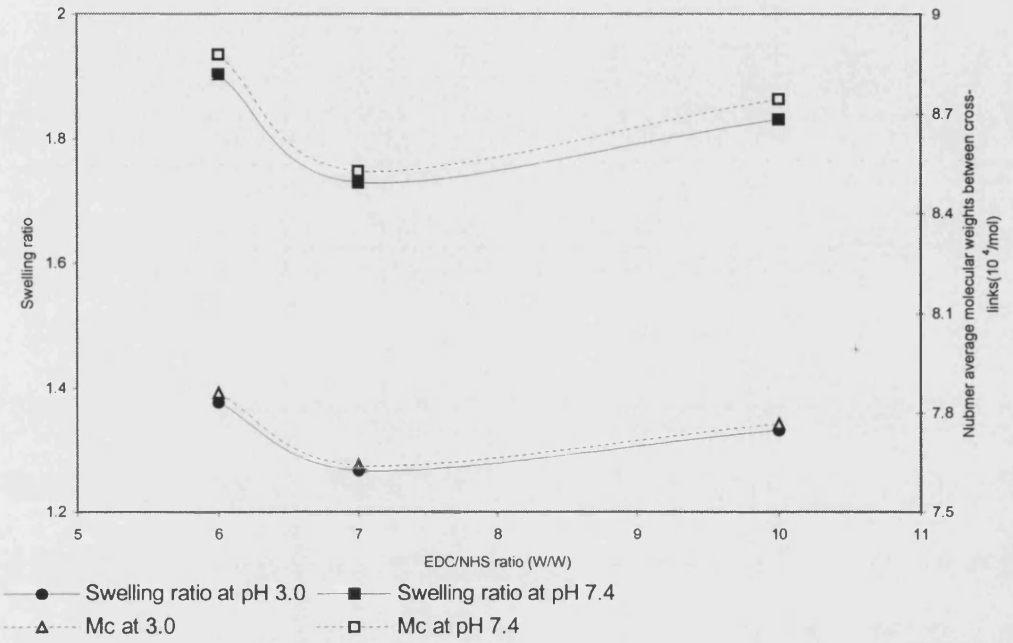

Figure 5.5: Dependence of SRE and $\overline{M_c}$ on the proportion of EDC to NHS cross-linking reagents used in the formation of CM-dextran hydrogels.

The dependence of SRE and $\overline{M_c}$ on the molecular weight of dextran is illustrated in Figure 5.6. As the molecular weight of the dextran molecule was increased from 482,000 Da to 2,000,000 Da, both $\overline{M_c}$ and SRE decreased. This was probably due to an increase in the formation of entanglements as a higher molecular weight of dextran was used. A similar trend was also reported by Hovgaard - Brondsted (Reinhart *et al.*, 1981) when investigating the suitability of dextran hydrogels cross-linked with diisocyanate for colon-specific drug delivery.

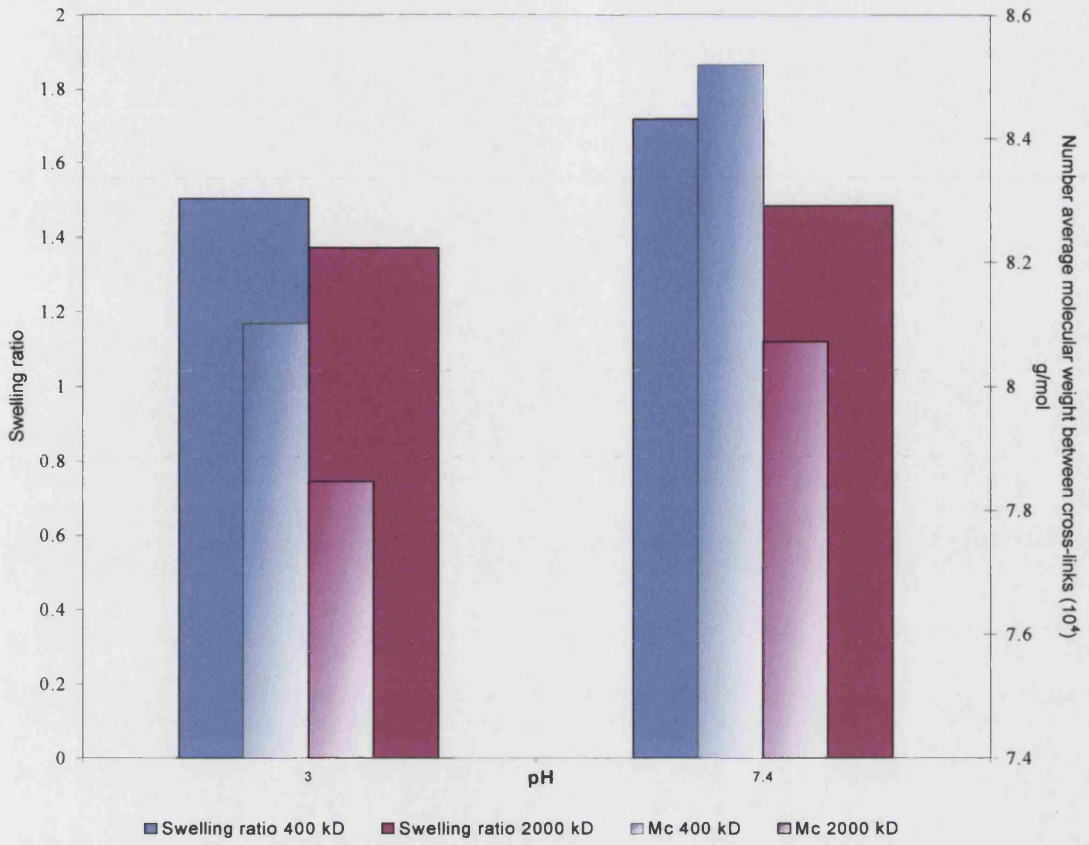

Figure 5.6: Dependence of SRE and $\overline{M}_c$ on the molecular weight of dextran used in the formation of the CM-dextran hydrogels.

5.4.2 Mass Transfer and Releasing Properties via Protein Studies

According to Lino Ferreira *et al.*(2002), the average mesh pore size for dextran-containing hydrogels synthesized by enzymes showed a correlation with the monomer concentration and the degree of substitution of the dextran molecules. For an initial monomer concentration of 8 weight to volume percentage (w/v %), the average mesh size calculated ranged from 0.49nm to 1.82nm depending on the degree of substitution, while the values ranged from 0.23nm to 0.52nm for an initial monomer concentration of 20%. In general, as the reaction time and concentration of monomer increased, a decrease in the average mesh pore size was observed.

For this study, the CM-dextran used was between the ranges used in the experiment conducted by Lino Ferreira. (Since 1 ml of water is approximately equal to 1 cm^3 of water, a weight ratio of 0.15 is equal to a 0.15 w/v). For a maximum ratio of 15 w/v (%), we can predict that the minimum average mesh pore size for CM-dextran

hydrogels is at least 0.34nm. (Note: pore diameter can be roughly estimated at 900 nm based on the SEM structure shown in Chapter 4). For the protein-related experiments, cytochrome C was selected as the protein to be used as it is extremely water soluble, stable and has a relatively small size: 0.34nm.

Results of the protein loading experiment were treated according to Equations 8 and 9 whereby the amount of protein that diffused into the gel was normalized by the amount of CM-dextran in the hydrogel. This method was favoured over 'concentration of protein in the gel' as the hydrogel volume was changing continuously over time due to swelling effects. Fitting the protein/CM-dextran results against time, it was found that the loading studies could be best fitted to a sigmoidal plot. The results for an initial protein solution of 0.197 mg/ml for different CM-dextran weight ratio used is illustrated in Figure 5.7. For plots of protein/CM-dextran at 25^0C and pH 7.4 against time for different hydrogel compositions, with initial protein concentrations of 0.197 mg/ml and 0.410 mg/ml.

The sigmodial fit implies that the rate of protein diffusion into the CM-dextran hydrogels increased and then decreased. Initially, the CM-dextran hydrogels were in a relaxed state. When the buffer solutions were placed above the gel, interaction between the COOH groups and water resulted in the swelling effect that increased the mesh sizes, leading to an increase in diffusion rate.

At pH 7.4, the cytochrome C protein is positively charged as the pH is below its isoelectric point of 10.2. As the protein diffuses into the hydrogel, it binds to the negatively charged COOH groups, hence reducing electrorepulsion effects between the charged COOH groups. Together with a reduction in the driving force due to less protein molecules in the buffer solutions, the rate of diffusion decreases gradually and equilibrium is reached.

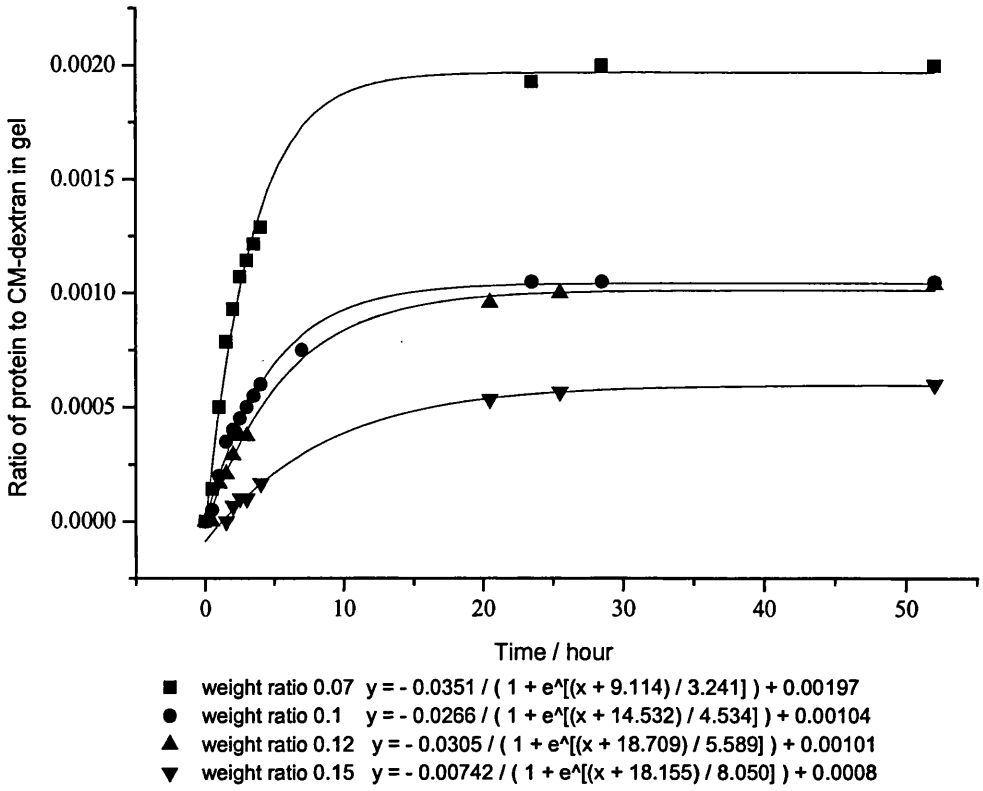

Figure 5.7: Plot of protein/CM-dextran at 25^{0}C and pH 7.4 in CM-dextran hydrogels of different weight ratios over time with initial protein concentration of 0.197mg/ml.

Since we are interested in finding the overall permeability, *k'*, of the protein in the hydrogel according to Fick's law, for nonporous, homogeneous, polymeric hydrogels, the system can be represented by Equation 9. Using 'Scentist', computer fitting of the experimental results to find *k'* resulted in Equation 10. Iteration was carried out by Excel and the calculated hydrogels' permeability coefficient, *k'*, are tabulated in Table 5.3.

SRE, $\overline{M_c}$ and ρ_x are characteristics of the hydrogels. Since the composition of the gels remained the same (except for the hydrogel formed from 10 COOH/CM-dextran (10^{-4} Mol/g)), they are assumed to be same as the results obtained in the first experiment. The $\overline{M_c}$ and ρ_x for hydrogel formed from 10 COOH/CM-dextran (10^{-4} Mol/g) are based on extrapolation from existing data.

Variation		Hydrogel permeability coefficient (Initial protein concentration (g/cm^3)) cm^{-2} s^{-1}				Swelling ratio	Number average molecular weight between crosslinks, $\overline{M_c}$ (10^4) g/mol	Cross-linking density, ρ_x (10^{-} mol/cm^{-}
		k' (0.197)	R^2	k' (0.410)	R^2			
CM dextran weight ratio	0.07	0.3027	2.574E-08	0.4048	2.526E-07	1.4502	8.4776	1.9025
	0.1	0.2268	6.96E-08	0.3027	1.79E-08	1.4224	4.5051	3.5802
	0.12	0.1508	8.21E-09	0.2354	2.20E-08	1.5190	3.6921	4.3685
	0.15	0.0591	5.17E-09	0.1374	2.64E-08	1.8387	4.4395	3.6331
glucose number/ COOH	43.5	0.1374	2.37E-08	0.2882	3.20E-08	1.8412	8.7512	1.8431
	12	0.2268	6.96E-08	0.3027	1.79E-08	1.7300	8.5284	1.8912
	8.5	0.2888	4.35E-08	0.3187	4.77E-08	NA	97.896	0.1647
EDC/NHS ratio	6	0.2559	1.75E-08	0.4480	4.02E-08	1.9047	8.8804	1.8163
	7	0.2268	6.96E-08	0.3027	1.79E-08	1.7300	8.5284	1.8912
	10	0.2099	1.12E-08	0.3307	1.11E-08	1.8325	8.7459	1.8442

Table 5.3: CM-dextran hydrogel permeability coefficient, k', calculated based on computer fitting to Fick's law.

The dependence of the hydrogel permeability coefficient on the cross-linking density for an initial protein concentration of 0.197 mg/ml at pH 7.4 is examined in Figure 5.8. As the weight ratio of CM-dextran was increased, the cross-linking density increased. An increased in cross-links implies that the number of junction points increased. As the diffusing molecule faces increasing barriers, or an increased screening effect, the solute diffusion coefficient in the polymer, D_{im}, would decrease, leading to a smaller value in the hydrogel permeability coefficient. This effect was also observed by Reinhart *et al* who studied the diffusion of proteins and drugs through amorphous cross-linked hydrogels (Reinhart *et al.,* 1981).

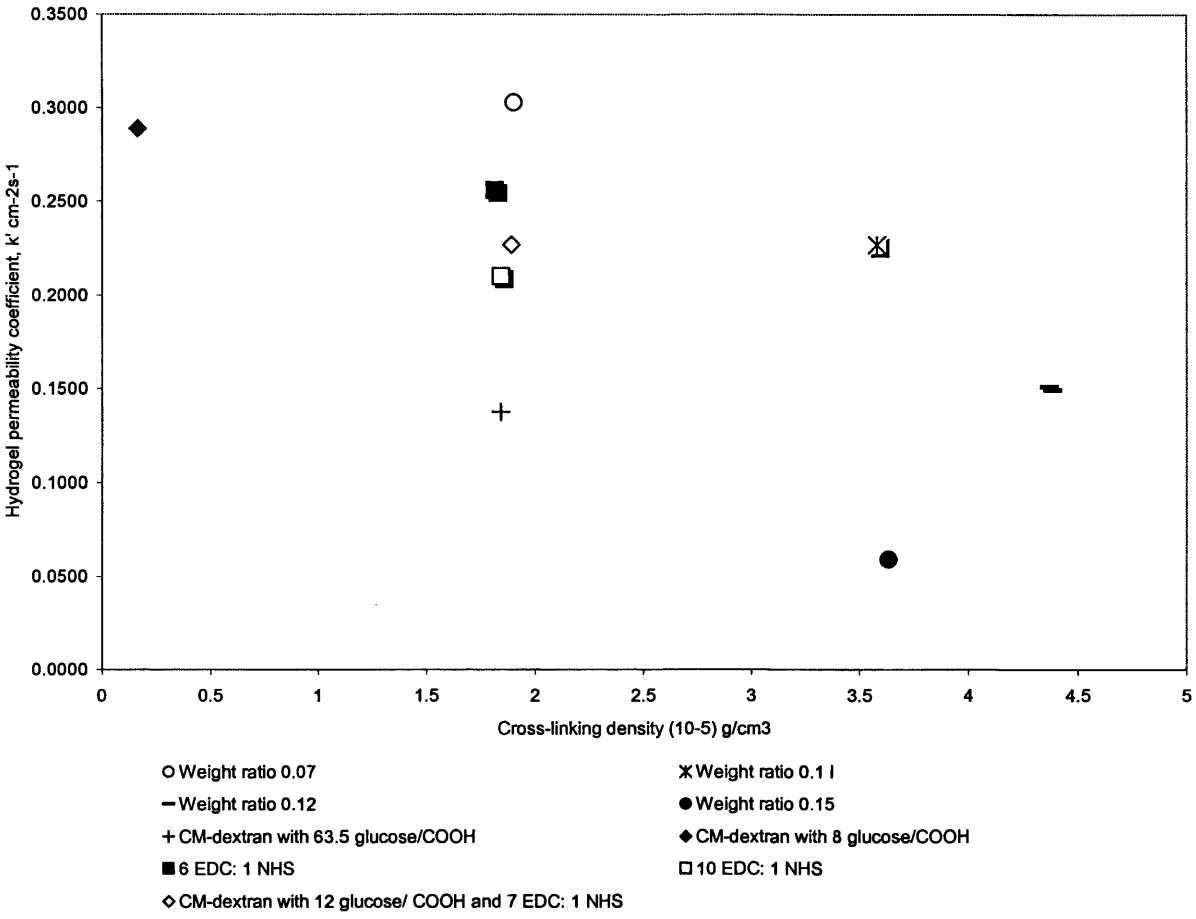

Figure 5.8: Dependence of k' on ρ_x

Based on earlier studies for the weight ratio of CM-dextran and ratio of EDC/NHS used at pH 7.4, an optimum cross-linking density is achieved with a 2-5 COOH/CM-dextran(10^{-4} Mol/g). With all other factors remaining constant, an increased number of COOH groups attached resulted in an increased swelling ratio.

In this study, CM-dextran with a 5 COOH/CM-dextran (10^{-4} Mol/g) was used. This implied that there would be an increased ratio of 'free' COOH groups. Under alkaline conditions, the carboxymethyl groups become protonated and carry negative charges, leading to an increased swelling ratio. This implies that the mesh size of the polymer may have increased.

Under these conditions, the cytochrome C molecules carry a positive charge as the environmental pH is below that of its isoelectric point. Stronger attraction between

the cytochrome C molecules and the dextran backbone resulted in an increase in the solute partition coefficient, K_i, while increased mesh for diffusion resulted in an increase in the solute diffusion coefficient, D_{im}. This lead to an increase in hydrogel permeability coefficient, k'.

The increased in K_I is large enough to compensate for the increased sieving effect of the cross-linkages. This is reflected in the close k' values of CM-dextran hydrogels with a 6COOH/CM-dextran (10^{-4} Mol/g) and when a low weight ratio of CM-dextran is used. Based on earlier studies for the composition of CM-dextran used, an optimum proportion of EDC/NHS for cross-linking is 7:1. As expected, k' decreased as cross-linking increased.

The computer fit to Fick's law, Equation 10, provided a crude estimate of k' for cytochrome C. Besides diffusion, the fit does not account for the charge attraction between the protein and COOH groups and the swelling effect of the CM-dextran hydrogel that would have affected the rate of protein diffusion into the hydrogel.

In this study, the hydrogel is loaded with cyctochrome C while it is in a swollen state. It is then placed in environments in which the pH is either equivalent to or lower than the original environment. Upon contact with the new environment in which the pH is lower, the polymer matrix begins to contract. As a result, the rate in which the protein diffuses out of the polymer will be controlled by the rate of polymer 'contraction'. Such a protein release mechanism is referred to as a swelling-controlled system (Peppas *et al.*, 2000).

A simple expression given by Equation 11 was chosen over the more complex models as it is sufficient to correlate and evaluate the release data for $\frac{M_t}{M_\infty} \leq 0.7$ in most experiments (Sinclair *et al.*, 1981). The treated results for the protein release at different pH for different CM-dextran weight ratio used are tabulated in Table 5.4 – 5.6.

pH	CM-dextran weight ratio	Gradient (n)	y-intercept	K	R^2
3	0.07	0.4112	-0.3945	0.4032	0.9954
	0.1	0.4085	-0.4174	0.3825	0.9961
	0.12	0.4025	-0.4402	0.3629	0.993
	0.15	0.463	-0.4591	0.3475	0.9981
5.5	0.07	0.438	-0.4166	0.3832	0.9884
	0.1	0.4548	-0.4486	0.3560	0.9968
	0.12	0.435	-0.445	0.3589	0.9963
	0.15	0.4373	-0.4762	0.3340	0.9967
7.4	0.07	0.4305	-0.4212	0.3791	0.9836
	0.1	0.495	-0.4776	0.3330	0.9835
	0.12	0.4425	-0.4632	0.3442	0.9767
	0.15	0.4013	-0.476	0.3342	0.9753

Table 5.4: Tabulation of K and n proportionality constants as obtained by computer fitting for CM-dextran hydrogels with different CM-dextran weight ratios

As is evident from the high values of correlation coefficients of the linear regression of ln $(\frac{M_t}{M_\infty})$ against ln t plots ($R^2 > 0.99$ for most situations), the quality of the data obtained is high. Since most of the obtained n values were below $n < 0.5$, according to Peppas, (Fisher *et al.*, 1960) for protein release through a slab, this indicates that another process in addition to diffusion occurs.

pH	D-glucose/COOH	Gradient (n)	y-intercept	k	R^2
3	43.5	0.4327	-0.4227	0.3778	0.9962
	12	0.4085	-0.4174	0.3825	0.9961
	8.5	0.477	-0.461	0.3459	0.9939
5.5	43.5	0.4117	-0.4063	0.3924	0.9985
	12	0.4548	-0.4486	0.3560	0.9968
	8.5	0.4318	-0.467	0.3412	0.9975
7.4	43.5	0.3828	-0.4036	0.3948	0.9855
	12	0.495	-0.4776	0.3330	0.9835
	8.5	0.4901	-0.5	0.3162	0.9879

Table 5.5: Tabulation of K and n proportionality constants as obtained by computer fitting for CM-dextran hydrogels with different amount of COOH

pH	EDC/NHS ratio	Gradient (n)	y-intercept	k	R^2
3	6:1	0.4375	-0.4352	0.3671	0.9932
	7:1	0.4085	-0.4174	0.3825	0.9961
	10:1	0.3455	-0.4101	0.3890	0.9917
7.4	6:1	0.4264	-0.4228	0.3777	0.9930
	7:1	0.495	-0.4776	0.3330	0.9835
	10:1	0.4636	-0.4612	0.3458	0.9934

Table 5.6: Tabulation of K and n proportionality constants as obtained by computer fitting for CM-dextran hydrogels with different ratio of cross-linking agents

5.4.3 Biodegradability Studies

In most enzymatic degradation experiments, the rate of degradation of the hydrogels is evaluated based on the time for complete dissolution of the hydrogels. Methods of calculating the rate of degradation include the computation of the loss in the dry weight as a percentage of the initial dry weight, loss in height of the hydrogels and the

accompanied release of sugars from the gels (Stubbe *et al.*, 2001, Hovgaard *et al.*,1995).

In this study, degradation was measured by the rate of release of sugar from the hydrogel as dextran is hydrolysed by dextranase. This method was chosen as the small volume of the gel in the petri dish made it impossible to detect either the weight loss or the loss in height of the gel over time. Since a large amount of buffer (10ml) containing dextranese was placed into the petridish, the small amount of solution (~μl) lost during the analysis of the solution was negligible.

Dextranase belongs to a class of enzymes also known as glucanases, which can be classified as exo-glucanases or endo-glucanases. Based on Fisher and Stein, (1960) dextranase catalysed the endo-hydrolysis of the C-O and C-C bond by cleaving randomly along the dextran chain.

During the experiment, it was observed that the microbial degradation of the dextran gels proceeded from the surface of the gels. Such an observation is in accordance with the fact that dextranase might be sterically hindered from diffusing into the hydrogel. For the gel in which there was no exposure to dextranase, degradation of the gel did not occur during the time frame of the experiment

The dependence of enzymatic degradation on the weight ratio of CM-dextran is illustrated in Figure 5.9. The amount of glucose present in the system is related to the rate of enzymatic degradation. The faster the rate of degradation, the higher the amount of glucose present. Based on the slopes of the curves, the rate of enzyme degradation depended on the weight ratio used - the lower the weight ratio, the faster the rate of degradation. From earlier experiments, it was concluded that the cross-linking density increased as the weight ratios increased. As such, greater steric hindrance of the enzyme into the gel resulted in slower rates of degradation. Such a trend is in accordance with the ones observed by Marvis *et al* who reported a slower enzymatic degradation rate when cross-linking increased (Stubbe *et al.*, 2001).

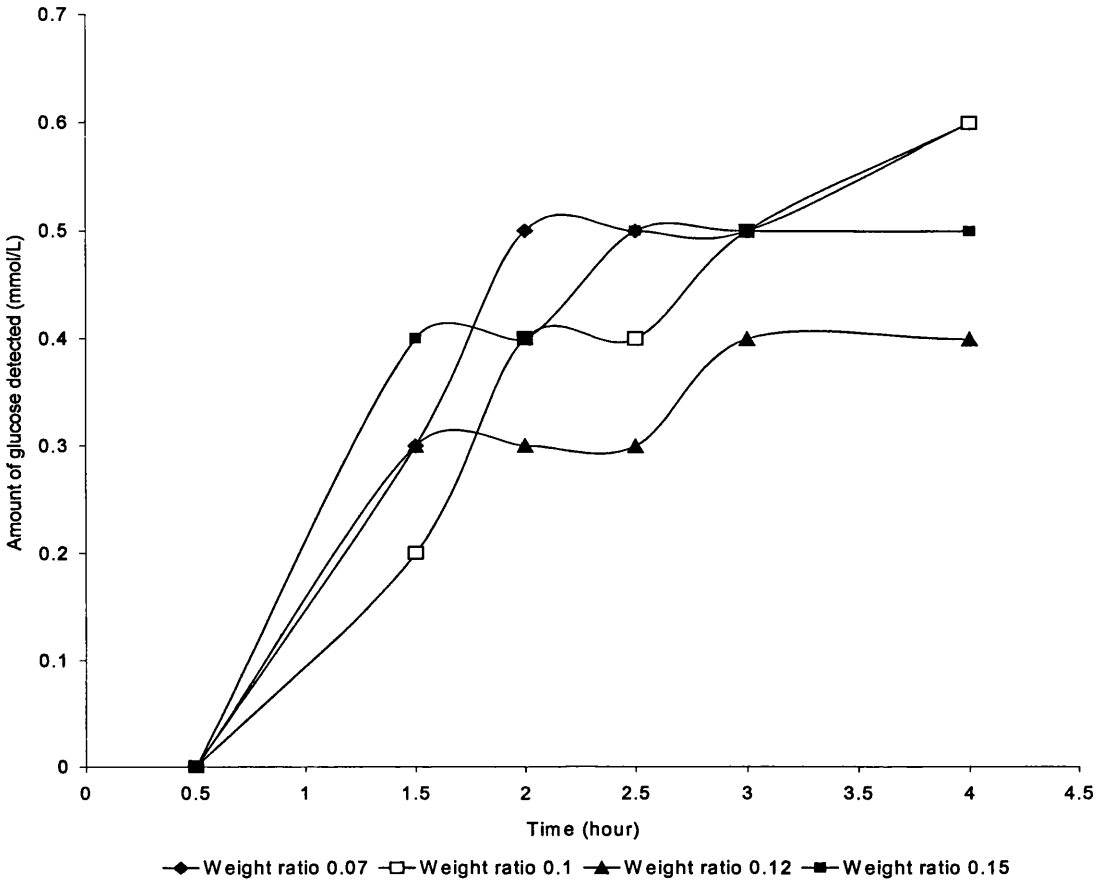

Figure 5.9: Dependence of enzyme degradation of CM-dextran hydrogels on the number of CM-dextran monomers present in the gel.

The effects described above were more pronounced when an enzyme with reduced activity was used in the degradation experiments, as illustrated by Figure 5.10.

At a temperature of 37^0C, bacterial activity is enhanced and the amount of NaN_3 present was insufficient to suppress bacterial growth. As a result, a competitive reaction between the production of glucose and the usage of glucose by bacteria is present. This is evident by the reduction of glucose to 0 in a timeframe of 2 hours and the noted increased in the level of carbon dioxide present in the system.

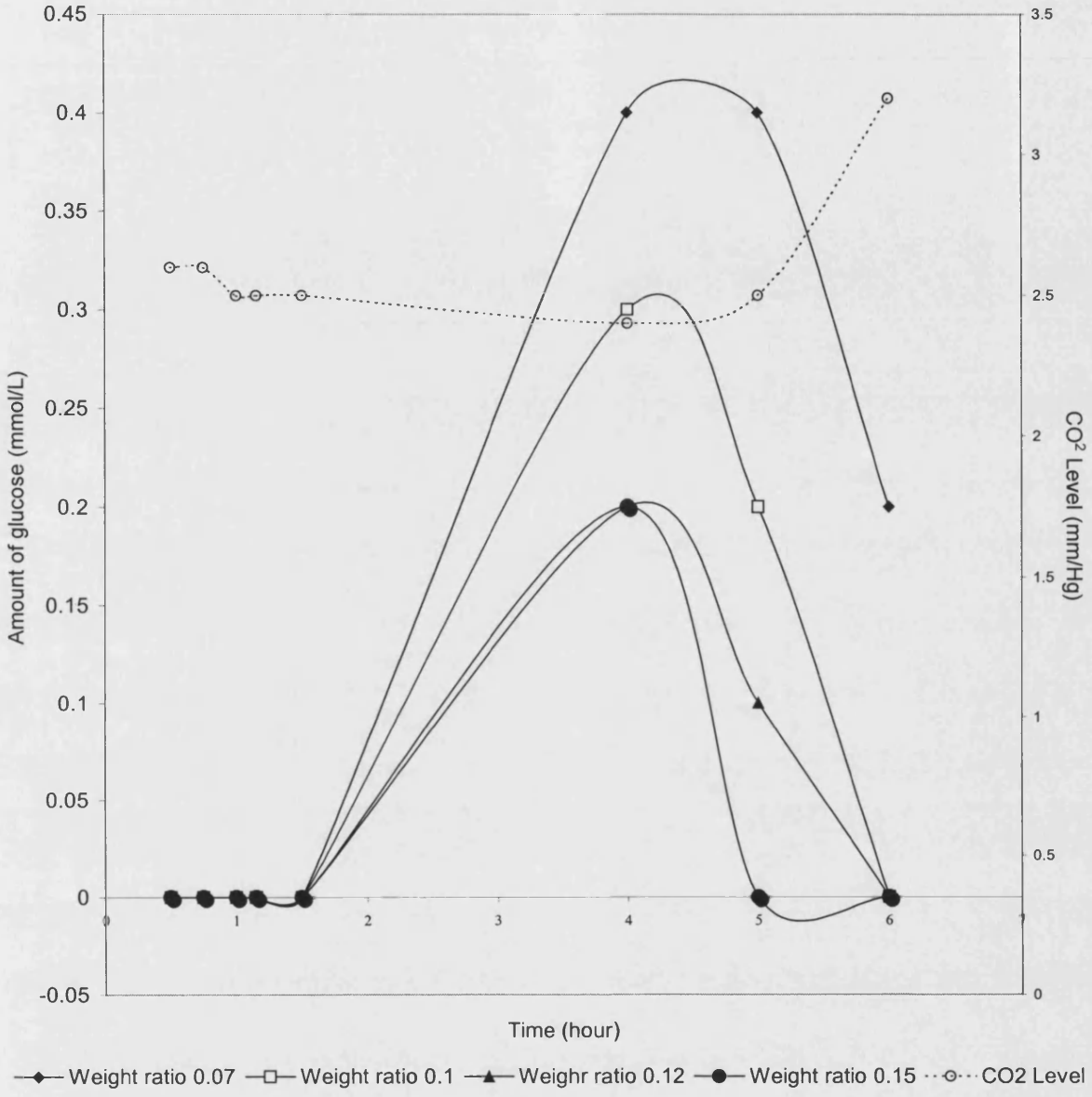

Figure 5.10: Dependence of reduced enzyme activity degradation of CM-dextran hydrogels on the number of CM-dextran monomers present in the gel.

The dependence of enzymatic degradation on COOH number in CM-dextran is illustrated in Figure 5.11. From the first experiment, it was concluded that the optimum COOH number in CM-dextran for the formation of maximum cross-linkages at pH 7.4 (all else constant) was 63.5 glucose/COOH. This was followed by the hydrogel from a 12 glucose/COOH. I would have expected that the rate of degradation to be the slowest at this point due to the formation of more cross-linkages hindering the diffusion of dextranase into the gel. However, results indicated that this

was not so. A possible explanation could be found in the recent findings of Franssen *et al* (Frannssen *et al.*, 1999) who indicated that the degradation of dextran by dextranase was via a 'two substrate model'. They suggested that the length of the chain segments of dextran affected the rate of degradation due to their different affinity to dextranase. A chain segment of eighteen or more unsubstituted glucose units had a much higher affinity for dextranase (primary substrate) compared to the shorter chain segments of six to eight unsubstituted glucose units (secondary substrate).

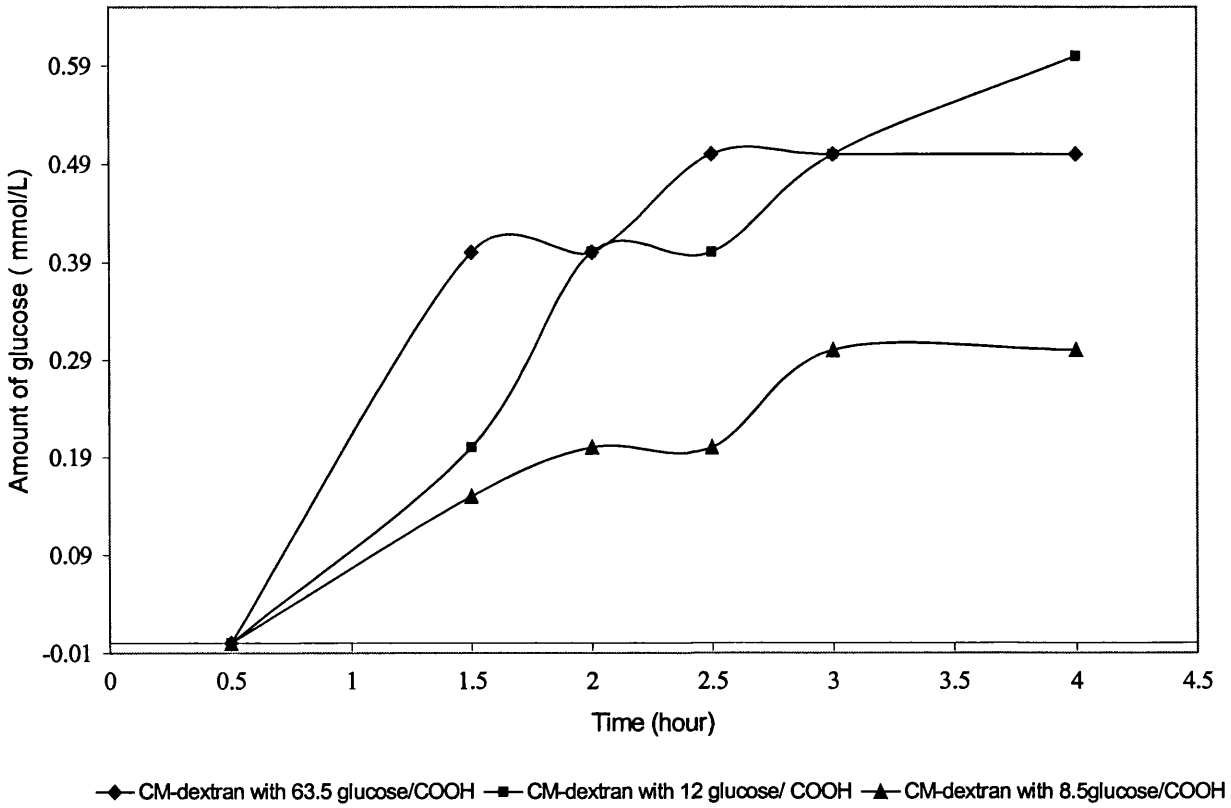

Figure 5.11: Dependence of enzyme degradation of CM-dextran hydrogels on COOH number in CM-dextran used in the formation of the gel

The dependency of enzymatic degradation of CM-dextran hydrogels on the proportion of EDC/NHS used in the formation of the gel is illustrated in Figure 5.12. The initial rate of increase was fastest at a ratio of 10 EDC/NHS and slowest at a ratio of the 7 EDC/NHS. This corresponded to earlier experimental results that indicated that the densest cross-links were formed at a proportion of 7 EDC/NHS (hence increased

steric hindrance). The overall rate of increase was slowest at a ratio of 6 EDC/NHS, which corresponded to the highest swelling ratio at 6 EDC/NHS. Since the isoelectric point of dextranase is 4.55 (http://www.worthington-biochem.com/DEX/default.html) the enzyme would be negatively charged at a pH of 7.4. The electrostatic repulsion between similarly charged molecules (i.e. COOH and dextranase) could have hindered the diffusion of the molecule into the gel, resulting in the slowest rate of initial increase.

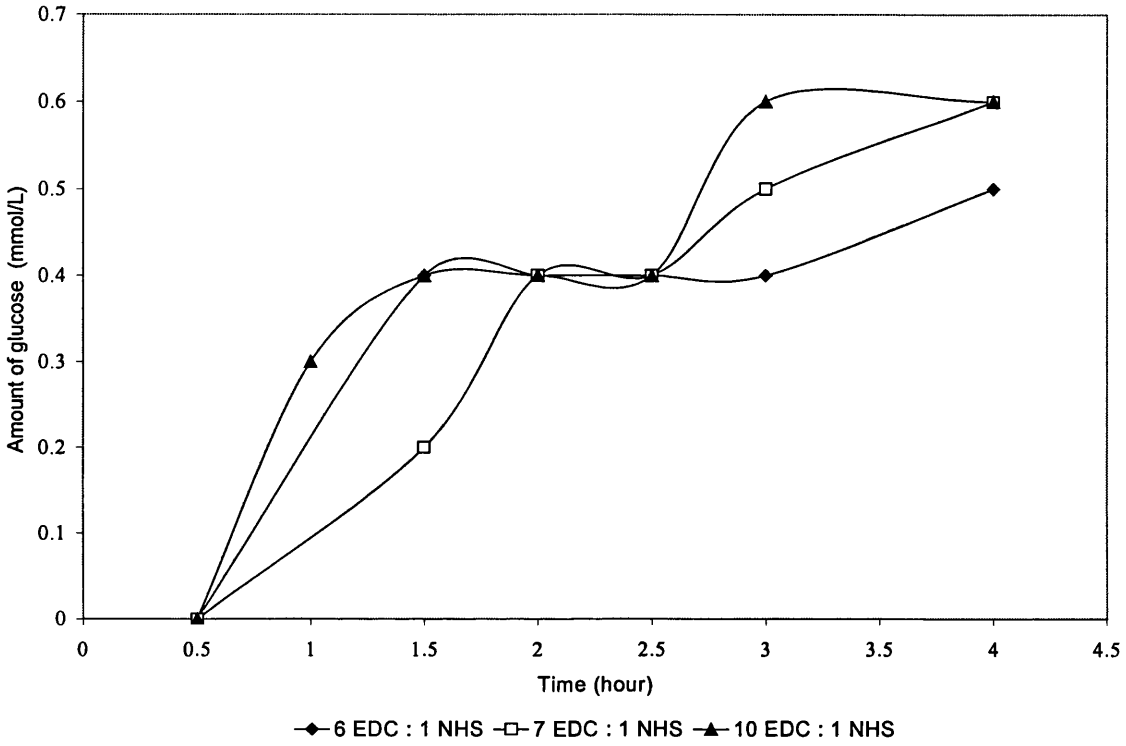

Figure 5.12: Dependence of enzyme degradation of CM-dextran hydrogels on the proportion of EDC/NHS cross-linking agent used in hydrogel formation

In addition, it was noted that the CM-dextran hydrogel degradation by dextrose was observed to phase change from gel to sol during first 4 hrs, after that, microbe contamination has more significant effect on the glucose detection. This suggests the CM-dextran hydrogel could be an effective biomaterial for drug release application.

5.5 Conclusions

The properties of the hydrogels produced are strongly determined by their network structure. In the analysis of the network structure of CM-hydrogel, equilibrium

swelling theory (Peppas, 1986) was used. The pH sensitivity of the CM-dextran hydrogels was shown. At higher pH, in addition to osmotic pressure, the driving force for water diffusion into the hydrogels was higher due to the following reasons:

(1) Ionization of COOH groups resulting in increased hydrophilicity;
(2) Increased electrostatic repulsion between neighbouring similarly charged molecules;
(3) Increased counter-ion diffusion into the gel to maintain electroneutrality.

These resulted in the observed higher swelling ratios (as given by Equation 2) of the hydrogels. It was noted that the hydrogels have a relatively low swelling ratio when compared to other synthesized hydrogels. This would give the CM-dextran hydrogels an advantage over other hydrogels in applications where mechanical strength and low water intake is required.

It was also concluded that for a CM-dextran with 5 COOH/CM-dextran (10^{-4} Mol/g) and a proportion of cross-linking agents at 7 EDC/NHS (W/W), a weight ratio of 0.10 (CM-dextran / hydrogel (W/W)) was the optimum for forming cross-linkages. Subsequent experiments were carried out while maintaining the other variables constant at these initial values. Variation in the proportion of cross-linking agents proved that the ratio of 7 EDC/NHS (W/W) was optimum for cross-linkages formation. Variation in the length of carboxymethylation reaction at 50 °C suggested that a timeframe of 20 minutes to 1.5 hours was the optimum for fabricating pH-sensitive hydrogel.

The movement of solutes through the hydrogel is through convection or diffusion, and the dominant effect is determined by the pore size available for mass transfer. As far as CM-dextran hydrogels are concerned, diffusion is the main transport effect. The hydrogel permeability coefficient, k', is dependent on 2 factors – the solute diffusion coefficient, D_{im}, and the solute partition coefficient, K_i. When calculating k', interaction between the solute and the polymer structure must be taken into account. In the treatment of the results, k' was calculated using Equation 10, which is a computer fit to Fick's law. The fit gave a rough estimate of the actual values of k'. This is due to an invalidity to take into account other factors, such as charge attraction

and gel swelling, which would have affected the transport process. In general, hydrogels with increased cross-linking have a lower k' value.

The fractional protein release experimental data were fitted to the Equation 11 and the proportionality constants – K and n, determined. The n values were all less than 0.5 with a correlation coefficient of the linear regression $R^2>0.99$ for most cases. The analysis by Peppas, who studied the values of exponent n as a means of identification of the transport mechanism of a solute through a polymer slab, suggested that this indicated that another process in addition to diffusion is taking place (Peppas, 1986). However, due to the limited data available, a further 95% confidence interval calculation would be necessary to support this point.

For the degradation of the CM-dextran hydrogels, the rate of degradation depended on the cross-linking density and charge forces between the enzyme and the unreacted COOH groups. When the hydrogel was least dense, the rate of degradation was highest. For intermediate densities, the rate of degradation would be a function of the interaction between the electrostatic repulsion between similar charged molecules (i.e. COOH and dextranese) and the mesh size.

Chapter 6. A Novel pH- and Ionic-Strength-Sensitive Carboxyl Methyl Dextran Hydrogel

6.1 Background

Stimuli-responsive hydrogels can exhibit dramatic changes in their swelling behaviour, network structure, permeability or mechanical strength in response to changes in the pH or ionic strength of the surrounding fluid, temperature, bimolecular and applied electrical or magnetic fields (Peppas, 2000). Because of their nature, these materials can be used in a wide variety of applications, such as separation membranes, biosensors, drug delivery devices and tissue engineering (Lee *et al.*, 2001).

All pH-sensitive polymers are produced by adding pendant acidic or basic functional groups to the polymer backbone; these either accept or release protons in response to appropriate pH and ionic strength changes in aqueous media (Qui *et al.*, 2001). The network porosity in these hydrogels is a result of electrostatic repulsion. For example, ionic hydrogels containing carboxylic or sulphuric acid show either sudden or gradual changes in their dynamic and equilibrium swelling behaviour as a result of changing the external pH (Katchalsky *et al.*, 1955, Peppas *et al.*, 1991). The degree of ionisation of these hydrogels depends on the number of pendant acidic groups in the hydrogel, which results in increased electrostatic repulsions between negatively charged carboxyl groups on different chains, as shown in Figure 6.1. This, in turn, results in an increased hydrophilicity of the network, and greater swelling ratios. On the other hand, a hydrogel containing basic pendant groups, such as amines, ionises extensively at low pH, also causing increased electrostatic repulsions.

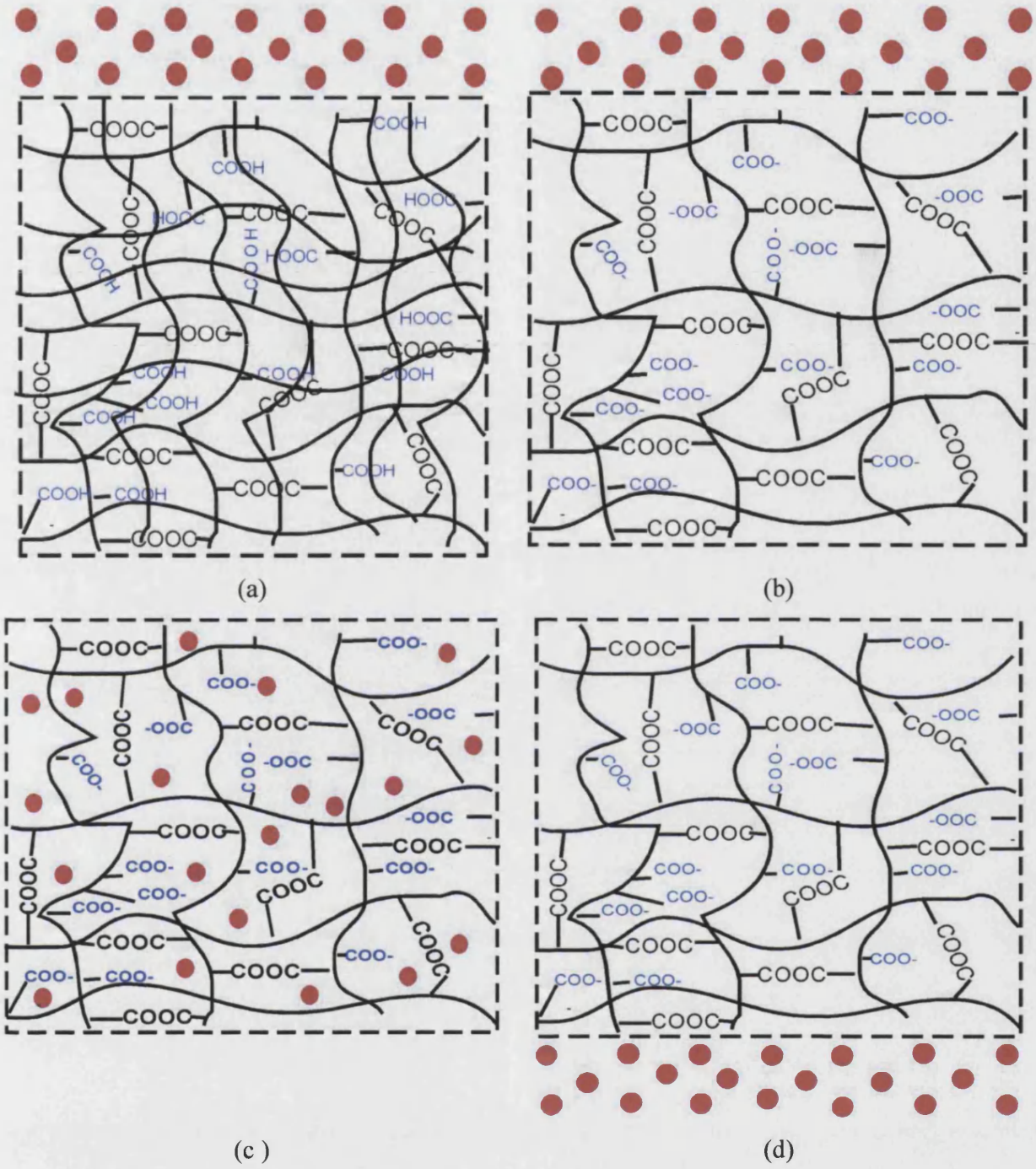

Figure 6.1: Schematic of the composite hydrogel (bold lines denote covalent links)

(a) Gel porosity reduced by cross-links in pH 5.5 that exclude protein. e.g. lysozyme

(b) The porosity increases in high pH leading to ionization of the carboxylic groups.

(c) Protein enters the more highly porous gel.

(d) Protein diffuses through the membrane.

Hydrogels currently used, or with potential applications, in drug delivery or tissue engineering are divided into two categories, according to their natural or synthetic origin. Hydrogels from various synthetic polymers have been widely investigated by using neutral co-monomers, such as 2-hydroxyethyl methacrylate, methyl methacrylate and maleic anhydride (Falamarzian *et al.,* 1988, Kuo *et al.* 1988, Brannon-Peppas *et al.,* 1990, Khare *et al.,* 1993). While considerable effort has been made to synthesize and characterize acrylate-based ionic hydrogels, these materials are not biologically degradable by either hydrolytic or enzymatic mechanisms. As a result, acrylate systems are limited in their potential as biodegradable drug-delivery platforms. To overcome this liability, a range of natural polymers has been used to prepare cross-linked hydrogel networks. For example, pH-sensitive hydrogels based on polypeptides, proteins and polysaccharides have all been produced (Chui *et al.,* 1999, Markland *et al.,* 1999).

However, limitations of hydrogels from natural polymers have motivated approaches to modify these polymers as well as to use various synthetic polymers. A wide range of synthetic polymers may potentially have suitable chemical and physical properties for these applications. Dextran is a polysaccharide mainly composed of 1,6-linked D-glucopyranose residues. Owing to their low tissue-toxicity and high enzymatic degradability at desired sites, dextran hydrogels have been frequently considered as a potential matrix system for drug delivery or controlled release of bioactive agents (Chui *et al.* 2002). Several approaches to the preparation of dextran hydrogels have been adopted. Hydrogels were prepared directly by cross-linking dextran with either 1,6-hexanediisocyanate or glutaraldehyde (Hovgaard *et al.,* 1995, Bronsted *et al.* 1998). Sequential reactions of dextran with glycidyl acrylate, followed by polymerization of acrylated dextran also led to the formation of the polymer network (Yamamoto *et al.* 1996). Methacrylation of dextran has been conducted with full control of the degree of substitution by transesterification of glycidyl methacrylate with dextran in dimethyl sulphoxide (Van Dijk-Wolthius *et al.* 1995, Van Dijk-Wolthius *et al.* 1997). Kim and Chu (2000) and Kim *et al.* (1999) obtained dextran hydrogels by UV irradiation of methacrylated and acrylated dextrans that were synthesized by reacting dextran with methacrylic anhydride, and then bromoacetyl bromide and sodium acrylate. Recently, Chiu *et al.* (2002) have reported dextran hydrogels prepared by radical copolymerization of methacrylate-dextran with acetic

anhydride in borate buffer at room temperature, using ammonium peroxydisulfate and N,N,N',N'-tetramethylethylenediamine as an initiation system.

Chapter 3 reported the synthesis of a D-glucose-sensitive dextran hydrogel and demonstrated that the release of proteins (insulin, lysozyme, and BSA) from this hydrogel varied with D-glucose concentration (Tang *et al.* 2003). It was also shown that hydrogels synthesized by grafting Cibacron Blue and lysozyme to dextran can yield a reversible and specific controlled release of both cytochrome C and haemoglobin in response to changes in environmental NAD concentration (Tang *et al.* 2002). This chapter reports the synthesis of a novel pH-responsive dextran hydrogel produced by the intermolecular cross-linking of carboxymethyl dextran (CM-dextran) using 1-Ethyl-(3-3-dimethylaminopropyl) carbodiimide hydrochloride (EDC) and N-hydroxysuccinimide (NHS). In view of the toxicity of the crosslinking agent in the work reported here, EDC was used for preference as it is not incorporated into the cross-linked structure, but is simply changed to a water-soluble urea derivative. The cytotoxity of the urea derivative has been found to be quite low compared with that of EDC (Benslimane *et al.* 1988). The hydrogel described here is formed by ester bonds between hydroxyl and carboxyl in CM-dextran in the presence of EDC and NHS. In this respect the synthesis method is similar to that of Tomihata and Ikada (1997) who synthesised an uncharged hydrogel for tissue engineering applications. The primary targets here are to demonstrate that pH-sensitive hydrogel membranes can be produced by including an excess of carboxylic groups, that these change their porosity reversibly in response to changes in environmental pH, and that this response can control the delivery of a protein (lysozyme) though the membrane.

6.2 Materials and methods

6.2.1 Materials

Dextran and lysozyme were obtained from Sigma-Aldrich, UK. All other chemicals were of reagent grade and obtained from Lancaster Synthesis Ltd., UK.

6.2.2 Hydrogel membrane synthesis

The synthesis procedure was described in Chapter 4(Page 73), and is summarised in Figure 6.2. The number of COOH groups in the above two CM-dextrans were calculated by means of acid titration (Chapter 4 Page 73). The ratio of COOH groups per dextran is 1-COOH:13-glucose for the pH-sensitive hydrogel and 1-COOH:63-glucose for the non-pH-sensitive hydrogel.

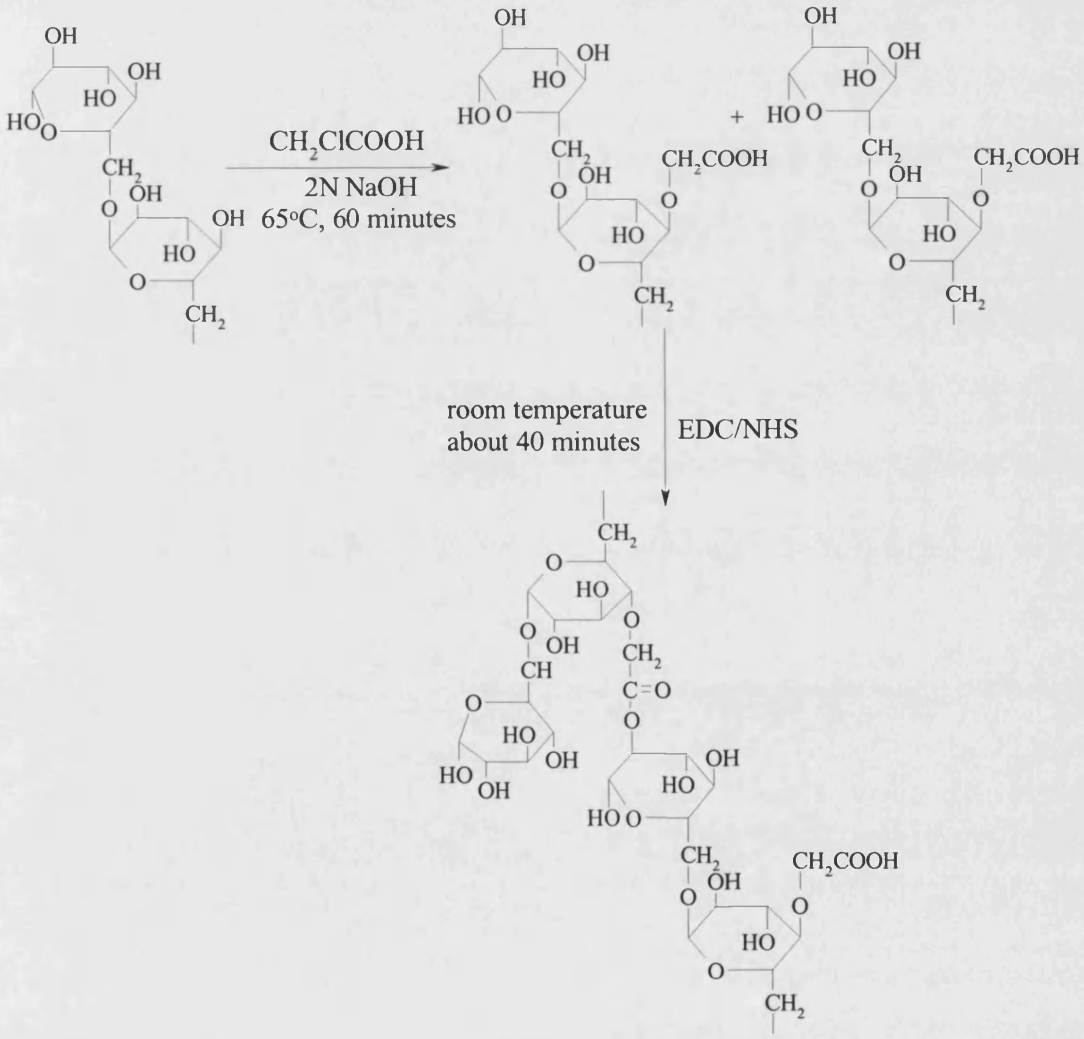

Figure 6.2: Gel synthesis protocol

To make a pH-sensitive hydrogel membrane, 0.5 g CM-dextran was weighed and dissolved using 3 ml distilled water while stirring thoroughly. 160 mg EDC and 25 mg NHS were weighed and dissolved in 1 ml distilled water. If no bubbles were found in the CM-dextran solution, 1 ml of the EDC/NHS mixture was added and stirred for 30 minutes. The solution was then cast on a nylon gauze mechanical support (pore size 0.1 mm, thickness of 0.05 mm) between two glass plates using spacers to give the required total membrane thickness.

Non-pH sensitive hydrogels were produced by a similar procedure using a CM-dextran with a lower degree of carboxylic group substitution (1-COOH:63-Glucose; see above)

6.2.3 Lysozyme diffusion experiments

The trans-membrane transport of lysozyme was studied using a diffusion cell consisting of donor and receptor chambers of equal volumes of 4.4 ml, as described in chapter 3 and by Tang *et al.* (2003). Hydrogel membranes with a surface area of 4.58 cm^2 were mounted between the two chambers. Once the membranes were mounted, both chambers were filled with 20 mM phosphate buffer. The donor chamber was connected to the lysozyme reservoir via a pump. The receptor chamber was connected to a UV-Visible spectrophotometer, to allow lysozyme diffusion across the membrane to be automatically monitored and logged from optical density changes (see Figure 3.3). Lysozyme diffusion across to the receptor chamber was calculated using calibration data for lysozyme at 280 nm. The effect of pH and ionic strength was investigated by varying pH and ionic strength levels in the lysozyme solution feed to the donor chamber and following the resultant changes in transport rate. Lysozyme (2 mg/ml) was dissolved in 20 mM phosphate buffer containing 50 mM NaCl. Transport was monitored at room temperature (25 °C).

6.2.4 Morphology of the pH-sensitive hydrogel membrane in different pH environments

The morphology of the hydrogel in different pH phosphate buffers was examined using a Jeol 6310 SEM equipped with a cryo-stage and energy-dispersive X-ray (EDX). A sample of the hydrogel was clamped between two pieces of aluminium sheet and rapidly frozen in liquid nitrogen then introduced into the SEM-chamber pre-cooled to a temperature of ca. –160 °C. The stage was the heated to a temperature of ca-80 °C to sublime the surface water. After cooling to –160 °C, the sample was gold sputtered for 3 minutes. The sample was scanned at a magnification of 2000x.

6.2.5 Physicochemical properties of the hydrogel

Infrared spectroscopy was performed on a Bruker-equinox 55 FT-IR spectrometer. Freeze-dried samples were mixed with potassium bromide powder and pressed into tablets under vacuum. For each sample 100 scans were recorded from 4000-400 cm^{-1} with a resolution of 2 cm^{-1}.

6.3 Results

6.3.1 Hydrogel characterization

As shown in Figure 6.2, the carboxylic groups can be grafted into dextran in the presence of sodium chloroacetate. Adjusting both reaction temperature and time can control the degree of carboxylic substitution. In this experiment, two CM-dextran preparations were made. The first, containing one COOH group per 13 glucose residues, was produced using a reaction temperature of 65 °C for 90 minutes. The second, containing one COOH per 65 glucose residues was attained at 50 °C for 15 minutes.

Carbodiimide chemistry was employed to cross-link carboxylic groups and hydroxyl groups in CM-dextran. According to the expected cross-linking mechanism, EDC can react with the carboxyl groups in CM-dextran to form an activated O-urea. This intermediate may either react with available hydroxyl to form an ester linkage or

release a soluble urea derivative. To get a pH-sensitive hydrogel, not all carboxyl groups should be crosslinked; the extra hydroxyl group will play the key role in the response to environmental pH changes. Therefore, the degree of sensitivity will be decided by the amount of extra carboxyl groups in the hydrogel. As in the similar method reported by Tomihata and Ikada (1997), hyaluronic acid (HA) hydrogel was prepared by the means of intermolecular formation of ester bonds between hydroxyl and carboxyl groups.

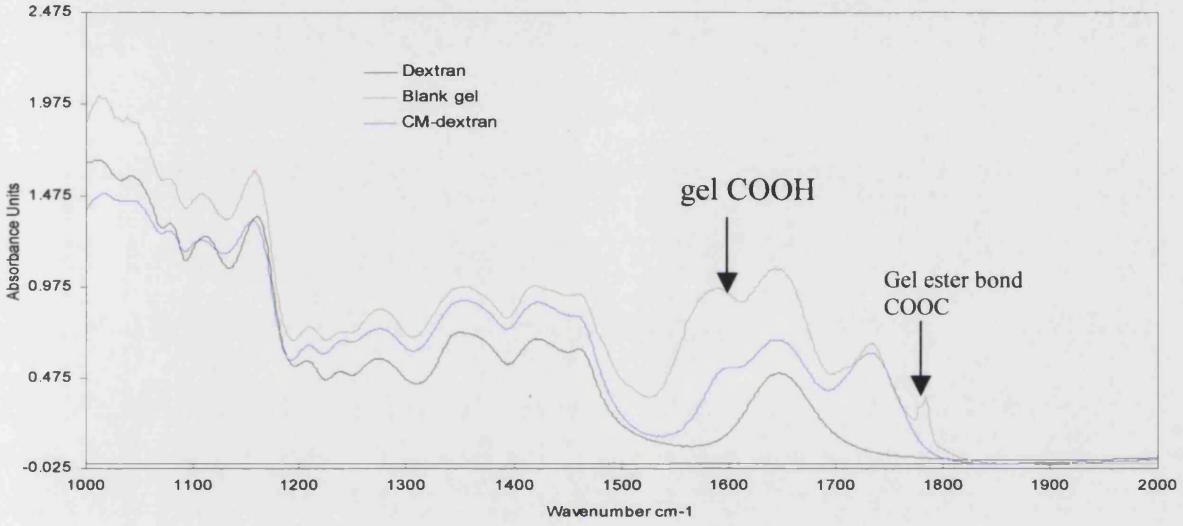

Figure 6.3: Dextran hydrogel characterized by FTIR. Peak from the carbonyl (C=O) stretching of CM-dextran and gel appeared at ca.1734 cm^{-1} and 1580 cm^{-1}. The peak of the carbonyl of gel ester bond appears at ca.1775 cm^{-1}.

The successful incorporation of the COOH group into dextran is demonstrated by the presence of a carboxylic FT-IR band from the carbonyl (C=O) stretching of CM-dextran at ca.1734 cm^{-1} and 1580 cm^{-1} as shown in Figure 6.3. This indicates that activated carboxyl groups can react with hydroxyl groups in CM-dextran to form ester linkages.

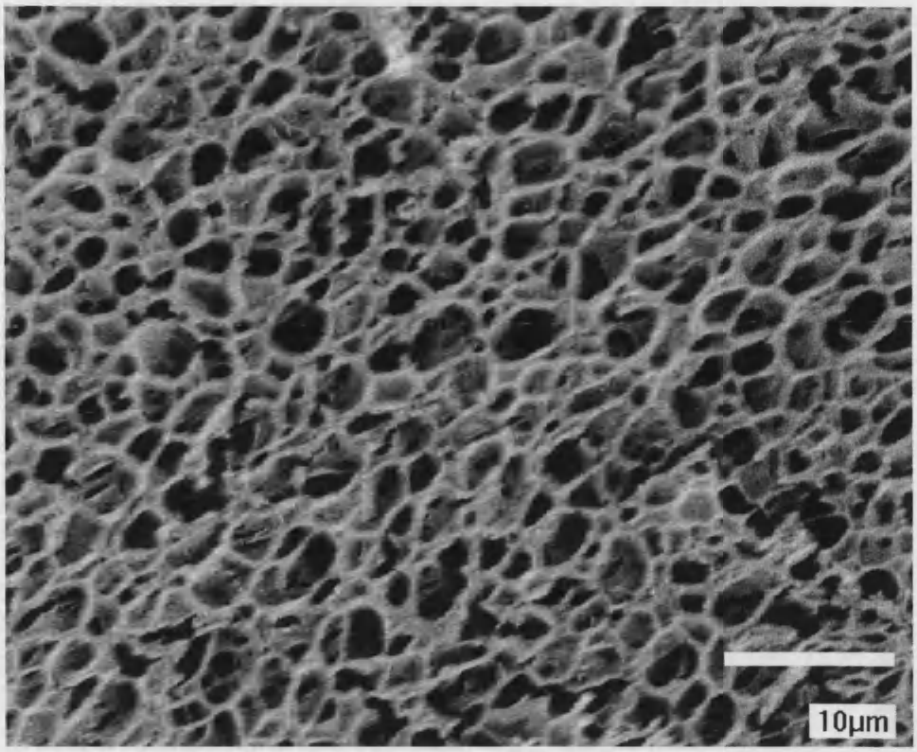

SEM of hydrogel in pH 5.0 buffer with magnification of 2000

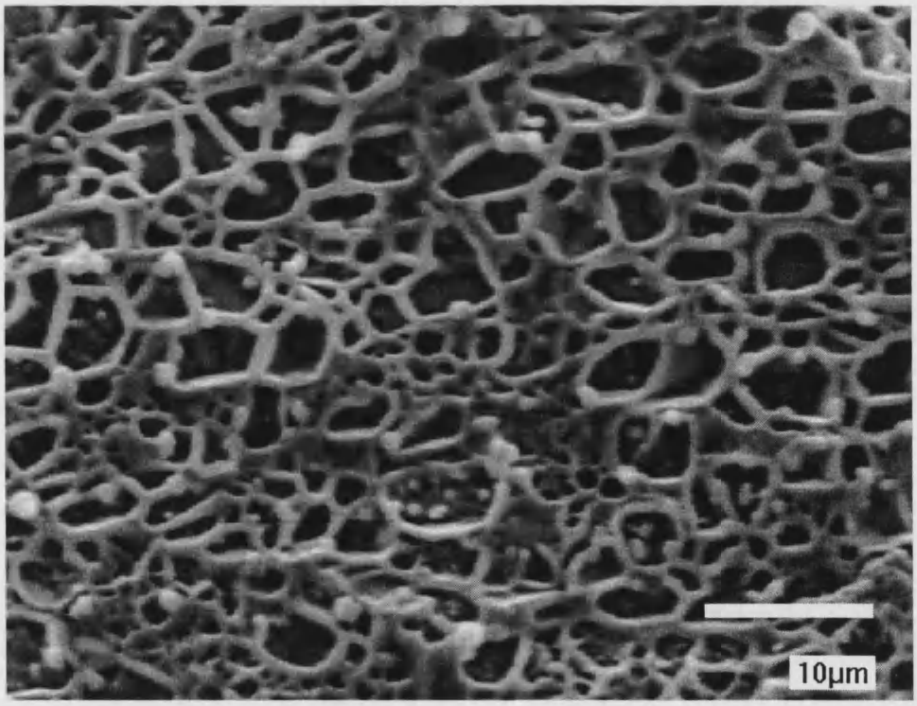

SEM of hydrogel in pH 7.4 buffer with magnification of 2000

Figure 6.4: SEM structure comparison of hydrogel kept in pH 5.0 and 7.4 phosphate buffer.

The cross-sectional interior structure of swollen hydrogels kept in pH 7.4 and 5.5 phosphate buffer were revealed by the SEM. Two different structures were observed

as shown in Figure 6.4. The porosity of the hydrogel in pH 5.5 is seen to be compact compared with that in pH 7.4. The pH-responsive feature of the hydrogel is thought to exist in the pore walls. The relatively loose structure at pH 7.4 is ascribed to expanded pore walls, which results from the response of the hydrogel to the pH change.

6.3.2 Reversibility of the pH response

The reversibility of the pH effect was studied by switching between lysozyme solutions in pH 5.5 and 7.4 phosphate buffer (20 mM) while maintaining the same ionic strength (0.1M) using sodium chloride. In the experiment shown in Figure 6.5, lysozyme (2.0 mg/ml in a 100ml reservoir) was used for the first 200 minutes at pH 5.5, providing the baseline diffusion curve. At 200 minutes, the pH 5.5 solution was replaced by protein solution at pH 7.4. As the total amounts of lysozyme in the reservoir were much higher than the corresponding amounts in the receptor side of the diffusion cell the effective driving concentration can be assumed constant throughout the run. A significant increase in the rate of lysozyme diffusion occurred about 20 minutes after the switch to the high-pH solution. This cycle was repeated: at 350 minutes protein solution in pH 5.5 was reintroduced. The diffusion curve became stable after 50 minutes. Repetition of this procedure gave a similar response. The results obtained with lysozyme show that the pH-sensitive membrane exhibits a reversible response in protein diffusion in response to pH changes under the condition of the same ionic strength (0.1M).

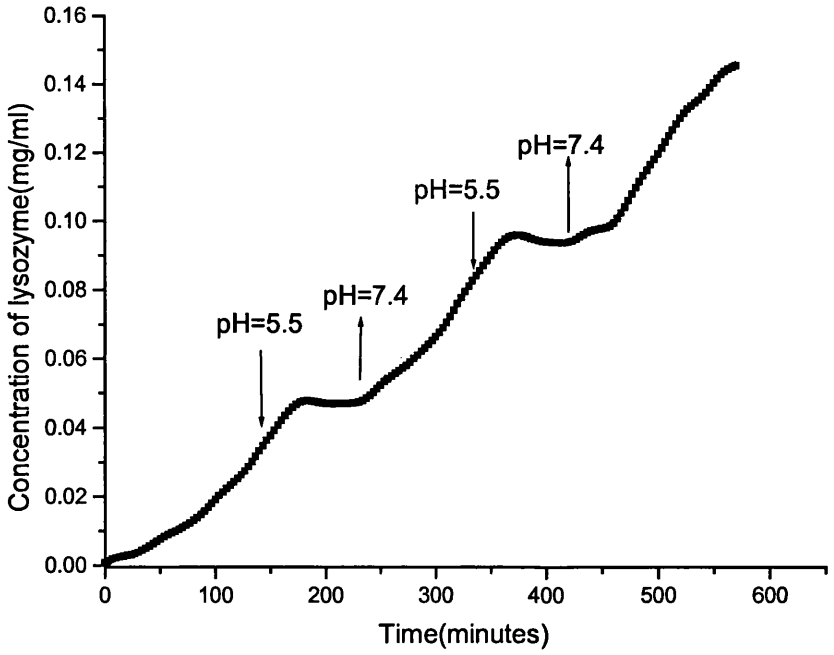

Figure 6.5: Reversible of hydrogel response to pH change. pH 7.4 phosphate buffer plus 2.0 mg/ml lysozyme was added at the down-arrows. pH 5.0 phosphate buffer plus 2.0 mg/ml lysozyme was used at the beginning and restored at the up-arrows. (Temperature 25°C, fixed ionic strength 0.1M).

6.3.3 Effect of pH on diffusion rate

2mg/ml lysozyme was used to examine the diffusion rate across the hydrogel membrane in response to pH changes adjusted by phosphate buffer of 20 mM with the same ionic strength (0.1M) attained by the addition of sodium chloride). Figure 6 shows lysozyme transport through the membrane when pH was varied from 5.0 to 9.0. All these experiments were conducted with a single membrane. To avoid artefacts arising from diffusion lags after pH changes, a pre-incubation period was allowed before data collection took place. The results show that the transport rate of lysozyme across the hydrogel increased as the pH increased as the acidic moieties of the CM-dextran became increasingly ionised. Similar results have been observed with pH-sensitive polypeptide hydrogels, methacrylated dextran hydrogels, polyacrylamide-*g*-guar gum microgels and chitosan–polyvinyl pyrrolidone hydrogels (Markland *et al.*, 1999, Risbud *et al.*, 2000, Soppimath *et al.*, 2001, Chiu *et al.*, 2002). We therefore assume that the pH-sensitive hydrogel grafted carboxyl groups are similar to polyvalent weak acids. At high pH, the COOH groups may be ionised or dissociate, which induces the electrostatic repulsion depicted in Figure 6.1. As a consequence,

the distance between chains increases and the hydrogel becomes swollen. The inset curve in Figure 6.6 shows that the rate/pH response fits to a titration curve giving a pKa value of 6.1.

6.3.4 The effect of ionic strength on diffusion rate

The ionic strength characteristics of the hydrogels were investigated by measuring the diffusion rate of lysozyme across the membrane under a range of ionic strengths between 0.045 M and 0.3 M at pH 5.5 and 7.4 respectively. Considering the hydrogel as a polyelectrolyte suggests porosity should decrease as ionic strength increases. As shown in Figure 7, at pH 7.4 the diffusion rate of lysozyme firstly increased with increasing ionic strength up to 0.15M; however after that, it decreased with higher ionic strengths. A similar result was attained at pH 5.5, with a shift of the concentration of ionic strength to 0.2 M at which the diffusion rate reaches its maximal point. Ju *et al.* (2002) have also reported similar results in alginate/PNIPAAm-NH_2 comb-type graft hydrogels.

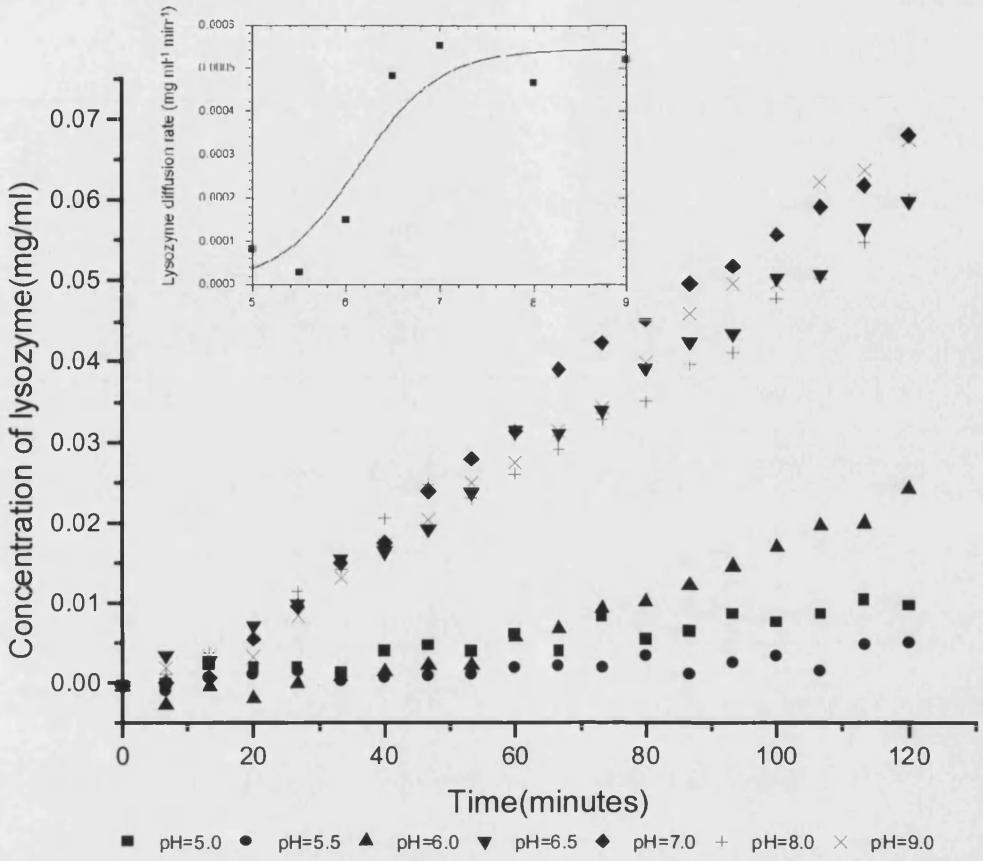

Figure 6.6: Effect of pH on lysozyme diffusion. Lysozyme 2.0 mg/ml, temperature 25°C. 20 mM phosphate buffer of constant ionic strength of 0.1 M (adjusted using NaCl).

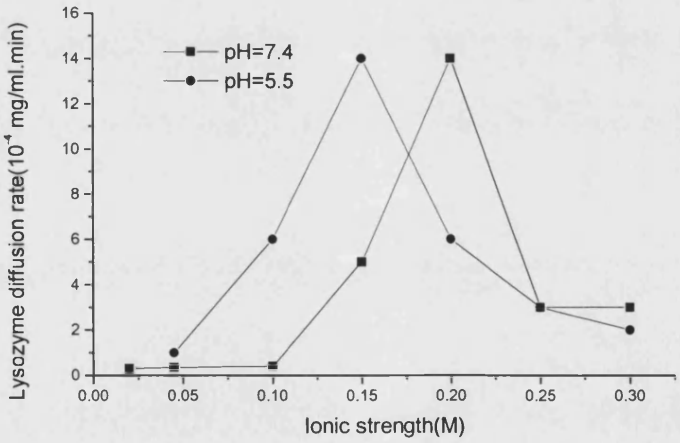

Figure 6.7 The profile of rate of Lysozyme diffusion rate as a function of ionic strength at pH 7.4 and 5.5. All other conditions as for Figure 6.6.

6.3.5 Osmotic pressure effects

Diffusion experiments were conducted using a 0.5mm membrane with different osmotic pressures induced by changes in sucrose concentration at 25 °C in pH 7.4 phosphate buffer of 20 mM (I=0.1M). Sucrose at 0.2M and 0.5M were introduced after 100 minutes. In both cases there was no observable effect on transport rate, suggesting that the diffusion-rate fluctuation seen with changes in pH and salt concentration are not the result of changes in osmotic pressure.

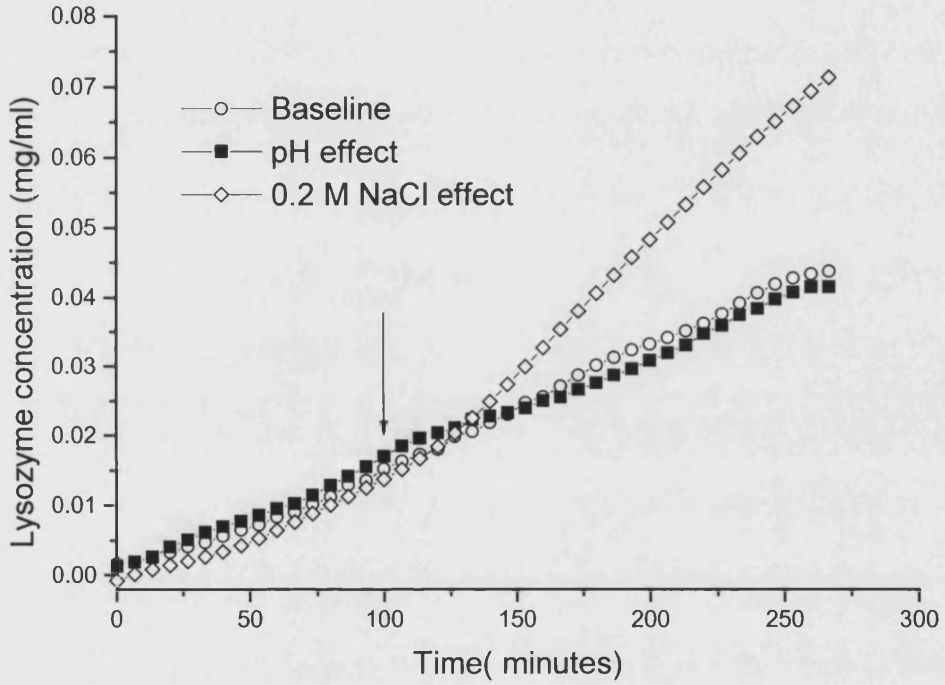

Figure 6.8. The pH and ionic strength effect on 2mg/ml lysozyme through non-pH-sensitive hydrogel membrane at room temperature (25 °C). At 100 minutes, the pH 7.4 phosphate buffer of 20 mM (ionic strength 0.1M) or pH 5.5 phosphate Buffer containing 0.2M NaCl were used minutes as shown down arrow. pH 5.5 phosphate buffer was used at the beginning. The baseline was conducted at pH 7.4 and ionic strength as 0.1 M.

6.3.6 pH and ionic strength effects on control hydrogels

The operational mechanism of the pH hydrogel membrane is based on extra COOH groups in the hydrogel. As seen in Figure 6.1, the hydrogel membrane can work only in ionised carboxylic group after exposure to high pH. In contrast, hydrogels with a

lower carboxylic acid substitution would not be expected to show a significant pH response. From the curve in Figure 6.8, the diffusion rate of lysozyme across a hydrogel made from CM-dextran with 1 COOH per 65 glucose units shows no change as external pH increased form 5.5 to 7.4. However, ionic strength effects are still apparent as 0.2 M NaCl is added to the buffer used.

6.4 Discussion

pH-sensitive hydrogels were successively prepared by chemical cross-linking of carboxy methyl dextran (CM-dextran) using 1-Ethyl-(3-3-dimethylami-nopropyl) carbodiimide hydrochloride (EDC) and N-hydroxysuccinimide (NHS). These cross-linking agents introduce 'zero length' ester-crosslinks between carboxylic acid groups and hydroxyl groups in CM-dextran. When compared with commonly used methacrylated dextran hydrogels, prepared by radical polymerization of methacrylated dextran in the presence of cross-linking agents, hydrogels based on CM- dextran with EDC and NHS have several advantages. Firstly, the preparation procedure is simple and rapid. More importantly, variation of carboxylic group density and cross-linking reagent concentration allow control of both charge density and degree of cross-linking in the hydrogel so that the balance between degradation rates and mechanical properties can be easily controlled. Lastly EDC/NHS does not chemically bind to dextran molecules, in contrast with conventional cross-linking agents (Nakajima *et al.,* 1995), instead it reacts to form a water-soluble urea derivative which has far lower cytotoxity and is easily washed out.

The formation of an ester bond as the cross-link bridge was confirmed by FT-IR. It is obvious that the chemically reactive groups responsible for the cross-linking of CM-dextran molecules must be hydroxyl and carboxyl from Figure 6.3. Proof of the presence of COOH groups in the hydrogel is also provided by the evidence from FT-IR.

The prominent transition of the hydrogel structure in response to pH is shown in Figure 6.4. Although the sizes of pores in the hydrogel as shown by the SEM are much larger than the protein's diameter, I assume that pores shown by the SEM are

water-filled. The functional properties stem from the polymer layer comprising the pore wall, where ionic components will produce changes in electrostatic repulsion with pH change. As explained above, the pores should be regarded as water reservoirs that can be measured from the swelling ratio of the hydrogel. In addition, the COOH content of the hydrogel determines whether the hydrogel is sensitive to pH. As seen in Figure 6.8, the hydrogel will lose sensitivity to external pH change when there are few or no COOH groups in the hydrogel. It follows that the sensitivity of this hydrogel can be predicted from the substituted degree of carboxymethyl in the dextran. However, transport will also be influced by the effect of pH on the charge on the lysozyme molecular as described in Chapter 4 (Page, 90-91).

The diffusion data for lysozyme across the hydrogel at different pH or ionic strengths show the porosity response of the hydrogel to its external environment. The results in Figure 6.6 indicate that by increasing pH from 5.5 to 7.4, a considerable increase in diffusion rate results. The apparent pKa of 6.1 observed for the CM-dextran, as determined by the bulk titration method, is basically in agreement with the values observed for the center of the relationship curve between diffusion rates against pH in Figure 6.6 (inset). As far as the ionic strength effect is concerned, the dissociation of COOH in CM-dextran may be enhanced as the ionic strength increases up to a fixed value; but with ionic strength continuously increasing, the anionic groups in the hydrogel are screened by Na^+ ions. As a result, the conformation in the hydrogel changes from an expanded free-draining matrix to that of a more compact and non-free-draining matrix, so the diffusion rate will dramatically drop with increasing ionic strength. Another possible contribution to this result is that chloride ions present in the external solution might have neutralized the carboxylic (COO-) group as described by Soppimath *et al.* (2001).

In addition, this response to pH is reversible as seen in Figure 6.5. The shorter lag time of diffusion at pH 7.4 than that at pH 5.5 results from the time taken for the system pH to reach equilibrium after the new buffer is introduced.

Chapter 7. The Evaluation of Carboxyl Methyl Dextran as a Potential Tissue Engineering Extracellular Matrix for Human Cell Culture

7.1 Introduction

Over the years, various synthetic and natural polymers and their hybrids have been utilised as cell support scaffolds (Hansbrough *et al.,* 1998). Various hydrogels have been used as extracellular matrices (ECM) for cell immobilisation, transplantation and tissue engineering (Rowley *et al.,* 1999, Lim *et al.,* 1980, Atala *et al.,* 1994, Jen *et al.,* 1996). Hydrogels with three-dimensional, hydrophilic polymeric networks can potentially mimic some of the many roles found *in vivo* (Lee *et al.,* 2001). ECMs compromising of various amino acids and sugar based macromolecules, coupled to hydrogels, provide a hydrated microenvironment to orientate cells, give mechanical integrity and permit the diffusion of nutrients, metabolites and growth factors. Hydrogels from natural polymers such as collagen, gelatin, fibrin, alginate, agarose and chitosan have already been widely used for tissue engineering applications (Putnam *et al.,* 1996, Suh *et al.,* 2000, Trudela *et al.,* 2002, Draye *et al.,* 1998, Groot *et al.,* 2001, Kuijpers *et al.,* 2001, Tomihata *et al.,* 1997, Pieper *et al.,* 2000, Wissink *et al.,* 2001). Previously, reconstituted collagen in the form of gels, sponges or films, has been extensively used to support cell cultures both *in vitro* and *in vivo*. These materials have proved valuable but recent concerns regarding potential viral infection and problem of limited availability have highlighted a need for ECMs derived from non-animal sources.

The availability of dextran possessing a range of different molecular weights, its solubility in polar organic solvents (which enable chemical modification) and its biocompatibility make this natural polysaccharide immediately attractive. Indeed, the low tissue toxicity, high enzymatic degradability at desired sites and ease of chemical modification mean that dextran hydrogels have been frequently considered as a potential matrix system for cell culture (Ferreiraa *et al.,* 2002). Existing dextran hydrogels are prepared directly by crosslinking dextran with either 1,6-

hexanediisocyanate or glutaraldehyde (Chiu *et al.,* 2002, Hovgaard *et al.,* 1995). Sequential reactions of dextran with glycidyl acrylate and the subsequent polymerisation have also been reported (Brondsted *et al.,* 1998, Yamamoto *et al.,* 1996). Nearly all of the existing studies focus on crosslinking using methacrylate dextran hydrogels. Methylacrylation (MA) of dextran has been conducted with full control of the degree of substitution by transesterification of glycidyl methacrylate with dextran in DMSO (Van *et al.,* 1995, 1997). Kim *et al.* (2000) obtained hydrogels by UV irradiation of methacrylic anhydride and with bromoacetyl bromide and sodium acrylate (Kim *et al.,* 1999, 2000). Recently, Chiu *et al.* (2002) also reported hydrogels prepared by radical copolymerisation of MA-dextran with Aac in borate buffer, using ammonium peroxydisulfate and N,N,N',N'-tetramethylethylenediamine as an initiation system(Chiu, et. al., 2002).

For applications in cell and tissue culture it may also be beneficial to incorporate coupled proteins in order to facilitate cellular adhesion and morphology. Using MA-dextran, the proteins or attachment ligands can be grafted onto the surface. Synthesising gels using the method described here for CM-dextran with carbodiimide chemistry permits protein distribution throughout the hydrogel.

The ability of the CM-dextran to support cells would open up new potential applications for this material in tissue engineering. Presently, despite many years of research and development, the only commercially available tissue engineered product is a dermal replacement material (Dermagraft, Smith and Nephew, USA). It is for the same flat sheet application that the potential of CM-dextran as an ECM is considered. The preferential use of autologous split-thickness skin grafting to cover wounds is severely restricted by donor availability. Therefore, the ability to rapidly and efficiently create a suitable sterile replacement that is conducive to optimal healing, it minimises infection, shock, desiccation, wound contraction and eventual scar formation, would be highly desirable. Replacement dermis material function as a scaffold for local cells migrating from the wound periphery and supports subsequent grafts of partial thickness or cultured epithelial sheets. Presence of a dermal component has long been shown to improve epithelial acceptance, function and aesthetic appearance, in addition to providing strength and ease of clinical handling. For the following study, the potential of CM-dextran to perform the task of a dermal

replacement or cell delivery system was examined by using flat sheets for the maintenance of human dermal fibroblasts. To maintain clinical relevance, primary human cells were used.

7.2 Materials and methods

7.2.1 Materials

Dextran and lysozyme were obtained from Sigma-Aldrich, UK. All other chemicals were of reagent grade and obtained from Lancaster Synthesis Ltd., UK.

7.2.2 Tissue culture

Human fibroblast cells was generously supplied by Dr Marcus Jarman-Smith (Smith, *et al*, thesis 2000) and were cultured at 37°C with a 95% air, 5% CO_2 gaseous composition and 100% humidity, and used between passage 2 and 4.

7.2.3 Hydrogel membrane synthesis for tissue culture

Gels were synthesized as described in Chapter 4. To give a control, Substitution of COOH was 1 COOH: 13 glucose for pH-sensitive gels and 1 COOH: 63 glucose for non - sensitive gels.

All methods for preparation were carried out under sterile conditions. The lyophilised dextran (3g) was dissolved in 20ml of fibroblast medium and sterilised using a 0.2μm filter. Separately, 1.5g of EDC and 300mg NHS were dissolved in 5ml of distilled water and also filtered. The EDC/NHS solution was added to the CM-dextran and pipette into 12 well tissue culture plates. Some hydrogels were additionally modified by the inclusion of additional adhesive factors: 1ml of either poly (L-lysine), fibronectin (50 $\mu g\ ml^{-1}$) or concanavadin A was added into the CM-dextran solution and mixed.

Hydrogels were incubated at 37°C until gelation occurred (approximately 1 hour), and were then washed several times using 0.1M phosphate buffer solution (PBS) at pH 7.4 followed by fibroblast media. Hydrogels were produced using both pH-sensitive gels and non-sensitive CM-dextran gels. Finally, all gels were soaked overnight in fibroblast

media. Early passage primary human dermal fibroblasts were seeded onto the gels at a density of $5x10^4$ cells cm^{-2} of gel surface and maintained in a humidified incubator at 37°C and 5% CO_2/95% air. Media was replenished every second day and samples were observed at various time points during culture up to 7 days.

7.2.4 Analysis of samples

Images were obtained using a light microscope (Carl Zeiss 68040) utilising a colour video camera (JVC 3-CCD KY-F55B) fitted with an imaging system (KS 300, Imaging Associates Ltd, UK).

Samples of unseeded CM-dextran were characterised when hydrated at pH 7.4 in PBS, using cryo-SEM. Samples were observed in the field emission SEM (JSM-6210, JEOL, Japan) operated at 1.5-30kV and maintained at a temperature of 148-163K.

7.3 Results

The internal structure of the hydrogel has a high voidage as shown in Figure 6.4. and should allow the unrestricted passage of nutrients throughout the nascent tissue construct. In addition, the structure should also provide suitable for maintenance of cells in a three-dimensional orientation as tissue develops. Fibroblast cultures served to demonstrate the increased biological interaction that is possessed by the covalently modified (non-sensitive) CM-dextran. Hydrogels that were additionally modified by the inclusion of adhesive factors (fibronectin, Con A or poly(L-lysine)) showed the beginnings of attachment and spreading of cells by 4 hours post-inoculation on all samples (Figure 7.1). However, qualitatively there appeared to be no improvement over samples of the CM-dextran possessing no additional adhesive factors. Control pH-sensitive dextran hydrogels with a ratio 1 COOH: 13 glucose demonstrated no cellular attachment by the same time (4 hours), nor at any subsequent time period. Cells were maintained upon the hydrogels for 7 days. An increasing number of cells were observed during this period indicating that cells were proliferating. This occurred on all non-sensitive CM-dextran hydrogels. By the end of this 7 day period entire confluent cell sheets had formed upon the surface of the gels. Cells showed an

affinity for alignment along natural cracks and cavities that had formed in the gel upon gelation (Figure 7.2).

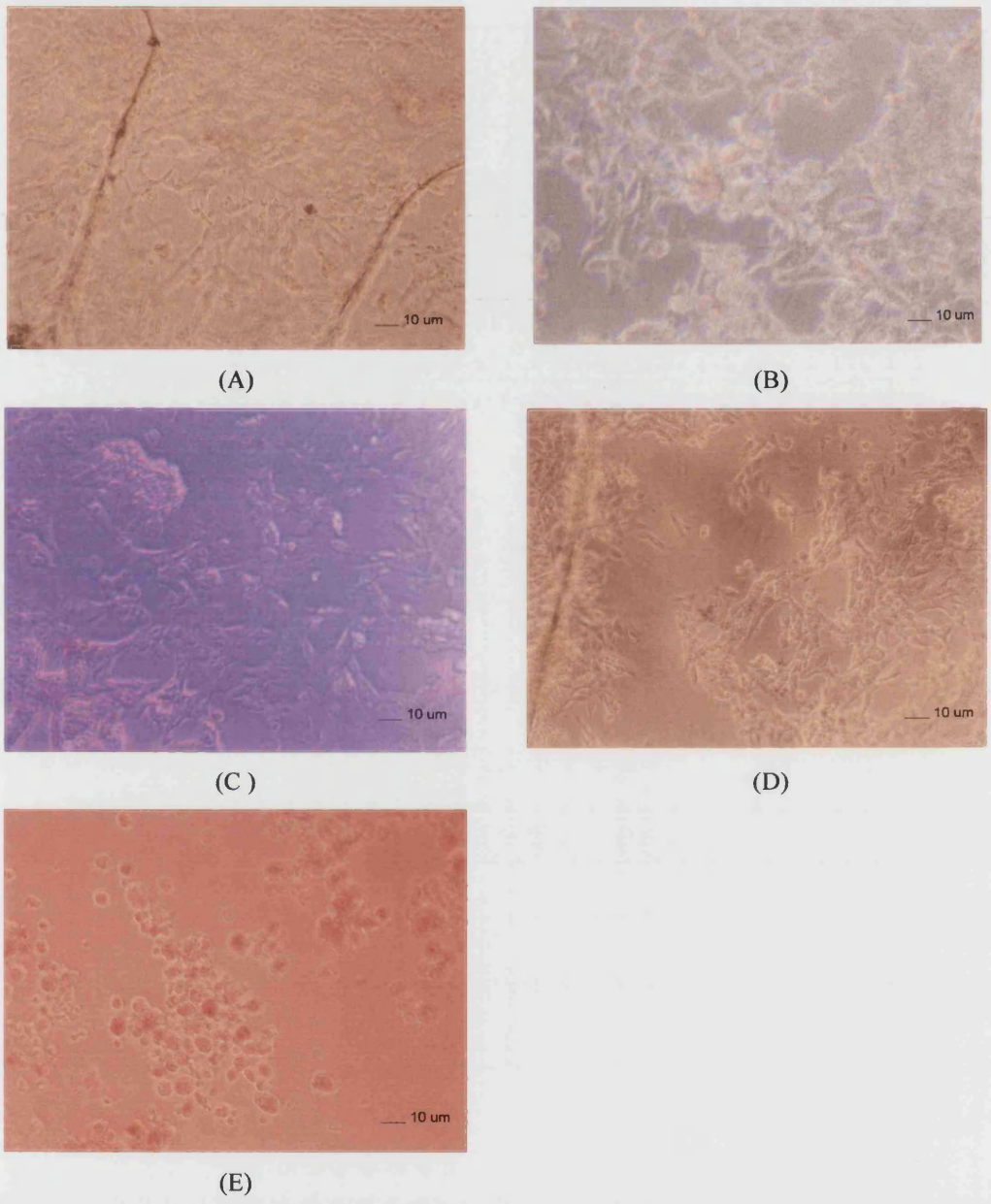

(A) (B)

(C) (D)

(E)

Figure 7.1. Light micrographs showing attachment of primary human dermal fibroblasts onto CM-dextran after X hours post-seeding. Cellular attachment was present on all non-sensitive hydrogels whether possessing additional adhesion factors or not (A- CM-dextran only, B- with fibronectin, C- with poly L-lysine, D- with concanavadin A, E- All pH sensitive gels showed no attachment).

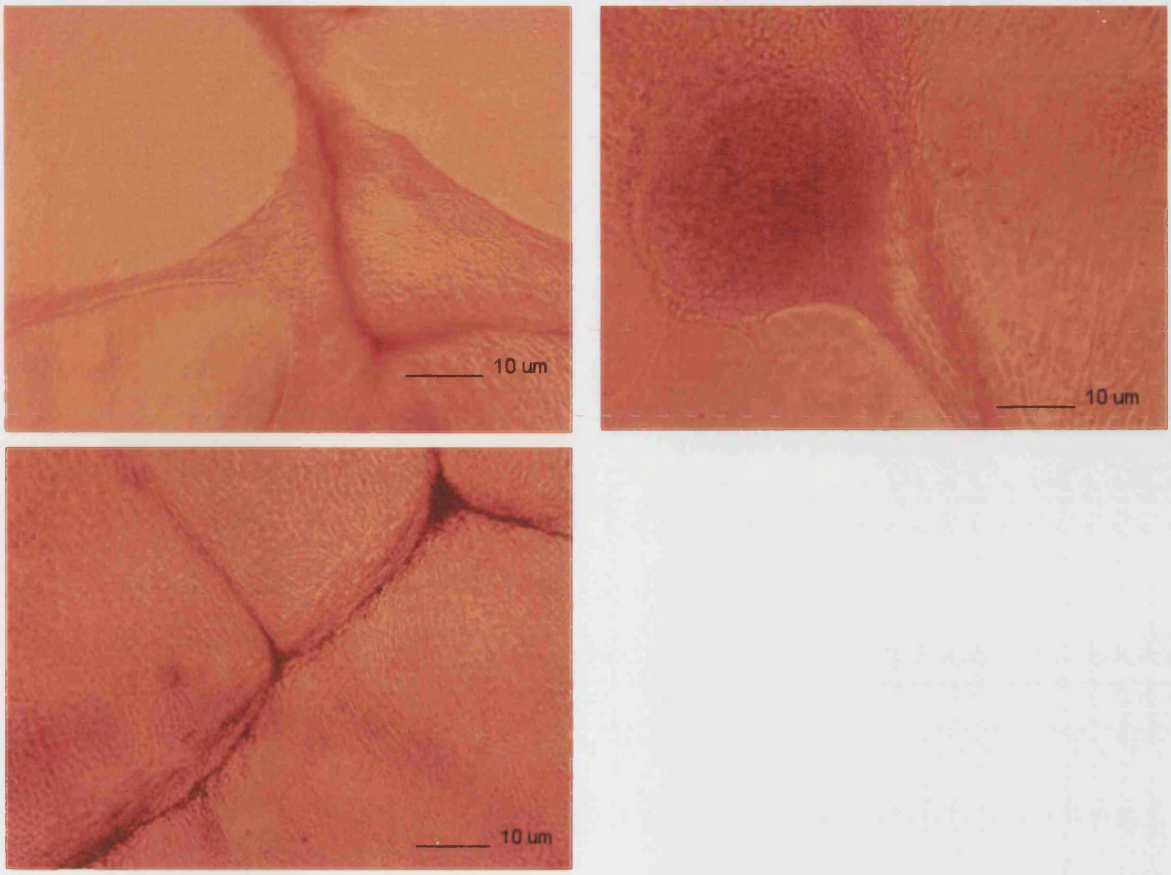

Figure 7.2: Light microscopy demonstrating the confluent sheets of primary human dermal fibroblasts that have formed on CM-dextran hydrogels after 5 days culture. The gels shown are non-sensitive and contained no additional adhesion factors.

7.4 Discussion

Obviously, the incorporation of these additional features could be beneficial in three dimensional cell culture as it would permit some microenvironmental response to the changing culture conditions. This will have implications for cellular migration, timed release of growth factors, and facilitation of diffusion of nutrients and toxic metabolites (such as lactic acid).

Carbodiimide chemistry was employed to crosslink carboxylic and hydroxyl groups in CM-dextran. The expected mechanism would result in EDC reacting with the carboxyl of the CM-dextran and form activated O-urea. This is an intermediate and may subsequently react with available hydroxyl to form ester linkages or release a soluble urea derivative. The extent of crosslinking of the carboxyl groups has

implications for the reactivity of the gel to physicochemical conditions such as pH, and also to the cell affinity for the matrix. Similar methods have been reported for hyaluronic acid hydrogels, which were prepared utilising intermolecular formation of ester bonds between hydroxyl and carboxyl groups (Tomihata *et al.*, 1997).

Cell culture experiments using primary human dermal fibroblasts were utilised to demonstrate the ability of the matrix to support clinically relevant cells and demonstrate the potential to extend its use as a delivery system or tissue engineering scaffolding. The failure of fibroblasts to attach to the pH-sensitive CM-dextran hydrogels may have been due to the negative influence of the ionic charge present in these gels. The absence of fibroblasts on these gels suggested that it was the ratio of COOH to glucose that predicted whether attachment would occur. The inability of this pH-sensitive gel to support cells was disappointing, however, the presence of fibroblasts on all forms of the non-sensitive CM-dextran was encouraging. This demonstrated that the presence of additional adhesion molecules were not a prerequisite for improving cell attachment, spreading or survival. This obviously makes the synthesis of matrices more cost effective, rapid and simple.

The CM-dextran gels were successfully prepared by chemically crosslinking CM-dextran using EDC and NHS. These crosslinking agents introduce "zero length" ester linkages between carboxylic acid and hydroxyl groups in CM-dextran. The CM-dextran has the following advantages when compared with commonly used methylacrylated form crosslinked with the same agents. Firstly, the procedure for preparation is simple and rapid. Secondly, variation of carboxylic group density and crosslinking reagent concentration permits control of the charge density and the degree of crosslinking. This means that the balance between the degradation rate and mechanical properties can be easily controlled. Importantly for cell culture, the EDC/NHS does not chemically bind to the dextran molecules, in contrast with conventional crosslinking agents, and the chemicals are changed into water soluble urea derivatives which are less cytotoxic and can be removed by adequate washing. The presence of cells upon the non-sensitive CM-dextran suggested that the only cytotoxicity present was due to variations in the number of COOH groups. The observation that cell numbers increased over 7 days also indicated that the dermal fibroblasts were not merely remaining attached or surviving. The proliferation would

also suggest that no toxicity was present due to leachables from the process leaving the hydrogels.

The ability of the matrix to support human cells may have an immediate application as a flat sheet supporting dermal fibroblasts for the tissue engineering replacement of: venous/arterial, decubitus, diabetic ulceration; burns; or loss of tissue due to accident or disease. In the example of ulcers, chronic wounds require significant maintenance and cost. The Global wound care market in 2002 was estimated at $15 billion (*Clinica Reports, 2000*) and venous ulcers had a reported worldwide incidence of 2.8 million due to venous insufficiency (Baker *et al.,* 1994). A matrix synthesised from dextran could be easily sourced and inexpensive to produce. The matrix also offers the additional potential benefits: biocompatible; rapid gelation; malleable; controllable degradation; controllable porosity; ability to be chemically modified; transparent for clinical evaluation and microscopic examination. In addition, although constituent solutions were filter sterilised in this study, we have found that the hydrogel remains intact when steam sterilised post-gelation.

Previously, implantation of collagen dermal replacements have been enhanced by the inclusion of additional dermal components, such as the glycosaminoglycans. The CM-dextran also offers the ability to combine these factors easily as additional solutions or compounds pre-gelation. Longer-term studies will be required to examine whether cells have the ability to infiltrate the matrix.

This research has initially shown that a CM-dextran hydrogel is capable of maintaining primary human dermal fibroblasts over a period of 7 days without any apparent adverse effects in vitro. Based upon these findings, the CM-dextran hydrogel offers significant possibilities for development as an extracellular matrix substrate for use in cell culture or tissue engineering applications.

Chapter 8. An Intelligent Hydrogel with Diffraction Grating Structure: Novel Biosensor Materials

8.1 Background

Biosensors use biological molecules to recognize sample molecules of interest via hydrogen bonding, charge-charge interactions, and other biochemical interactions. They are commonly used for analysis of biomolecular interactions and can give detailed information on binding affinity, and in many cases also on binding kinetics (McFadden, 2002).

Biosensors generally consist of two components: a highly specific recognition element (receptor) and a transducer that converts the molecular recognition event into a quantifiable signal (Lin *et al.*, 1997). The receptor is always a biological element such as an enzyme, an antibody, a nucleic acid, a microorganism or a cell. Signal transduction has been accomplished using electrochemical, field-effect transistors, optical absorption, fluorescence and interferometric and other devices.

In the past decade, optical biosensors that exploit surface plasmon resonance, waveguides and resonant mirrors have been used widely to analyse biomolecular interactions (Cooper, 2002). These sensors allow the determination of the affinity and kinetics of a wide variety of molecular interactions in real time, without the need for a molecular tag or label.

The successful commercialization of real-time optical biosensors based on surface plasmon resonance (SPR) has provided a powerful new tool for the research community and to the pharmaceutical industry in particular (Turner, 2000). Commercial SPR devices detect alterations in the optical evanescent waves that result from small changes in refractive index at the interface between the sample and the device, which are caused by, for example, an antibody binding to an antigen. The advantage of these label-free biosensors is that they detect a binding event directly by monitoring the change in a physical property.

Recently, with the advent of sophisticated advanced microfabrication facilities and new material technologies, diffractive and miniaturized optical gratings have been widely used in optical systems such as integrated optics, quantum electronics, holography and spectroscopy. Several techniques, which included mechanical processes, holographic interference, the phase mask method and photolithography, and electron-beam lithography, are widely applied to manufacture diffraction gratings. In these methods, the fabrication processes are divided into two main steps. The first step involves the fabrication of the grating structure on a photoresist thin film. The second step involves the transfer of the grating surface relief structure to the substrate by etching. The two-step patterning and transferring processes are routine procedures in the conventional microfabrication on photoresist-based materials. They are typically complicated in the etching process and this is especially true for grey-level surface relief structures.

Until now, intelligent hydrogels as sensor materials have been limited by the lack of accurate techniques to gauge their volume change in response to any stimulus. To solve this problem, some research groups fabricated a hydrogel by encapsulating colloidal crystals within the gel or engineering surface patterns on the gel. Therefore, the optical properties of these hydrogels respond directly to small environmental stimuli (Grier, 1997).

The Asher group in Pittsburg University (U.S.A.) fabricated a novel sensing hydrogel material that reports on analyte concentrations via diffraction of visible light from a polymerized crystalline colloidal array (PCCA). The PCCA is a mesoscopically periodic crystalline colloidal array (CCA) of spherical polystyrene colloids polymerized within a thin, 'intelligent' polymer hydrogel film. CCAs are brightly colored, and they efficiently diffract visible light meeting the Bragg condition. The intelligent hydrogel incorporates chemical molecular recognition agents that cause the gel to swell in response to the concentration of particular analytes; the gel volume is a function of the analyte concentration. The color diffracted from the hydrogel film is, thus, a function of analyte concentration: the swelling of the gel changes the periodicity of the CCA, which results in a shift in the diffracted wavelength (Holtz *et al.,* 1997).

Zhibing Hu in University of North Texas (U.S.A) used sputter deposition to imprint the surface of a hydrogel with a square array of gold thin films. The periodicity of the array can be continuously varied as a function of temperature or electric field which alter the gel's volume, and so such an array might serve as an optical grating for sensor applications (Hu *et al.*, 1998, 2000).

Everhart patented one optical diffracting sensing device, which comprises one or more hydrogels coated onto patterned self-assembling monolayers onto some substrates and the diffraction pattern can change upon exposure to external stimuli (Everhart *et al.*, 2001).

The above-mentioned study results show some potential applications of modified gels in display and biosensor technology. However the fabrication procedures in the literature involved more complex steps compared with the needed for an intelligent hydrogel which can be created directly with an array structure in its surface. Such gels can be coupled with a ligand of interest, for example, proteins, peptides, or functional, all of chemicals which can induce changes of the hydrogel characteristic properties in response to many kinds of external stimuli, such as temperature, pH or a specific chemical trigger. e.g., glucose.

We have developed methods to fabricate directly intelligent hydrogels with diffraction gratings (IHDG). IHDG incorporates ligands that cause the gel to swell in response to the concentration of particular analytes. The gel volume is a function of the analyte concentration and the diffraction or reflection effect change of the IHDG is thus a function of analyte concentration. The swelling of the IHDG changes the periodicity of IHDG surface, which results in a change in the diffraction grating distance. Thus, the brightness or irradiance or position of a diffraction or reflection spot is related to the statistical average physical shape, size, and refractive index of the gel and the wavelength of the laser.

Previously Chapter 3 reported on the synthesis of differently functioning dextran hydrogels which demonstrated that the release of proteins (insulin, lysozyme, or BSA) from these hydrogels could be regulated by varying D-glucose concentration, NAD concentration or pH (Tang *et al.*, 2003). This chapter will look at the structural

properties of these materials with a view to developing novel biosensor applications. Specifically the development of diffraction gratings based on responsive hydrogels which change their diffractive properties in response to specific changes in environmental conditions.

8.2 Materials and method

8.2.1 Materials

Dextran and bovine serum albumin (BSA) were obtained from Sigma-Aldrich, UK. All other chemicals were of reagent grade and obtained from Lancaster Synthesis Ltd., UK. ESSIL 291 resin (RE Z00728, Axson), ESSIL 291 catalyser (REF Z000729, Axson)

8.2.2 Method

8.2.2.1 Fabrication of intelligent hydrogel with diffraction grating (IHDG)

The diffraction gratings are made using a soft lithography approach. Gratings are first cast in a siloxane polymer from an original etched master. This soft secondary master is used as a template for the formation of a hydrogel grating. Polysaccharide polymer is mixed with cross-linking reagents and poured onto the siloxane master or directly onto the original metal master. The polymer is then allowed to react until a stable hydrogel is formed. Once gelation has occurred the gel and master are left to air-dry whereupon a slight residual shrinkage of the hydrogel allows separation of it from the master with minimal surface damage.

Another method of fabrication is that the solution is first cast onto the master and then covered by a cellulose nitrate microfiltration membrane. This not only provides mechanical support but allows the analyte to be applied from the reverse face of the hydrogel such that the grating surface is protected from attritional forces and the optical path is not compromised in the case of turbid samples. Additionally, the hydrogel is easily peeled off from the master after partial drying.

To investigate the pattern formed in the IHDG in both methods, the IHDG was coloured using Cibacron Blue to make it dark before using.

8.2.2.2 Submaster preparation of silicone rubber

100 g ESSIL 291 resin was weighed and mixed with 10 g catalyser using a stirrer. The mixture was degassed using a vacuum pump for 20 minutes. The mixture was then poured onto glass or metal with diffraction grating on its surface and degassed for a further 25 minutes. The mixture was kept in an oven at 40 °C until set.

Hydrogels in this study were prepared from polysaccharide with a natural or a modified carboxyl acid group and then intercrosslinked by using carbodiimide chemistry as described in Chapter 4. Polysaccharide with carboxyl acid or modified carboxymethyl groups (for example alginate or CM-dextran) can be inter-crosslinked by exposure to EDC/NHS as shown Figure 8.1.

Briefly, 0.5 g CM-dextran was weighed and dissolved using 2.5 ml distilled water while stirring thoroughly. 160 mg EDC and 25 mg NHS were weighed and dissolved in 1 ml distilled water. If no bubbles were found in the CM-dextran solution, 1 ml of the EDC/NHS mixture was added and stirred for 30 minutes. And then 50 mg BSA dissolved in 1ml distilled water was added into the mixture with stirring for another 5 minutes. The solution could be cast onto the silicon rubber diffraction grating master until gelation.

In the case of alginate hydrogel, 5-g 4% alginate solution (W%W) was intercrosslinked by catalysing using 2ml EDC/NHS(140mg/20mg). This solution could be poured onto the diffraction grating master until gelation.

The preparation method of carboxymethyl (CM)-dextran is shown as Figure 8.1 B and the details can be seen in Chapter 6.

To identify the physicochemcal properties of the hydrogel, infrared spectroscopy was performed on a Bruker-equinox 55 FT-IR spectrometer. Freeze-dried samples were mixed with potassium bromide powder and pressed into tablets under vacuum. For

each sample 100 scans were recorded from 4000 to 400 cm^{-1} with a resolution of 2 cm^{-1}.

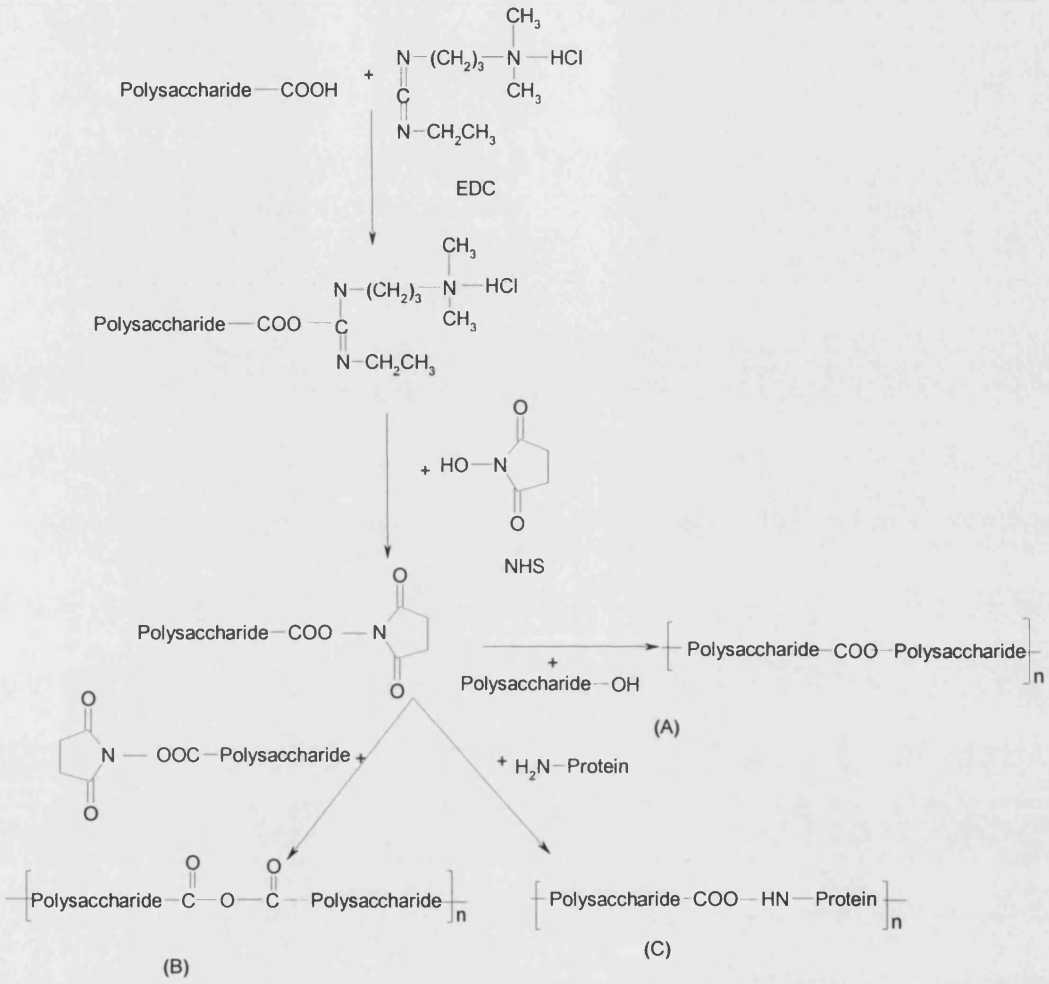

Figure 8.1: The chemistry of hydrogel preparation based on carbodiimide chemistry.

8.2.2.3 Sensor testing

The test flow cell layout is shown in Figure 8.2. The IHDG is mounted over a flow channel and covered by a glass slide to keep constant humidity during the experiment. The arrows denote the direction of fluid flow. A Helium-Neon laser is shine at the surface of the IHGD. A digital camcorder was employed to record the reflection or diffraction effect upon a detection screen. The bulk solution was pumped through the flow channel from the solution reservoir using a peristaltic pump.

8.2.2.4 The optical theory of IHDG

The theory description of refraction is illustrated as Figure 8.3 and 8.4. When monochromatic light is incident on a grating surface, it is diffracted into discrete directions. We can picture each grating groove as being a very small, slit-shaped source of diffracted light. The light diffracted by each groove combines to form a diffracted wavefront. The usefulness of a grating depends on the fact that there exists a unique set of discrete angles along which, for a given spacing λ between grooves, the diffracted light from each facet is in phase with the light diffracted from any other facet, so they combine constructively (http://www.gratinglab.com/library/handbook/).

Diffraction by a grating can be visualized from the geometry in Figure 8.3, which shows a light ray of wavelength *l* incident at an angle a and diffracted by a grating (of groove spacing λ, also called the pitch) along angles β_m. These angles are measured from a line normal to the grating (shown as the dashed line perpendicular to the grating surface at its centre). The sign convention for these angles depends on whether the light is diffracted on the same side or the opposite side of the grating as the incident light. In Figure 8.3, which shows a reflection grating, the angles $\alpha > 0$ and $\beta_1 > 0$ (since they are measured counter-clockwise from the grating normal) while the angles $\beta_0 < 0$ and $\beta_{-1} < 0$ (since they are measured clockwise from the grating normal). By convention, angles of incidence and diffraction are measured from the grating normal to the beam. This is shown by arrows in the diagram. The sign convention for angles is shown by the plus and minus symbols located on either side of the grating normal.

A laser is a device that controls the way that energized atoms release photons laser is an acronym for light amplification by stimulated emission of radiation, which describes very succinctly how a laser works. When the laser is used to illuminate the hydrogel with a diffraction grating (a collection of reflecting (or transmitting) elements separated by a distance comparable to the wavelength of light under study http://science.howstuffworks.com/laser2.htm). The diffraction effect results from an electromagnetic wave incident on a grating, having its electric field amplitude, or phase, or both, modified in a predictable manner after diffraction (http://www.gratinglab.com/library/handbook/). But when the groove distance λ

between grating lines changes, the diffraction effect also changes. In the case of IHDG, this change will be observed by the size and shape of the diffraction or reflection spot which will increase when the grating area shrinks in response to an environmental trigger as seen in Figure 8.4. This effect is reversible consistent with the reverse alteration of hydrogel.

8.2.2.5 Morphology of the hydrogel

The morphology of the IHDG was examined using a Jeol 6310 SEM equipped with a cryo-stage and energy-dispersive X-ray (EDX). A sample of the hydrogel was clamped between two pieces of metal sheet and rapidly frozen in liquid nitrogen. It was then introduced into the SEM-chamber pre-cooled to a temperature of ca. –160 °C. The stage was then heated to a temperature of ca-80 °C to sublimate the surface water. After cooling to –160 °C, the sample was gold sputtered for 3 minutes. The sample surface with the diffraction grating was scanned.

In the case of the alginate hydrogel, one piece of hydrogel was split to two halves, one was kept in Tris buffer of 20 mM, another in Tris buffer of 20 mM with 0.1 M $CaCl_2$ solution to cause it to shrink before SEM detection.

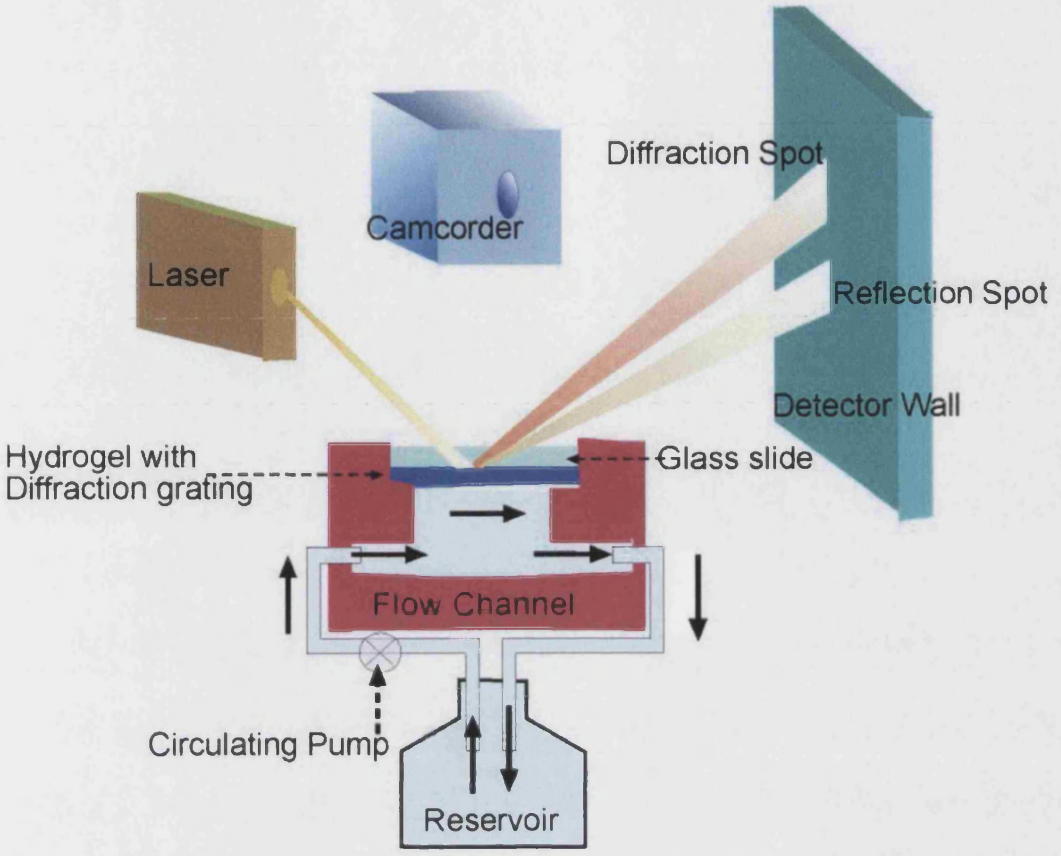

Figure 8.2: The set-up rig of the hydrogel with diffraction grating to response to flow stimulus in exposure to laser.

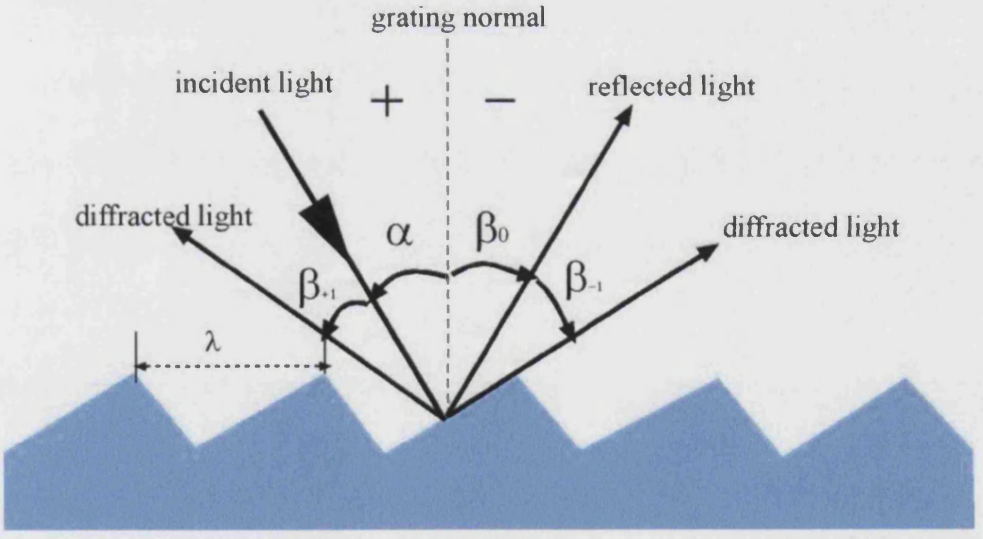

Figure 8.3: Diffraction by a plane reflection grating: the incident and diffracted rays lie on the same side of the grating. A beam of monochromatic light of wavelength *l* is incident on a grating and diffracted along several discrete paths. The triangular grooves come out of the page; the rays lie in the plane of the page. The sign convention for the angles α and β is shown by the + and – signs on either side of the grating normal.

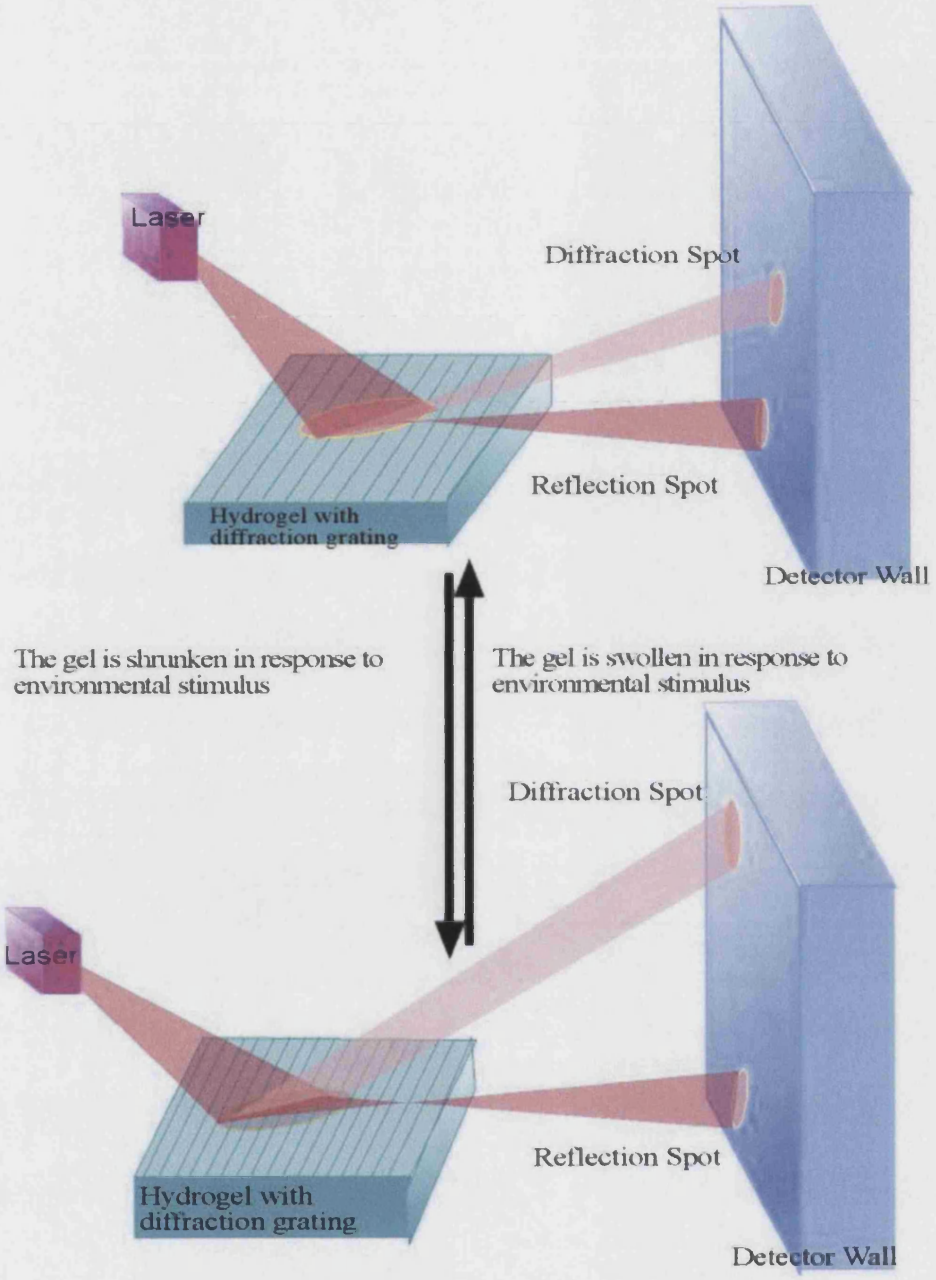

Figure 8.4: Functional changes in the intelligent hydrogel with diffraction grating (IHDG) function method in response to environmental stimuli.

8.3 Results

8.3.1 Hydrogel characterization

1-Ethyl-3-(3-dimethylaminopropyl)-carbodiimide (EDC) catalyses the formation of amide bonds between carboxylic acids and amines by activating carboxyl to form an O-urea derivative. This derivative reacts readily with nucleophiles. The reagent can also be used to make ether links from alcohol groups ester links from acid alcohols and peptide bonds from acids and amines (Tedder *et al.*, 1972). *N*-Hydroxysuccinimide (NHS) is often used to assist the carbodiimide coupling in the presence of EDC. The reaction includes formation of the intermediate active ester (the product of condensation of the carboxylic group and *N*-hydroxysuccinimide) that further reacts with the amine function finally to yield the amide bond.

As shown in the Figure 8.1B, the carboxylic groups can be first grafted onto dextran in the presence of sodium chloroacetate. The carboxyl methyl group modified on dextran can be confirmed by the presence of a carboxylic FT-IR band from the carbonyl (C=O) stretching of CM-dextran at ca.1734 cm^{-1} and 1580 cm^{-1} as shown in Figure 8.5a. The CM-dextran hydrogel can be prepared by carbodiimide chemistry, thus cross-linking carboxylic groups and hydroxyl groups in the CM-dextran without any protein. But according to the expected cross-linking mechanism, the successful incorporation of the protein into the polysaccharide is demonstrated by strong absorption at 1570-1515cm^{-1} (Figure 8.5), which are the characteristic peaks of the secondary amide bond in the solid phase mainly due to N-H bending motion (Socrates, 1997). This indicates that activated carboxyl groups can react with amino acid groups in protein to form amide linkages. Additional, the FT-IR spectrum of the alginate hydrogel in Figure 8.5 B showed evidence of an ester bond at 1450-1475cm^{-1}.

Briefly, a part of the carboxyl groups in modified carboxymethyl-modified dextran or alginate give reactive ester functions by treatment with an aqueous solution of N-hydroxysuccinimide and N-(3-dimethyl-aminopropyl)-N'-ethylcarbodiimide hydrochloride(EDC) together with NHS. The actived ester is easily reacted with hydroxyl groups in CM-dextran or another actived ester and thus the hydrogel can be formed based on the ester bond or carboxylic acid anhydrides (Figure 8.1 A or B). As

far as method B is concerned, the bonds of carboxylic acid anhydrides were always thought to be unstable under normal condition because they are more reactive towards water to form acid (unless the water was removed from the hydrogel on purpose). But a strong band in the range 1300-1210 cm^{-1} for a strained-ring in alginate hydrogel might be noticed due to C-O-C stretching vibrations as seen in Figure 8.5B (Socrates, 1997). With this activated matrix at least two important advantages are obtained: (1) It contains unreacted carboxyl groups which, in low ionic strength conditions, will act as ion exchangers, and by electrostatic interaction the ligand which is to be immobilized is connected to the dextran matrix (reaction C); (2) This matrix will very efficiently bind the ligand thus concentrated at the surface or inside the hydrogel by condensation of ligand aldehyde groups with the hydrazide function of the matrix. In the same way as in the example described above, actived carboxyl groups can be reacted with amine group on ligands (for example, proteins and peptides) by covalent bonds which contribute to effecting a concentration of ligands on the surface or inside.

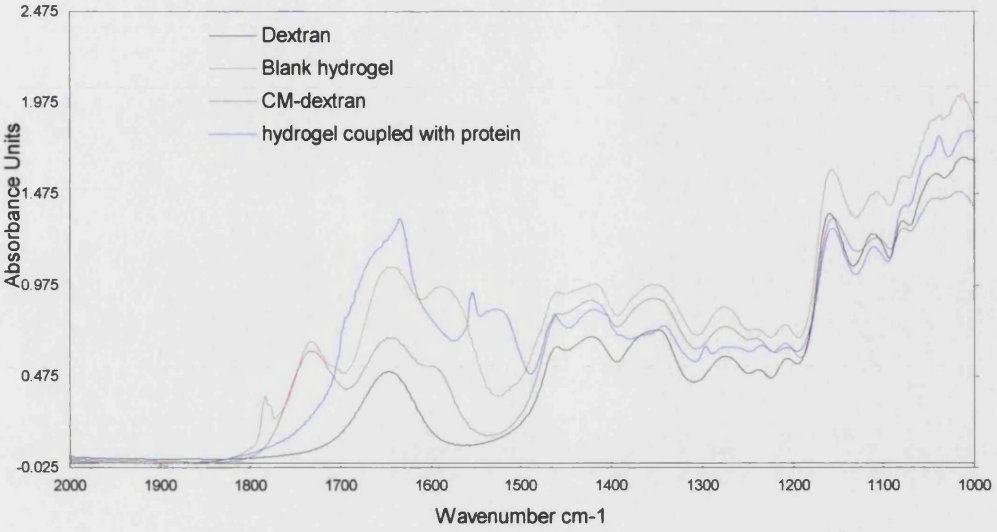

(A)

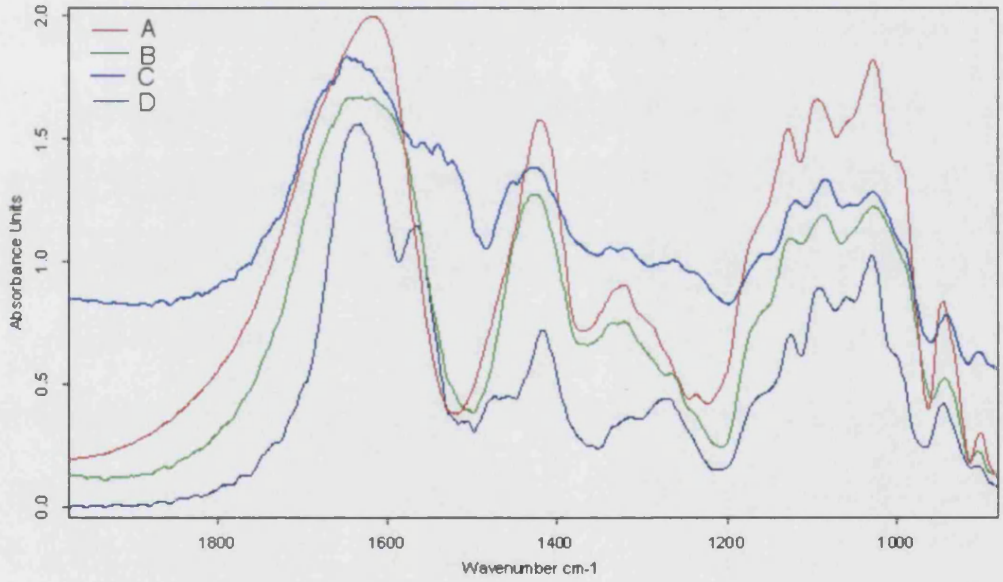

A ---- Alginate, B---- Alginate hydrogel based on ca2+ cross-linkage, C----Alginate hydrogel coupled with protein, D---- Alginate hydrogel based on carbodiimide chemistry

(B)

Figure 8.5: CM-Dextran hydrogel (A) and alginate hydrogel (B) were characterized by Fourier Transform Infrared Spectroscopy (FT-IR). Peaks from the carbonyl (C=O) stretching of CM-dextran and gel appeared at wavenumber as 1734 cm^{-1} and 1580 cm^{-1}. The peak of the carbonyl of gel ester bond at wavenumber as 1775 cm^{-1} also appeared.

8.3.2 Images from of intelligent hydrogel with a diffraction grating

As described in the Introduction to this chapter, master holographic diffraction gratings are normally recorded in a photoresist material whose intermolecular bonds are either strengthened or weakened by exposure to light. Photoresist gratings are chemically developed after exposure to reveal the fringe pattern. A photoresist may be *positive* or *negative*, nevertheless the latter is rarely used. During chemical development, the portions of a substrate covered in positive photoresists that have been exposed to light are dissolved, while for negative photoresist the unexposed portions are dissolved. Upon immersion in a chemical developer, a surface relief pattern is formed: for positive photoresist, valleys are formed where the bright fringes were, and ridges where the dark fringes were. At this stage a master holographic grating has been produced; its grooves are sinusoidal ridges. This grating may be coated and replicated like master ruled gratings.

IHDG fabrication was based on a microcontact printing technique for forming patterns on the hydrogel's surface with micron and submicron lateral dimensions. This method can offer experimental simplicity and flexibility in forming certain types of patterns from a master ruled grating. As showed in Figure 8.6 and 8.7, the pattern image of IHDG (Figure 8.6 B and 8.7B) was apparently replicated from the metal (Figure 8.6 A) or silicon rubber master (Figure 8.7 A). It should be noted that the IHDG in Figure 8.6 B was engineered by the intercrosslinking of CM-dextran with BSA as described in Figure 8.1 C and the IHDG in Figure 8.7 B was cast alginate hydrogel on a cellulose nitrate microfiltration membrane as described in the second fabrication method. The pattern photographs of both the IHDG and the master were taken by digital camera. To enhance effect, the contrast and brightness of these images were adjusted using Jasc Paint Shop Pro^{TM} 6 software, but no other changes to them were made.

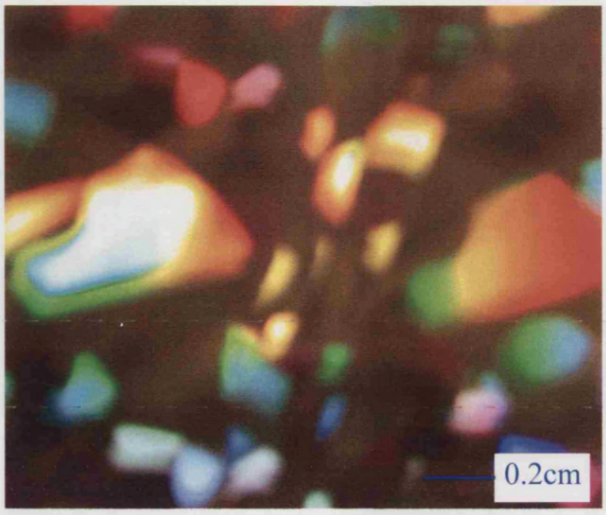

(A)

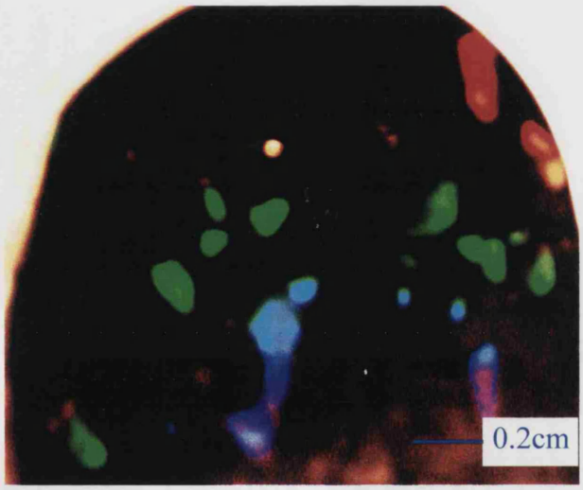

(B)

Figure 8.6: Comparison of the effects of master (A- Metal) and BSA-CM-dextran hydrogel (B- hydrogel without any support) with the same diffraction grating pattern in exposure to strong incident white light.

(A)

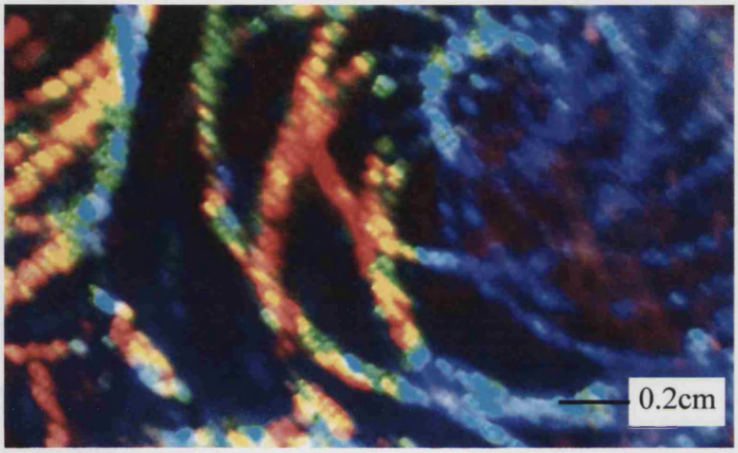

(B)

Figure 8.7: Comparison of the effects of master (A- silicon rubber) and BSA-CM-dextran hydrogel (B-hydrogel cast on the a cellulose nitrate microfiltration membrane) with the same diffraction grating pattern in exposure to strong incident white light. (Dimension approximated as gel swelling varies)

8.3.3 Morphology of the IHDG

Figure 8.8 and 8.10 show the surface array of a swollen hydrogel surface with diffraction grating investigated by optical microscope(Nikon Eclipse E400) and SEM (Jeol 6310 SEM equipped with a cryo-stage). The hydrogel diffraction grating was replicated from metal master with a specific pattern as seen in Figure 8.9 and Figure 8.10 and 8.11. It is noticeable from these images that the hydrogel holds the groove profiles and replicated them from the master. More importantly, the structure of the hydrogel layer with a diffraction grating demonstrates the periodic array in Figure 8.10 A and B, rather then a random distribution like a normal hydrogel structure. Obviously, this array can change with the whole structure of the intelligent hydrogel with environmental stimuli. Although the surface arrays discussed here have a

periodic square structure, many other structural arrays can be created by using different masters. These include strip, rectangular, hexagonal, and even non-periodic surface arrays. The periodicity of the surface array is clearly demonstrated by both optical and diffraction observations.

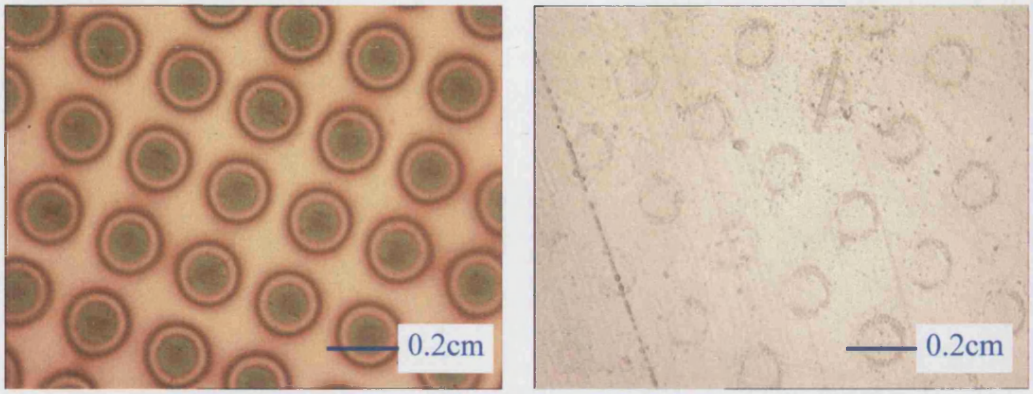

(A) (B)

Figure 8.8: Comparison of the surface pattern of metal master (A) and hydrogel (B) with the same diffraction grating patter detected by optical microscope.

This specific structural changes generated by an applied analyte will lead to changes in the diffraction grating, which will be observable from changes in the diffraction pattern obtained when a laser is diffracted from the gel's surface.

In addition, an alginate hydrogel with simple pattern was fabricated to make an IHDG. Owing to Ca^{2+} having enhanced further crosslinking of alginate, this hydrogel was anticipated to be shrunken by Ca^{2+} in its environment. This result can be confirmed by the SEM of its structure in Figure 8.11. The SEM in Figure 8.11 A appeared looser than that in Figure 8.11 B because the hydrogel in Figure 8.11 B was shrunken after exposure in $CaCl_2$ solution.

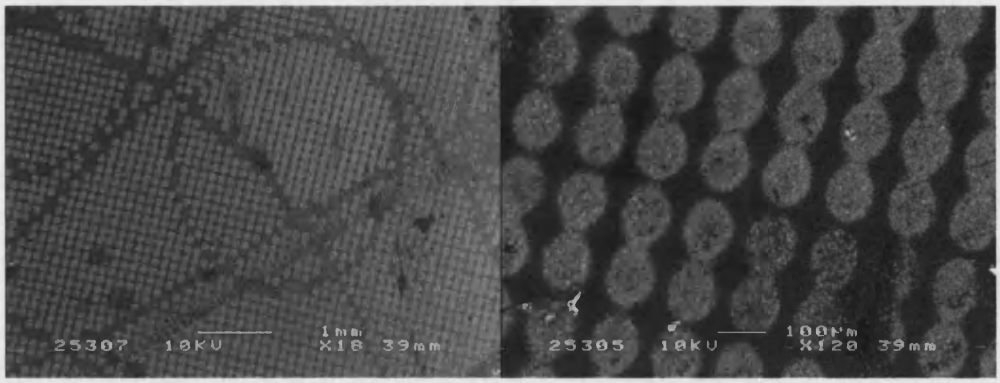

(A) (B)

Figure 8.9 SEM structure of metal master (A, B) with the diffraction grating pattern detected by Jeol 6310 SEM

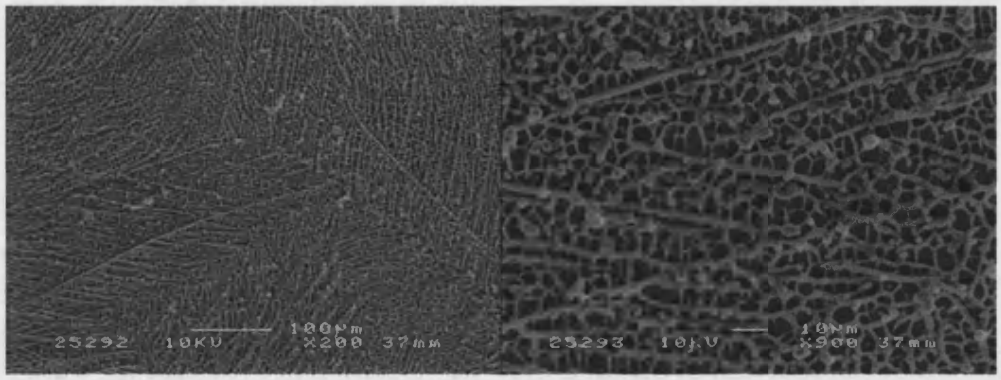

(A) (B)

Figure 8.10: SEM of hydrogel (C, D) with the regular structure detected by Jeol 6310 SEM.

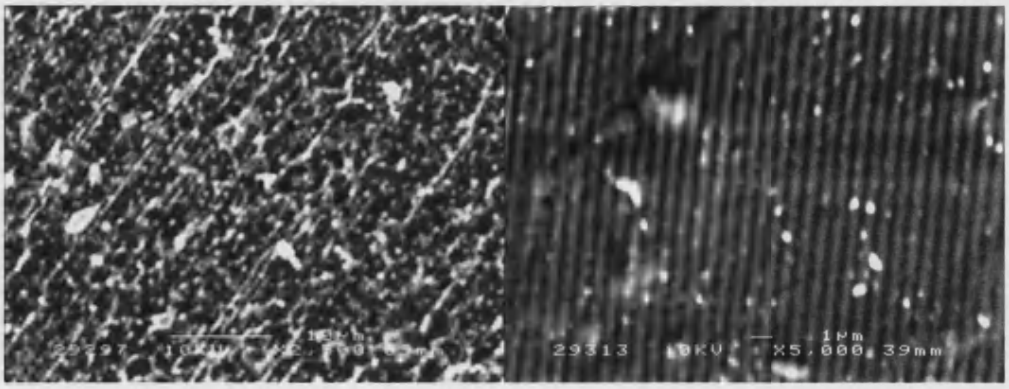

(A) (B)

Figure 8.11: Comparison of SEM structure of diffraction grating alginate hydrogel with simple pattern detected by Jeol 6310 SEM. (A: the hydrogel was kept in Tris buffer of 20 mM (magnification as 2500), B: the hydrogel was kept in Tris buffer of 20mM and 0.1 M $CaCl_2$ (magnification 5000))

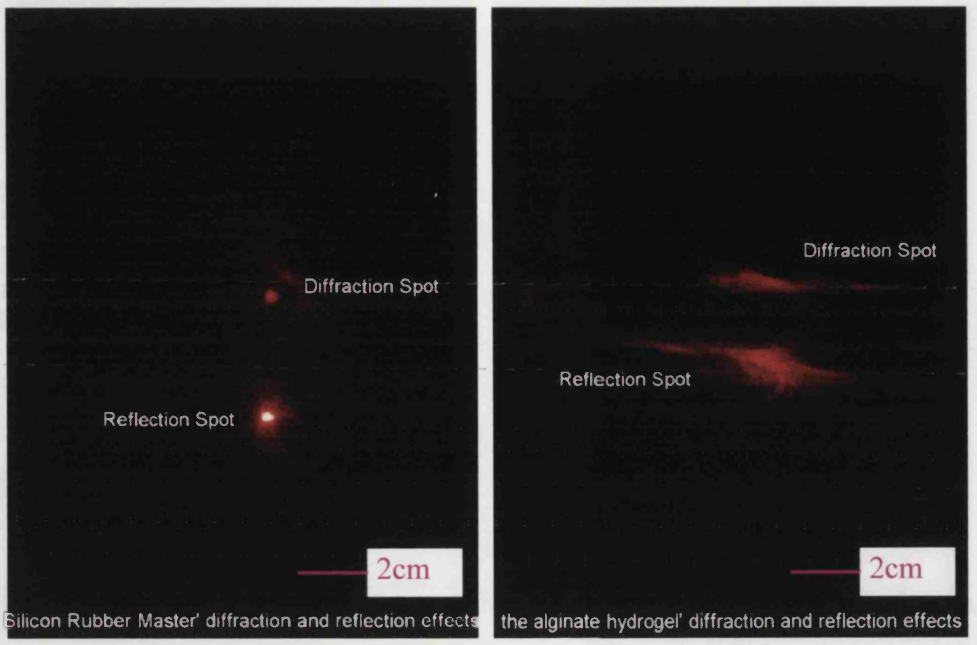

(A) (B)

Figure 8.12: Comparison of the silicon rubber master and the CM-dextran hydrogel with the same diffraction grating pattern illustrated incidented by laser. The image are of the detector screen in Figure 8.2.

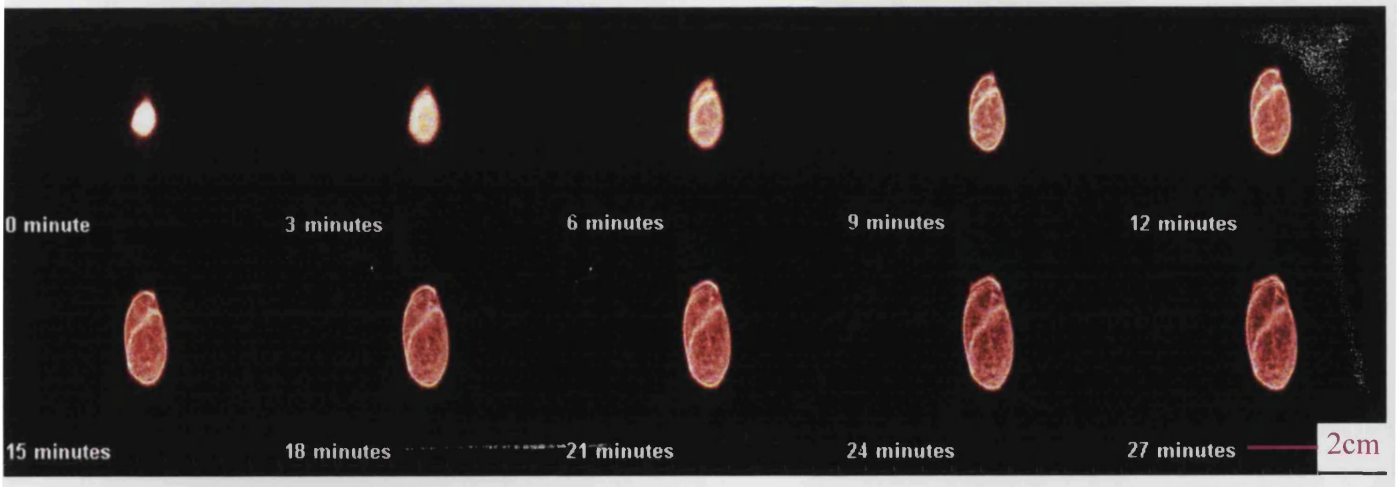

(A)

Figure 8.13: The reflection spot's from the alginate hydrogel with a diffraction grating changes against the time in exposure to 0.1 M $CaCl_2$ solution.

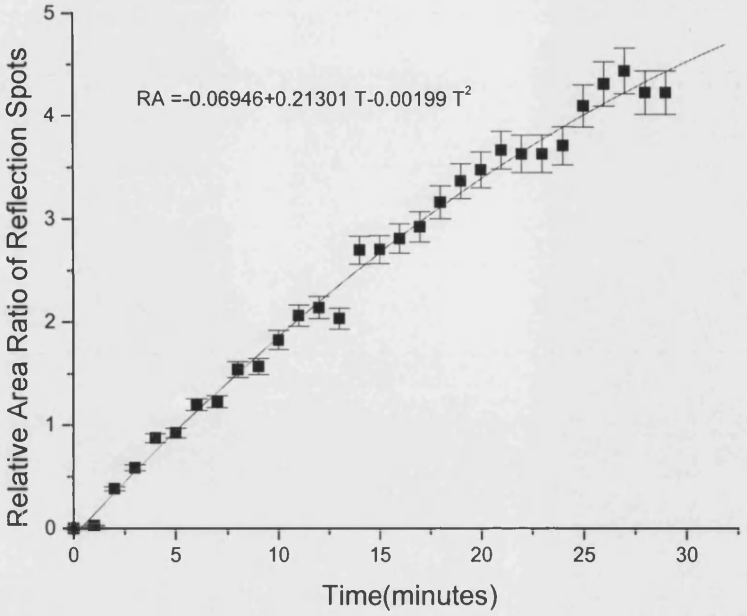

(B)

Figure 8.14: The relative area ratio of the reflection spot is plotted against time. (Note: $RA = \frac{A_t - A_0}{A_0}$)

8.3.4 Testing diffraction gratings on the hydrogels

The diffraction experiment was performed by placing the hydrogel samples in the set-up shown in Figure 8.2. In this case, CM-dextran hydrogel coupled with BSA was used to test the effects on exposure to laser light. It is mentioned the hydrogel used to test was engineered the diffraction grating with simple pattern in order to easily observe out the difference between the reflection and diffraction. The changes of diffraction or the reflection spots on the screen was recorded using a digital camera when the IHDG surface was illumined the by He-Ne laser. As expected, the IHDG replicates the optical effect of a diffraction grating master such as metal or silicon rubber as seen in Figure 8.12A. The limitation of this appears to be that the spot doesn't look as well determed in Figure 8.12 B as that from rubber submaster. This possibly results from irregularities in the surface of hydrogel. To investigate the optical properties of of IHDG from the hydrogel's structural deformation, alginate hydrogel was mounted in the detector set-up. Alginates are well known to be generally acid-stable and heat resistant, with calcium ions causing crosslinking and

controlling the hydrogel's strength. In this study, alginate hydrogel with a diffraction grating was first made in the presence of EDC/NHS, and then 5 mM $CaCl_2$ solution was pumped into the flow channel. Hence the alginate hydrogel underwent shrinkage (as shown in Figure 8.11). As observed in Figure 8.4, the diffraction or reflection spot is anticipated to move in response to the shrinkage of the hydrogel. The converse effect should be seen in response to hydrogel swelling. This phenomenon results from the periodic array density enhance are given by the contracted hydrogel under the condition of constant laser irradiation. But the different results are observed as shown in Figure 8.13. Further experiment will investigate the cause of this result. The interesting consequence is that the shape of reflection spot was recorded by digital camcorder (Canon MV530i) against time during the diffusion of Ca^{2+} into hydrogel. The spot area appears to dramatically enlarge after 30 minutes, however, the brightness of the spot was declined. To track this relationship between reflection shapes with time, the relative area ratio (*RA*) was calculated based on the area of these shapes. To determine the absolute area of these shapes, the images were displayed in the same size window using Paint Shop Pro 6.02 (PSP), the grid spacing of image can be read out. The RA value can be attained according to $RA = \frac{A_t - A_0}{A_0}$, where A_t is the readout area of spot shape in PSP at different time and A_0 is readout area at the beginning of experiment. The curve in Figure 8.14 demonstrated the RA increases quickly at the earlier 15 minutes and then tails off.

8.4 Discussion

This study was carried out as a proof of concept for an intelligent hydrogel with a diffraction grating. When compared with a hydrogel with a square array of gold thin films (Hu *et al.*, 1998) or entrapped crystalline colloidal arrays (Holtz *et al.*, 1998). Firstly the method of hydrogel fabrication used simplified the manufacturing procedure allowing the diffraction grating to be directly replicated from a suitable submaster grating. From the previous study of pH-sensitive hydrogels, variation of carboxylic group density and cross-linking reagent concentration in a CM-dextran hydrogel allow control of both charge density and degree of cross-linking in the hydrogel so that the balance between degree of swelling and mechanical properties can be easily controlled. In addition, EDC/NHS does not chemically bind to

polysaccharide molecules, in contrast with conventional cross-linking agents (Nakajima *et al.,* 1995), instead reacting to form a water-soluble urea derivative which has far lower cytotoxity and also is easily washed out. More importantly, the carboxyl groups in carboxymethyl-tailored or natural carboxyl acid polysaccharide are modified so as to give reactive ester functions by treatment with EDC/NHS, hence enhancing the ligands containing amine groups such as, for example, proteins and peptides, be coupled to hydrogel by covalent bonds. The protein of interest binding to a target drug or other substance is attached in hydrogel with a diffraction grating and then arranged in microarray chips. One novel protein chip created will combine protein coupled in the support material with easily detection. Together these simultaneously meet the two crucial requirements of protein microarray: that is to choose a suitable surface chemistry to allow immobilized protein of diverse types retain to biological activity and devise a practical means of measuring the degree of protein binding, assuring both sensitivity and a suitable range of operation (Mitchell, 2002). This novel material has potential application in protein microarray or drug discovery.

The hydrogels' physiochemical characteristics after gelation of alginate and CM-dextran based on carbodiimide chemistry has been confirmed by FT-IT spectrum as shown in Figure 8.5. Also different proteins, such as lysozyme, concanavalin A, and ovalbumin, have been coupled to CM-dextran hydrogel as shown in Chapter 3. The results from Con A –CM dextran hydrogel illustrated the porosity of this hydrogel can be adjusted by environmental D-glucose concentration owing to the D-glucose competitively binding to Con A resulting in the breakdown of the binding of dextran with concanavalin A (Tang *e. al.,* 2003).

The groove pattern of a silicon rubber grating is easily replicated from a submaster onto the hydrogel. This acted as the hydrogel submaster. Because of the silicon rubbers' hydrophobic properties, the hydrophilic hydrogel can be easily separated from the submaster with minimal damage. The response of hydrogel with specifically patterned diffraction gratings can be observed from color variations using incident white light as the structure of grating changes in response to specific environmental stimuli such as temperature, pH, or specific analyte.

8.5 Conclusion

A novel material with an embossed diffraction grating has been fabricated. The hydrogel optical characteristics have been confirmed both using monochromatic lasers and white light. The potential application of this functional hydrogel exists for a range of analytical applications has been demonstrated.

Chapter 9. Intrinsic Shielding Effects in Ligand-Receptor Substituted Affinity Membranes

9.1 Introduction

The potential for membrane chromatography as a high-throughput, high-selectivity purification scheme has been studied for many years, but as yet without significant commercial success (Reis *et al.,* 2001). Recent developments have stimulated further interest in this technology and several membrane chromatography products are expected to come to market in the next few years (Zeng *et al.,* 2000). Compared with conventional bead chromatography, micro-porous membranes have a number of potential advantages as supports for chromatography (Charcosset, 1998, Klein, 2000). The membrane acts as a very short, wide bed allowing high velocities with very short residence times coupled with modest trans-membrane pressure drops. Reduction of diffusional resistance by allowing a greater contribution from convective flow usually results in much faster binding kinetics. Affinity membranes represent a logical extension of these materials combining the selectivity of affinity and adsorption with the improved transport properties of membranes. Membrane systems similar in magnitude to packed columns operated using stepwise elution allows a rapid concentration of proteins by a factor of 10 or more, with 85-100% recovery (Charcosset *et al.*, 1995, Krause *et al.*, 1991, Luksa, 1994) . Similar analytical separations of proteins can be achieved using membrane stacks together with gradient elution methods and have been shown to be equivalent to chromatography column (Josic *et al.*, 1992, Tennikova *et al.*, 1993). Finally, the linear scalability of the membrane systems is attractive for processes aimed at purifying proteins and other biomolecules from biological fluids (Wang *et al.,* 1995, Elias, 2000).

To successfully apply affinity membranes in the biomedical field, low fouling hydrophilic membranes are needed with appropriate chemical groups on the pore surface that can serve as coupling sites for suitable ligands. A number of different methods have been described to prepare membranes with hydrophilic and/or

functionalizable surfaces, mainly derived from monomers containing reactive groups for polymerization and chemical or physical post-treatment of hydrophobic membranes (Avramescu *et al.*, 2003). The functional groups employed to couple ligands to membranes commonly include –OH, $–NH_2$, $–SO_3H$, –COOH, $–CONH_2$ or epoxy, achieved by chemical modification or graft polymerization (Rodemann *et al.*, 1994). Materials currently used or with potential applications in affinity membrane are divided into two categories, according to their natural or synthetic origin. The basic material from natural sources is cellulose, which has long been used in membrane preparation and is a good matrix for affinity ligand coupling (Charcosset, 1998). Recently, new macroporous chitin and chitosan membranes for protein purification have been also developed (Zeng *et al.*, 1997, 1998, 1999, 2000). The most common synthetic microporous membranes are produced from hydrocarbon polymers (polyethylene (PE) and polypropylene (PPr)), aromatic copolymers (polycarbonate (PC), polysulfone (PS) and polyethersulfone (PES)), aliphatic polyamides (nylon-6 and nylon-66), and a few specialty polymers, such as polyvinylalcohol (PVA) (Klein, 2000). The ligands employed in adsorptive membranes include amino acids, antigens, antibodies, mimetic dyes, metals, other biologicals, and ion exchange groups (Charcosset, 1998).

Since its introduction, dye ligand chromatography has played an important role in the separation, purification and recovery of numerous proteins and enzymes due to the overall similarity of their molecular shape, size and charge distribution to those of biological heterocycles such as coenzymes and nucleotides (Ruckenstein *et al.*, 1998, Biellmann *et al.*, 1979). They have a number of advantages over natural ligands including cost, stability and ease of coupling (Yu *et al.*, 2001). Initially dye ligand chromatography was limited in bead-based matrices (Zhang *et al.*, 2002, Tong *et al.*, 2002). However recently, dye-membranes have been reported for protein and enzyme separation (Ruckenstein *et al.*, 1997, 1998, Kassab *et al.*, 2000, Bayramoglu *et al.*, 2003). A range of dye ligands, including Cibacron Blue 3GA, Cibacron Blue F3GA, Active Red K2BP and Procion Blue MX-R, can be immobilized on a range of commercial membranes, including cellulous, titania, nylon (Suen *et al.*, 2000, Liu *et al.*, 1994, Champluvier *et al.*, 1994, Beeskow *et al.*, 1997) or novel polymerized membranes such as chitosan (Zeng *et al.*, 1996, 1998).

Considerable efforts have also been made to develop hydrogel membranes from dextran, a bacterial polysaccharide consisting essentially of a-1,6 linked d-glucopyranoside residues with a small percentage of a-1,3 linked side chains. The availability of dextran with different molecular weights, its solubility in polar organic solvents, enabling chemical modification, and its biocompatibility make this natural polysaccharide synthetically attractive. Owing to their low tissue toxicity and high enzymatic degradability at desired sites, dextran hydrogels have been widely investigated as potential matrix systems for both cell culture and drug delivery applications (Ferreiraa *et al.,* 2002, Tang *et al.*, 2003).

To improve the functionality of these dextran hydrogels we have developed synthetic protocols that allow the inclusion of the lectin Concanavalin A to produce a gel whose porosity changes in response to d-glucose concentration as seen in chapter 2 and 3. This method can also be used to graft a range proteins to a dextran backbone and that can be incorporated in to a hydrogel formulation. Once formed these gels can be further substituted with biomimetic dyes using standard coupling conditions via the reaction between the chlorine groups of the reactive dyes and the CH_2OH group of dextran.

The aim is a highly selective dye ligand affinity membrane capable of selectively recovering specific proteins from biological fluids by in a process stage where the effects of non-specific binding are minimized. To reduce non-specific binding, the affinity membranes described here include an immobilized protein such that, in the absence of external adsorbate, the dye will be weakly bound to the coupled protein. For external protein to displace this intrinsic adsorption its binding affinity for the dye must much be such that competitive displacement of the intrinsic binding occurs. By choosing appropriate dye/coupled protein combinations the aim is to allow the binding of a specific adsorbate while preventing the adsorption of more weakly interacting contaminants. The principle of operation is shown in Figure 9.1.

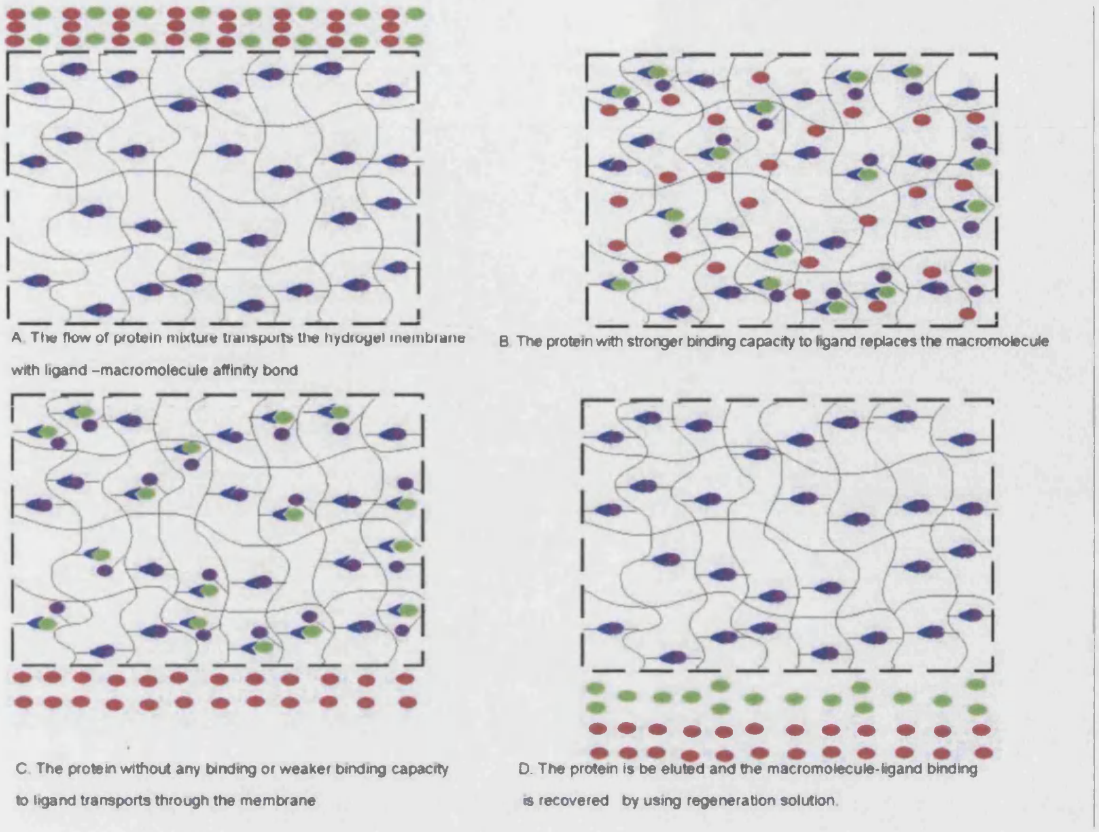

Figure 9.1: Hydrogel membrane with ligand-macromolecule binding exposed to protein with stronger binding capacity.

The concept is similar in principle to polymer shielding, as described by Mattiasson *et al.* (1996), where a non-ionic, water-soluble polymer is used to shield a dye matrix prior to column chromatography to prevent subsequent interactions. The advantage of the approach proposed here is that the need for an additional soluble reagent is eliminated.

Cibacron Blue F3-GA was chosen as the ligand in this study, as - while it has been widely used in the recovery of proteins from complex fluids e.g. human serum albumin (HSA) from blood plasma (Ruckenstein *et al.,* 1998, Kassab *et al.,* 2000) - purification factors can be limited by its ability to bind a variety of other proteins via a number of different mechanisms (Zhang *et al.,* 2001).

9.2 Materials and methods

9.2.1 Materials

Dextran, lysozyme, cytochrome C, cibacron blue F3GA, BSA and hemoglobin were obtained from Sigma-Aldrich, UK. All other chemicals were of reagent grade and obtained from Lancaster Synthesis Ltd., UK.

9.2.2 Hydrogel preparation

CM-dextran preparation was as described in Chapter 4. The reaction, utilizing carbodiimide chemistry catalyses the formation of amide bonds between carboxylic acids in CM-dextran and amines in protein, such as lysozyme, BSA and hemoglobin, by EDC and NHS (Figure 9.1). The reagent can also be used to make ester links from hydroxyl groups and carboxylic groups in CM-dextran (Tedder *et al.*, 1972, Grabarek, *et al.*, 1990). Furthermore, CB is covalently attached to the membrane via the reaction between the chloride groups of the reactive dyes and the hydroxyl groups of the dextran as shown in Figure 9.2 (Kopperschlager *et al.*, 1968). This structure should allow affinity binding between CB and the attached protein within the membrane (Figure 9.3).

1.

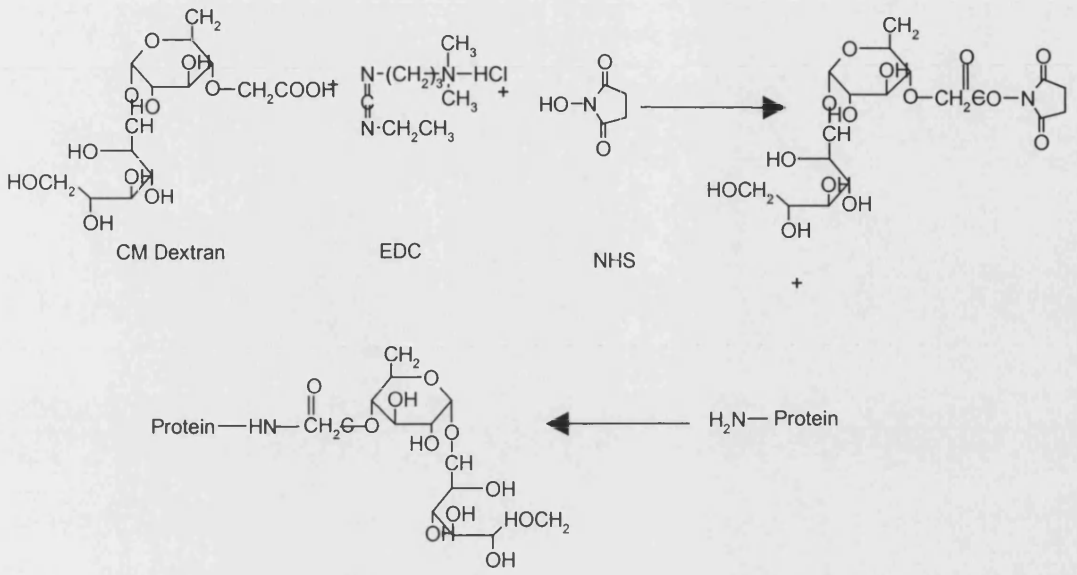

2.

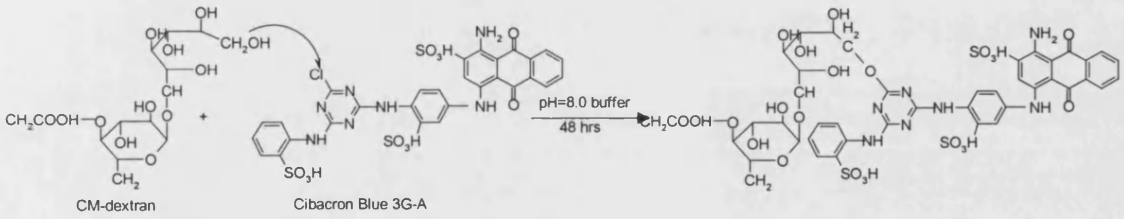

3.

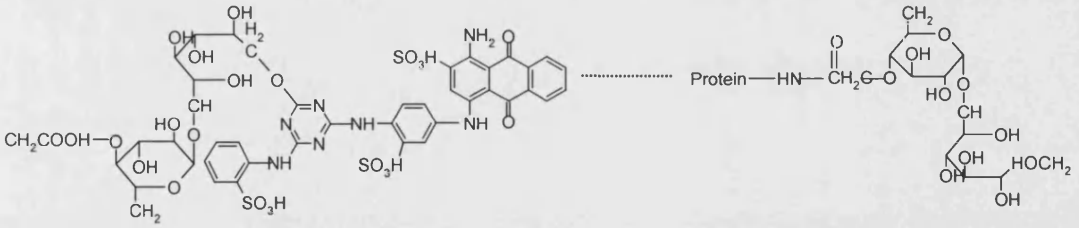

Figure 9.2: The chemistry of this gel

The CM-dextran used for hydrogel synthesis, has a COOH substitution ratio of 1 COOH per 65 glucose residues, as determined by acid titration. To produce hydrogel with coupled protein, 1 g CM-dextran was dissolved in 5 ml distilled water by stirring. The resulting solution was degassed and 500mg EDC plus 75mg NHS was dissolved in 2 ml distilled water added and stirred for 10 minutes. 200 mg of the protein to be attached, dissolved in 3.0ml distilled water, was then added. For the

higher molecular weight proteins (BSA and haemoglobin) gelation occurred after approximately 30 minutes, at which point it could be cast as required. For the membranes used here casting was onto a nylon gauze support, pore size 0.1 mm, thickness of 0.5 mm mounted between two glass plates using spacers to give the required membrane thickness. In the case of the lower molecular weight proteins gelation starts after approximately 50 minutes and the sol-gel transition period is very short (approximately 1 minute) requiring careful casting.

After initial gelation the gels were allowed to stabilize for a further 8 hours before being removed from the casting plates by immersion and subsequent extensive washing in 20 mM Tris buffer of pH 8.5 to remove unreacted material. These membranes were then placed in 5mg/ml CB in Tris buffer (pH 8.5) and allowed to react for 12 hrs. Before use, the membranes were washed in pH 7.4 Tris buffer with 1M NaCl to remove non-covalently binding CB.

Control membranes were produced with CB but no coupled protein using the same synthesis protocol.

9.2.3 Physicochemcal properties of the hydrogel

Infrared spectroscopy of samples taken at different stages of the reaction sequence was performed using a Bruker-equinox 55 FT-IR spectrometer. Freeze-dried samples were mixed with potassium bromide powder and pressed into tablets under vacuum. For each sample 100 scans were recorded from 4000 to 400 cm^{-1} at a resolution of 2 cm^{-1}.

9.2.4 Hydrogel morphology

The morphology of the hydrogel was examined using a Jeol 6310 scanning electron microscope (SEM) equipped with a cryo-stage and energy-dispersive X-ray (EDX). Samples of hydrogel were clamped between two pieces of aluminum sheet and rapidly frozen in liquid nitrogen and then introduced into the SEM chamber pre-cooled to a temperature of ca. –160 °C. The stage was then heated to a temperature of ca-80 °C to sublimate off the surface water. After cooling to –160 °C, the sample was gold sputtered for 3 minutes. Samples were scanned at a magnification of 5000.

9.2.5 Characterization of binding interactions

In spite of the extensive studies and applications of dye-ligand adsorbents, fundamental interactions between the reactive dye and target proteins remain poorly understood. In this study, the binding properties of soluble CB towards the proteins used in membrane preparation (lysozyme, cytochrome C, BSA and hemoglobin) were studied using Isothermal Titration Calorimetry (ITC) in an OMEGA ITC (Microcal Ltd). The instrument was calibrated and experiments conducted in accordance with the manufacturer's operating instructions.

Before use, CB was treated by 0.1M NaOH and adjusted to pH 7.4 with HCl to block the chemically reactive chloride groups. The deactivated dye was diluted in 20 mM Tris buffer pH 7.4, 0.1M (adjusted with NaCl), and 0.02% NaN_3 was added as a preservative. Before use, the solution was filtered through a 0.1 μm PVD/PE syringe filter and the concentration adjusted to 0.092 mM. Protein samples were diluted to a final concentration of 27.8 mM. Titrations were run at 20°C with all samples degassed at 15°C prior to use. In each case 54 injections of 5 μl of CB solution were automatically added at 2 minutes intervals into the protein solution stirred at 300 rpm. The heat evolved after each injection was determined from the energy input required to maintain the temperature of the sample cell equal to that of the reference cell. In all cases control experiments were carried out using CB injections into a cell containing buffer without protein and relative heats of dilution and mixing subtracted from the heats of binding relative to the real titration experiment.

Final experimental results, represented by heat evolved versus cell ligand/lectin ratio, were fitted to a range of binding models using the Origin ITC Data Analysis package (Microcal Ltd).

9.2.6 Protein diffusion and adsorption experiments

The trans-membrane transport, protein transport, and adsorption were investigated using solutions of the proteins used to make the membranes tested i.e. each membrane type was challenged with each protein in turn. Diffusion experiments were conducted in a diffusion cell consisting of donor and receptor chambers of equal volumes of 4.4 ml as seen in Chapter 3. Hydrogel membranes with a surface area of 4.58 cm^2 were mounted between the two chambers. Once the membranes were

mounted, both chambers were filled with 20 mM Tris buffer. The donor chamber was connected to the protein reservoir (4mg/ml) via a pump. The receptor chamber was connected to a UV-Visible spectrophotometer (Shimadzu 1601), to allow protein diffusion across the membrane to be automatically monitored and logged from optical density changes. The amount of protein diffusing across to the receptor chamber was calculated using calibration data for lysozyme, BSA at 280 nm, cytochrome C at 410nm, and hemoglobin at 418nm. Adsorption and desorption cycles were conducted by recycling the solutions through donor and receptor chambers in a closed loop configuration with a total loop volume for each chamber of 6 ml. A protein feed of 4mg/ml protein was loaded into the donor side and allowed to absorb into membrane for 5 hours while recycle flow was maintained. The membrane was then washed using 20 mM Tris buffer (I= 0.1M) recycled in both chambers until no further protein release was observed in the receptor chamber. Desorption was accomplished by pumping 1M NaCl into donor side (Zhang *et al.,* 2001, 2002). Eluted protein was determined as function of time while the solution was recycled thought the receptor chamber. All experiments were conducted at 25°C.

9.3 Results

9.3.1 Hydrogel characterization

The successful incorporation of the COOH group into dextran is demonstrated by the presence of a carboxylic FT-IR band from the carbonyl (C=O) stretching of CM-dextran at ca .1734 cm^{-1} and 1580 cm^{-1} as shown in Figure 9.3. In the absence of protein, carboxyl groups activated by EDC/NHS can react with hydroxyl groups in CM-dextran to form ester linkages as described in Chapter 5. For proteins containing gels primary amides show a weak-to-medium intensity band at 1650-1620cm^{-1} that is generally too close to the strong carbonyl band to be resolved. However, as seen in Figure 9.2, a strong band at 1580-1520cm^{-1} from the sym-triazine ring of CB covers the amide II band (1570-1515cm^{-1}) arising from protein bound to dextran due to a motion combining both the N-H bending and the C-N stretching vibrations of the group –CO-NH- in its *trans*- form (Socrates, 1997).

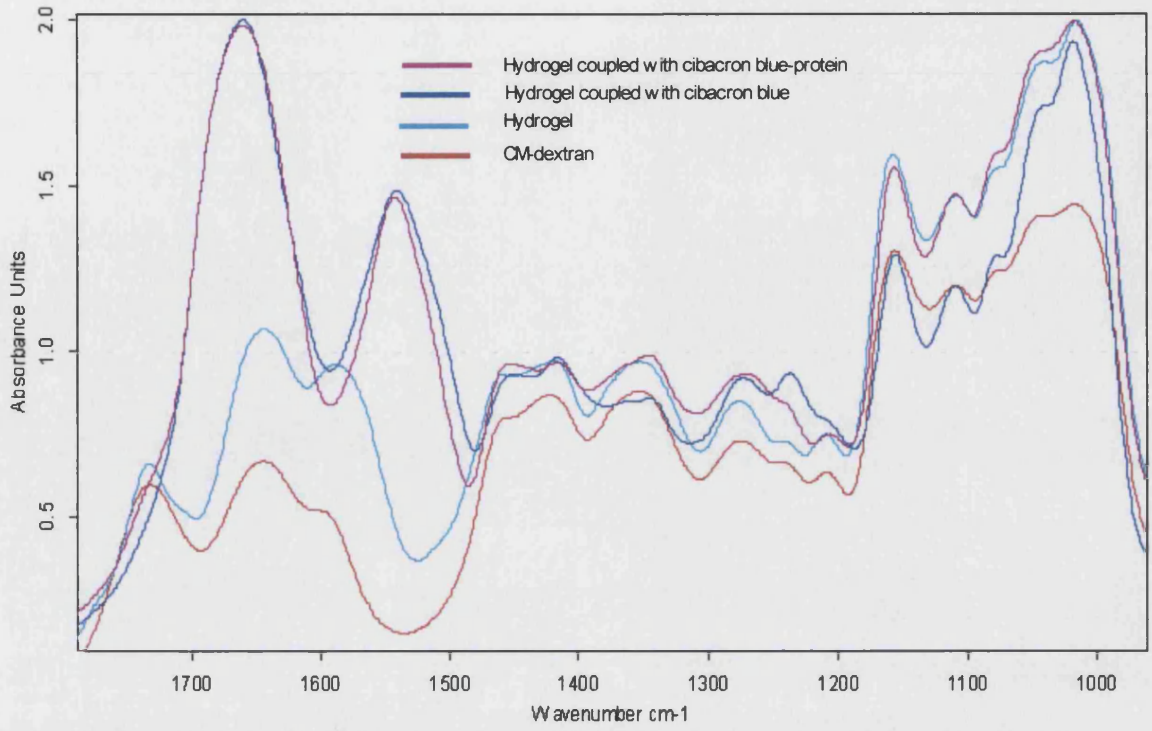

Figure 9.3: The comparison of CM-dextran, dextran hydrogel, hydrogel coupled with cibacron blue and hydrogel coupled with both cibacron blue and protein.

9.3.2 Morphology of hydrogel SEM

The SEM study of the cross-section morphology of the CM-dextran hydrogel clearly shows its three-dimensional network structure (Figure 9.4). It can be reasonably assumed that the structure observed by SEM was the original, or very close to the original, morphology without artifacts as no significant shrinkage of the gel volume (less than 1%) was observed after freeze-drying. This assumption also is supported by other reports (Hong *et al.,* 1998, Kim *et al.,* 2000) on the ability of cryofixation to conserve delicate structures of biological samples, such as tissue, which would be prone to deformation or to the release of their chemical constituents if chemical fixing agents were used. Cryofixation is regarded as eliminating artifacts such as distorted morphology generated by fixation processes that do not represent the true structure of a specimen (Bohrmann *et al.*, 1991).

Generally, the pores on the cross section of the CM-dextran hydrogel membrane were of similar size for all protein CB combinations. In comparison the hydrogel membrane without any ligand (Figure 9.4 A) shows pores, which are more compact.

A possible reason for this difference is that the ligands in membrane further strengthen the cross-linkage. The pore size of these membrane used in diffusion experiments was estimated as in the range of 0.1-0.4 um.

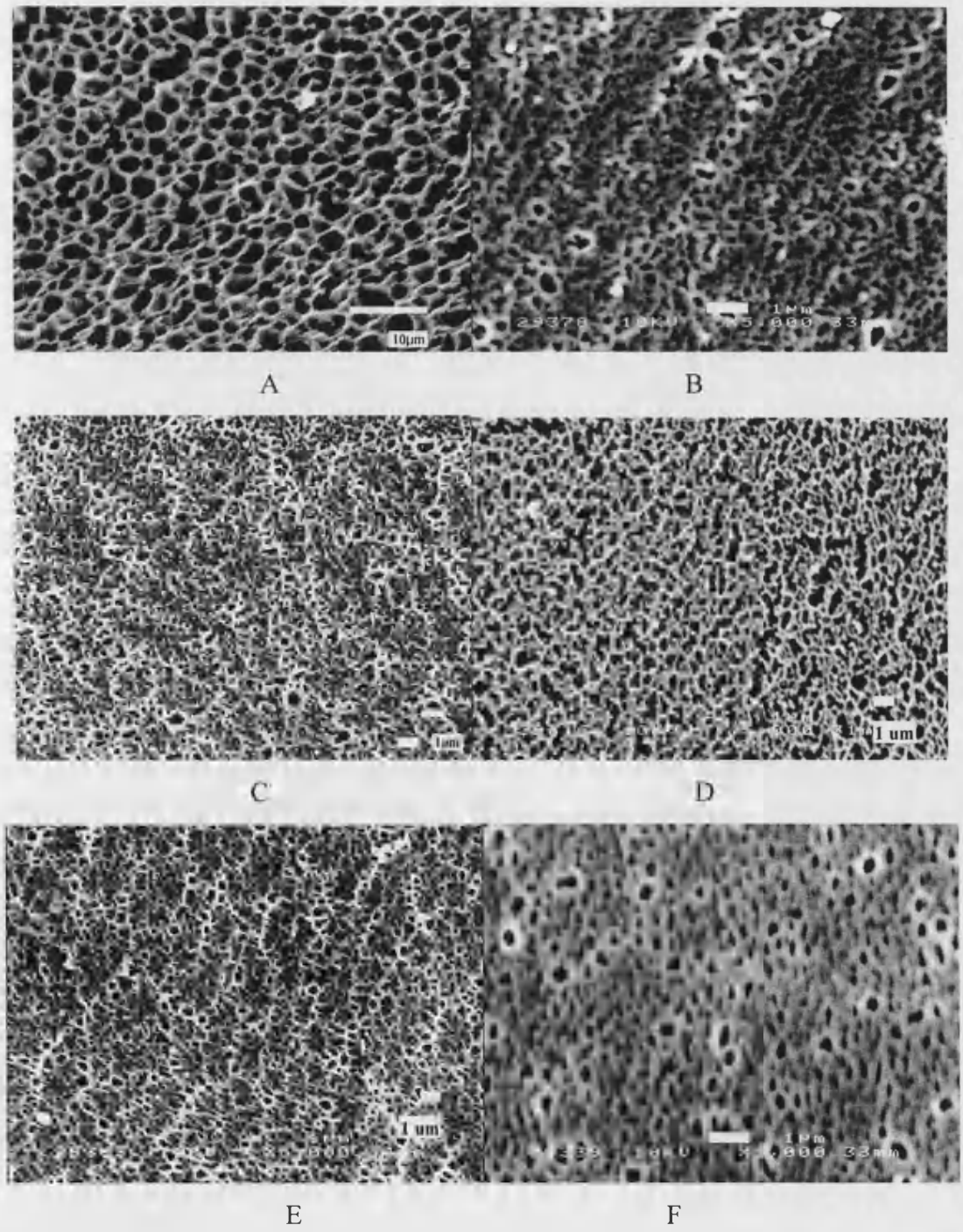

Figure 9.4: SEM micrograph of CM-dextran hydrogel membrane coupled with different ligands. A: without any ligands B: with CB C: with BSA D: with BSA-CB E: with hemoglobin-CB F: with lysozyme-CB.

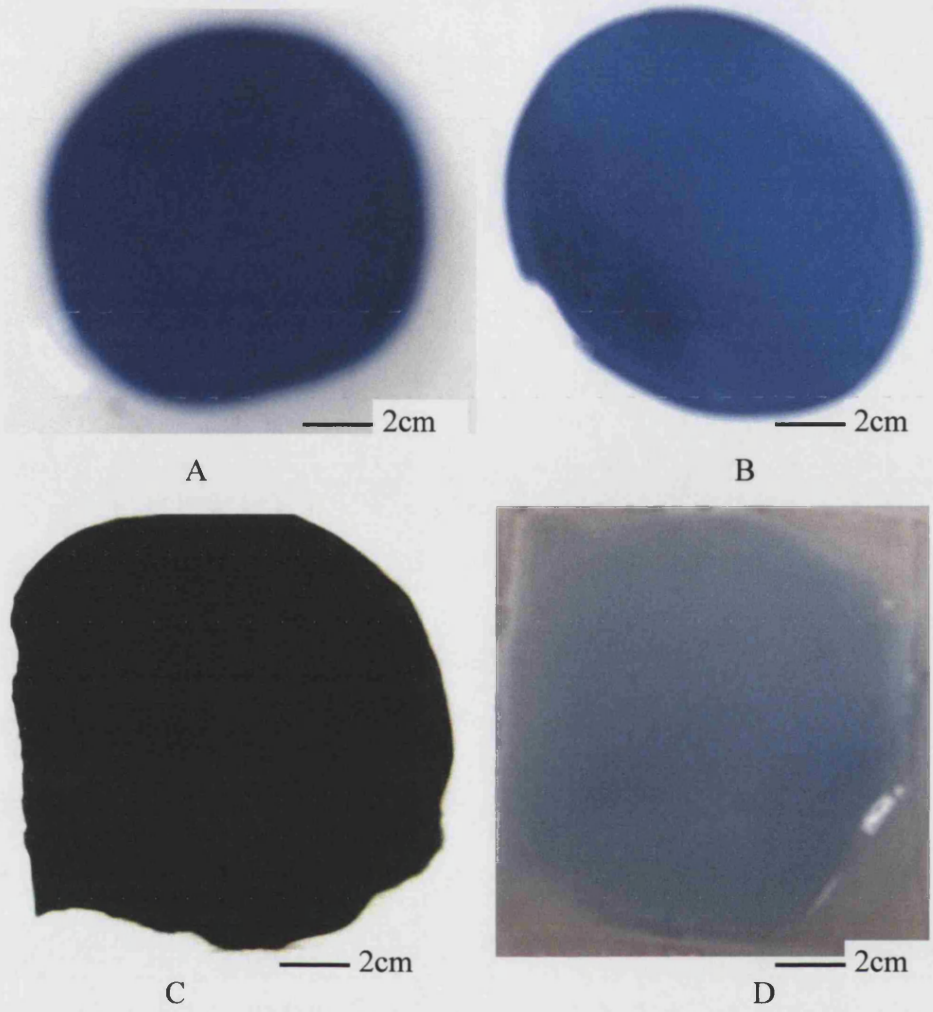

Figure 9.5: Photograph of A, B, C, D show hydrogel membranes coupled with BSA-CB, lysozyme-CB, haemoglobin-CB and CB respectively.

CB was immobilized onto CM-dextran hydrogel membrane. These membrane coupled protein developed a dark blue colouring in contrast to a very light blue tint of the membrane without any protein (as seen in Figure 9.5). These differences were caused by the protein enhancing binding of CB onto the membrane. Furthermore, the combination membrane with dark red hemoglobin and blue CB produce a deep dark coloured membrane in Figure 9.5 C.

9.3.3 ITC characterization of protein binding

ITC binding results are shown for CB with lysozyme, BSA, cytochrome C and hemoglobin in Figure 9.6. Panel 1 shows the raw calorimetric data for the titration of protein with CB, denoting heat evolved (negative exothermic peaks). Panel 2 shows the plot of heat evolved per injection as a function of the molar ratio of ligand to the

protein. The smooth solid line represents the best fit of the experimental data using a binding site model. The binding constants of different protein to CB are summarized in Table 9.1 together with relevant protein properties.

	Lysozyme	Cytochrome C	Hemoglobin	BSA
MW	14,300	12230	64,500	66200
Isoelectric point (pH)	11	10.6	6.8	4.9
Fit model	FourSites	TwoSites	OneSites	TwoSites
K_a (M^{-1})	K_1= (1.803±0.158)×10^5 K_2=(4.045±0.274)× 10^6 K_3=(2.477±0.089)×10^5 K_4=602.1±132.7	K_1=1614±107.3 K_2=(2.654±0.178)×10^4 K_3=3729±270	K=(4.203±0.058)×10^4	K_1=(8.203±6.565)×10^4 K_2=(3.515±4.776)×10^5

Table 9.1: The binding constants of different protein to CB together with protein relevant properties

Because CB is a triazine dye with three negative charges at pH 7.4, the binding relationship of CB with proteins can involve hydrophobic, electrostatic, or hydrogen bonding forces. As these effects will vary from protein to protein and will act in addition to more specific affinity interactions it was not possible to describe the interactions using the same model throughout. To attain good descriptions of the CB/protein binding data different models were evaluated for each case using the results of titrations conducted in triplicate. It was found that, based on the error range of the estimated parameters, a one-site binding model was plausible for hemoglobin-CB, two-sites for BSA-CB, four-sites for lysozyme-CB, and three-sites for cytochrome C-CB as shown in Figure 9.6 and 9.7. The exact mechanism of binding is still unclear but CB acts as a strong cationic ion exchanger because of its negative charge. It is postulated that the bilirubin and fatty-acid binding sites of albumin are significant in the interaction (Leatherbarrow *et al.*, 1980). The association constant of lysozyme and BSA binding with CB are consistent with other reports (Beeskow *et al.*, 1997, Mayes *et al.*, 1970), which lie in the range between 10^{-6} and 10^{-5} M. As far as cytochrome C and hemoglobin were concerned, they were used in relatively weaker

binding with CB in comparison with BSA or lysozyme. In this study, hemoglobin was also attached to the membrane with CB as a control experiment. To provide a common basis of comparison an effective half saturation constant was calculated for each interaction which suggested that the hierarchy of "operational affinity" is lysozyme>BSA>hemoglobin> cytochrome C.

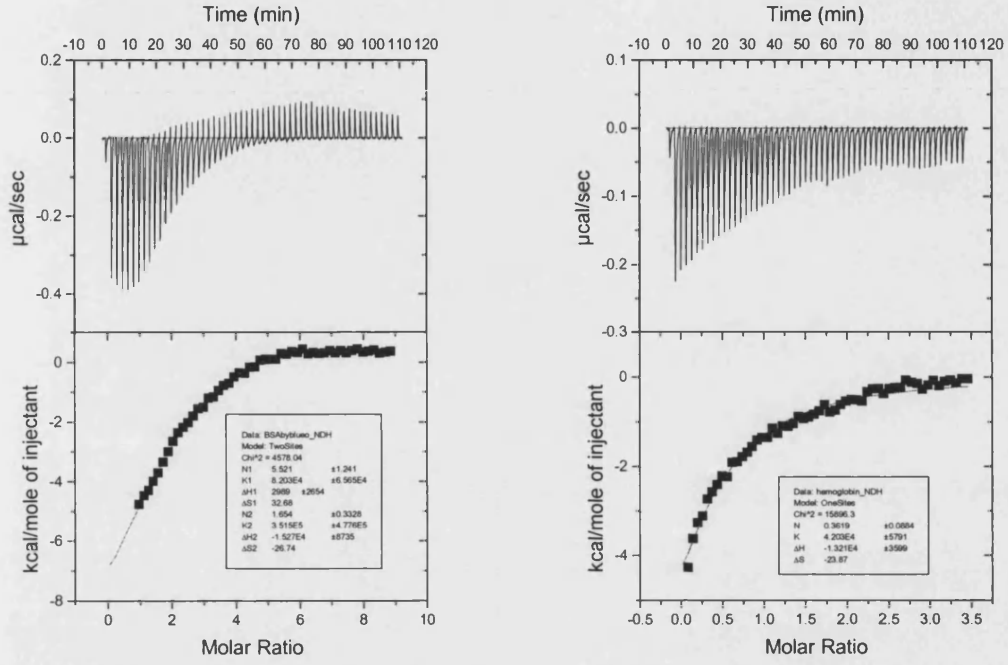

(A) (B)

Figure 9.6: (A) 2mg/ml Hemoglobin was titrated by 0.4mg/ml Cibacron blue. (B) 1 mg/ml BSA wad titrated by 0.5mg/ml cibacron blue.

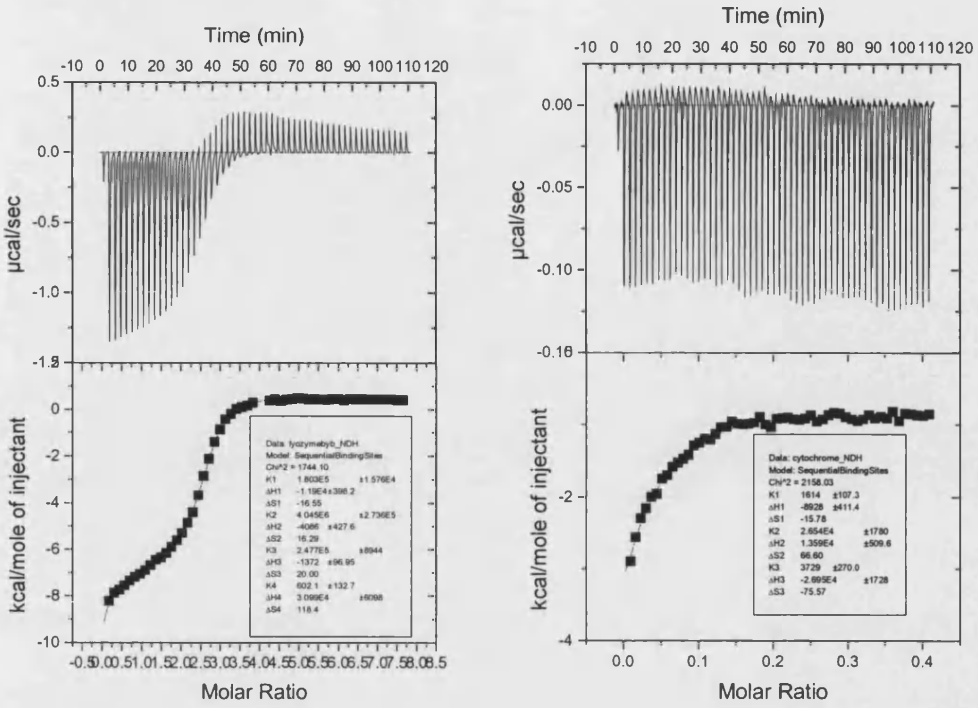

(A) (B)

Figure 9.7: (A) 0.5mg/ml lysozyme was titration by 1mg/ml cibacron blue. (B) 4mg/ml Cytochrome C was titrated by 0.5mg/ml Ciarcron blue.

9.3.4 Diffusion and elution of proteins through the hydrogel membrane coupled with different ligands

Diffusion experiments were conducted as described in the Methods section. To ensure binding saturation, protein was loaded until the transport rate into the receiving chamber had been constant for three hours. During this period the donor chamber concentration was maintained at 4 mg/ml. Once loading was complete the whole system was washed with 20 mM Tris buffer at pH 7.4 (I=0.1) until no further removal of protein from the membrane was observed. Elution was achieved using 1M NaCl in Tris buffer (pH 7.4) recycled through the receiving chamber. A typical elution curve is shown in Figure 9.8.

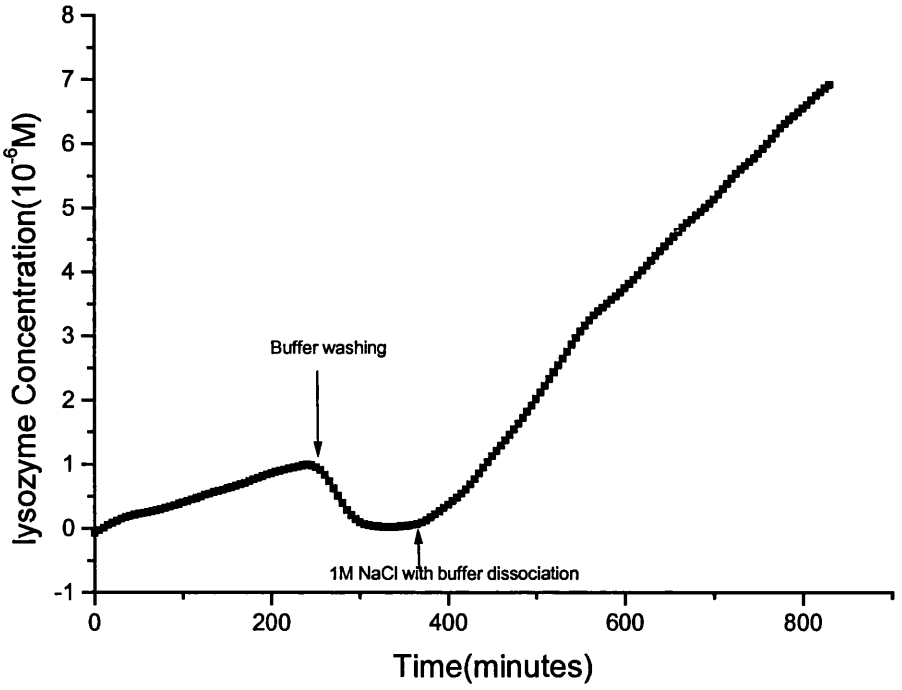

Figure 9.8: Diffusion and elution curves of lysozyme through BSA-CB hydrogel membrane. The lysozyme concentration was 4.0 mg/ml in donor side before washing at 250 minutes. Tris buffer was used to wash two sides of the diffusion systems until no lysozyme was detected from 250 to 350 minutes. 1 M NaCl with Tris buffer eluted the lysozyme from the membrane after 350 minutes. All experiments were conducted at temperature 25°C.

The loading and desorption profiles are shown in Figure 9.9-9.12 with diffusion rate of protein controlled by both protein size and membrane porosity. The general similarity of the gross membrane morphology suggests that membrane porosity should be similar for all preparations such that protein size and binding capacity should determine these profiles. This is supported by the observation that cytochrome C exhibits faster transport during the loading stage with all membranes than is seen with the larger proteins, while hemoglobin, the largest protein, appears completely excluded. Although the CB density in each membrane was not determined, a single membrane of each type was used allowing direct comparison of protein amounts bound for each membrane type. Table 9.2 shows the amount of eluted protein (M) for the various membranes. Direct comparison can be made for each membrane type as shown in lower panels in Figure 9.9-9.12.

Lysozyme diffusion was not obviously faster than BSA through the membranes despite obvious size differences and charge properties at pH 7.4 where lysozyme is positive in comparison with the negative charge of BSA. These results could be explained by the combined involvement from electrostatic and binding forces among protein, CB and membrane.

Comparison of BSA with lysozyme showed systematic variations between the different membranes. As expected from the ITC results lysozyme showed higher binding levels than BSA to all membranes. The differences were similar for native CB membranes and CB-hemoglobin membranes suggesting that hemoglobin has little shielding effect. However, in the case of CB-BSA membranes there was proportionally higher adsorption of lysozyme, consistent with the enhanced ability of the tighter-binding lysozyme to displace the intrinsic interaction than soluble BSA with a similar half saturation constant. In the case of CB-lysozyme membranes there is significant lysozyme adsorption as equilibrium is established between soluble and immobilized lysozyme with CB. However, in this case the higher dissociation constant of BSA for CB means that it is not able to displace the intrinsic lysozyme-CB interactions and so binding is reduced.

Cytochrome C shows low binding to native CB and CB-hemoglobin membranes as expected from the ITC results. However, in the case of membranes with immobilized lysozyme and BSA there is clear evidence of increased Cytochrome C binding. This suggests that there is a binding interaction between Cytochrome C and the immobilized protein in these cases. It is probable that in the case of the highly charged lysozyme this results from an ion exchange effect. With the BSA-CB membrane the binding capacity for Cytochrome C is higher than for lysozyme and suggests that there is a high affinity interaction between Cytochrome C and BSA.

These studies of protein elution from membranes coupled with CB-lysozyme suggest that electrostatic interaction between protein and membrane are significant. CM-dextran hydrogel exhibited negative charge at pH 7.4 owing to ionization of the carboxylic group in CM-dextran and also not all CB was affinity bound with lysozyme coupled in the membrane, so the free lysozyme, cytochrome C and BSA could still have an effect within the membrane as seen in Figure 9.12.

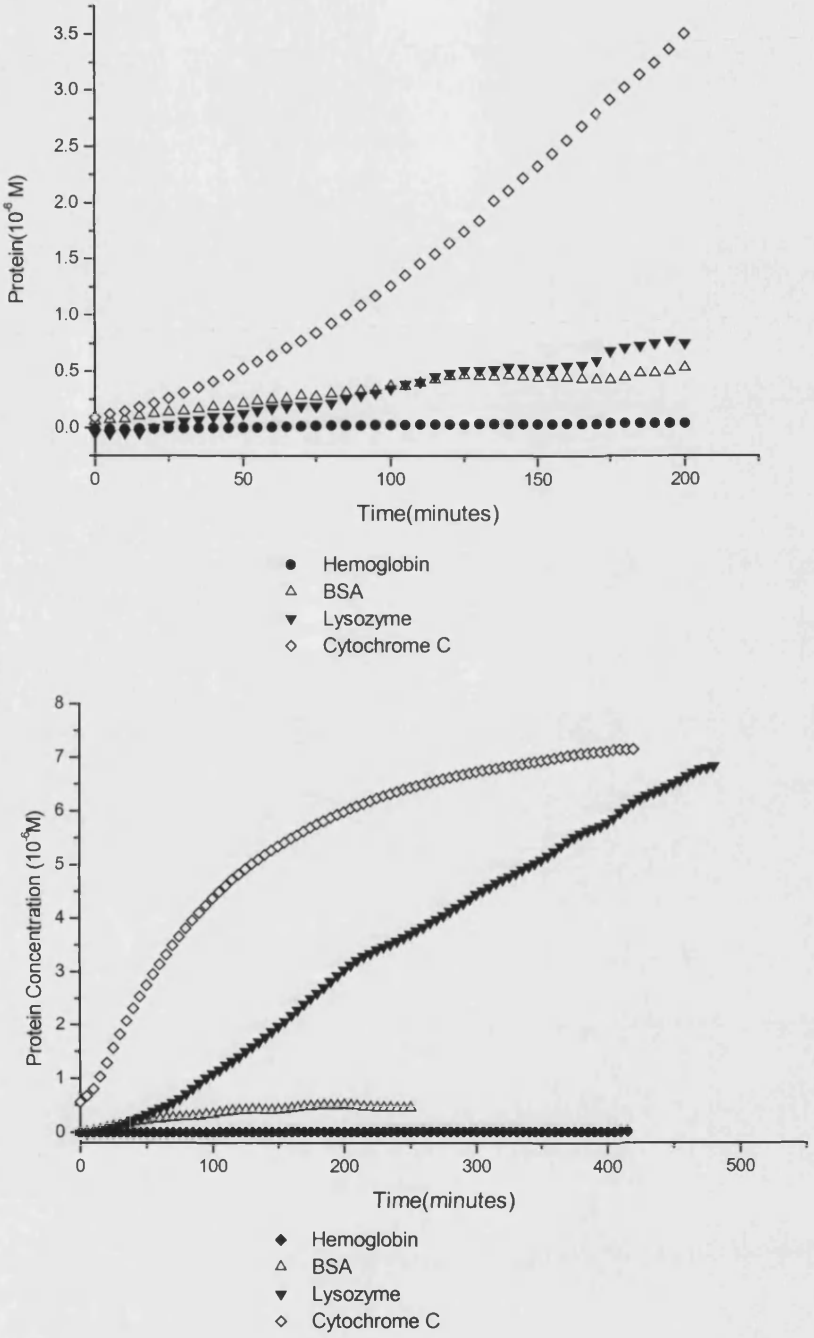

Figure 9.9: Protein diffusion (top panel) and elution (bottom panel) profiles through hydrogel membranes coupled with BSA-CB. Protein of 4mg/ml in 20mM pH 7.4 Tris buffer (I =0.1M) was used in donor side. 1 M NaCl with Tris buffer at pH 7.4 eluted the protein from the membrane. All experiments were conducted at temperature 25°C.

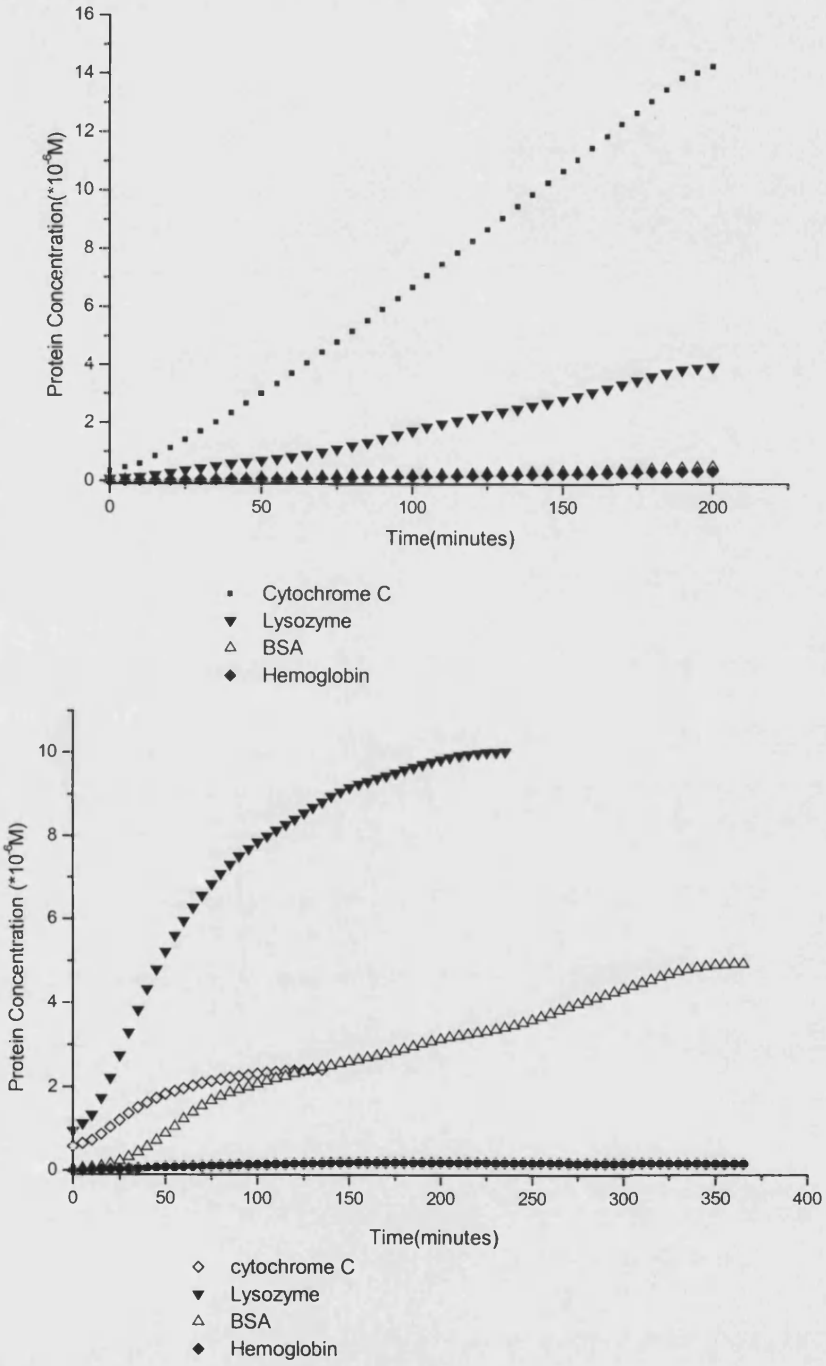

Figure 9.10: Protein diffusion (top panel) and elution (bottom panel) profiles through hydrogel membranes coupled with CB. Protein of 4mg/ml in 20mM pH 7.4 Tris buffer (I =0.1M) was used in donor side. 1 M NaCl with Tris buffer at pH 7.4 eluted the protein from the membrane. All experiments were conducted at temperature 25°C.

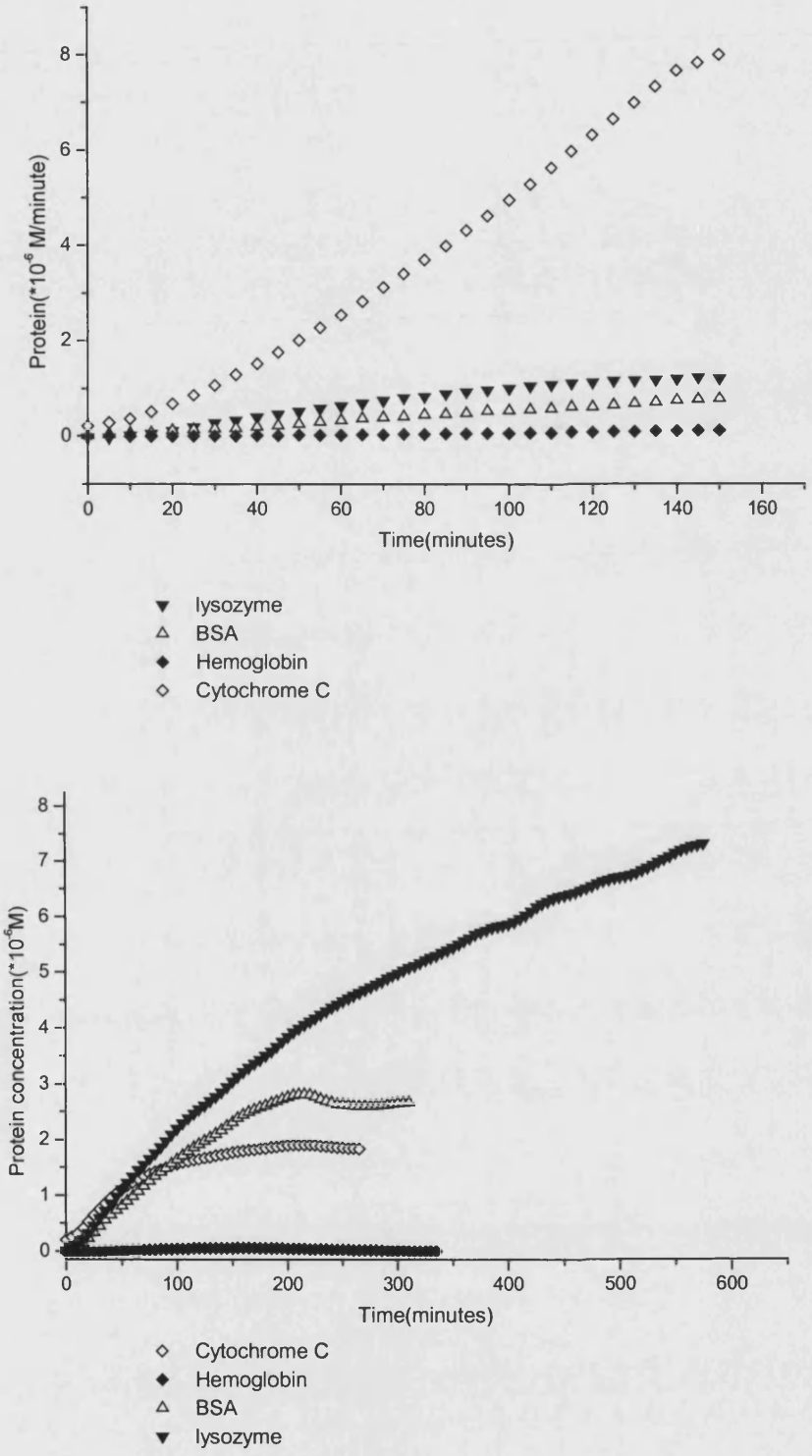

Figure 9.11 Protein diffusion (top panel) and elution (bottom panel) profiles through hydrogel membranes coupled with hemoglobin-CB. Protein of 4mg/ml in 20mM pH 7.4 Tris buffer (I =0.1M) was used in donor side. 1 M NaCl with Tris buffer at pH 7.4 eluted the protein from the membrane. All experiments were conducted at temperature 25°C.

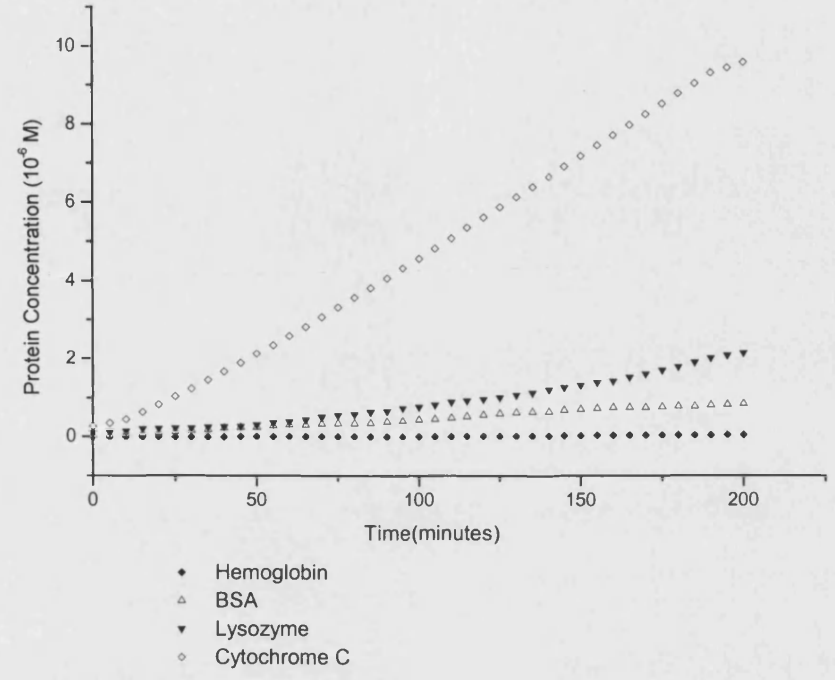

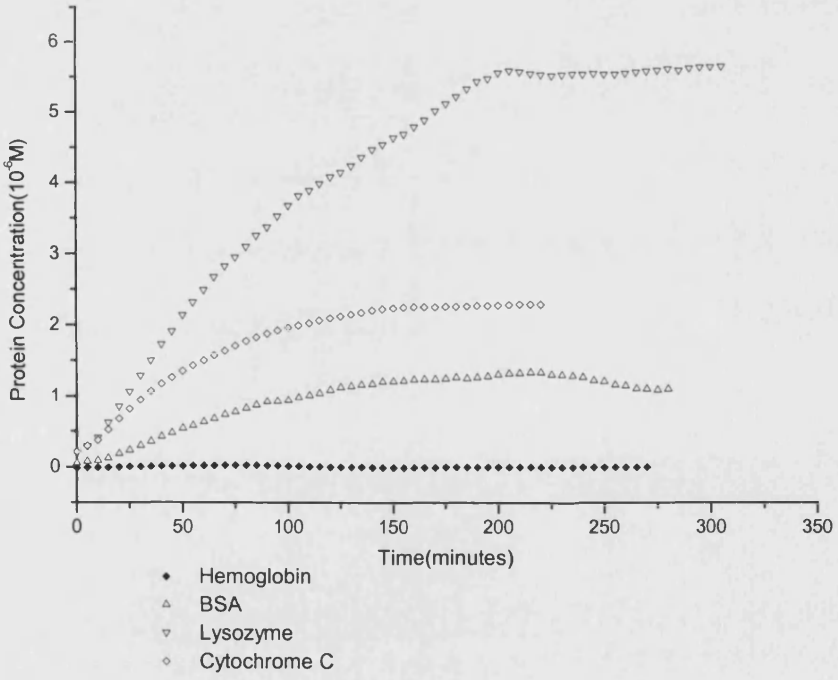

(D) Lysozyme-CB

Figure 9.12: Protein diffusion (top panel) and elution (bottom panel) profiles through hydrogel membranes coupled with lysozyme-CB. Protein of 4mg/ml in 20mM pH 7.4 Tris buffer (I =0.1M) was used in donor side. 1 M NaCl with Tris buffer at pH 7.4 eluted the protein from the membrane. All experiments were conducted at temperature 25°C.

Ligand types	Cytochrome C	Lysozyme	BSA	Hemoglobin
CB	26.87	111.1	55	1.54
BSA -CB	78.65	More than 77	5.5	0.15
Lysozyme -CB	30.55	66.74	12.57	NS
Hemoglobin -CB	21.44	87.99	32.20	0.03

NS: not significant.

Table 9.2: Adsorption amount (10^{-6} Molar) of protein on CM-dextran hydrogel membrane coupled with different ligands.

9.4 Discussion and conclusion

This study describes a novel affinity membrane grafted with both ligand and receptor. Specifically, CM-dextran hydrogel membranes were produced containing a protein and the biomimetic dye Cibacron blue and studied with respect to their ability to bind a number of proteins. The structural similarity between CB and the coenzyme nicotinamide adenine dinucleotide (NAD) has led to it being widely used in the purification of kinases, hydrolases, polymerases and other nucleotide-dependent proteins. However, this binding is not totally specific and Cibacron Blue has also been used in the purification of various proteins with no nucleotide binding function. While this broadens the range of applications of affinity supports based on CB it can lead to significant reductions in selectivity as a result of secondary non-specific interactions with contaminant proteins.

By incorporating a weakly-bound protein into the affinity matrix my goal was to create an intrinsic shielding effect whereby weakly bound contaminants were excluded by virtue of their inability to displace the internal ligand receptor interaction. IR studies provided some confirmation that the synthesis proceeded as expected. SEM showed that gels of similar gross structure are produced irrespective of protein coupled. However, some differences in gel kinetics were observed with the different proteins used. While not part of the current study, other results have shown that the mechanical properties of these hydrogels can be controlled by adjusting the weight

ratio of CM-dextran, protein, EDC/NHS, or substitution ratio of COOH in CM-dextran.

Isothermal titration calorimetry confirmed that the proteins used all showed binding interaction with CB, albeit with the suggestion of different mechanisms in some cases, and showed that an affinity hierarchy in terms of half saturation constants existed.

The results of loading and elution experiments showed that composite membranes of this type were capable of adsorbing proteins showing a range of half saturation constants. As originally hoped the results demonstrate that the inclusion of a weak binding protein (BSA) could reduce the binding of soluble BSA while having little effect on the capacity for a more strongly bound protein (lysozyme). Table 9.2 illustrates that using a membrane coupled with CB alone to adsorb lysozyme and BSA, gives an adsorbed lysozyme concentration twice that of BSA. If a membrane coupled with BSA-CB is used the adsorbed lysozyme is 14-fold that of BSA.

The fact that haemoglobin was excluded from all membranes shows that further selectivity gains can be made by controlling the molecular weight cut-off of the membrane such that the final performance is dictated by a function of both molecular size and bio-affinity.

While this study shows the potential of the principle of intrinsic shielding, clear evidence of secondary interactions between applied protein (e.g. cytochrome C) and coupled BSA highlight the importance of choosing an appropriate shielding molecule for the separation system to be targeted.

Chapter 10. Chromatographic Elution Characteristics of Protein Using D-Glucose Sensitive Hydrogel Beads

10.1 Introduction

In addition to flat membranes, the hydrogel can also be made into beads as well. Hydrogel beads have been used in practical drug delivery and are easily fabricated into self a self-regulated system. Many reports relate the application of hydrogels in drug delivery focused on bead preparation. In recent years, beads have been proposed for the treatment of many diseases needing constant drug concentration in the blood, or drug targeting to specific cells or organs (Cortesia *et al.,* 1999). For instance, beads encapsulating antineoplastic drugs have been made with the aim of: (a) maintaining constant drug levels in the blood possibly reducing the need for multiple administrations (Arshady, 1990); (b) obtaining higher drug concentrations at the tumour site (Nastruzzi, 1994); and (c) possibly targeting the antitumor agents to the lesion site (Lee *et al.,* 1990).

In the study reported in this chapter, D-glucose sensitive hydrogel was fabricated into beads using the same method as in previous chapters. In order to improve the mechanical strength of the beads for use in this study, sodium alginate was used to partly or wholly replace dextran as the backbone, and a Con A coupling agent was used. Sodium alginate forms a mechanically strong gel and it was proposed that it could replace dextran as the backbone polymer in a responsive gel. It was also proposed that Con A could react in a similar way in alginate as it does in dextran, and therefore have the same biological properties, but exhibit a higher degree of mechanical strength. The experiments shown in here were conducted using two types of hydrogel. A CM-dextran hydrogel coupled with Con A mixed with alginate hydrogel mechanical strength was further enhanced by Ca^{2+} crosslinkage. The other was directly made by first grafting Con A onto alginate and then forming beads using Ca^{2+} solution. To investigate these beads' response to D-glucose, size exclusion chromatography (SEC) was employed to detect the effect of D-glucose.

SEC, also called gel-permeation chromatography (GPC), uses porous particles to separate molecules of different sizes. It is generally used to separate biological molecules by size and to determine the molecular weights and molecular weight distributions of polymers. Molecules that are smaller than the pore size can enter the particles and therefore have a longer path and longer retention time within the column than larger molecules that cannot enter the particles (Stulýka *et al.*, 2003).

For this study, SEC was used to find the elution profiles of specific proteins when the column was operated under varying buffer conditions. The buffer composition was varied by including D-glucose at various concentrations. The bead particles of D-glucose-sensitive hydrogel were suspended in this buffer; so in theory the D-glucose change would affect the bead's porosity. This change in porosity would in turn change the retention times of the protein samples.

10.2 Materials

The dextran and proteins used here were obtained from Sigma-Aldrich, UK. All other chemicals were of reagent grade and obtained from Lancaster Synthesis Ltd., UK.

10.3 Methods

10.3.1 Bead Preparation

Two typical beads from different polysaccharides, dextran or sodium alginate, were prepared by using carbodiimide chemistry and ionic crosslinkage.

10.3.1.1 Preparation of CM-dextran –Con A –alginate gel beads

The CM-dextran preparation is as described in chapter 4. The gel physic-chemical characteristics were confirmed by FT-IR in as the previous study. To make the beads, the chemistry of bead preparation was showed as in Figure 10.1A. Briefly, 1g CM-dextran with 1-COOH:65-glucose residues, was dissolved in 4.2ml distilled water and stirred thoroughly. 210mg EDC and 30mg NHS were dissolved in 1.5 ml distilled water. After degassing the solution for several minutes. 1.5 ml EDC/NHS was added to the CM-dextran solution and the reaction allowed to proceed for 5 minutes. Next

130mg Con. A dissolved in 3ml distilled water-containing trace ions (Ca^{2+}, Mn^{2+}) was added. The gelation was allowed to take place at room temperature overnight. The resulting gel was placed in a beaker containing 20ml 3% sodium alginate solution and homogenised until all the gel was broken up into fine particles. Using a peristaltic pump, the mixed alginate solution was dropped into 0.2M $CaCl_2$, varying the speed and tube diameter to get sized appropriately beads.

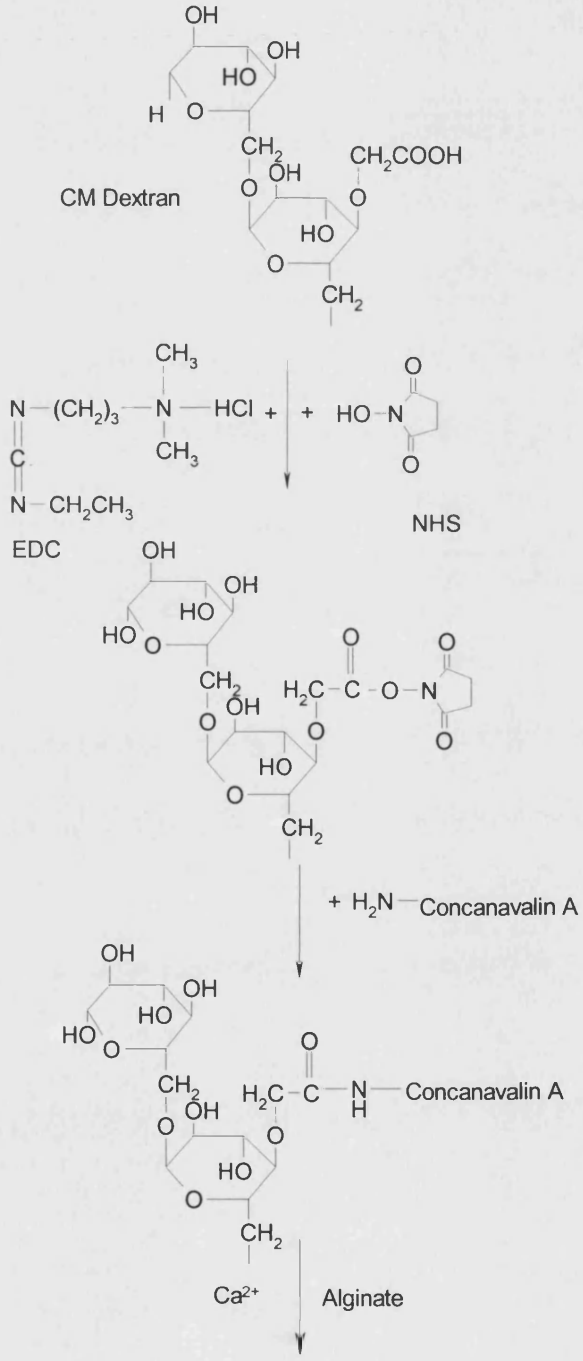

CM-dextran -Con A -alginate gel beads

(A)

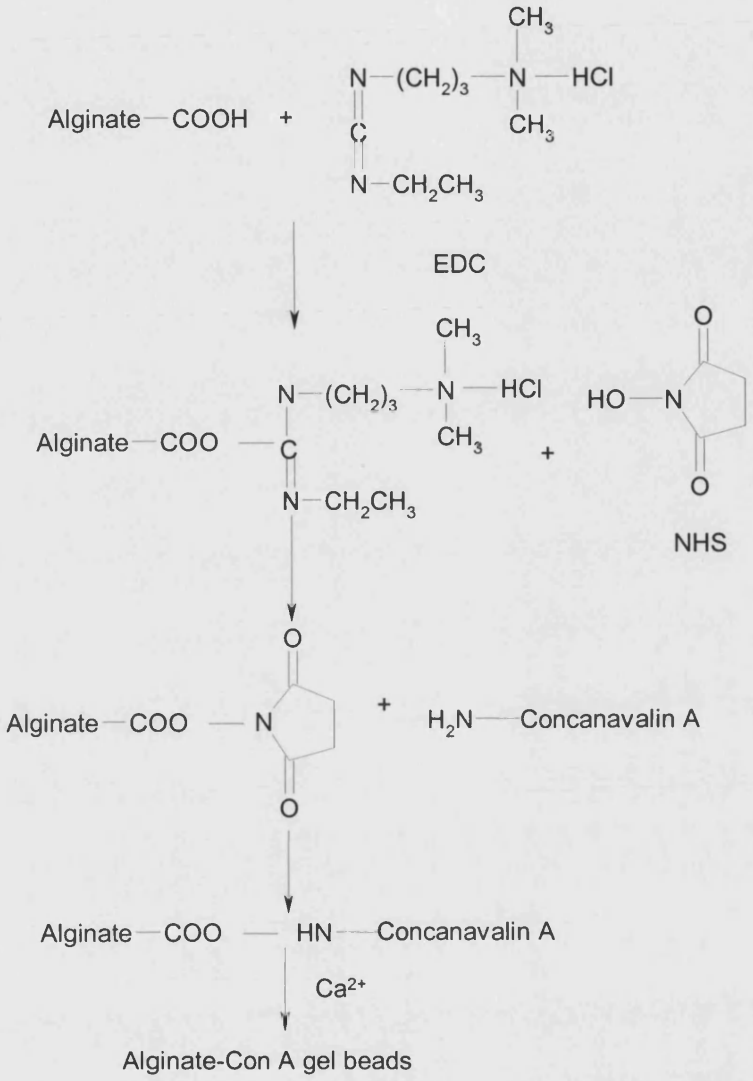

(B)

Figure 10.1: (A) Chemistry of CM-dextran-ConA-alginate gel beads preparation (B) Chemistry of alginate –ConA hydrogel beads preparation

10.3.1.2 Preparation of Alginate-Con A gel beads

Alginate beads coupled with Con A were prepared as shown in Figure 10.1 B. 200mg of con A was added to 5ml of distilled water and left to dissolve. 210mg of EDC and 30mg NHS were mixed in 3ml distilled water and stirred for 1 minute to ensure they were fully dissolved. The 3ml of EDC/NHS mix was added into 14 ml 2% alginate solution and allowed to activate sodium alginate for 2 minutes. The 5ml of Con A solution was added to the activated alginate mixture and left for 2 minutes being

slowly stirred. To form the solution into beads, the alginate-Con A polymer solution was dripped via a peristaltic pump (Eyela Micro Tube Pump MP3-Tokyo Rikakikai Ltd) through an air stream, from a height of approximately 5cm into a gently stirred 0.2M $CaCl_2$ solution. The bead size was controlled by altering the pump speed and the intensity of the air stream.

The prepared beads from above were cured for 1-3hours, followed by decanting the beads into the desired buffer and equilibrating overnight. The beads' shape was photographed using a light microscope with X25 magnification in Figure 10.2.

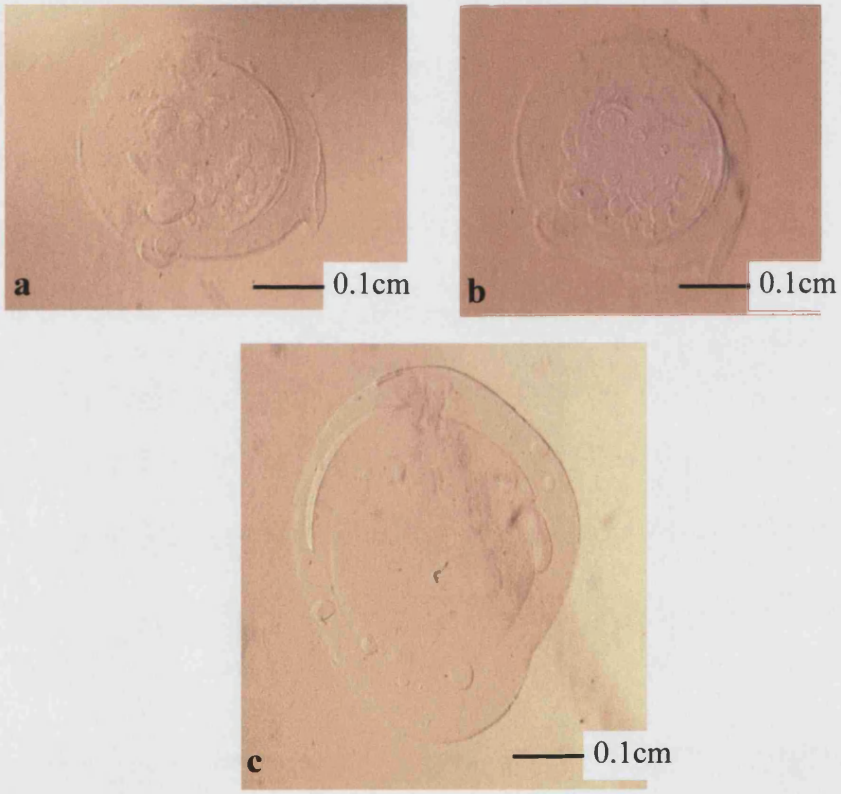

Figure 10.2: Images of hydrogel beads made and used in this project. A light microscope with X25 magnification was used together with photo-image capture. Bead a, has a length and width of 1.1mm. Bead b, has a width of 1.1mm and a length of 1.0mm. Bead c, has a width of 1.3mm and a length of 1.8mm.

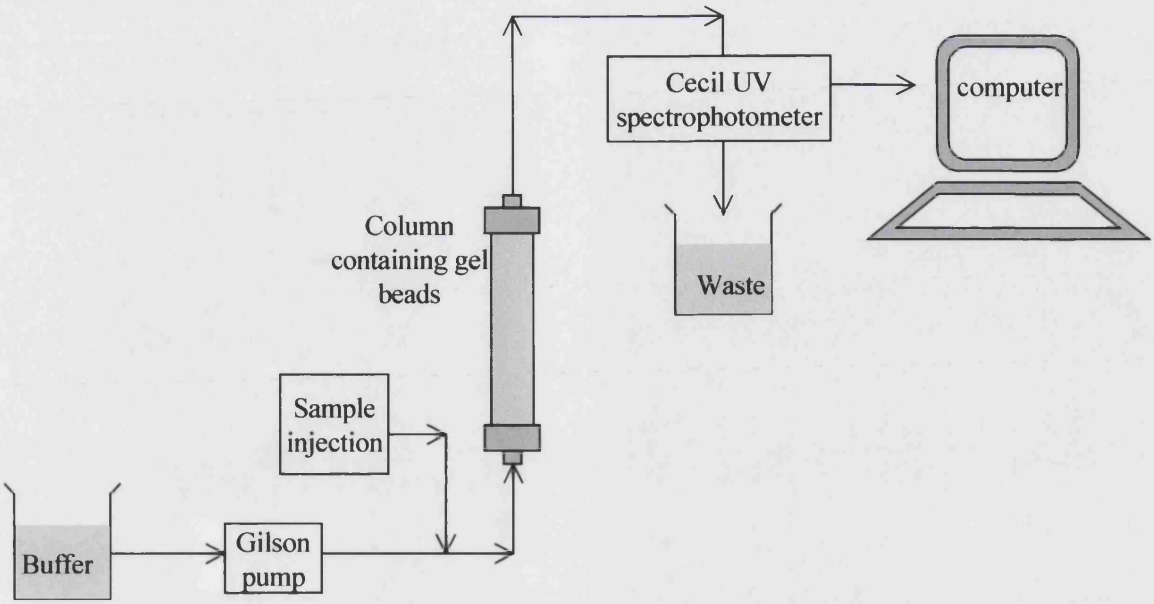

(A)

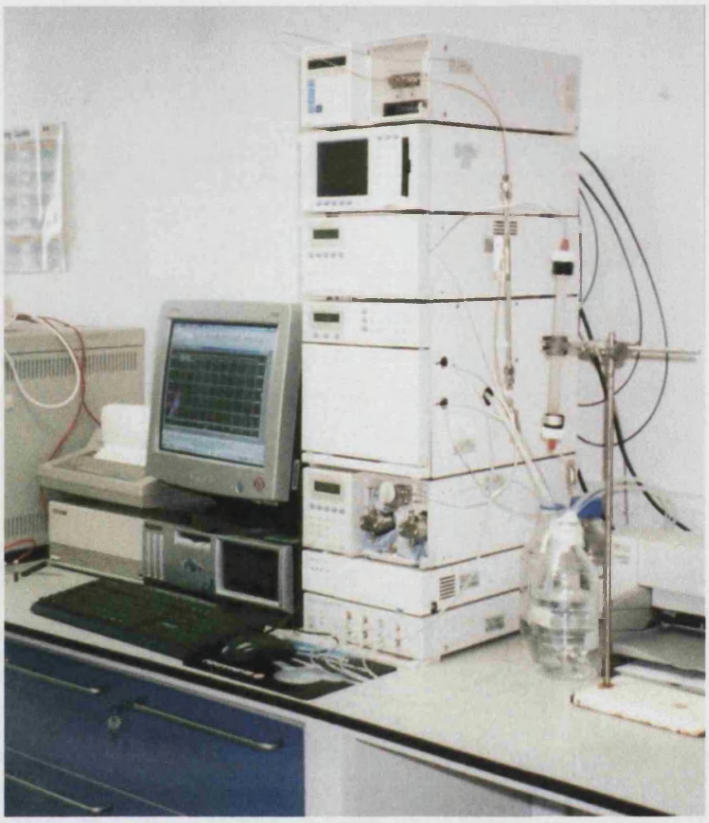

(B)

Figure 10.3: (A) Schematic representation of the experimental setup for size-exclusion chromatography. The direction of the arrows indicates the flow of buffer or sample through the system. (B) Photograph of the actual Shimadzu HPLC instrument with an SEC column and a UV detector.

10.3.2 Packing the beads into the column

Water calibration of the column was carried out before the packing of the beads. The total bed volume (V_t) of the column used in this project was 19ml. Beads were packed under vacuum, to ensure the beads were packed tightly in a uniform manner throughout the column. The buffer (0.02mol/l Tris buffer pH7.4, 0.1M NaCl, 1.0M $CaCl_2$, 1.0 mM $MnCl_2$, 1.0mM NaN_3) was filtered using 0.45μM membrane filters and degassed (using helium) to prevent bubbles and contamination of the very small diameter tubing.

Two detector systems were used. Firstly, the beads of dextran-alginate gel were packed into the column, which was attached to the pump (Gilson Autosampler Model 231 Gilson, Inc. Middleton, USA) and UV spectrophotometer (Gilson UV detector model 116, Gilson, Inc. Middleton, USA). Degassed buffer was pumped through the column from the bottom at a constant rate. Continuous and automatic detection of the sample was achieved (VisiTech International, Sunderland, UK) and recorded. The set-up of this system was seen in Figure 10.3 A. The second instrument system controller and automatic data collection components were co-ordinated by the computer using the Shimadzu Class VP software, version 5.02 (1997). The column packed with alginate gel beads was attached to the Shimadzu HPLC (UV detector) instrument, seen in Figure 10.3 B.The UV detector HPLC has a degasser unit built in, so the buffer only has to be filtered (0.45μM membrane filters) when using this machine.

10.3.3 Running samples

The proteins used were Cytochrome C (MW 12.3 KD), BSA (MW 67 KD) and hemoglobin (MW 68 KD), ovalbumin (MW 43 KD). The samples were made up in buffer (0.02mol/l Tris buffer pH7.4, 0.1M NaCl, 1.0M $CaCl_2$, 1.0mM $MnCl_2$, 1.0mM NaN_3) and filtered using 0.45μM membrane filters.

1 M $CaCl_2$ was included to maintain gel stability. While this would not be suitable for practical application, it allowed the potential of the responsive gel principle to be evaluated using a simple bead synthesis protocol.

In the first UV-detector system, a sample of 100µl and a protein concentration of 4mg/ml were used to produce reliable results at a UV absorbance of 280nm.

When the second UV-detector system was employed, 500µl of each protein sample was placed in individual 1.2ml Chromacol autoinjector vials with crimp push-on lids. An injection volume of 100µl and a UV absorbance of 280nm were programmed. Samples could be run individually or run in a sequence, again programmed into the Class VP software. Each protein was run with 10mM, 20mM, 50mM, 100mM and 150mM D-glucose present in the buffer. A glucose-free buffer was also prepared and the protein samples run as a control.

10.3.4 Characterisation of binding interactions between Con A with alginate

The binding properties of Con A towards alginate were studied using Isothermal Titration Calorimetry (ITC) in an OMEGA ITC (Microcal Ltd). The instrument was calibrated and experiments conducted in accordance with the manufacturers' operating instructions. Before use, Con A was dissolved in and dialysed against 20 mM Tris buffer pH 7.4 containing 0.5mM $CaCl_2$, 0.5 mM $MnCl_2$, 0.5 mM $MgCl_2$, 150 mM NaCl, and 0.02% NaN_3 at 4 °C, filtered with PVD/PE syringe filters and the monomer concentration (MW:27 KD) adjusted to 0.092 mM. Titrant of D-glucose was diluted to a final concentration of 27.8 mM. Titrations were run at 20 °C and all the samples degassed at 15°C prior to use. In each case 54 injection of 5 ul of sugar solution were automatically added at 2 minutes intervals into the lectin solution stirred at 300 rpm. The heat evolved after each injection was measured by the cell's feedback network as differential heat effects between sample and reference cell. The binding capacity between alginate with Con A was investigated by displacing the binding of alginate to Con A by D-glucose. In brief, 1.25mg/ml Con A was firstly mixed with 2 mg/ml alginate and then titrated with 5mg/ml D-glucose.

Final experimental results of heat developed versus cell ligand/lectin ratio were fitted to a one-binding-sites-per-monomer model using Origin ITC Data Analysis Software (Microcal Ltd).

10.4 Results

The primary goal of this series of experiments was to demonstrate that the glucose-sensitive gel beads could respond the changes in external glucose in the buffer, and thus affect the passage of macromolecules through the gel matrix. Competitive displacement reactions are postulated to occur in the presence of glucose that increases the gel's porosity and therefore effect the passage of macromolecules through the gel as their accessibility to the gel is greater. Increased access to the gel matrix will be shown as a shift of the elution profile corresponding to a longer elution time compared to control experiments in the absence of glucose.

Between each experiment, the system was equilibrated with at least 5 bed volumes of buffer to wash away any unwanted products within the gel matrix. Samples were only injected into the column when the absorbance readings had reached a steady baseline level.

10.4.1 Binding capacity comparison of alginate with concanavalin A by ITC

Con A titrated against alginate did not give strong evidence of a binding relationship between Con A and alginate because Ca^{2+} and Mn^{2+} in buffer, (which is essential to for the activity of Con A), bound to the algiante. The replacing binding experiment was conducted by ITC.

Figure 10.4 shows the calorimetric data for titration of native Con A with D-glucose and Con A-alginate mixture with D-glucose. Comparison of the binding constants obtained for free Con A and alginate-Con A conjugates with D-glucose, show a reduction in the association constant from 166.3 to 121.1 M^{-1}, indicating a reduced affinity. This reduction resulted from competitive binding of alginate to Con A with D-glucose. On the other hand, weak binding of alginate with Con A was confirmed.

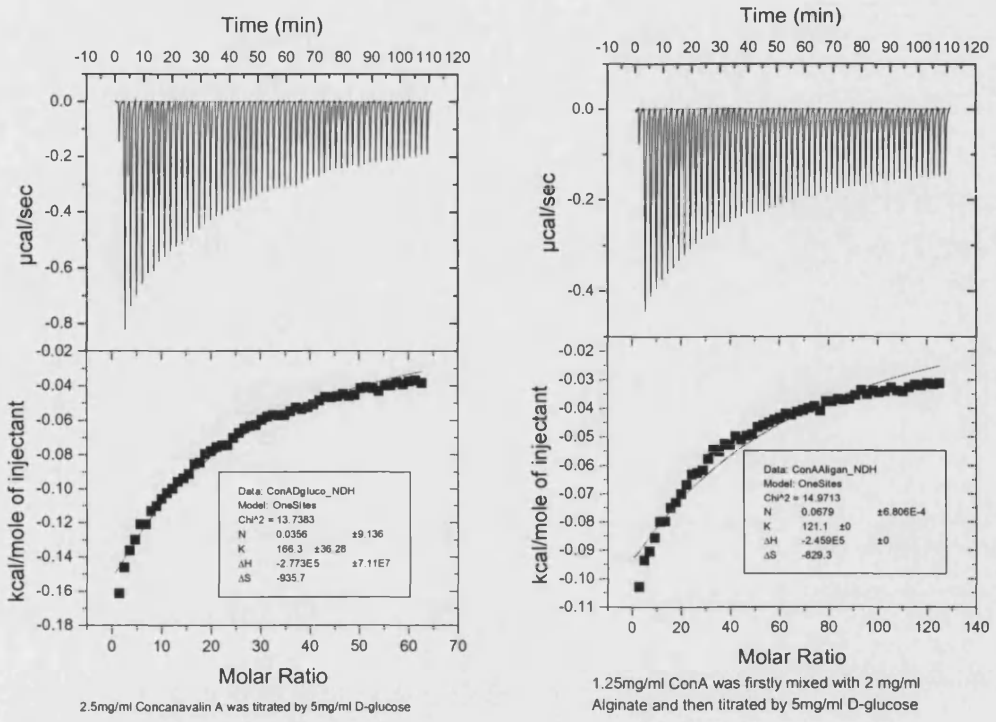

(A) (B)

Figure 10.4: ITC results of Con A titrated against sugar under different conditions with a one binding site model and parameter results (N - Stoichiometry, K- Association constant [M^{-1}], H – Enthalpy [cal mol^{-1}], S - Entropy [cal mol^{-1} K^{-1}]). 0.092 mM of Con A titrated against 27.8mM of D-glucose (1) and (2) showed the D-glucose (27.8 mM) completely bound the mixture of alginate (2mg/ml) with Con A (0.092mM) respectively at 20 °C.

10.4.2 CM-dextran Con A alginate beads using the first detector system

The passage of cytochrome C through the column using CM-dextran-alginate-Con A beads was recorded. The $CaCl_2$ concentration was altered to ensure the best elution profiles were obtained.

As shown in Figure 10.5, the elution profile for the data corresponding to 1M $CaCl_2$ yielded the best elution curve as it reflected a bell-shaped curve and had a shorter lag phase than the results for 0.5M $CaCl_2$. The results were reproducible, as shown for the results for 0.5M $CaCl_2$, although for simplicity not all the data is shown. 20mM Tris buffer with 1M $CaCl_2$ was therefore used in subsequent experiments.

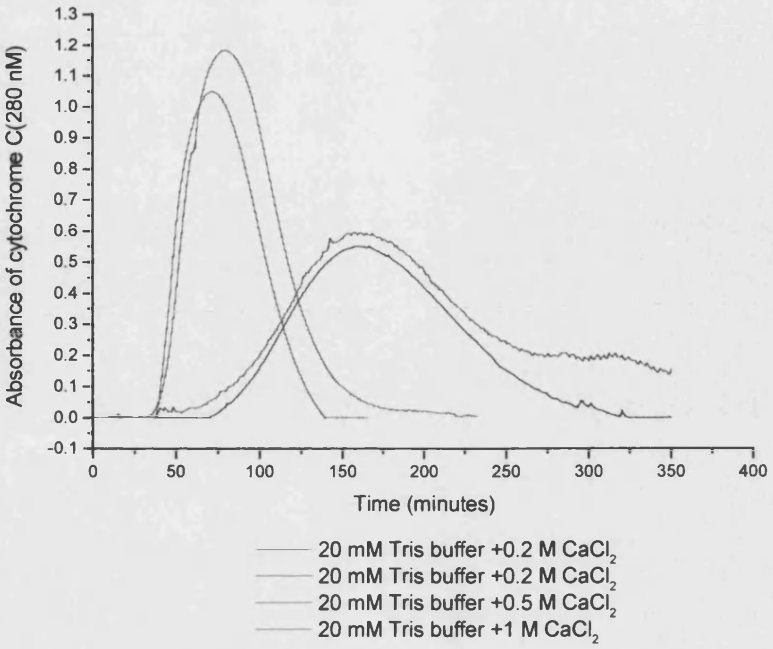

Figure 10.5: The passage of cytochrome C through the column packed with CM-dextran-Con A-alginate hydrogel beads at varying $CaCl_2$ concentrations.

The effect of glucose on the elution profile of cytochrome C through the column is shown in Figure 10.6. As the results were reproducible, glucose was added to the buffer. Studies showed that a 0.1M glucose buffer gave rise to an observable shift in the elution profile of cytochrome. The peak elution time for cytochrome C in the absence of buffer was recorded at 71 mins. The peak elution time for cytochrome C in the presence of glucose was 77 mins. This showed a clear shift to the right, which was as expected as it shows that the gel responds to glucose. The results have been normalised so that the absorbance was expressed as a fraction of the highest absorbance reading for that profile.

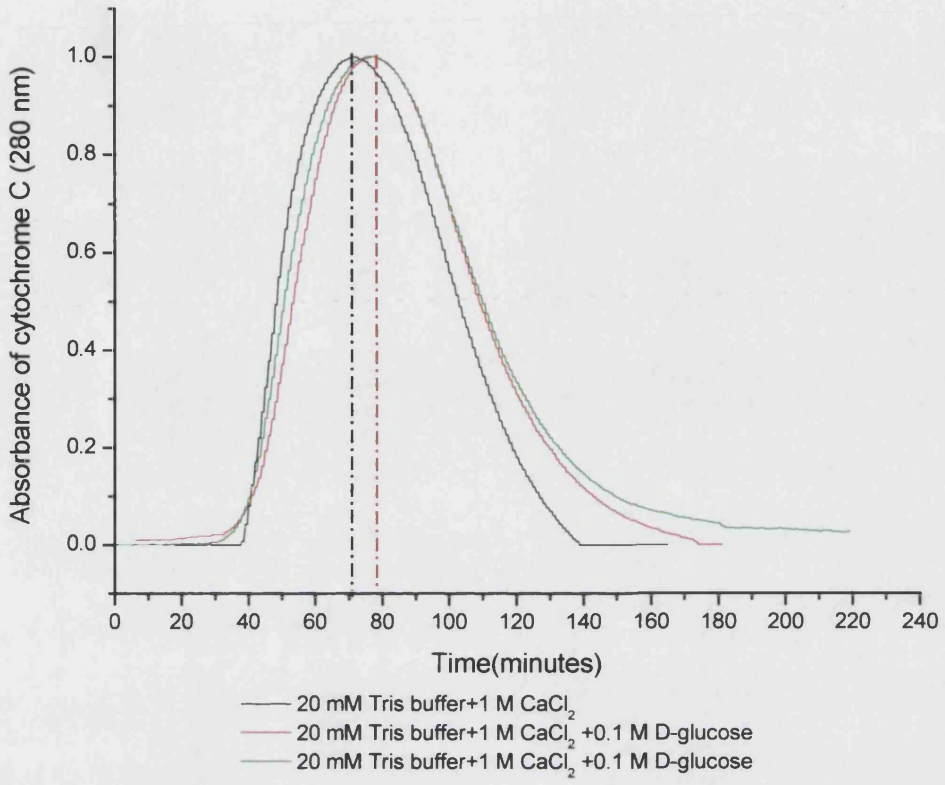

Figure 10.6: The effect of glucose in the passage of cytochrome C through the column packed with CM-dextran-Con A-alginate hydrogel beads.

It was important to test whether macromolecules of different molecular weights showed the expected profiles through the column. Larger molecules should be eluted before cytochrome C as they have less accessibility to the gel matrix. As shown in Figure 10.7, the peak elution time for cytochrome C was 71 mins, and the elution times for BSA and ovalbumin were 66 mins and 70 mins respectively. These molecules were then eluted in the presence of glucose to determine whether they were also affected. The maximum absorbance for BSA and ovalbumin is lower than that for cytochrome C as their absorbance spectra are different.

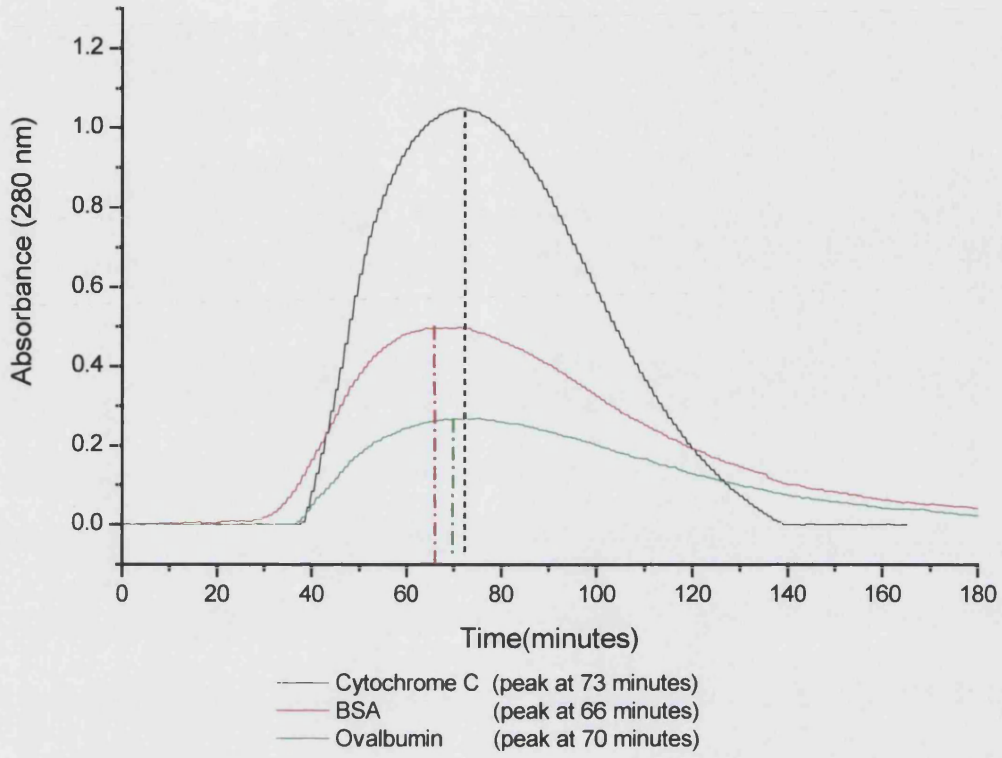

Figure 10.7: Cytochrome C, BSA and Ovalbumin injected into the column packed with CM-dextran-Con A-alginate hydrogel beads.

Glucose was then added to the buffer to test what effect this would have on other macromolecules. The peak elution time for BSA without glucose was 66 mins, and in the presence of glucose 72 mins (Figure 10.8 A). Therefore, elution profile for BSA was shifted to the right as was seen for Cytochrome C. However, the peak elution time for ovalbumin in the absence of glucose was 70 mins, and in the presence of glucose, 66 mins (Figure 10.8 B). Ovalbumin is a glycosylated protein which will bind to Con A. As expected, the elution profile of ovalbumin in the presence of glucose shifted to the left because ovalbumin lost the binding capacity to Con A in the present of D-glucose.

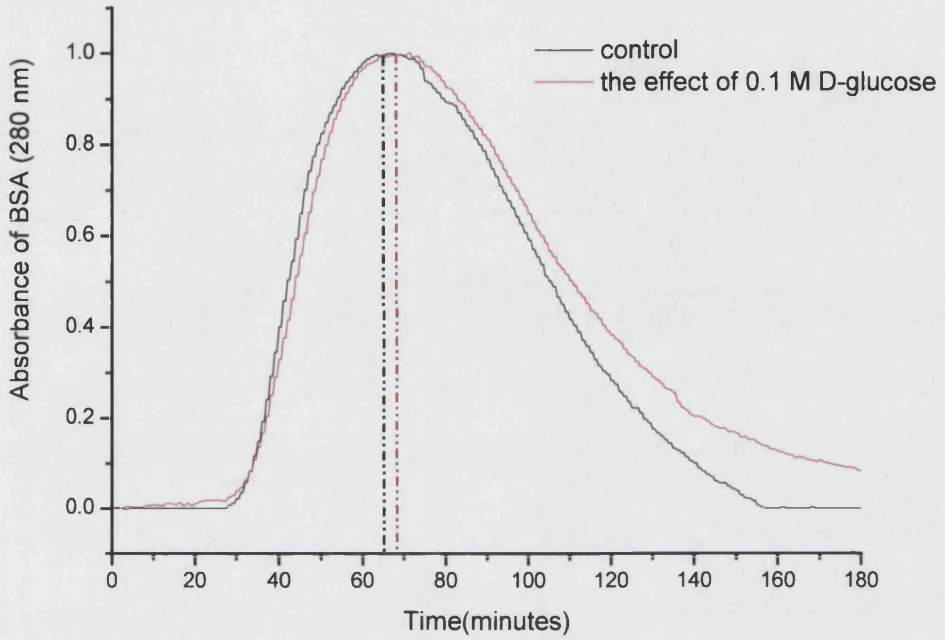

(A)

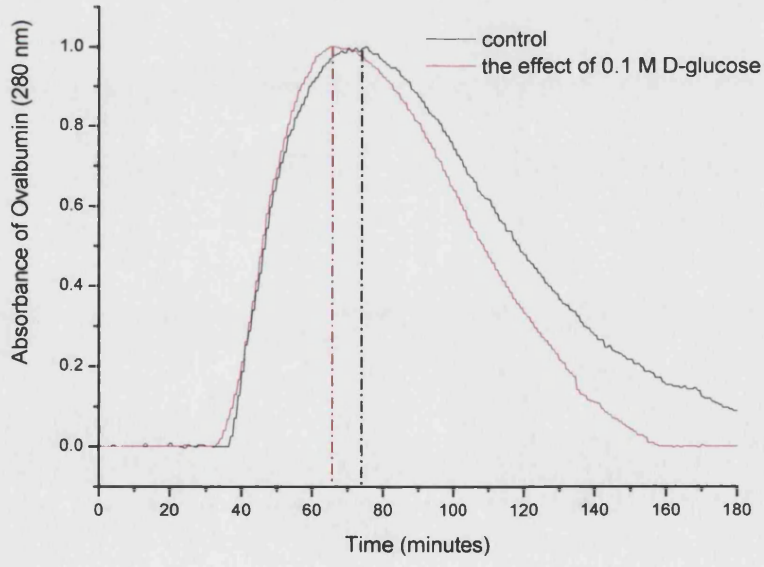

(B)

Figure 10. 8: The effect of glucose on BSA (A) and ovalbumin (B) elution through the column packed with CM-dextran-Con A-alginate hydrogel beads.

10.4.3 Experiments of alginate beads using the second detector system

The data for the following experiments using the second detector system have been exported from the Class VP software to Microsoft Excel. Their axes have been modified from minutes and volts to number of column volumes passed (x-axis) and absorbance units (y-axis).

$$\text{Number of column volumes passed} = \frac{\text{Time (hours) x flow rate (mls/hour)}}{\text{Original column volume (mls)}}$$

Where flow rate = 15ml/hour, and original column volume = 19mls. For the y-axis manipulation, 1 volt is equal to 1 absorbance unit (AU).

Figure 10.9 shows the duplicate runs for Cytochrome C, BSA and hemoglobin. Although the shoulders of the peaks differ slightly between Runs 1 and 2, the summits of the elution peaks show very little variation between runs. Duplicate runs were carried out for all the following experiments, but will not be shown. The examples in Figure 10.9 are all with Tris buffer plus 50mM D-glucose.

The proteins were run through the column without free glucose molecules present in Figure 10.10. The pores of the beads would be governed solely by the crosslinkages of alginate and Con A. The elution peaks for each of the proteins vary in magnitude, as does the volume of buffer it takes for the peaks to emerge. Cytochrome C has a maximum absorbance of 0.044AU and elutes at 0.7 column volumes. BSA has a maximum absorbance of 0.025AU and the summit of its peak is after 0.522 column volumes of buffer has passed through the column. Hemoglobin's elution peak has the sharpest incline and the highest maximum absorbance of 0.055AU. It also has the shortest elution volume of 0.493 column volumes. Even though there is a difference in the elution volumes and magnitudes of the peaks owing to their absorbance spectra being different, they all take approximately 2.7 column volumes of buffer to return to the baseline absorbance and the larger molecules are eluted before the smaller as they have less accessibility to the gel matrix.

Cytochrome C

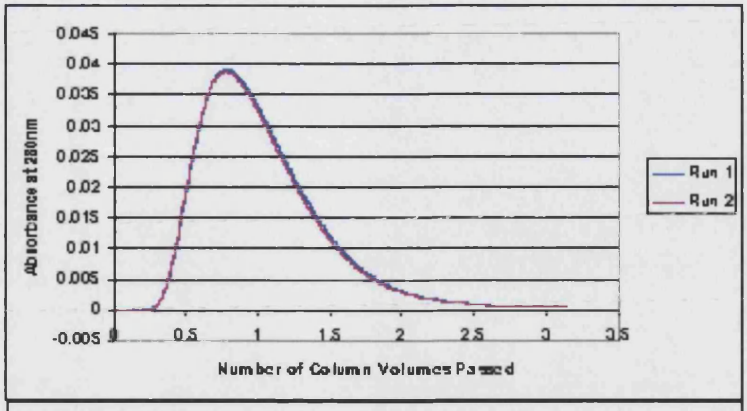

BSA

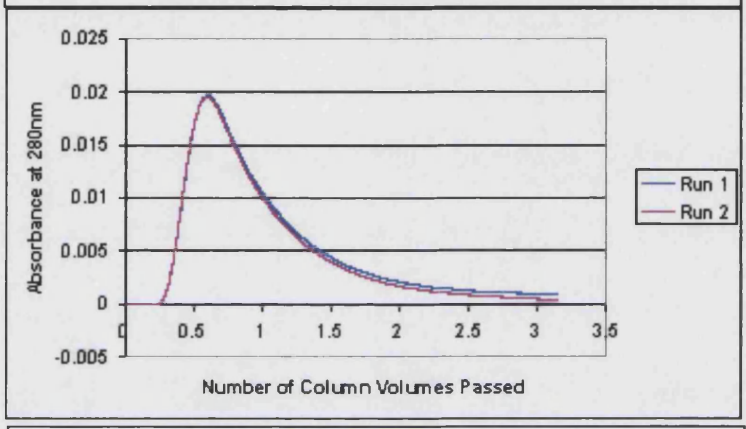

Haemoglobin

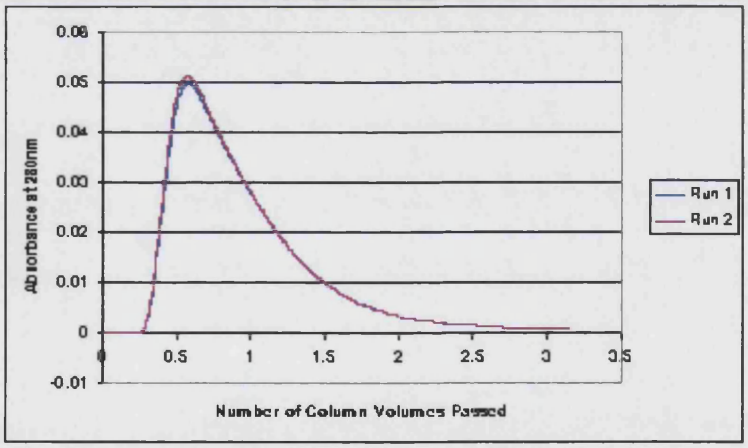

Figure 10.9: Graphs to show the reproducibility of the data when cytochrome C, BSA and haemoglobin are injected into a Con A-alginate bead packed column. (50mM D-glucose).

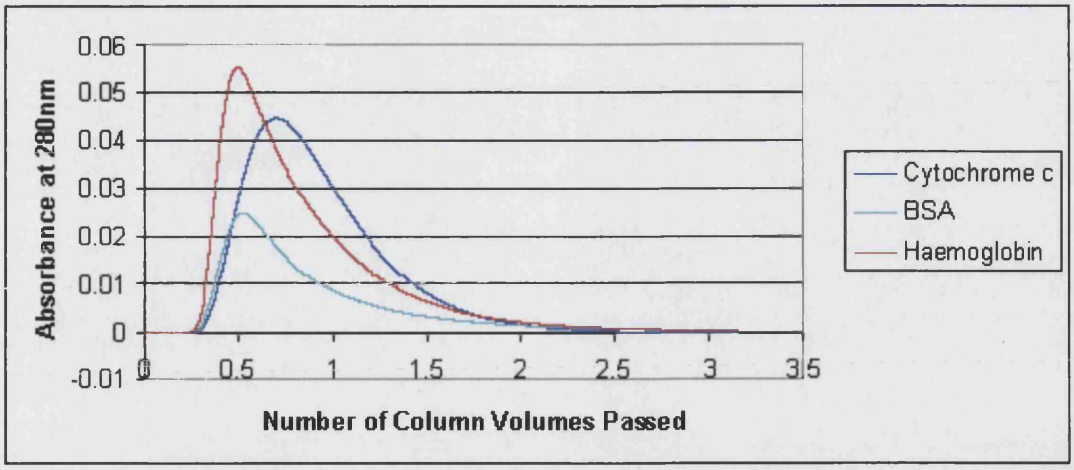

Figure 10.10: The passage of Cytochrome C, BSA and hemoglobin through the SEC column packed with Con A-alginate beads.

The concentration of D-glucose in the buffer was varied (10mM, 20mM, 50mM, 100mM and 150mM) in Figures 10.11-10.13. Each protein was run in duplicate using the Shimadzu sequence function. Between each set of experiments (different glucose concentrations) the column was run at 0.25ml/min for 24 hours (19 column volumes) to allow the beads to equilibrate to the new, higher free D-glucose concentration.

The results of varying the concentration of D-glucose for Cytochrome C are shown in Figure 10.11. It is hard to precisely quantify the number of column volumes passed from Figure 10.11. For values of column volumes passed at each glucose concentration see the Table 10.1 and Figure 10.14. Looking at Figure 10.11 in a qualitative manner shows that there is an increase in the column volumes passed between 20mM and 50mM glucose concentration. The elution peak has slightly shifted to the right on the graph. The further increases of D-glucose have no effect on the elution volume.

The same trend of the elution peaks shifting slightly to the right between 20mM and 50mM of glucose is also seen with BSA (Figure 10.12) and hemoglobin (Figure 10.13). The maximum absorbance also varies under the varying D-glucose concentrations. The degree of variation differs for each protein: 0.039-0.045AU for Cytochrome c, 0.020-0.025AU for BSA and 0.050-0.062AU for hemoglobin. For Cytochrome c and BSA the maximum absorbance is correlated with the shift to the right of the peak maximum, the further the shift to the right, the lower the maximum

absorbance. This trend is not seen with hemoglobin, but there is still a variation in maximum absorbance.

The Table 10.1 quantitatively shows the effect D-glucose has on the elution peaks of the proteins. For all three proteins tested, there is no obvious difference between the number of column volumes of buffer passed through the column for the peak maximum to appear for no glucose, 10mM glucose and 20mM glucose. At 50mM glucose there is a shift of the elution peaks to the right. Further increases in glucose concentration to 100mM and 150mM give similar graphs to the 50mM peaks. This data is shown graphically in Figure 10.14. All three proteins show a similar line trend, with a slight dip in absorbance at 20mM, before the larger increase at 50mM.

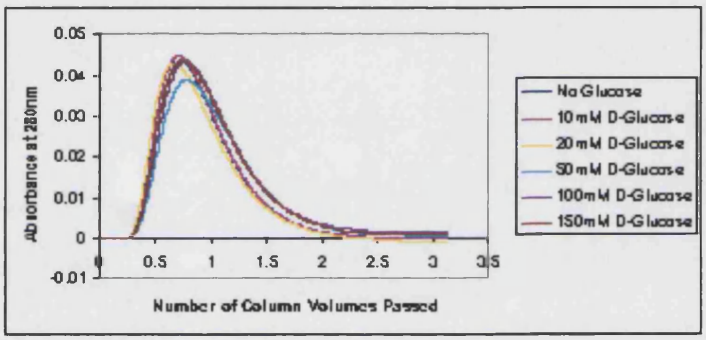

(A)

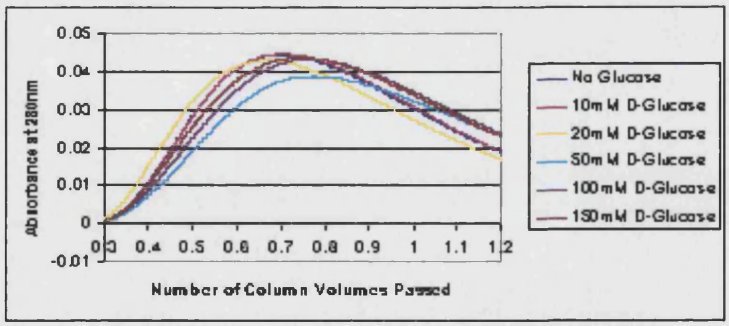

(B)

Figure 10.11: (A) The effect that varying the free glucose concentration has on the elution volumes needed to remove cytochrome c from the column. (B) The effect of glucose on the elution volume of cytochrome C (a zoomed-in version of Figure (A)).

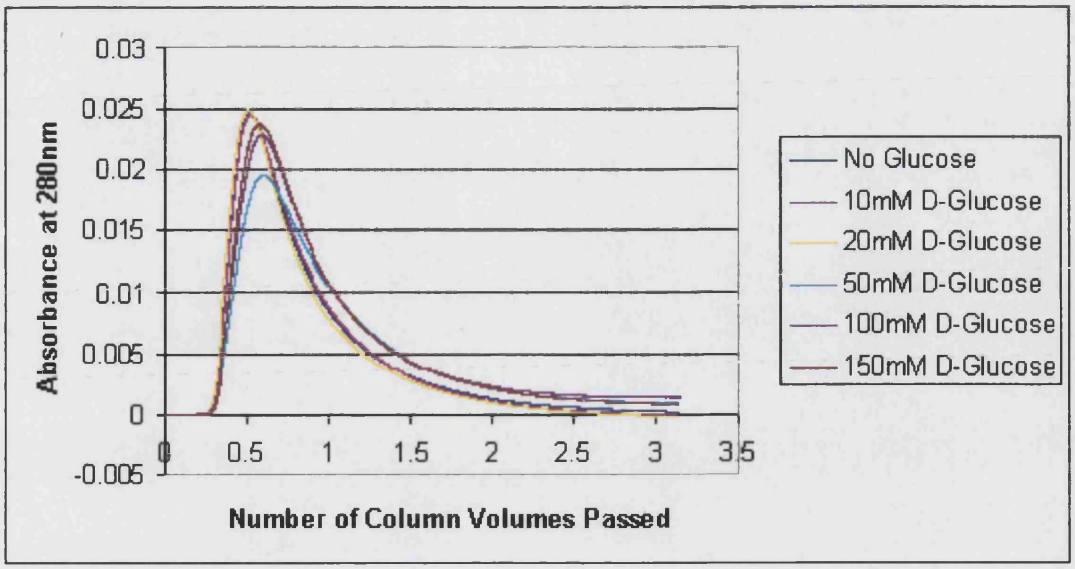

(A)

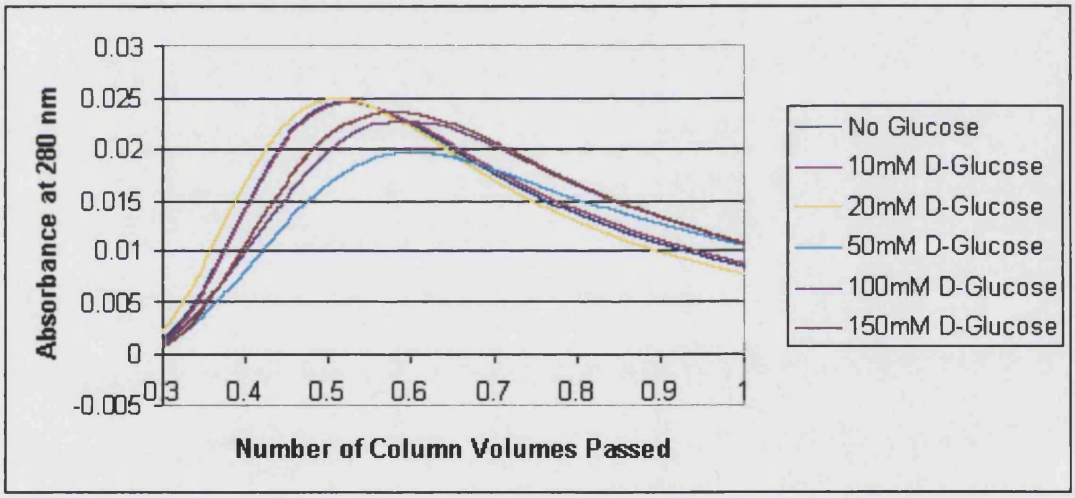

(B)

Figure 10.12: (A) The effect that varying the free glucose concentration has on the elution volumes needed to remove BSA from the column. (B) The effect of glucose on the elution volume of BSA. (a zoomed-in version of Figure (A)).

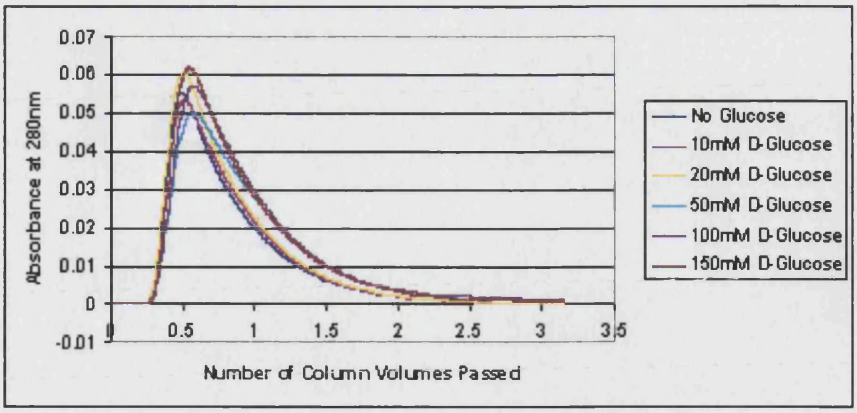

(A)

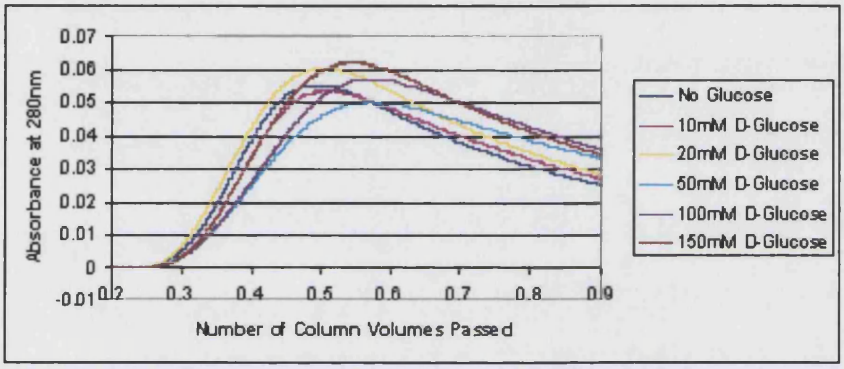

(B)

Figure 10.13: (A) The effect that varying the free glucose concentration has on the elution volumes needed to remove haemoglobin from the column. (B)The effect of glucose on the elution volume of haemoglobin (a zoomed-in version of Figure (A)).

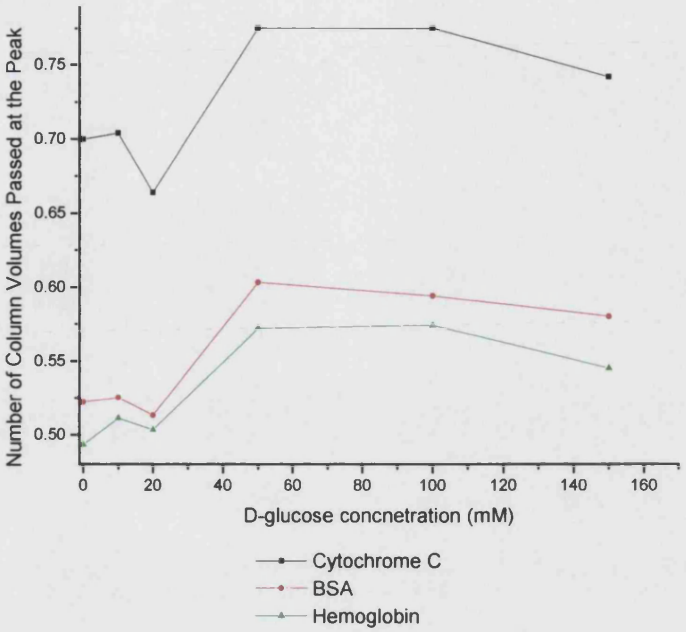

Figure 10.14: A graph to show the effect of D-glucose on the movement of the proteins, Cytochrome c, BSA and hemoglobin, though con A-alginate beads.

Column Volumes Passed						
	No Glucose	10mM Glucose	20mM Glucose	50mM Glucose	100mM Glucose	150mM Glucose
Cytochrome c	0.700	0.704	0.664	0.775	0.775	0.742
BSA	0.522	0.525	0.513	0.603	0.594	0.580
Hemoglobin	0.493	0.511	0.503	0.572	0.574	0.545

Table 10.1. A table accumulating the numeric data from the graphs shown in figures

10.5 Discussion

The CM-dextran – Con A gel suspended in the sodium alginate gel yielded some interesting results. As expected, the elution profile for cytochrome C was shifted to the right in the presence of glucose. This indicates that the porosity of the gel beads is affected thus allowing cytochrome C to have greater accessibility to the matrix.

Altering the buffer composition had a profound effect on the elution profiles of cytochrome C. Increasing the ion concentration saturates the ion exchange effects and reduces the chances of non-specific ion-exchange-based adsorption of the transported protein to the immobilised Con A. Adsorption is the process where a solute in the liquid phase becomes bonded to the surface of a solid, and therefore increasing the $CaCl_2$ concentration in the buffer helps to elute bound protein in the same way as used in ion exchange chromatography. A variety of ions could be used to achieve this, but in these experiments, $CaCl_2$ was used as it will help maintain the stability of the alginate gel.

The results for the passage of BSA and ovalbumin through the column were also as expected, with the elution profile shifting to the right and the left. The molecular weight of BSA and cytochrome C is 69KD, and 12.3KD respectively. As BSA is larger that cytochrome C, it is expected to eluted faster as it has less accessibility to the pores in the gel beads. The molecular weight of ovalbumin is 46KD. Therefore, as expected, the elution time for ovalbumin is faster than that for cytochrome C. In the presence of glucose, the BSA profile is shifted to the right. This shows that the passage of BSA through the column is also affected by glucose due to its ability to enter a larger volume of the gel matrix. Ovalbumin is a glycosylated protein and will therefore form affinity interactions with Con A (Ambrosino *et. al.,* 1987), retarding its passage through the column. However, as the gel porosity changes in response to glucose, the ovalbumin will also have more access to the column. These two competing factors will affect the overall elution of ovalbumin, depending on the strength of the interactions with Con A, and the degree of porosity change. In this experiment, the predominating factor is the interaction between Con A and glycosylated ovalbumin, which leads the shift of the elution profile to the left. Altering the balance between the amount of Con A in the gel and the glucose concentration would therefore give rise to either a shift to the left or the right of the elution profiles depending on the interaction or lack of it between Con A and the protein concerned.

Overall, this set of experiments using alginate-CM-dextran-Con A beads has provided more information on the function of these particular hydrogel beads, and has shown some essential properties that are required for self-regulating drug delivery systems.

The data on alginate beads obtained using the second UV-detector system was reliable and reproducible. The shoulders of the peaks slightly varied, but there was no significant difference in the retention times between duplicates, so much so that the peaks were virtually superimposable.

When there were no free D-glucose molecules present in the system, the three proteins, Cytochrome C, BSA and hemoglobin, all gave different retention times. This was due to their different molecular weights. Cytochrome c, the smallest protein of the samples at 12.3 KD, gave the longest retention time of 0.700 column volumes. Like conventional SEC, the greater the protein interaction with the gel, the longer the retention time. Because the larger proteins BSA and hemoglobin have molecular weights of 67 KD and 68 KD respectively, their retention times are shorter than Cytochrome C, with BSA slightly longer: 0.522 column volumes to hemoglobin's 0.493 column volumes. BSA and hemoglobin are both too large to interact with the pores and have to travel around the beads, giving them a shorter pathlength within the column and therefore shorter retention times.

The presence of 10mM and 20mM D-glucose has no effect on the bead pore size, as the retention times for movement of all three proteins are virtually the same as when free glucose molecules are absent from the system. In theory, free glucose will compete for the binding of the Con A, but at low concentrations, this is not sufficient enough to disturb the Con A crosslinkages to the alginate. However, at a 50mM D-glucose concentration, there is a peak shift to the right giving longer retention times. At this concentration free glucose is successfully competing with alginate for the binding of Con A, breaking a number of the crosslinkages and slightly increasing the bead pore size. The proteins now have increased interaction with the bead pores and take longer to elute from the column.

It was expected that the peak shift to the right would carry on increasing at 100mM and 150mM D-glucose. This did not occur; the retention times were not significantly different from the 50mM glucose concentration.

When the concentration of D-glucose was increased the absorbance maximum of the peaks also varied. For Cytochrome C and BSA, a trend was seen: the higher the D-

glucose concentration, the lower the maximum absorbance. For hemoglobin the absorbance maximums gave no pattern.

The conditions required for optimum SEC results were fully investigated using these two systems. It was interesting to see that similar results could be achieved when the experimental set up changed a little.

Although the results stated in this set of experiments show potential for both alginate beads and Con A dextran gels in SEC. SEC would yield the most accurate results if the beads within the column were of uniform size and shape. However, the viscosity of the alginate solution meant that when the solution was added drop-wise to $CaCl_2$, the drops that formed resulted in strong beads, but were too big for use with SEC. If the alginate were forced to drop into the calcium chloride solution before forming a natural bead in accordance with surface tension alone, the resulting beads would be smaller and more desirable. Many methods were tried to achieve this. Physically tapping the tube through which the solution emerged resulted in beads of a desirable size, but was unsuitable and tedious. The second method tried involved using a spinning disk onto which the solution was applied. Centrifugal forces resulted in the solution being spun off the disk and landing in the $CaCl_2$ solution, but in order for the beads to be of a suitable size, the speed at which the disk needed to be rotated was high. This meant that the solution was projected about 40cm from the disk, and no suitable container was available for the collection of the beads. It also required a large volume of $CaCl_2$, which was uneconomical. Finally a method was devised using an air supply that blew the solution from the tube and into the container below allowed for good bead formation. Altering the flow rate and the intensity of the air supply allowed for beads of a desirable size to be obtained.

Generally, the method of bead preparation was rather crude in these experiments, making it very hard to finely control the size of the beads. The beads vary in size and shape as shown in Figure 10.2, causing a variation in the size of the pores. In order to achieve more accurate results, the method of bead preparation needs to be optimised to ensure that the beads are spherical and of an even size distribution, thus a smaller concentration of glucose would have an effect on the retention times of the sample proteins.

To substantiate the data and ideas shown in this study, the effect of D-glucose experiments should be repeated in duplicate with additional data points (more glucose concentrations tested between 0 and 150mM), to determine if there is a glucose saturation effect like that seen by Tang *et al.*(2003) with dextran con A hydrogels. With the increased number of runs for each buffer condition, the standard deviation for each set of results could be calculated. This would determine if the change in retention times were due to the presence of D-glucose or just normal experimental variation. This could subsequently be backed up by a control experiment that used another sugar, for example L-glucose, in place of D-glucose, which could confirm the special response to D-glucose, rather than other factors.

10.6 Conclusion

This study has shown that the presence of 50mM D-glucose does have a significant effect on the retention times of the proteins Cytochrome C, BSA and hemoglobin through alginate beads.

The mechanical strength of the beads was not a problem, as the beads at the end of this project held their shape, even though they had buffer continuously flowing through them for 6 weeks (approximately 15 litres of buffer). It was the process of making the beads that was the limiting factor inaccuracy.

If responsive chromatographic beads could be successfully manufactured, they could find some applications in the bioseparations area. While the use of alginate beads allowed a convenient preliminary evaluation of the potential of this technique. It is clear that further development would require the formation of covalently cross linked beads which would not require high calcium concentrations to maintain stability. The same beads could be used to separate molecules according to their molecular weight, when they are dissolved in a specific glucose-concentration-containing buffer. This would eradicate the need for numerous types of beads, but could have some limitations. The molecules being injected to the column could not contain any glucose (e.g. glycoproteins) or free hydroxyl groups, as they would bind to the beads. They would

also have to not interact or react with glucose molecules. These might be too many constraints for the dynamic beads to have an application in the general chromatographic consumable market, but they could have specialized application.

Overall, this study has shown that the presence of D-glucose at a specific concentration does effects somewhat the pore size of both Con A -dextran-alginate and Con A-alginate beads.

Chapter 11. Conclusions and Future Work

11.1 Conclusions

The results of the studies presented in this thesis show that dextran hydrogels can be fabricated for a number of potential biomedical engineering applications. The most promising hydrogel developed was based on CM-dextran by the introduction of crosslinks using N-(3-dimethylaminopropyl)-N'-ethylcarbodiimide (EDC) in combination with N-hydroxysuccinimide (NHS). Detailed applications of this method in various fields were investigated. The results illustrate the potential of smart hydrogels in fabrication, tissue engineering, biosensors and bioseparation.

In summary:

- Dextran/Con-A hydrogel membranes can be synthesized via a nucleophilic replacement reaction in a triazine ring, such that both gel formation and Con-A fixation occurred at the same synthesis step. The resulting hydrogels are capable of releasing insulin in a dose-dependent response to changes in D-glucose concentrations. The response observed is selective to sugars that are bound by Con A and is repeatable reversible. Unlike sol-gel systems, this membrane retains structural integrity in the presence of elevated D-glucose concentrations and needs no additional external membrane containment. The synthesis protocol can be extended to the formation of gels based on other ligand-receptor interactions and provides a basis for developing a wide range of responsive materials. However the synthesis is complex and the triazine group is potentially toxic.

- A simple procedure was developed for the synthesis of D-glucose responsive hydrogels by carbodiimide chemistry. This allows production of gels with varying levels of protein substitution and with a controllable degree of carboxylic group substitution. There are two major advantages of this material. (i) The gel no longer requires the use of a potentially cytotoxic triazine group, and hence is more likely to be biocompatible. (ii) The use of CM dextran allows the intrinsic charge properties of the gel to be easily

controlled such that gels can be tailored for use in environments of different pH and ionic strengths. In the course of these studies it was found that the gelation time and the mechanical strength of the final gel produced are dictated by the initial degree of substitution of carboxylic groups and subsequently by the concentration of coupled protein e.g. the gelation time for hydrogel-grafted Con A is far shorter than that of gels without protein produced using the same procedure. This suggest that mechanical properties can be modified independently of response levels by including inert proteins or other amine-containing compounds to increase the degree of covalent cross-linking.

❖ The properties of the hydrogel are closely related to its network structure. In the analysis of the network structure of CM-hydrogel, equilibrium swelling theory was used. pH sensitivity of the CM-dextran hydrogels was shown. At higher pH, in addition to osmotic pressure, the driving force for water diffusion into the hydrogels was higher due to the following: (1) Ionization of COOH groups resulting in increased hydrophilicity; (2) Increased electrostatic repulsion between neighboring similarly-charged molecules; (3) Increased counter-ion diffusion into the gel to maintain electroneutrality. It was also concluded that for a CM-dextran with 5 COOH/CM-dextran (10^{-4} Mol/g) and a proportion of cross-linking agents at 7 EDC/NHS(W/W), a weight ratio of 0.10 (CM-dextran / hydrogel (W/W)) was the optimum for forming cross-linkages. In general, hydrogels with increased cross-linking have a lower k' value. The fractional protein release experimental data were fitted to equation $\frac{M_t}{M_\infty} = K t^n$ and the proportionality constants – K and n – determined. The n values were all less than 0.5 with a correlation coefficient of the linear regression R^2>0.99 for most cases. For the degradation of the CM-dextran hydrogels, the rate of degradation depended on the cross-linking density and charge forces between the enzyme and the unreacted COOH groups. The rate of degradation was the highest for the lowest density gels. For intermediate densities, the rate of degradation was a function of the interaction between the electrostatic repulsion between similar charged molecules (i.e. COOH and the dextranase used) and the mesh size.

- pH-sensitive hydrogels were formed by the intermolecular cross-linking of CM-dextran using EDC and NHS. Infrared spectra of the hydrogels suggested that intermolecular formation of ester bonds occurred between the hydroxyl and carboxyl groups in CM-dextran. The porosity of the hydrogels produced, as shown by protein diffusion, increased in response to changes in the pH and the ionic strength of the external medium. The result show pH-dependent swelling behavior arising from the acidic pedant groups in the polymer network. The diffusion of the protein lysozyme through the hydrogel membranes increased with increases in both pH (5.0-9.0) and ionic strength. The effect of changes of both pH and ionic strength on the hydrogel's permeability was shown to be reversible. Cryofixation and cryofracturing techniques were used to confirm pH-induced changes in their interior cross-sectional structure.

- The ability of a novel dextran-based biomaterial to support human cells was examined, as a precursor to its use as an extracellular matrix (ECM) for tissue engineering purposes. Alteration of the ratio of carboxylic and hydroxyl groups in the CM-dextran gel was possible and enabled creation of specific properties such as pH-sensitivity and porosity. It was found that a non-sensitive form of the CM-dextran hydrogel was optimal for attachment and maintenance of primary human dermal fibroblast cultures and that attachment did not appear to be facilitated by the additional presence of adhesion factors (fibronectin, Con A or poly(L-lysine)). Cell cultures over a period of 7 days showed normal morphological and proliferative capabilities. The CM-dextran gel demonstrated initial potential for development as a tissue engineered dermal replacement.

- A proof-of-concept study was conducted to see if an intelligent hydrogel with a diffraction grating could be fabricated in one-step. The CM-dextran hydrogel coupled BSA was prepared using carbodiimide chemistry; simultaneously the grating pattern was engineered onto its surface. The results of FT-IR confirmed the chemical mechanism of hydrogel preparation and also

cryofixation and cryofracturing techniques give evidence of the grating structure. It was shown that this functional hydrogel had the same optical properties as the silicon rubber submaster. A simple non-patterned hydrogel diffraction grating was manufactured from alginate using the same chemistry. In test with this alginate grating it was shown that the shapes of diffraction or reflection spots derived from an incident laser beam in response to changes in the gel as Ca^{2+} was varied. It is anticipated that this response could provide the basis for a new type of biosensor.

- A novel affinity membrane was fabricated from CM-dextran, protein and cibacron blue (CB). ITC results provided evidence for binding differences between CB and lysozyme, Cytochrome C, BSA, and hemoglobin. Results from diffusion and elution across hydrogel membranes with different proteins proved there was displaceable competitive binding between CB and protein. This hydrogel membrane was able to purify proteins in the presence of contaminant more effectively than a conventional affinity membrane grafted with CB ligand as the intrinsic binding interaction was only displaced by the more strongly bound protein.

- D-glucose sensitive hydrogel was fabricated into bead. Sodium alginate was used to partly or wholly replace dextran as the backbone in order to improve the mechanical strength of the gel. Experiments were conducted using two types of hydrogel. One was based on a CM-dextran hydrogel coupled with Con A combined with alginate which further enhanced the mechanical strength allowing additional Ca^{2+} crosslinkage. The second was directly attained by grafting Con A onto alginate and then forming beads using Ca^{2+} solution. Size exclusion chromatography (SEC) was employed to detect the effect of D-glucose on the size exclusion properties of the gels. The results show that 50mM D-glucose has a significant effect on the retention times of the proteins Cytochrome C, BSA and hemoglobin. Overall, this study has shown that SEC can be used to characterize the response properties of these gels.

11.2 Future work

Many researchers have investigated the rate of hydrogel response to change in vitro. The response speed is dictated by both polymer and functional mechanisms. For example, temperature-responsive hydrogel can be formed using poly(N-isopropylacryamide) (PNIPAAm) which has a lower critical solution temperature at around 32 °C in aqueous solution. The properties and applications of these hydrogels will be enhanced if response to various stimuli in different conditions, such as pH, temperature, and D-glucose. Recently, hydrogels which respond to both pH and temperature accounted for most studies. However, no reports mention dual function where a biomolecular response is combined with a temperature response. Based on the results in this project, the hydrogel produced should respond to a combination of D-glucose with pH. The next step is to make pH and temperature sensitive CM-dextran hydrogels by grafting PNIPAAm into the hydrogel. This should be feasible as PNIPAAm can be substituted with an amino group which will favor PNIPAAm incorporating into the CM-dextran backbone during the EDC/NHS crosslinking step.

An attractive application of these hydrogels lies in the fabrication of a novel biosensor. The proof of principle experiments confirmed that a diffraction grating can be imprinted on the gel. Further work could aim to produce new devices whose physical dimensions change in an a structured way in response to the presence of specific actuating molecules allowing direct observation from the change of optical characteristics of a hydrogel grating. It should be possible to form protein chips based on a number of different protein/receptors grafted into this hydrogel diffraction grating, allowing a number of analytes to be determined simultaneously.

Further experiment could investigate mammalian cell growth on these gels as a novel extracellular matrix. Stable and repeatable results will be attained only if the optimum conditions can be determined for this matrix. In all, these further experiments should substantiate the commercial potential of these gels.

References

Afify, A. M., Stern, M., Guntenhöner, M., and Stern, R. (1993). Purification and characterization of human serum hyaluronidase, *Arch. Biochem. Biophys.*, **305**, pp434-441

Akala, E. O., Kopeckova, P., Kopecek, J., (1998). Novel pH-sensitive hydrogels with adjustable swelling kinetics, *Biomaterials*, **19**, pp1037–1047.

Alberts, B., Bray, D., Lewis, J., Raff, M., Roberts, K. and Watson, J.D. (1994). *Molecular biology of the cell*, 3rd ed. New York: Garland Publishing,Inc.,.

Albin, G. W., Horbett, T. A., Miller, S. R. and Ricker, N. L. (1987). Theoretical and experimental studies of glucose sensitive membranes, *J. Controlled Release*, **6**, pp267–291.

Albin, G., Horbett, T. A. and Ratner, B. D. (1985). Glucose sensitive membranes for controlled delivery of insulin: Insulin transport studies, *J. Controlled Release*, **2**, pp153–164.

Ambrosino, R., Barone, G., Castronuovo, G., Ceccarini, C., Cultrera, O. and Elia, V., (1987). Protein-Ligand interaction: A calorimetric study of the interaction of oligosaccharides and hen ovalbumin glycopeptides with concanavalin A. *Biochemistry*. **26(13),** pp. 3971-3975

Aoki, T., Nagao, Y., Sanui, K., Ogata, N., Kikuchi, A., Sakurai, Y., Kataoka, K. and Okano, T. (1996). Glucose-sensitive lower critical solution temperature changes of copolymers composed of N-isopropylacrylamide and phenylboronic acid moieties, *Polym. J.*, **28**, pp371–374.

Arshady, R. (1990). Albumin microspheres and microcapsules: methodology of manufacturing techniques, *J. Control. Rel.*, **14,** pp111–131.

Arvidsson, P., Plieva, F. M., Lozinsky, V. I., Galaev, I. Y. and Mattiasson, B. (2003). Direct chromatographic capture of enzyme from crude homogenate using immobilized metal affinity chromatography on a continuous supermacroporous adsorbent, *Journal of Chromatography A*, **986(2),** pp275-290.

Arvidsson, P., Plieva, F. M., Savina, I. N., Lozinsky, V. I., Fexby, S., Bülow, L., Galaev, I. Y. and Mattiasson, B. (2002). Chromatography of microbial cells using continuous supermacroporous affinity and ion-exchange columns, *Journal of Chromatography A,* **977(1),** pp27-38.

Aryca, Y. (2000). Epoxy derived pHEMA membrane for use bioactive macromolecules immobilization: covalently bound urease in a continuous model system, *J. Appl. Polym. Sci.,* **77,** pp2000–2008.

Atala, A., Kim, W., Paige, K. T., Vacanti, C. A. and Retik, A. B. (1994). Endoscopic treatment of esicoureteral reflux with a chondrocyte–alginate suspension. *J Urol*, **152,** pp641–643.

Avramescu, M. E., Sager, W. F. C. and Wessling, M. (2003). Functionalised ethylene vinyl alcohol copolymer (EVAL) membranes for affinity protein separation, *Journal of Membrane Science,* **216,** pp177–193.

Baker and Stacey, (1994). Epidemiology of chronic leg ulcers in Australia. *Autralian and New Zealand Journal of Surgery*, **64(4),** pp258.

Baldwin, S. P. and Saltzman W. M. (1998), Materials for protein delivery in tissue engineering, *Advanced Drug Delivery Reviews*, **33,** pp71–86.

Ballerstadt, R. and Ehwald, R. (1994). Suitability of aqueous dispersions of dextran and Concanavalin A for glucose sensing in different variants of the affinity sensor. *Biosens. Bioelectron.,* **9,** pp557–567.

Ballerstadt, R. and Schultz, J. S. (1998). Kinetics of dissolution of concanavalin A/dextran sols in response to glucose measured by surface plasma response. *Sensors and Actuators B*, **46** p50-55.

Bayramo¡glu, G., Yilmaz, M., Arica, M. Y. (2003). Affinity dye–ligand poly(hydroxyethyl methacrylate)/chitosan composite membrane for adsorption lysozyme and kinetic properties, *Biochem. Eng. J*, **13,** pp35–42.

Bayramoglu, G., Yýlmaz, M. and Arýca, M. Y. (2003). Affinity dye–ligand poly(hydroxyethyl methacrylate)/chitosan composite membrane for adsorption lysozyme and kinetic properties. *Biochemical Engineering Journal*, **13,** pp35–42.

Beebe, D. J., Moore, J. S., Bauer, J. M. Yu, Q., Liu, R. H., Devadoss, C. and Jo, B. H. (2000). Functional hydrogel structures for autonomous flow control inside microfluidic channels, *Nature*, **404,** pp588-590.

Beeskow, T., Kroner, K. H. and Anspach, F. B. (1997). Nylon-Based Affinity Membranes: Impacts of Surface Modification on Protein Adsorption, *Journal of Colloid and Interface Science,* **196,** 278–291.

Benslimane, S., Guidoin, R., Marceau, D., Merhi, Y., King, M. W. and Sigo–Luizard, M. F. (1988). Characteristics of polyester arterial grafts coated with albumin, the role and importance of the crosslinking chemicals. *Eur Surg Res*, **20,** pp8 –28

Biellmann, J. F., Samama, J. P., Branden, C. I. and Eklund, H. (1979). X-ray studies of the binding of cibacron blue F3GA to liver alcohol dehydrogenase. *Eur. J. Biochem.* **102,** pp107–110.

Bikales, M. and Menges, O. (1987). *Encyclopedia of polymer science and engineering Volume 7,* Wiley-Interscience publication, New York, pp798.

Bohrmann, B., Villiger, W., Johansen, R. and Coralline K. E. (1991). Shape of the bacterial nucleoid after cryofixation., *J Bacteriol*, **173,** pp3149–3158.

Borzacchiello, A. and Ambrosio, L. (2001). Network formation of low molecular weight hyaluronic acid derivatives. *J Biomater Sci: Polym Ed*, **12** pp307–316.

Brahim, S., Narinesingh, D. and Guiseppi-Elie, A. (2002). Bio-smart hydrogels: co-joined molecular recognition and signal transduction in biosensor fabrication and drug delivery, *Biosensors and Bioelectronics,* **17(11-12),** pp973-981.

Brahim, S., Narinesingh, D. and Guiseppi-Elie, A. (2002). Polypyrrole-hydrogel composites for the construction of clinically important biosensors, *Biosensors and Bioelectronics,* **17(1-2),** pp53-59.

Brannon-Peppas, L. and Peppas, N. A. (1990). Dynamic and equilibrium swelling behaviour of pH-sensitive hydrogels containing 2- hydroxyethyl methacrylate, *Biomaterials*, **11**, pp635– 644.

Brannon-Peppas, L. and Peppas, N. A. (1991). Equilibrium swelling behavior of pH-sensitive hydrogels, *Chem. Eng. Sci.*, **46**, pp715.

Brondsted, H., Anderson, C. and Hovgaard. (1998). Crosslinked dextran F new capsule material for colon targeting of drugs. *J Contr Rel*, **53,** pp7 –13.

Brownlee, M. and Cerami, A. (1979). Glucose-controlled insulin- delivery system: semisynthetic insulin bound to lectin, *Science*, **206**, pp1190–1191.

Brownlee, M. and Cerami, A. (1983). Glycosylated insulin complexed to concanavalin A. Biochemical basis for a closed-loop insulin delivery system, *Diabetes,* **32,** pp499–504.

Bryant, S. J. and Anseth, K. S. (2001). The effects of scaffold thickness on tissue engineered cartilage in photocrosslinked poly(ethylene oxide) hydrogels. *Biomaterials*, **22**, pp619–626.

Byrne, M. E., Park, K. and Peppas, N. A. (2002). Molecular imprinting within hydrogels, *Advanced Drug Delivery Reviews*, **54(1),** pp149-161.

Cadee, J. A., de Groot, C. J., Jiskoot, W., den Otter, W. and Hennink, W. E. (2002). Release of recombinant human interleukin-2 from dextran-based Hydrogels, *Journal of Controlled Release,* **78**, pp1–13.

Cai, Q., Yang, J., Bei, J. Z. and Wang, S. G. (2002). A novel porous cells scaffold made of polylactide–dextran blend by combining phase-separation and particle-leaching techniques, *Biomaterials*, **23,** pp4483–4492.

Cartier, S., Horbett, T. A. and Ratner, B. D. (1995). Glucose-sensitive membrane coated porous filters for control of hydraulic permeability and insulin delivery from a pressurized reservoir, *J. Membr. Sci.,* **106**, pp17–24.

Champluvier, B. and Kula, M. R. (1992). Dye-ligand membranes as selective adsorbents for rapid purification of enzymes: A case study, *Biotechnol. Bioeng.*, **40** pp33-40.

Charcosset, C. (1998). Purification of Proteins by Membrane Chromatography: Review, *J. Chem. T echnol. Biotechnol.*, **71**, 95-110

Charcosset, C., Su, Z., Karoor, S., Daun, G. and Colton, C. K., (1995). Protein A immunoaffinity hollow fiber membranes for immunoglobulin purification: experimental characterization, *Biotech. Bioeng.*, **48**, pp415-427.

Chegel, V., Shirshov, Y., Avilov, S., Demchenko, M. and Mustafaev, M. (2002). A novel aldehyde dextran sulfonate matrix for affinity biosensors, *Journal of Biochemical and Biophysical Methods,* **50(2-3),** pp201-216.

Chen, Y. F. and Yi, M. (2001). Swelling kinetics and stimuli-responsiveness of poly (DMAEMA) hydrogels prepared by UV-irradiation, *Radiation Physics and Chemistry*, **61(1),** pp65-68.

Chenite, A., Chaput, C., Wang, D., Combes, C., Buschmann, M. D., Hoemann, C. D., Leroux, J. C., Atkinson, B. L. and Binette, F. S. (2000). A. Novel injectable neutral solutions of chitosan form biodegradable gels in situ., *Biomaterials*, **21**, pp2155–2161.

Chiu, H. C., Hsiue, G. H., Lee, Y. P. and Huang, L. W. (1999). Synthesis and characterization of pH-sensitive dextran hydrogels as a potential colon-specific drug delivery system, *J Biomater Sci Polym Edn,***10**, pp591–608.

Chiu, H. C., Lin Y. F. and Hsu, Y. H. (2002). Effects of acrylic acid on preparation and swelling properties of pH-sensitive dextran hydrogels, *Biomaterials*, **23(4),** pp1103-1112.

Chiu, H. C., Wu, A. T. and Lin, Y. F. (2001). Synthesis and characterization of acrylic acid-containing dextran hydrogels, *Polymer*, **42**, pp1471–1479.

Choi, Y. S., Hong, S. R., Lee, Y. M., Song, K. W., Park, M. H.and Nam, Y. S. (1999). Study on gelatin-containing artificial skin: I. Preparation and characteristics of novel gelatin-alginate sponge, *Biomaterials*, **20,** pp409.

Cooper, M. A. (2002). Optical Biosensors in Drug Discovery, *Nature*, **1,** pp515-528.

Cortesia, R., Espositoa, E., Ostia, M., Squarzonia, G., Menegattia, E., Davisb, S. and Nastruzzia, S. C. (1999). Dextran cross-linked gelatin microspheres as a drug delivery system, *European Journal of and Biopharmaceutics*, **47,** pp153–160

Dagani, R. (1997). Intelligent gels, *Chem. Eng. News,* **75**, pp26–36.

De Groot, C. J., Van Luyn, M. J. A., Van Dijk-Wolthuis, W. N. E., CadeH, J. A., Plantinga, J .A., Otter, W. D. and Hennink, W. E. (2001). In vitro biocompatibility of biodegradable dextran-based hydrogels tested with human fibroblasts, *Biomaterials*, **22,** pp1197-1203.

de Jong , S. J., van Eerdenbrugh , B., van Nostrum , C. F., Kettenes-van den Bosch J. J. and Hennink, W. E. (2001). Physically crosslinked dextran hydrogels by stereocomplex formation of lactic acid oligomers: degradation and protein release behavior, *Journal of Controlled Release,* **71**, pp261–275.

de Jong, S. J., De Smedt , S. C., Demeester, J., van Nostrum , C. F., Kettenes-van den Bosch, J. J. and Hennink, W. E. (2001). Biodegradable hydrogels based on

stereocomplex formation between lactic acid oligomers grafted to dextran, *Journal of Controlled Release,* **72,** pp47–56.

Dennis, S. E., Rosann, M.K. and Mark, L. J., (2001). Gel Sensors and Method of use Thereof, *US patent*: 6180288B1.

Dong, S. J. and Chen, X. (2002). Some new aspects in biosensors, *Reviews in Molecular Biotechnology,* **82,** pp303-323.

Draye, J. P., Delaey, B., Van de Voorde, A., Van Den Bulcke, A., Reu, B. D. and Schacht, E. (1998). In vitro and in vivo biocompatibility of dextran dialdehyde cross-linked gelatin hydrogel films, *Biomaterials*, **19,** pp1677–1687.

Drury, J. L. and Mooney, D. J. (2003). Hydrogels for tissue engineering: scaffold design variables and applications, *Biomaterials,* **Available online 26 June.**

Edman, P., Ekman, B. and Sjoholm, I. (1980). Immobilization of proteins in microspheres of biodegradable polyacyldextran., *J Pharm Sci*, **69,** pp838–842.

Ehwald, R., Ballerstadt R. and Dautzenberg, H. Viscosimetric affinity assays Anal. Biochem. 234 (1996), pp. 1–8

Eiselt, P., Lee, K. Y. and Mooney, D. J. (1999). Rigidity of two-component hydrogels prepared from alginate and poly(ethylene glycol)-diamines, *Macromolecules*, **32,** pp5561–5566.

Evans, D. F., Pye, G., Bramly, R., Clark, A. G., Dyson, T. J. and Hardcastle, D. J. (1988). Measurement of gastrointestinal pH profiles in normal ambulant human subjects, *Gut*, **29,** pp1035.

Everhart, D.S., Kaylor, R.M. and Jones, M.L. (2001). Gel Sensors and Mthods of Use thereof, *Patent US6180288 B1.*

Falamarzian, M. and Varshosaz, J. (1998). The effect of structural changes on swelling kinetics of polybasic /hydrophobic pH sensitive hydrogels, *Drug Dev. Ind. Pharm.*, **24,** pp667.

Ferreira, L., Gil, M. H. and Dordick, J. S. (2002). Enzymatic synthesis of dextran-containing hydrogels, *Biomaterials*, **23,** pp3957 – 3967.

Fisher, E., Stein, E., Boyer, P., Lardy H. and Myrback, K. (1960). *The Enzymes 4A*, Academic Press, New York, pp304.

Fitzpatrick, J., Fanning, L., Hearty, S., Leonard, P., Manning, B. M. and Quinn, J. G., (2000). Applications and recent developments in the use of antibodies for analysis, *Anal Lett*, **33(13),** pp263–2609.

Flory, P. J. and Rehner, R. J. (1943). Statistical mechanics of cross-linked polymer networks. I. Rubberlike elasticity, *Journal of Chem. Phys.*, **11,** pp521.

Francis Suh, J. K. and Matthew, H. W. T. (2000). Application of chitosan-based polysaccharide biomaterials in cartilage tissue engineering: a review, *Biomaterials*, **21,** pp2589-2598

Frannssen, O., van-Ooijen, R. D., de-Boer, D., Maes, R. A. A. and Hennink, W.E. (1999). Enzymatic degradation of cross-linked dextrans, *Macromolecules*, **32,** pp2896 – 2902.

Franssen, O. and Hennink, W. E. (1998). A novel preparation method for polymeric microparticles without the use of organic solvents, *International Journal of Pharmaceutics,* **168,** pp1–7.

Franssen, O., Stenekes,R. J. H. and Hennink, W. E. (1999). Controlled release of a model protein from enzymatically degrading dextran microspheres, *Journal of Controlled Release*, **59,** pp219–228.

Franssen, O., Vandervennet, L., Roders, P. and Hennink, W. E. (1999). Degradable dextran hydrogels: controlled release of a model protein from cylinders and microspheres, *Journal of Controlled Release,* **60,** pp211–221.

Franssen, O., Vos O. P. and Hennink, W. E. (1997). Delayed release of a model protein from enzymatically-degrading dextran hydrogels, *Journal of Controlled Release,* **44(2-3),** pp237-245.

Galaev, I. Y. and Mattiasson, B. 1999. 'Smart' polymers and what they could do in biotechnology and medicine. *Trends in Biotechnology*, **17,** 335-340.

Gamini, A., Paoletti, S., Toffanin, R., Micali, F., Michieli, L. and Bevilacqua, C. (2002). Structural investigations of cross-linked hyaluronan, *Biomaterials*, **23,** pp1161–1167.

Gehrke, S. H. and Lee, P. I., (1990). *Hydrogels for drug delivery systems. In Specialized Drug Delivery Systems* (Tyle, P., ed.), Marcel Dekker, pp. 333–392,

George S. (1997). *Infrared characteristic Group Frequencies*: Tables and Charts (second edition). London: John Wiley & Sons, pp105.

Gombotz, W. R. and Wee, S. F. (1998). Protein release from alginate matrices, *Advanced Drug Delivery Reviews*, **31(3),** pp 267-285

Grabarek, Z. and Gergely, J. (1990). Zero-Length Crosslinking Procedure with the Use of Active Esters, *Analytical Biochemistry,* **185,** pp131-135.

Grier, D. G. (1997). New age crystals, *Nature*, **389**, pp784-785.

Griffith, L. G. (2000). Polymeric biomaterials, *Acta Materialia*, **48, 1(1),** pp263-277.

GuÈ vena, O., Sena, M., Karadag, E. and Saray, D. (1999). A review on the radiation synthesis of copolymeric hydrogels for adsorption and separation purposes, *|nc Radiation Physics and Chemistry,* **56**, pp381-386.

Guilherme, M. R., Silva, R. E., Girotto, M., Rubira A. F. and Muniz, E. C. (2003). Hydrogels based on PAAm network with PNIPAAm included: hydrophilic–hydrophobic transition measured by the partition of Orange II and Methylene Blue in water, *Polymer*, **44(15),** pp4213-4219.

Guo, W., Shang, Z., Yu, Y. and Zhou, L. (1994). Membrane affinity chromatography of alkaline phosphatase., *J. Chromatogr*, **685**, pp344-348.

Gupta, P., Vermani, K. and Garg, S. (2002). Hydrogels: from controlled release to pH-responsive drug delivery, *Drug Discovery Today*, **7(10),** pp569-579.

Habeck, M. (2001).Temperature-sensitive gels: from tissue engineering to drug delivery, *Drug discovery today*, **6(11),** pp553-554.

Haeberlin, B. and Friend, D. R (1992). *Anatomy and physiology of the gastrointestinal tract: Implications for clolonc drug delivery*, iln: D.R.Friend(Ed). Oral Colon-specific Drug Delivery, CRC Press, Boca Raton, FL, p1

Hansbrough, J. F. and Franco, E. S. (1998). Skin replacements. *Clinics in Plastic Surgery.* **25**, pp3.

Harvey, J. A. (1995). *Smart materials, In Encyclopedia of Chemical Technology (Kroschwitz, J.I. and Howe-Grant, M., eds),* John Wiley & Sons , pp. 502–514,

Hassan, C. M., Doyle, F. J. I. and Peppas, N. A. (1997). Dynamic behavior of glucose-responsive poly (methacrylic acid–g-ethylene glycol) hydrogels, *Macromolecules*, **30,** pp6166–6173.

Heller, J., Chang, A. C., Rodd, G. and Grodsky, G. M. (1990). Release of insulin from pH-sensitive poly(ortho esters), *J. Controlled Release*, **13**, pp295–302.

Hennink, W. E. and van Nostrum, C. F. (2002). Novel crosslinking methods to design hydrogels, *Advanced Drug Delivery Reviews*, **54**, 13–36.

Hennink, W. E., Franssen, O., van Dijk-Wolthuis, W. N. E. and Talsma, H. (1997). Dextran hydrogels for the controlled release of proteins, *Journal of Controlled Release,* **48(2-3),** pp107-114.

Heskins, M. and Guillet, J. E. (1968). Solution-properties of poly(N-isopropylacrylamide)., *J. Macromol. Chem. A*, **2**, pp1441.

Hinchcliffe, M. and Illum L., (1999). Intranasal insulin delivery and therapy, *Adv Drug Delivery Rev,* **35**, pp199-234.

Hoffman, A. S. Intelligent Polymers, in: K. Park (Ed.), (1997). *Controlled Drug Delivery: Challenge and Strategies*, American Chemical Society, Washington, DC, , pp. 485–497.

Hoffman, A. S., Hydrogels for biomedical applications (2002), *Advanced Drug Delivery Reviews*, **43**, pp3–12

Holtz, J. H. and Asher, S. A. (1997). Polymerized colloidal crystal hydrogel films as intelligent chemical sensing materials, *Nature*, **389**, pp829-832.

Holtz, J. H. Holtz, J. S. W., Munro, C. H. and Asher, S. A. (1998). Intelligent Polymerized Crystalline Colloidal Arrays: Novel Chemical Sensor Materials, *Anal. Chem.*, **70**, pp780-791.

Hong, P. D. and Chen, J. H. (1998). Network structure and chain mobility of freeze-dried polyvinyl chloride/dioxane gels., *Polymer*, **39**, pp5809–5817.

Hou, K. C. and Zaniewski, R. (1991). The effect of hydrophobic interaction on endotoxin adsorption by polymeric affinity matrix, *Biochimica et Biophysica Acta.*, **1073(1)**, pp149–154.

Hou, K. C., Zaniewski, R. and Roy, S. (1991). Protein A immobilized affinity cartridge for immunoglobulin purification, *Biotechnol. Appl. Biochem.*, **13(2)**, pp257–268.

Hovgaard L. and Brøndsted, H. (1995). Dextran hydrogels for colon-specific drug delivery, *Journal of Controlled Release*, **36(1-2)**, pp159-166.

http://science.howstuffworks.com/laser2.htm (link 1, 2003- 06-05)

http://www.affinity-sensors.co.uk/

http://www.gratinglab.com/library/handbook/chapter1.asp#1.1 (link 2, 2003- 06-05)

http://www.sigmaaldrich.com/

http://www.worthington-biochem.com/DEX/default.html

Hu, Z. B., Chen, Y. Y., Wang, C. J., Zheng, Y. D. and Li, Y. (1998). Polymer gels with engineered environmentally responsive surface patterns, *Nature*, **393**, pp149-152.

Hu, Z. B., Lu, X. H., and Gao, J. (2000). Hydrogel Opals, *Optics Communications*, **185**, pp19-24.

Huang, S. and Ingber, D. E. (1999). The structural and mechanical complexity of cell growth control., *Nat. Cell Biol.*, **1**, pp131-138.

Invitski, D., Abdel-Hamid, I., Atanasov, P. and Wilkins, E. (1999). Biosensors for the detection of pathogenic bacteria., *Biosens Bioelectron*, **14**, pp599–624.

Ishihara, K. and Matsui, K. (1986). Glucose-responsive insulin release from polymer capsule, *J. Polym. Sci. Polym. Lett. Ed.*, **24**, pp413–417.

Jen, A. C., Wake, M. C. and Mikos, A. G. (1996). Review: hydrogels for cell immobilization. *Biotechnol Bioeng*, **50**, pp357–364.

Jeong, B., Bae, Y. H., Lee, D. S. and Kim, S. W. (1997). Biodegradable block copolymers as injectable drug-delivery systems, *Nature*, **388**, pp860–862.

Jeong, B., Kim, S. W. and Bae, Y. H. (2002). Thermosensitive sol–gel reversible hydrogels, *Advanced Drug Delivery Reviews*, **54**, pp37–51.

Jon A. Rowley, Gerard Madlambayan, David J. Mooney, (1999). Alginate hydrogels as synthetic extracellular matrix materials, *Biomaterials*, **20,** pp45–53.

Josic, D., Reusch, J., Loster, K., Baum, O. and Reutter, W., (1992). High-performance membrane chromatography of serum and plasma membrane proteins., *J. Chromatogr.*, **590**, pp59-76.

Ju, H. K., Kim, S. Y. and Lee, Y. M. (2002). pH/temperature-responsive behaviors of semi-IPN and comb-type graft hydrogels composed of alginate and poly(N-isopropylacrylamide), *Polymer*, **42,** pp6851.

Kang, S. Il and Bae, Y. H. (2003). A sulfonamide based glucose-responsive hydrogel with covalently immobilized glucose oxidase and catalase, *Journal of Controlled Release*, **86,** pp115–121.

Kassab, A., Yavuz, H., Odabas, M. and Denizli, A. (2000). Human serum albumin chromatography by Cibacron Blue F3Gaderived microporous polyamide hollow-fiber affinity membranes, *Journal of Chromatography B*, **746,** pp123–132

Kataoka, H. K., Okano, T. and Sakurai, Y. (1997). Glucose-responsive gel from phenylborate polymer and polyvinylalcohol: prompt response at physiological pH through the interaction of borate with amino group in the gel, *Pharm. Res.*, **14,** pp289–293.

Kataoka, K., Miyazaki, H., Bunya, M., Okano, T. and Sakurai, Y. (1998). Totally synthetic polymer gels responding to external glucose concentration: their preparation and application to on– off regulation of insulin release, *J. Am. Chem. Soc.*, **120,** pp12694–12695.

Kataoka, K., Miyazaki, H., Okano, T. and Sakurai, Y. (1994). Sensitive glucose-induced change of the lower critical solution temperature of poly[N,N-dimethylacrylamide-co-3-acrylamido]phenylboronic acid] in physiological saline, *Macromolecules*, **27,** pp1061–1062.

Katchalsky, A. and Michaeli, I. (1955). Polyelectrolyte gels in salt solution, *J Polym. Sci.***15**, pp69.

Khare, A. R. and Peppas, N. A. (1993). Release behavior of bioactive agents from pH-sensitive hydrogels, *J. Biomater. Sci. Poly. Ed.*, **4**, pp275–289, (published erratum appears in J. Biomater. Sci. Polym. Ed. 1994;6 (6):following 598).

Kikuchi, A. and Okano, T. (2002). Pulsatile drug release control using hydrogels, *Advanced Drug Delivery Reviews*, **54**, pp53–77

Kim, J. J. and Park, K. (2001). Glucose-binding property of pegylated concanavalin A. *Pharmaceutical Research,* **18**, pp794-799.

Kim, J. J. and Park, K.(2001). Modulated insulin delivery from glucose-sensitive hydrogel dosage forms, *Journal of Controlled Release*, **77**, pp39–47.

Kim, S. H and Chu, C. C. (2000). Synthesis and characterization of dextran-methacrylate hydrogels and structural study by SEM. *J Biomed Mater Res*, **49,** 517 – 527.

Kim, S. H., Won, C. Y. and Chu, C. C. (1999). Synthesis and characterization of dextran-based hydrogels prepared by photocrosslinking., *Carbohydro Polym*, **40,** pp183–190.

Kim, S. H., Won, C. Y. and Chu, C. C. (1999). Synthesis and characterization of dextran-maleic acid based hydrogel, *J Biomed Mater Res*, **46,** pp160–170.

Kim, S. H., Won, C. Y. and Chu, C. C., (1999). Synthesis and characterization of dextran-based hydrogels prepared by photocrosslinking, *Carbohydr Polym*, **40,** pp183 –190.

Kim, S. J., Park, S. J. and Kim, S. I. (2003). Synthesis and characteristics of interpenetrating polymer network hydrogels composed of poly(vinyl alcohol) and poly(N-isopropylacrylamide), *Reactive and Functional Polymers,* **55(1),** pp61-67.

Kim, S. W., Pai, C. M., Makino, K., Seminoff, L. A., Holmberg, D. L., Gleeson, J. M. Wilson, D. E. and Mack, E. J. (1990). Self-regulated glycosylated insulin delivery, *J. Controlled Release,* **11,** pp193–201.

Kissel, T., Li, Y. X. and Unger, F. (2002). ABA-triblock copolymers from biodegradable polyester A-blocks and hydrophilic poly(ethylene oxide) B-blocks as a candidate for in situ forming hydrogel delivery systems for proteins, *Advanced Drug Delivery Reviews,* **54(1),** pp99-134.

Kitano, S., Koyama, Y., Kataoka, K., Okano, T. and Sakurai, Y. (1992). A novel drug delivery system utilizing a glucose responsive polymer complex between poly(vinyl alcohol) and poly(N- vinyl-2-pyrrolidone) with a phenyl boronic acid moiety, *J. Controlled Release*, **19,** pp162–170.

Klech, C. M. (1990). *Gels and jellies.*, In Encyclopedia of Pharmaceutical Technology (Swarbrick, J. and Boylan, J.C., eds), Marcel Dekker, pp. 415–439,

Klein, E. (2000). Affinity membranes: a 10-year review, *Journal of Membrane Science,* **179,** pp1–27.

Kokufuta, E., Matsukawa, S., Ebihara, T. and Matsuda, K., (1994). *In Macro-ion Characterization: From Dilute Solutions to Complex Fluids* (Schmitz, K. S., ed.), American Chemical Society, Washington, DC, USA, pp. 507–516.

Kopperschlager, G., Freyer, R., Diezel, W. and Hoffman, E. (1968). Kinetic and molecular properties of yeast phosphofructokinase., *FEBS Letter*, **1,** pp137-141

Kost, J. (1999). *Intelligent drug delivery systems.* In Encyclopaedia of Controlled Drug Delivery (Mathiowitz, E., ed.), John Wiley & Sons, pp. 445–459.

Kou, J. H., Amidon, G. L. and Lee, P. I. (1988). pH-dependent swelling and solute diffusion characteristics of poly(hydroxyethyl meth- acrylate–co-methacrylic acid) hydrogels, *Pharm. Res.*, **5,** pp592–597.

Krause, S., Kroner, K. H. and Deckwer, W. D., (1991). Comparison of affinity membranes and conventional affinity matrices with regard to protein purification. *Biotechnol. T ech.*, **5(3),** pp199-204.

Kubota, N., Nakagawa, Y. and Eguchi, Y. (1996). Recovery of serum proteins using cellulosic affinity membrane modified by immobilization of Cu2C ion, *J. Appl. Polym. Sci.*, **62,** pp1153–1160.

Kuijpers, A. J., Engbers, G. H. M., Feijen, J., De Smedt, S. C., Meyvis, T. K. L., Demeester, J., Krijgsveld, J., Zaat, S. A. J., and Dankert, J., (1999). Characterization of the network structure of carbodiimide cross-linked gelatin gels, *Macromolecules*, **32,** pp3325-3333.

Kuijpers, A. J., Engers, G. H. M., Meyvis, T. K. L., de Smedt, S. C. Demeester, J., Krijgsveld, J., Zaat, S.A.J., Dankert, J. and Feijen, J. (2000). Combined gelatin-chondroitin sulfate hydrogels for controlled release of cationic antibacterial proteins, *Macromolecules*, **33**, pp3705–3713.

Kuijpers, A. J., van Wachum, P. B., van Luyn, M. J. A., Engbers, G. H. M., Krijsveld, J., Zaat, S.A.J., Dankert, J. and Feijen, J. (2000). In vivo and in vitro release of lysozyme from cross-linked gelatin hydrogels: a model system for the delivery of antibacterial proteins from prosthetic heart valves, *J. Controlled Release*, **67**, 323–336.

Kumar, N., Ravikumar, M. N. V. and Domb, A. J. (2001). Biodegradable block copolymers, *Advanced Drug Delivery Reviews,* **53(1),** pp23-44.

Langer, R. (2000). Biomaterials in Drug Delivery and Tissue Engineering: One Laboratory's Experience, *Acc. Chem. Res.*, **33,** pp94-101.

Larsen, C., Harboe, E., Johansen, M., and Olesen, H. P., (1989). Macromolecular prodrugs. XVI. Colon-targeted deliverycomparison of the rate of release of naproxen from dextran ester prodrugs in homogenates of various segments of the pig gastrointestinal (GI) tract., *Pharm. Res.*, **5**, pp995–999.

Lawrence, E. (1995). *Henderson's Dictionary of Biological Terms*, Eleventh Edition, Longman Singapore Publishers (Pte) Ltd.

Leatherbarrow, R. J. and Dean, P. D. G. (1980). Studies on the mechanism of binding of serum albumins to immobilized Cibacron blue F3GA., *Biochem J,* **189**, pp27–34.

Lee, C. H. Singla, A and Lee, Y. (2001). Biomedical applications of collagen., *Int J Pharm*, **221**, pp1–22.

Lee, C. R., Grodzin sky, A. J. and Spector, M. (2001). The effects of cross-linking of collagen-glycosaminoglycan scaffolds on compressive stiffness, chondroc yte-mediated contraction,proliferation, and biosynthesis. *Biomaterials*, **22**, pp3145–54.

Lee, K. C., Lee, Y. J., Kim, W. B. and Cha, C. Y. (1990). Monoclonal antibodybased targeting of methotrexate-loaded microspheres, *Int. J. Pharm.,* **59**, pp27–33.

Lee, K. Y. and Mooney, D. J. (2001). Hydrogels for Tissue Engineering, *Chemical Reviews*, **101(7)**, pp1869-1879

Lee, K.Y., Rowley, J. A., Eiselt, P., Moy, E. M., Bouhadir, K. H. and Mooney, D. J. (2000). Controlling Mechanical and Swelling Properties of Alginate Hydrogels Independently by Cross-linker Type and Cross-linking Density, *Macromolecules*, **33**, pp4291-4294.

Leonard, P., Hearty, S., Brennan, J., Dunne, L. and Quinn, J. Trinad Chakraborty c, Richard O'Kennedy, (2003). Advances in biosensors for detection of pathogens in food and water, *Enzyme and Microbial Technology: Review* **32**, pp3–13.

LeRoux, M. A., Guilak, F. and Setton, L. A. (1999). Compressive and shear properties of alginate gel: effects of sodium ions and alginate concentration., *J Biomed Mater Res*, **47**, pp46–53.

Lim, F. and Sun, A. M. (1980) Microencapsulated islets as bioartificial endocrine pancreas, *Science*, **210**, pp908–910.

Lin, V. S. Y., Motesharei, K., Dancil, K. P. S., Sailor, M. J. M. and Ghadiri, R. (1997). A Porous Silicon-Based Optical Interferometric Biosensor, *Science,* **278**, pp840-843.

Liu H. C. and Fried, J. R. (1994). Breakthrough of lysozyme through, an affinity membrane of cellulose-Cibacron Blue 3GA, *AIChE J.*, **40**, pp40-49.

Loris, R., Hamelryck, T., Bouckaert, J., and Wyns, L., (1998). Legume lectin structure., *Biochimica et Biophysica Acta,* **1383**, pp9-36.

Lowman, A. M., Morishita, Kajita, M., Nagai, M. T., and Peppas, N. A. (1999). Oral Delivery of Insulin Using pH-Responsive Complexation Gels, *Journal of Pharmaceutical Sciences*, **88(9)**, pp933-937

Luksa, J., Menart, V., Milicic, S., Kus, B., Gaberc-Porekar, V. and Josic, D., (1994). Purification of human tumour necrosis factor by membrane chromatography., *J. Chromatogr. A*, **661**, pp161-168.

Marchand, R., Woerly, S., Bertrand, L. and Valdes, N. (1993). Evaluation of two cross-linked collagen gels implanted in the transected spinal cord, *Brain Research Bulletin*, **30(3-4)**, pp415-422.

Markland, P., Zhang, Y., Amidon, G. L. and Yang, V. C. (1999). A pH- and ionic strength-responsive polypeptide hydrogel: synthesis, characterization, and preliminary protein release studies, *J. Biomed. Mater. Res.*, **47**, pp595.

Martin, B. D., Linhardt, R. J. and Dordick, J. S. (1998). Highly swelling hydrogels from ordered galactose-based polyacrylates, *Biomaterials*, **19**, pp69 – 76

Masci, G., Bontempo D. and Crescenzi, V. (2002). Synthesis and characterization of thermoresponsive N-isopropylacrylamide/methacrylated pullulan hydrogels, *Polymer,* **43(1)**, pp5587-5593.

Matejtschuk, P. (1997). *Affinity Separations: A practical Approach*, Oxford UK, University Press, pp4.

Mayes, A. G., Moore, J. D., Eisenthal, R., Hubble, J. , (1990). Investigation of binding site density: effects on the interaction between Cibacron blue-dextran conjugates and lysozyme, *Biotechnology & Bioengineering*, **36**, pp1090-1096.

McFadden, P. (2002). Broadband Biodetection: Holmes on a Chip, *Science,* **297**, pp2075-2076

Mi, F. L., Kuan, C. Y., Shyu, S. S., Lee, S. T. and Chang, S. F., (2000). The study of gelation kinetics of chain-relaxation properties of glutaraldehyde-cross-linked chitosan gel and their effects on microspheres preparation and drug release., *Carbohydr Polym*, **41**, pp389–396.

Mitchell, P. (2002). A perspective on protein microarrays, *Nature biotechnology*, **20,** pp225-229.

Miyata, T., Asami, N. and Uragami, T., (1999). A reversibly antigen-responsive hydrogel. *Nature*, **399**, pp766-769.

Miyata, T., Jikihara, A., Nakamae, K. and Hoffman, A. S. (1996). Preparation of poly(2-glucosyloxyethyl methacrylate)–concanavalin A complex hydrogel and its glucose-sensitivity, *Macromol. Chem. Phys.*, **197,** pp1135–1146.

Miyata, T., Uragami, T., and Nakamae, K. (2002). Biomolecule-sensitive hydrogels, *Advanced Drug Delivery Reviews*, **54,** pp79–98.

Molteni, L., (1979). In: Gregoriadis, G. (Ed.), *Drug Carriers in Biology and Medicine*, Academic Press, London, pp107–125.

Mun, G. A., Nurkeeva, Z. S., Khutoryanskiy, V. V., Sergaziyev, A. D. and Rosiak, J. M. (2002). Radiation synthesis of temperature-responsive hydrogels by copolymerization of [2-(methacryloyloxy)ethyl]trimethylammonium chloride with N-isopropylacrylamide, *Radiation Physics and Chemistry*, **65(1),** pp267-270.

Murat, E. and Arzu, Y. (2001). Controlled release of antifungal drug terbinafine hydrochloride from poly (N-vinyl 2-pyrrolidone/itaconic acid) hydrogels, *International Journal of Pharmaceutics,* **228(1-2),** pp33-41.

Murat, E., Uzun, C. and Güven, O. (2000). Controlled release of terbinafine hydrochloride from pH sensitive poly (acrylamide/maleic acid) hydrogels, *International Journal of Pharmaceutics,* **203(1-2)**, pp149-157.

Nakajima N. and Ikada, Y. (1995). Mechanism of amide formation by carbodiimide for bioconjugation in aqueous media, *Bioconjugate Chem.*, **6**, pp123–130.

Nakamae, K., Miyata, T., Jikihara, A. and Hoffman, A. S. (1994). Formation of poly(glycosyloxyethyl methacrylate)–concanavalin A complex and its glucose sensitivity, *J. Biomater. Sci. Polm. Edn.*, **6**, pp79–90.

Nastruzzi, C., Pastesini, C., Cortesi, R., Esposito, E., Gambari, R. and Menegatti, E. (1994). Production and in vitro evaluation of gelatin microspheres containing an antitumor tetra-amidine, *J. Microencaps.*, **11**, pp249–260.

Nguyen, K. T. and West, J. L. (2002). Photopolymerizable hydrogels for tissue engineering applications, *Biomaterials*, **23(22),** pp4307-4314.

Nishikawa, A. H., Bailon, P., and Ramel, A. H., (1976). Design parameters in affinity chromatography., *J. Macromol. Sci. – Chem.*, **A10,** pp149–190.

Obaidat, A. A. and Park, K. (1997). Characterization of protein release through glucose-sensitive hydrogel membranes., *Biomaterials,* **18,** pp801-806.

Oerther, S., Maurin, A. C., Payan, E., Hubert, P., Lapicque, F., Presle, N., Dexheimer, J., Netter, P. and Lapicque, F. (2000). High interaction alginate–hyaluronate associations by hyaluronate deacetylation for the preparation of ef.cient biomaterials., *Biopolymer*, **54**, pp273–281.

Ó'Fágáin, C. (2003). Enzyme stabilization—recent experimental progress, *Enzyme and Microbial Technology*, **33(2-3),** pp137-149.

Ono, K., Saito, Y., Yura, H., Ishikaw, K., Kurita, A., Akaike, T. and Ishihara, M.(2000). Photocrosslinkable chitosan as a biological adhesive., *J Biomed Mater Res*, **49**, pp289–295.

Ozmen, M. M. and Okay, O. (2003). Swelling behavior of strong polyelectrolyte poly(N-t-butylacrylamide-co-acrylamide) hydrogels, *European Polymer Journal,* **39(5),** pp877-886.

Palumbo, P. F. S., Giammona, G., Casadei, M. A. and Moracci, F. M. (2003). Biodegradable hydrogels obtained by photocrosslinking of dextran and polyaspartamide derivatives, *Biomaterials,* **24(23),** pp4301-4313G.

Park, K., Shalaby, W. S. W. and Park, H. (1993). *Biodegradable Hydrogels, for Drug Delivery,* Technomic Publishing, Lancaster-Basel.

Park, S. N., Lee, H. J., Lee, K. H. and Suha, H. (2003). Biological haracterization of EDC-crosslinked collagen–hyaluronic acid matrix in dermal tissue restoration, *Biomaterials,* **24**, pp1631–1641.

Park, S. N., Park, J. C., Kim, H. O., Song, M. J. and Suh, H. (2002). Characterization of porous collage/hyaluronic acid scaffold modi.ed by 1-ethyl-3-(3-dimethylaminopropyl)carbodiimide cross-linking, *Biomaterials*, **23**, pp1205–1212.

Parker, R. S., Doyle III, F. J. and Peppas, N. A. (1999). A model-based algorithm for blood glucose control in type I diabetic patients, *IEEE Trans. Biomed. Eng.*, **46**, pp148–157.

Patel, V. R. and Amiji, M. M. (1996). Preparation and characterization of freeze-dried chitosan–poly (ethylene oxide) hydrogels for site-specific antibiotic delivery in the stomach, *Pharm. Res.* , **13**, pp588–593.

Peppas, N. A (1986). *Characterization of the cross-linked sructure of hydrogels, Hydrogels in Medicine and Pharmacy Volume I Fundamentals Chapter 2*, CRC Press, Boca Raton, Florida, pp27 – 56.

Peppas, N. A (1986). *Dynamically swelling hydrogels in controlled release applications Hydrogels in Medicine and Pharmacy Volume III Properties and Applications Chapter 6*, CRC Press, Boca Raton, Florida pp109 – 135.

Peppas, N. A (1986). *Solute diffusion in hydrophilic network structures Hydrogels in Medicine and Pharmacy Volume I Fundamentals Chapter 3*, CRC Press, Boca Raton, Florida, pp57 – 83.

Peppas, N. A and Merrill, E. W. P. (1976). Hydrogels: reinforcement of radiation crosslinked networks by crystallization, *Journal of Polymer Science Polymer Chemistry,* **14,** pp441.

Peppas, N. A. (1986). *Solute diffusion in hydrophilic network structures, Hydrogels in Medicine and Pharmacy Volume I Fundamentals Chapter 1*, CRC Press, Boca Raton, Florida, pp1 – 25.

Peppas, N. A. (2000). Hydrogels in pharmaceutical formulations, *Eur. J. Pharm. Biopharm.*, **50**, pp27–46.

Peppas, N. A. and Khare, A. R. Preparation, (1993), Structure and diffusional behaviour of hydrogels in controlled release, *Advanced Drug Delivery Reviews*, **11**, pp1 – 36.

Peppas, N. A. and Klier, J. (1991). Controlled release by using poly- (methacrylic acid–g-ethylene glycol) hydrogels, *J. Controlled Release,* **16,** pp203–214.

Peppas, N. A. and Mikos, A. G. (1986). *Preparation methods and structure of hydrogels, in: N.A. Peppas (Ed.), Hydrogels in Medicine and Pharmacy*, Vol. 1, CRC Press, Bocca Raton, FL, pp1–27.

Peppas, N. A. and Sahlin, J. J. (1996). Hydrogels as mucoadhesive and bioadhesive materials: a review, *Biomaterials,* **17(16),** pp1553-1561.

Peppas, N. A., and Langer, R. (1994). New challenges in biomaterials, *Science,* **263**, pp1715-1720.

Peppasa, N. A., Buresa, P., Leobandunga, W. and Ichikawa, H. (2000). Hydrogels in pharmaceutical formulations, *European Journal of Pharmaceutics and Biopharmaceutics,* **50**, pp27-46.

Perka, C., Spitzer, R. S., Lindenhayn, K., Sittinger, M. and Schultz, O. (2000). *J. Biomed. Mater. Res.,* **49**, pp305.

Pieper, J. S., Hafmans, T., Veerkamp, J. H. and van Kuppevelt, T. H. (2000). Development of tailor-made collagen glycosaminoglycan matrices: EDC/NHS crosslinking, and ultrastructural aspects, *Biomaterials,* **21,** pp581-593.

Pitarresi, G., Palumboa, F. S., Giammona, G., Casadeib, M. A. and Moraccib, F. M. (2003). Biodegradable hydrogels obtained by photocrosslinking of dextran and polyaspartamide derivatives, *Biomaterials*, **24**, pp4301–4313

Pitt, C. G. (1990). The controlled parentral delivery of polypeptides and proteins. *Int J Pharm,* **59**, pp173-196.

Podual, K., Doyle III, F. J. and Peppas, N. A. (2000). Preparation and dynamic response of cationic copolymer hydrogels containing glucose oxidase, *Polymer*, **41**, pp3975–3983.

Poznansky, M. J. and Cleland, L. G. 1980. In: Juliano, R.L. (Ed.), *Drug Delivery Systems*, Oxford University Press, New York, pp253–315.

Purohit, H. J. (2003). Biosensors as molecular tools for use in bioremediation , *Journal of Cleaner Production*, **11**, pp293–301.

Putnam, A. J. and Mooney, D. J. (1996). Tissue engineering using synthetic extracellular matrices, *Nature Med*, **2**, pp824–*826*.

Qiu Y. and Park K. (2001). Environment-sensitive hydrogels for drug delivery, *Advanced Drug Delivery Reviews*, **53**, pp321–339.

Ramakrishna, S., Mayer, J., Wintermantel, E. and Leong, K. W. (2001). Biomedical applications of polymer-composite materials: a review, *Composites Science and Technology*, **61(9),** pp1189-1224.

Ratner, B. D. and Hoffman, A. S. (1976). Synthetic hydrogels for biomedical applications, in: Andrade J. D. (Ed.), *Hydrogels for Medical and Related Applications, ACS Symposium Series,* **No. 31**, American Chemical Society,Washington, DC, , pp.1–36.

Ravichandran, P. K., Shantha, L. and Panduranga Rao, K. (1997). Preparation, swelling characteristics and evaluation of hydrogels for stomach specific drug delivery, *International Journal of Pharmaceutics,* **154(1),** pp89-94.

Reinhart, C. T., Korsmeyer, R. W. and Peppas, N. A. (1981). Macromolecular network structure and its effects on drug and protein diffusion, *International Journal Pharm Technol Prod Mfr*, **2**, pp9.

Risbud , M. V., Hardikar, A. A., Bhat, S. V. and Bhonde, R. R. (2000). pH-sensitive freeze-dried chitosan–polyvinyl pyrrolidone hydrogels as controlled release system for antibiotic delivery, *Journal of Controlled Release*, **68**, pp23.

Rodemann, K. and Staude, E. (1994). Synthesis and characterization of affinity membranes made from polysulfone, *J. Membr. Sci.*, **88,** pp271.

Rowley, J. A., Madlambayan, G. and Mooney, D. J. (1999). Alginate hydrogels as synthetic extracellular matrix materials, *Biomaterials*, **20**, pp45–53.

Ruckenstein, E. and Zeng, X. F. (1997). Macroporous Chitin Affinity Membranes for Lysozyme Separation, *Biotechnol Bioeng*, **56**, pp610–617,

Ruckenstein, E. and Zeng, X. F., (1998). Albumin separation with Cibacron Blue carrying macroporous chitin/chitosan membranes., *J. Membr. Sci.*, **142**, pp13-26.

Sanchez-Chaves, M. and Arranz, F., (1997). Preparation of dextran-bioactive compound adducts by the direct esterification of dextran with bioactive carboxylic acids. *Polymer,* **38(10),** pp2501–2505.

Sato, S., Ebert, C. D. and Kim, S. W. (1983). Prevention of insulin self association and surface adsorption, *J. Pharm. Sci* ., **72,** pp228-232.

Schild, H. G. (1992). Poly(N-isopropylacrylamide): experiment, theory and application., *Prog. Polym. Sci.*, **17,** pp163-249.

Schoof, H., Apel, J., Heschel, I. and Rau, G. (2001). Control of pore structure and size in freeze-dried collagen sponges., *J Biomed Mater Res,* **58**, 352–357.

Schuhmann, W. (2002). Amperometric enzyme biosensors based on optimised electron-transfer pathways and non-manual immobilisation procedures, *Reviews in Molecular Biotechnology,* **82,** pp425-441.

Sehgal, D. and Vijay, I. K. (1994). A Method for the High Efficiency of Water-Soluble Carbodiimide-Mediated Amidation, *Anal. Biochem*, **218**, pp87-91.

Seminoff, L. A., Olsen, G. B. and Kim, S. W. (1989). A self-regulating insulin delivery system I. Characterization of a synthetic glycosylated insulin derivative, *Int. J. Pharm.*, **54**, pp241–249.

Sery, T.W. and Hehre, E.J., (1956). Degradation of dextrans by enzymes of intestinal bacteria., *J. Bacteriol.,* **71,** pp373.

Shen, F., Cui, Y. L., Yang, L. F., Yao, K. D., Dong, X. H., Jia, W. Y. and Shi, H. D. (2000). A study on the fabrication of porous chitosan/gelatin network scaffolds for tissue engineering. *Polym Int*, **49,** pp1596–1599.

Shiino, D., Murata, Y., Kataoka, K., Koyama, Y., Yokoyama, M., Okano, T. and Sakurai, Y. (1994). Preparation and characterization of a glucose-responsive insulin-releasing polymer device, *Biomaterials*, **15**, pp121–128.

Shiino, D., Murata, Y., Kubo, A., Kim, Y.J., Kataoka, K., Kataoka, Y. K., Miyazaki, H., Okano, T. and Sakurai, Y. (1994). Sensitive glucose-induced change of the lower critical solution temperature of poly (N, N-dimethylacrylamide-co-3- crylamido) phenylboronic acid in physiological saline, *Macromolecules*, **27**, pp1061–1062.

Shiino, D., Murata, Y., Kubo, Kim, A. Y. J., Kataoka, K., Koyama, Y., Kikuchi, A., Yokoyama, M., Sakurai, Y. and Okano, T. (1995). Amine containing phenylboronic acid gel for glucose-responsive insulin release under physiological pH, *J. Controlled Release,* **37**, pp269–276.

Siegel, R. A., Falamarzian, M., Firestone, B. A. and Moxley, B. C. (1988). pH-controlled release from hydrophobic/ polyelectrolyte co-polymer hydrogels, *J. Controlled Release,* **8,** pp179–182.

Sierra, D.and Saltz, R., (1996). *Surgical Adhesives and Sealants: Current Technology and Application; Technomic;* Lancaster.

Sinclair, G. W. and Peppas, N. A. (1981). Analysis of non-fickian transport in polymers using simplified exponential expressions, *Journal of Membrane Science*, **17,** pp211.

Singh, R. S., Tiwary, A. K. and Kennedy, J. F. (1999). Lectins: sources, activities and applications., *Critical Reviews in Biotechnology*, **19**, pp45-178.

Soppimath, K. S., Kulkarni, A. R. and Aminabhavi, T. M. (2001). Chemically modified polyacrylamide-g-guar gum-based crosslinked anionic microgels as pH-sensitive drug delivery systems: preparation and characterization, *Journal of Controlled Release,* **75(3),** pp331-345.

Stenekes, R. J. H. and Hennink, W. E. (1999). Equilibrium water content of microspheres based on cross-linked dextran, *International Journal of Pharmaceutics*, **189**, pp131–135

Stenekes, R. J. H., Talsma, H. and Hennink, W. E. (2001). Formation of dextran hydrogels by crystallization, *Biomaterials,* **22**, pp1891-1898.

Stubbe, B., Maris, B., den Mooter, G. V., De Smedt, S. C. and Demeester, J. (2001). The in vitro evaluation of 'azo containing polysaccharide gels' for colon delivery , *Journal of Controlled Release* , **75**, pp103–114

Stulý ka, K., Paca kova, V. and Ticha, M. (2003). Some potentialities and drawbacks of contemporary size-exclusion chromatography, *J. Biochem. Biophys. Methods*, **56**, pp1 –13.

Suen, S. Y., Chen, R. L. and Tsai, Y. D. (2000). Comparison of lysozyme adsorption to immobilized Cibacron Blue 3GA using various membrane supports, *J. Liq. Chromatogr,* **23**, pp223–239.

Suen, S. Y., Lin, S. Y. and Chin, H. C. (2000). Effects of spaces arms on Cibacron Blue 3GA immobilization and lysozyme adsorption using regenerated cellulose membrane discs, *Ind. Eng. Chem.Res.,* **39**, 478–487.

Suh, J. K. F. and Matthew, H. W. T. (2000). Application of chitosan-based polysaccharide biomaterials in cartilage tissue engineering: a review, *Biomaterials*, **21**, pp2589-2598.

Tabata, Y. and Ikada, Y. (1998). Protein release from gelatin matrices, *Advanced Drug Delivery Reviews*, **31(3),** pp287-301.

Tan, W., Krishnara, J. R and Desai, T. A. (2001), Evaluation of nanostructured composite collagen–chitosan matricies for tissue engineering. *Tissue Eng,* **7**, pp203–210.

Tang, M., Zhang, R. Bowyer, A., Eisenthal, R. and Hubble, J. (2002). An NAD-sensitive hydrogel for the release of macromolecules, *ICOM Toulouse* (Supplementary book of abstracts page 40).

Tang, M., Zhang, R. Bowyer, A., Eisenthal, R. and Hubble, J. (2003). A reversible hydrogel membrane for controlling the delivery of macromolecules, *Biotechnology & Bioengineering,* **82(1),** pp47-53.

Tanna S. and Taylor, M. J. (1994). A self-regulating system using high-molecular weight solutes in glucose-sensitive gel membranes, *J. Pharm. Pharmacol.,* **46 (Suppl. 2),** pp1051b.

Tanna S., Sahota, T., Clark, J. and Taylor, M. J. (2002), Covalent coupling of concanavalin A to a Carbopol 934P and 941P carrier in glucose-sensitive gels for delivery of insulin, *Journal of Pharmacy and Pharmacology,* **54(11):** pp1461-1469.

Tanna, S., Sahota, T. S., Clark, J., and Taylor, M. J. (2002). A covalently stabilised glucose-responsive gel formulation with a Carbopol carrier., *J. Drug Target.,* **10,** pp411- 418.

Tanna, S., Taylor, M. J. and Adams, G. (1999). Insulin delivery governed by covalently modified lectin-glucogen gels sensitive to glucose. *J Pharm.Pharmacol,* **51,** pp1093-1098.

Tanna, S., Taylor, M. J. and Adams, G. (1999). Insulin Delivery Governed by Covalently Modified Lectin-glycogen Gels Sensitive to Glucose, *The Journal of Pharmacy and Pharmacology,* **51(10),** 1093-1098.

Taylor, M. J, Tanna, S., Taylor, P. M. and Adams, G. (1995). The delivery of insulin from aqueous and non-aqueous reservoirs governed by glucose sensitive gels, *J Drug Targeting,* **3,** pp209-216.

Taylor, M. J., Tanna, S., Cockshott, S. and Vaitha, R. (1994). A self -regulated delivery system using unmodified solutes in glucose-sensitive gel membranes, *J. Pharm. Pharmacol.,* **46 (Suppl. 2),** pp1051a.

Taylor, M. J., Tanna, S., Taylor, P. M. and Adams, G. (1995). Delivery of insulin from aqueous and nonaqueous reservoirs governed by Na glucose sensitive gel membrane, *J. Drug Target.*, **3,** pp209–216.

Tedder, J. M., Nechvatal, A. and Murray, A. W. (1972). Amino acids and proteins. In: *Basic organic chemistry.* London: John Wiley & Sons, Chapter 6, pp. 305-342

Tennikova, T. B. and Svec, F., (1993). High performance membrane chromatography: highly efficient separation method for proteins in ion-exchange, hydrophobic interaction and reversed-phase modes., *J. Chromatogr.,* **646,** pp279-288.

Theenot, D. R., Toth, K., Durst, R. A and Wilson, G. S., (1999). Electrochemical Biosensors: Recommended Definitions and Classification, *Pure Appl Chem,* **71,** pp2333-2348.

Thermes, F., Grove, J., Rozier, A., Plazonnet, B., Constancis, A. and Bunel, C. (1992). Mucoadhesion of copolymers and mixtures containing polyacrylic acid., *Pharm Res*; **9(12),** pp1563–1567.

Thommes, J. and Kula, M. R. (1995). Membrane Chromatography-An Integrative Concept in the Downstream Processing of Proteins: REVIEW, *Biotechnol. Prog.*, **11**, pp357-367.

Tomihata K. and Ikada, Y. (1997). Crosslinking of hyaluronic acid with water-soluble carbodiimide, *J Biomed Mater Res*, **37**, pp243–251.

Tong, X. D., Dong, X. Y. and Sun, Y. (2002). Lysozyme adsorption and purification by expanded bed chromatography with a small-sized dense adsorbent, *Biochemical Engineering Journal,* **12,** pp117–124.

Trudel, J. and Massia, S. P. (2002). Assessment of the cytotoxicity of photocrosslinked dextran and hyaluronan-based hydrogels to vascular smooth muscle cells, Biomaterials, 23(16), pp3299-3307.

Turner. A. P. F, (2000). Biosensors--Sense and Sensitivity, *Science,* **290**, pp1315-1317.

Van Dijk-Wolthuis W. N. E., Franssen, O., Talsma, H., Van Steenbergen, M. J., Kettenes-Van Den Bosch, J. J. and Hennink, W. E. (1995). Synthesis, characterization and polymerization of glycidyl methacrylate derivatized dextran, *Macromolecules*, **28**, pp6317–6322.

Van Dijk-Wolthuis W. N. E., Franssen, O., Talsma, H., Van Steenbergen, M. J., Kettenes-Van Den Bosch, J. J. and Hennink, W. E. (1997). Reaction of dextran with glycidyl methacrylate: an unexpected transesterification, *Macromolecules*, 30, pp3411–3413.

van Dijk-Wolthuis, W. N. E., Hoogeboom, J. A. M., van Steenbergen, M. J., Tsang S. K.Y. and Hennink, W. E. (1997). Degradation and release of dextran-based hydrogels, *Macromolecules*, **30**, pp4639 – 4645.

van Dijk-Wolthuis, W. N. E., Hoogeboom, J. A. M., van Steenbergen, M. J., Tsang S. K.Y. and Hennink, W. E. (1997). Reaction of dextran with glycidyl methacrylate:an unexpected transesterication, *Macromolecules,* **30,** pp3411-3418.

van Dijk-Wolthuis, W. N. E., Hoogeboom, J. A. M., van Steenbergen, M. J., Tsang S. K.Y. and Hennink, W. E. (1995). Synthesis, characterization and polymerization of glycidyl methacrylate derivatized dextran, *Macromolecules*, **28** pp6317-6323.

van Reis, R. and Zydne, A. (2001). Membrane separations in biotechnology, *Current Opinion in Biotechnology,* **12**, pp208–211.

Vandamme, Th. F., Lenourry, A., Charrueau, C. and Chaumeil, J. C. (2002). The use of polysaccharides to target drugs to the colon, *Carbohydrate Polymers,* **48**, pp219-231.

Vollhardt, K. P. C. and Schore, N. E. Editors, (1987). *Organic chemistry.* New York: W. H. Freeman and Company; pp776–777.

Wang N. S. Experiment No. 7b *Enzyme Immobilisation Protocol-Entrapment in Alginate* Gel. http://www.glue.umd.edu/~nsw/ench485/lab7b.htm (access in July, 2003)

Wang, W. K., Lei, S. P., Monbouquette, H. G. and McGregor, W. C., (1995). Membrane adsorber process development for the isolation of a recombinant immunofusion protein., *BioPharm.*, **June**, 52-59.

Wang, X. H., Li, D. P., Wang, W. J., Feng, Q. L., Cui, F. Z., Xu, Y. X., Song X. H. and van der Werf, M. (2003). Crosslinked collagen/chitosan matrix for artificial livers, *Biomaterials,* **24(19),** pp3213-3220.

Wichterle, O. and Lim, D. (1960). Hydrophilic gels for biological use, *Nature*, **185**, pp117–118.

Wissink, M. J. B., Beernink, R., Pieper, J. S., Poot, A. A., Engbers, G. H. M., Beugeling, T., van Aken W. G. and Feijen, J. (2001). Immobilization of heparin to EDC/NHS-crosslinked collagen. Characterization and in vitro evaluation, *Biomaterials,* **22(2),** pp151-163.

Wissink, M. J. B., Beernink, R., Pieper, J. S., Poot, A. A., Engbers, G. H. M., Beugeling, T., van Aken W. G. and Feijen, J. (2001). Binding and release of basic fibroblast growth factor from heparinized collagen matrices, *Biomaterials*, **22(16),** pp2291-2299.

Wissink, M. J. B., Beernink, R., Pieper, J. S., Poot, A. A., Engbers, G. H. M., Beugeling, T., van Aken W. G. and Feijen, J. (2000). Endothelial cell seeding of (heparinized) collagen matrices: effects of bFGF pre-loading on proliferation (after low density seeding) and pro-coagulant factors, *Journal of Controlled Release*, **67(2-3)**, pp141-155.

Wissink, M. J. B., Beernink, R., Pieper, J. S., Poot, A. A., Engbers, G. H. M., Beugeling, T., van Aken, W. G. and Feijen, J. (2001). Immobilization of heparin to EDC/NHS-crosslinked collagen. Characterization and in vitro evaluation, *Biomaterials*, **22,** pp151-163

Wissink, M. J. B., Beernink, R., Poot, A. A., Engbers, G. H. M., Beugeling, van Aken, T. W. G. and Feijen, J. (2000). Improved endothelialization of vascular grafts by local release of growth factor from heparinized collagen matrices, *Journal of Controlled Release,* **64(1-3)**, pp103-114.

Yamamoto, N., Kurisawa, M. and Yui, N. (1996). Double stimuli-responsive degradation based on phase separation of interpenetrating polymer networks consisting of gelatin and dextran, *Macromol. Rapid Commun.*, **17**, pp313-318.

Yang, L., Chu, J. S. and Fix, J. A. (2002). Colon-specific drug delivery: new approaches and in vitro/in vivo evaluation International, *Journal of Pharmaceutics* **235**, pp1–15.

Yang, L., Hsiao, W. W. and Chen., P. (2002). Chitosan–cellulose composite membrane for affinity purification of biopolymers and immunoadsorption, *Journal of Membrane Science,* **197**, pp185–197.

Yang, S., Leong, K. F., Du, Z. and Chua, C. K. (2001). The design of scaffolds for use in tissue engineering. Part I. Traditional factors., *Tissue Eng.*, **7,** pp679–89.

Yildiz, B., Belma, I. and Ki, M. (2002). Thermoresponsive poly(N-isopropylacrylamide-co-acrylamide-co-2-hydroxyethyl methacrylate) hydrogels, *Reactive and Functional Polymers*, **52(1)** pp3-10

Yu, Q., Bauer, J. M. and Moore, J. S. (2001). Responsive biomimetic hydrogel valve for microfluidics, *APPLIED PHYSICS LETTERS*, **78(17),** pp2589-2591

Yu, Y. H., Xue, B. and Sun, Y. (2001). Dye-ligand poly(GMA-TAIC-DVB) affinity adsorbent for protein adsorption, *Bioprocess and Biosystems Engineering*, **24**, pp25-31

Zeeman, R., Dijkstra, P. J., van Wachem, P. B., van Luyn, M. J. A., Hendriks, M., Cahalan, P. T. and Feijen, J. (1999). Successive epoxy and carbodiimide cross-linking of dermal sheep collagen, *Biomaterials,* **20(10),** pp921-931

Zeng, X. and Ruckenstein, E. (1996). Supported chitosan–dye affinity membranes and their protein adsorption, *J. Membr. Sci.,* **117**, pp271.

Zeng, X. F. and Ruckenstein, E. (1998). Cross-linked macroporous chitosan anion-exchange membranes for protein separation. *J. Membr. Sci.,* **148,** pp195-205.

Zeng, X. F. and Ruckenstein, E. (1998). Trypsin purification by paminobenzamidine immobilized on macroporous chitosan membrane. *Ind. Eng. Chem. Res.,* **37**, pp159-165.

Zeng, X. F. and Ruckenstein, E. (1999). Macroporous chitin affinity membranes for wheat germ agglutinin purification from wheat germ, *J. Membr. Sci.*, **156,** pp 97-107.

Zeng, X. F. and Ruckenstein, E. (2000). Membrane chromatography: preparation and applications to protein separation, *Biotechnol Prog*, **15,** pp1003-1019.

Zhang, S. P. and Sun, Y. (2001). Further Studies on the Contribution of Electrostatic and Hydrophobic Interaction to Protein Adsorption on Dye-Ligand Adsorbents, *Biotechnology and Bioengineering,* **75(1),** pp710-717.

Zhang, S. P. and Sun, Y. (2002). Ionic Strength Dependence of Protein Adsorption to Dye-Ligand Adsorbents, *Bioengineering, Food, and Natural Products*, **48(1),** pp178-186.

Zhao, L., Mitomo, H., Nagasawa, N., Yoshii, F. and Kume, T. (2003). Radiation synthesis and characteristic of the hydrogels based on carboxymethylated chitin derivatives, *Carbohydrate Polymers*, **51(2),** pp169-175.

Appendix

The standard curves of diffusant used in experiment.

All data were attained using SHIMADZU UV-visible Spectrophotometer (1601). The standard curve was created automatically by UV-probe software (version 1.01). The operation was done at 25 °C.

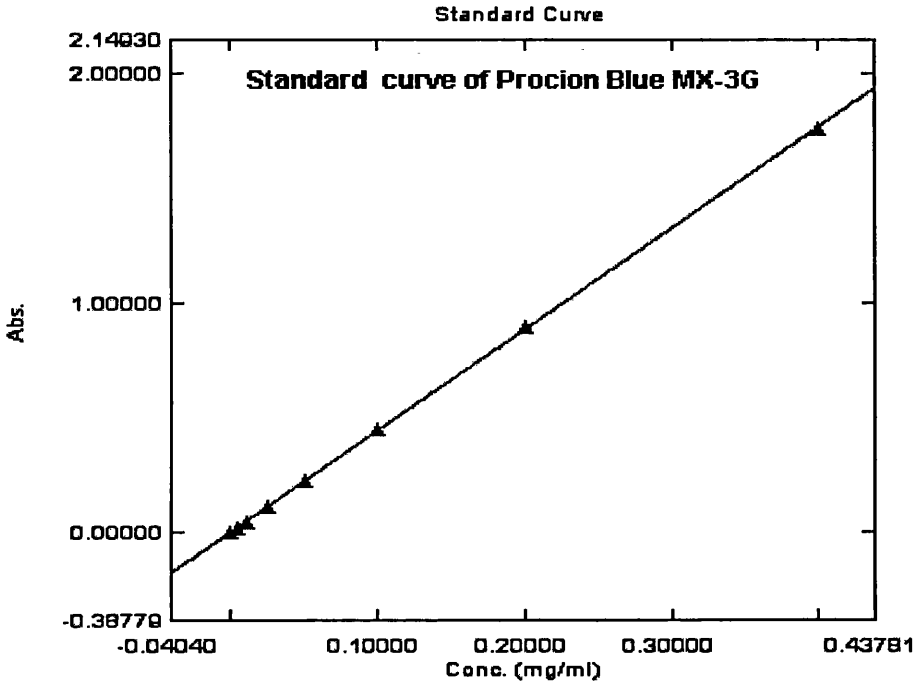

x = 0.22619 y - 0.00051
r2 Correlation Coefficient = 0.99991
Standard Error of Estimate = 0.00144

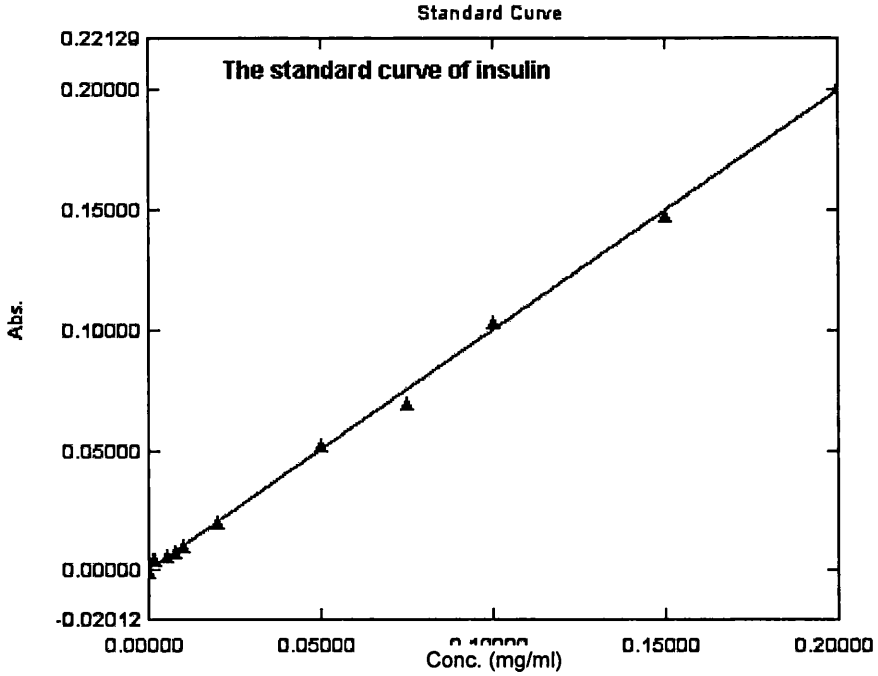

y = 0.99275 x + 0.00081
r2 Correlation Coefficient = 0.99882
Standard Error of Estimate = 0.00239

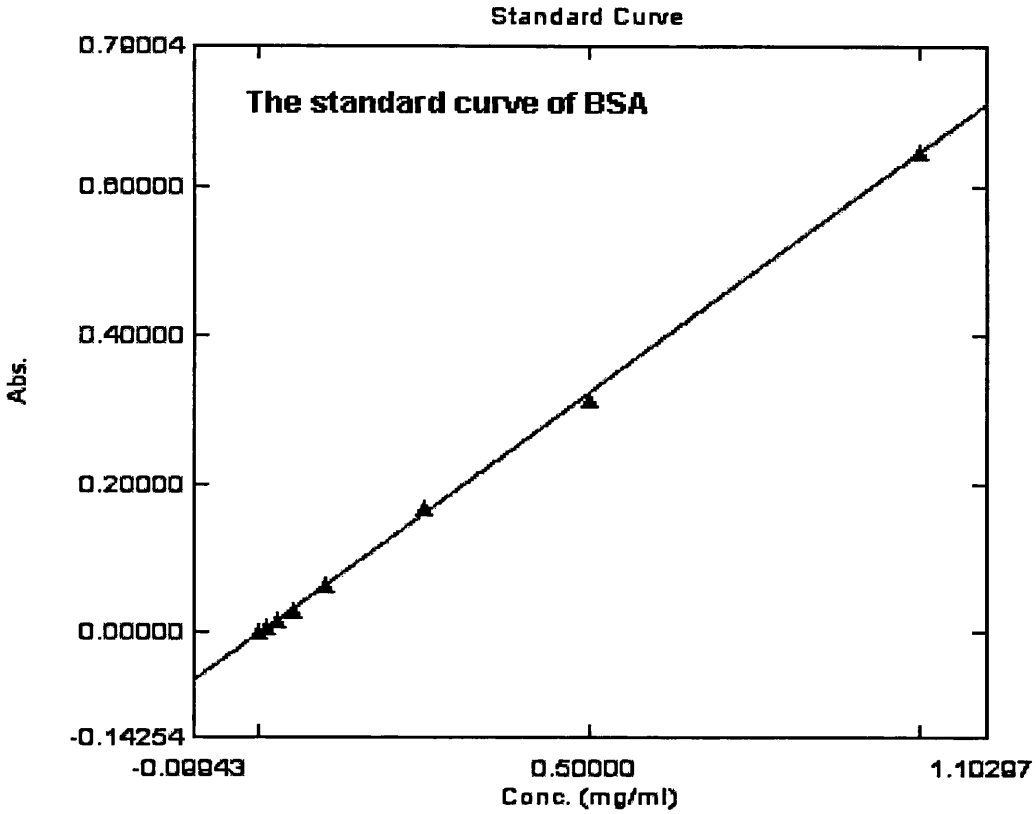

x = 1.54719 y + 0.00087
r2 Correlation Coefficient = 0.99959
Standard Error of Estimate = 0.00761

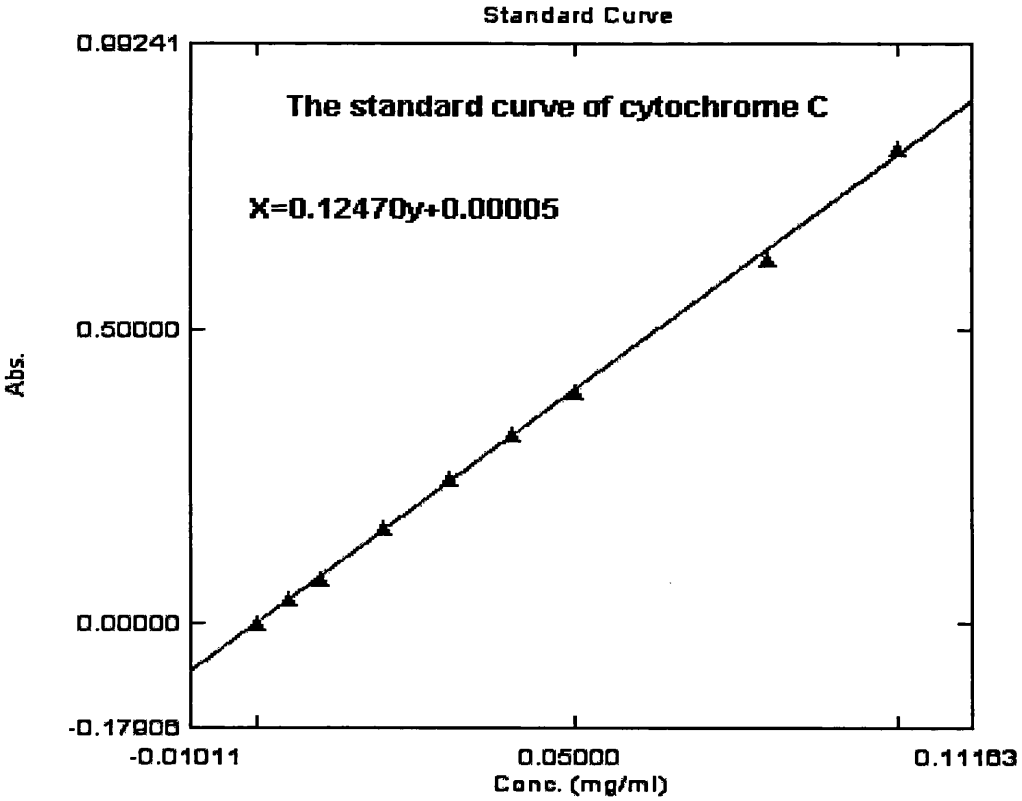

r2 Correlation Coefficient = 0.99884
Standard Error of Estimate = 0.00125

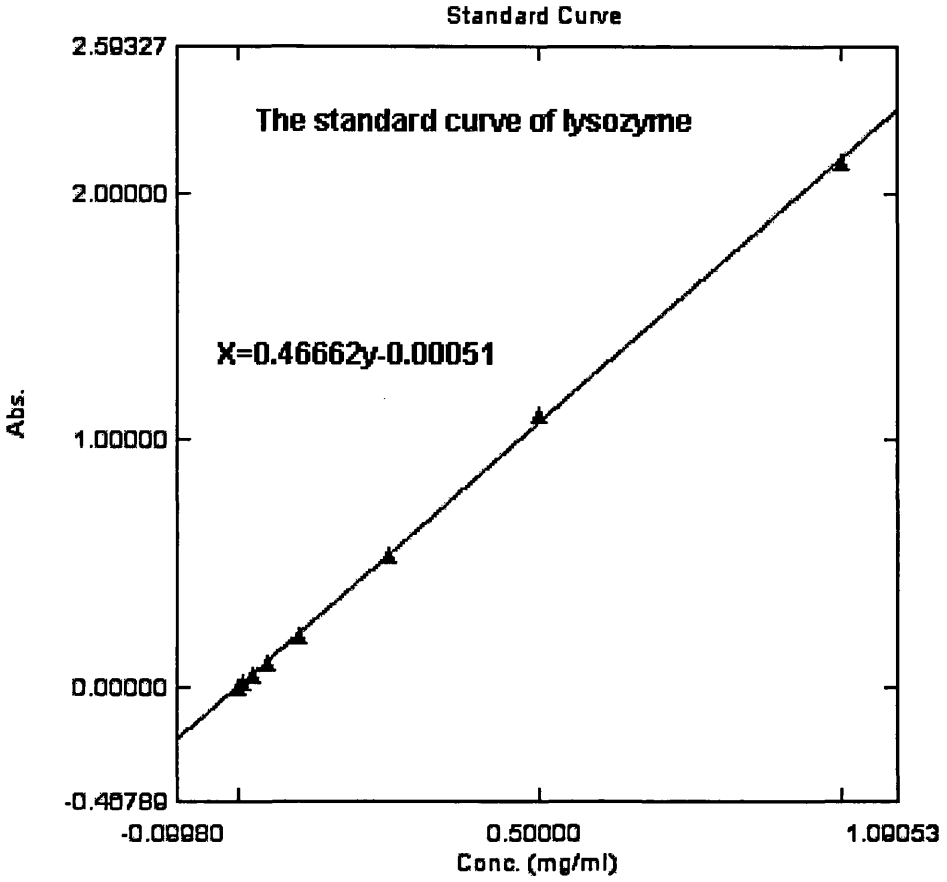

r2 Correlation Coefficient = 0.99965
Standard Error of Estimate = 0.00712

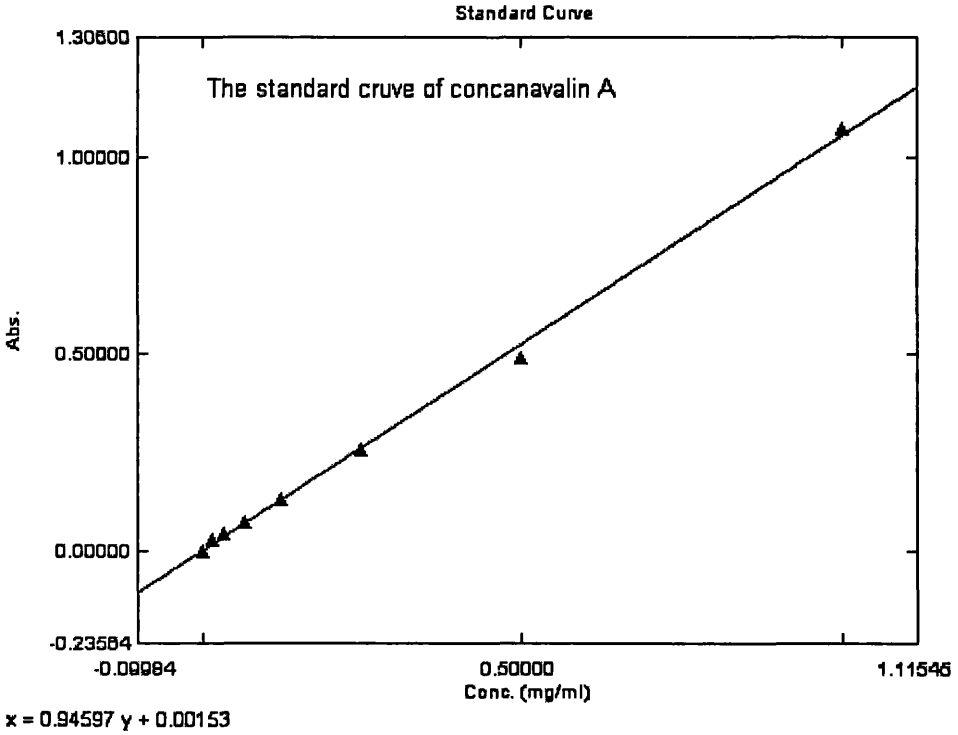

x = 0.94597 y + 0.00153
Standard Error of Estimate = 0.01553
Residual Standard Deviation = 0.01438

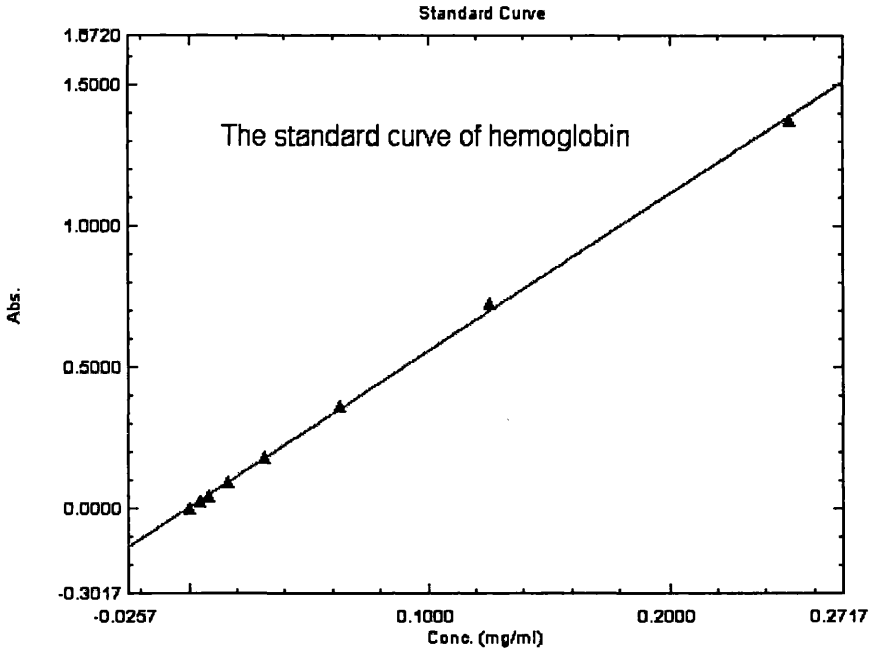

x = 0.18083 y - 0.00092
Standard Error of Estimate = 0.00246
Residual Standard Deviation = 0.00228

A Reversible Hydrogel Membrane for Controlling the Delivery of Macromolecules

M. Tang,[1] R. Zhang,[1] A. Bowyer,[2] R. Eisenthal,[3] J. Hubble[1]

[1]Department of Chemical Engineering, University of Bath, Claverton Down, Bath BA2 7AY, United Kingdom; telephone: + 44 1225 386221; fax: + 44 1225 386491; e-mail: j.hubble@bath.ac.uk
[2]Department of Mechanical Engineering, University of Bath, United Kingdom
[3]Department of Biology and Biochemistry, University of Bath, United Kingdom

Received 15 April 2002; accepted 5 September 2002

DOI: 10.1002/bit.10539

Abstract: Glucose-sensitive hydrogel membranes have been synthesized and characterized for their rate-of-delivery of macromolecules. The mechanism for changing this rate is based on variable displacement of the affinity interaction between dextran and concanavalin A (con A). Our main objective was to characterize the diffusion of model proteins (insulin, lysozyme, and BSA) through the membrane, in response to changes in environmental glucose concentrations. Membranes were constructed from crosslinked dextrans to which con A was coupled via a spacer arm. Changes in the porosity of the resulting hydrogel in the presence of glucose led to changes in the diffusion rate observed for a range of proteins. Gels of specified thickness were cast around to nylon gauze support (pore size, 0.1 mm) to improve mechanical strength. Diffusion of proteins through the gel membrane was determined using a twin-chamber diffusion cell with the concentrations being continuously monitored using a UV-spectrophotometer. Changes in the transport properties of the membranes in response to glucose were explored and it was found that, while 0.1*M* D-glucose caused a substantial, but saturateable, increase in the rates of diffusion of both insulin and lysozyme, controls using glycerol or L-glucose (0.1*M*) had no significant effect. Sequential addition and removal of external glucose in a stepwise manner showed that permeability changes were reversible. As expected, diffusion rates were inversely proportional to membrane thickness. A maximum increase in permeability was observed at pH 7.4 and at 37°C. The results demonstrate that this hydrogel membrane functions as a smart material allowing control of solute delivery in response to specific changes in its external environment. © 2003 Wiley Periodicals, Inc. *Biotechnol Bioeng* **82**: 47–53, 2003.

Keywords: affinity; membrane; responsive; lectin; insulin; biopolymer; release

Correspondence to: John Hubble
Contract grant sponsor: BBSRC; University of Bath
Contract grant number: 86/E12129

INTRODUCTION

In many clinical situations, controlled drug delivery systems, that deliver drugs at a predetermined rate, are replacing conventional drug formulations. However, in the case of diabetes mellitus, there is currently no entirely effective system for continuously controling blood glucose levels. The treatment of insulin-dependent diabetes requires the provision of insulin in response to increases in blood glucose concentration. Although a conventional oral route would be preferred, this is not practical for the systemic delivery of peptide and protein drugs, including insulin (Hinchcliffe and Illum, 1999). The consequent required daily injection of insulin may cause discomfort, and can lead to a number of the longterm complications associated with diabetes mellitus such as retinal damage and cardiovascular disease. Therefore, an insulin-delivery system capable of mimicking the pancreas and delivering insulin in response to increases in blood glucose would be highly attractive (Pitt, 1990).

The specific interactions between plant lectins with carbohydrates have been used to study the molecular basis of a range of biological recognition events (Loris et al., 1998; Singh et al., 1999). Such mechanisms have also been evaluated for use in drug delivery systems based on responding to chemical and biochemical stimuli, including pH, changes in specific ion concentration, and specific molecular recognition events (Qiu and Park, 2001). One approach is the development of a self-regulated insulin delivery system based on glucose-sensitive hydrogels capable of regulating the delivery of insulin in response to changes in blood glucose levels. Several such systems have been developed (Galaev and Mattiason, 1999; Qiu and Park, 2001), including pH-sensitive membrane systems, and two con-A based systems.

In the first approach, immobilized con A is used to control the delivery of a glycosylated insulin, which is initially bound by the con A. Interaction of environmental glucose

with the glycosylated insulin-con A complex leads to the displacement of glycosylated insulin (Brownlee and Cerami, 1979). A more recent approach has been the use of con-A/dextran mixtures to form a reversible sol-gel system (Obaidat and Park, 1997; Taylor et al., 1995; Tanna et al., 1999). In this system, a glucose-based polymer is mixed with con A to form a hydrogel, which is sandwiched between two porous membranes (Obaidat and Park, 1997; Tanna et al., 1999; Taylor et al., 1995). Gelation is reversible in response to changes in environmental glucose concentration such that the diffusion coefficient for insulin changes with degree of gelation. In earlier work, the gels were based solely on soluble components. However, leakage of con A through the membrane during del-sol transition led to revised systems with con A coupled to the polymer.

While reducing leakage, coupling of con A to the polymer still results in a system that is in a soluble form in the presence of glucose (Kim and Park, 2001; Tanna et al., 1999). Thus, support membranes are still required, leading to increased complexity and slow diffusion rates. To overcome these problems we report the synthesis of a mechanically stable, glucose responsive hydrogel membrane, which can be cast in a number of mechanical forms.

Our polymer is produced by crosslinking two dextrans with different molecular weights. The smaller dextran is functionalized with covalently grafted conA. This material is mixed with the larger, nonfunctionalized dextran, allowing easy control of the overall amount of grafted conA in the material. The affinity of ConA for dextran provides additional affinity crosslinks which are competitively inhibited by free glucose, resulting in a decrease in total crosslink density and increase in permeability to protein.

This is conceptually similar to the work of Miyata et al. (1999), who describe an antibody/antigen-based gel that swells in response to the free antigen. However, the use of the two dextran species allows greater control over the gel structure such that property changes can be restricted to changes in internal porosity. In this case the porosity increases because of the displacement of con-A/dextran interactions by the stimulus of soluble D-glucose.

To achieve this goal, gels were formed via a nucleophilic replacement reaction in a triazine ring, such that both gel formation and con-A fixation occurred in the same step of synthesis. A specific requirement of gel synthesis was to maintain the reaction pH below 9 to minimize con-A inactivation during coupling. In the results presented here, we demonstrate a material that is mechanically stable, changes permeability in response to changes in glucose concentration, and that shows negligible con-A leakage over extended periods.

MATERIALS AND METHODS

Materials

Dextran 40,000, dextran 500,000, divinyl sulfone, ethylenediamine, cyanuric chloride, concanavalin A (type IV from the jack bean), insulin, lysozyme, and BSA were obtained from Sigma-Aldrich, UK. All other chemicals were of reagent grade and obtained from BDH chemicals Ltd., UK.

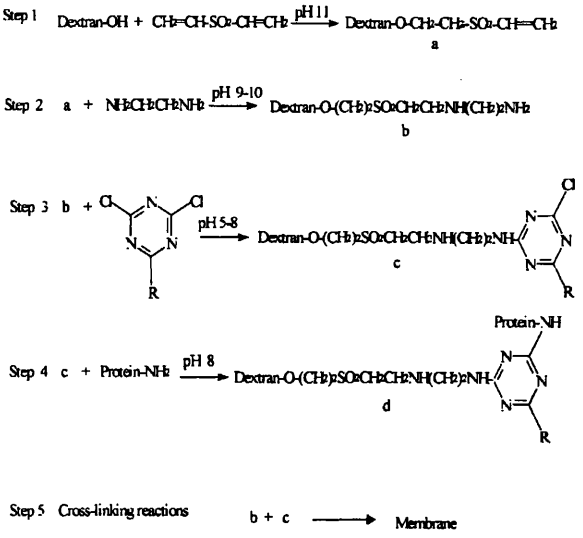

Figure 1. Synthetic route for the synthesis of concanavalin.

Smart Membrane Synthesis

The chemistry of hydrogel synthesis is shown in Figure 1. The procedure was as follows:

1. 10 g dextran was dissolved in 150 mL water, 0.795 g Na_2CO_3 was added, followed by the addition of 1.2 mL 97% divinyl sulfone. This was allowed to react at 18°C for 60 min, prior to the addition of 2.74 g ethylenediamine. The reaction was then allowed to proceed for 48 h after which the reaction mixture was dialyzed extensively against distilled water. The final dextran derivative solution was freeze-dried and then redissolved in distilled water to give a 14% dextran solution.
2. 20 mL solution of the dextran derivative was mixed with 0.17 g cyanuric chloride and allowed to react at room temperature for 24 h. The solution was centrifuged for 20 min at 4000 rpm at 4°C, and the supernatant was recovered. (The dextran derivative made with this procedure using a 40,000 mw dextran will be referred to as Solution A; the dextran derivative made using 500,000 mw dextran will be referred to as Solution B.)
3. 0.8 g of Solution A, 0.8 g of Solution B, 0.5 mL 0.8*M* $NaHCO_3$ and 40 mg con A (in 1.2 mL water) containing 1 mg $CaCl_2$ and 1.2 mg $MnCl_2$ were added and mixed fully. After mixing for 10 min, the solution was degassed and cast on a nylon gauze support (pore size 0.1 mm, thickness of 0.05 mm) between two glass plates using spacers to give the required total membrane thickness.

Gelation was allowed to proceed at 25°C for 16 h before the membrane was removed from the casting plates. The membrane was washed twice in distilled water and immersed overnight in 10 m*M* glycine solution in 20 m*M* acetate buffer, pH 6.0, containing 50 m*M* NaCl and 0.1% NaN_3 at 4°C. Finally, the gel was washed with distilled water twice and stored in 20 m*M* Tris buffer, pH 7.4, containing 1 m*M* $CaCl_2$, 1 m*M* $MnCl_2$, 50 m*M* NaCl, and 0.1% NaN_3, until it was used.

Protein Diffusion Experiments

The diffusion of model proteins (including insulin: mw 5800, lysozyme: mw 12400, and BSA: mw 66000) through the gel membranes was examined in a diffusion cell consisting of donor and receptor chambers with equal volume (4.4 mL), and with a surface area of 4.6 cm^2 available for diffusion. The gel membrane was mounted between the two chambers of the diffusion cell, and equilibrated with 20 m*M* Tris storage buffer as above. The donor chamber was connected to a protein reservoir through a pump. The receptor chamber was connected via a closed loop recycle through a flow cell mounted in the spectrophotometer (Shimadzu, UV-1601). The diffusion of the protein was continuously measured from absorbance changes at 280 nm logged to a computer. The effect of putative transport-enhancing agents was investigated by varying the composition of the donor buffer such that protein concentration remained constant.

For the experiments with insulin, the protein (from Bovine Pancreas, Sigma) was dissolved in a small amount of 0.05 N HCl and then adjusted at pH 7.4 with 0.05 N NaOH, and finally diluted with Tris buffer to give an insulin concentration of 2.0 mg/mL. In all experiments using insulin, urea was added to a final concentration of 2.0 mg/mL to inhibit insulin aggregation (Sato et al., 1983). Concentration-time courses were determined from absorbance changes using a conversion factor determined from a standard curve constructed using known insulin concentrations. For experiments with lysozyme and BSA, proteins were dissolved directly in Tris buffer to a concentration of 2.0 mg/mL. In each case the concentrations observed in the diffusion experiments were determined using calibration data from standard curves prepared using the specific protein.

RESULTS

Specificity Assessment

The specificity of the hydrogel membrane was determined using D-glucose, L-glucose, and glycerol. While D-glucose is specifically bound by con A, L-glucose and glycerol do not interact with it. Hence, membrane permeability changes would be expected in response to D-glucose, but not L-glucose or glycerol. Figure 2 shows the diffusion curves of insulin in response to glucose, L-glucose, or glycerol through a 0.4 mm membrane. In control experiments, where insulin solution without carbohydrate/glycerol was used little diffusion was observed. When L-glucose or glycerol was added to the protein reservoir of the donor side (final concentration 0.1*M*), there was a small increase in the diffusion rate in the initial stages, after which the profile mirrored that observed for the control. After a stabilizing period of 42 min D-glucose (0.1*M*) was added. Then, after a lag of about a further 18 min, there was a substantial increase in diffusion rate which was maintained for an extended period. The lag between addition and response matches the residence time in the donor cell such that diffusion limitations will be partially masked by the time course of D-glucose increase in the liquid phase.

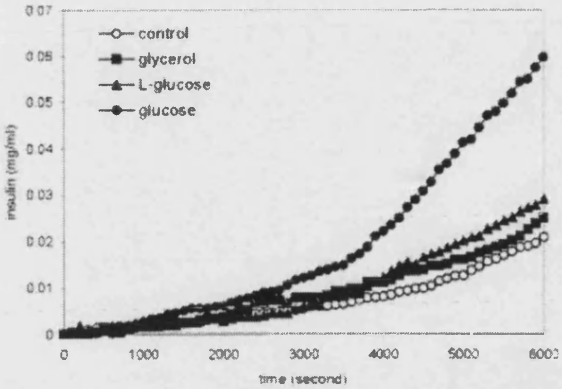

Figure 2. Insulin (2 mg/mL) diffusion curves in response to 0.1*M* D-glucose (●). L-glucose (■), or glycerol (▲). The control was carried out with insulin only (○). Putative activators were added at 2500 s. Measurements were conducted at 25°C.

The results show that the hydrogel membrane allows protein transport at a rate that is controllable using a soluble effector molecule, and that this effect is limited to molecules recognized by the con A receptor. This suggests that, as anticipated, changes in porosity of the membrane where dextran serves as both a ligand for con A affinity and a structural matrix results from a reduction of internal affinity crosslinks when a soluble competitor is introduced. It is also implicit in this result that a significant fraction of the total con A is not inactivated during membrane synthesis.

Effect of D-Glucose Concentration

Three proteins of different molecular sizes, insulin, lysozyme, and BSA, were used to examine the effect of glucose concentration on diffusion rates. Figure 3 shows the diffusion of insulin in response to changes in glucose concentrations over the range 0–200 mM. In these experiments, membranes were pre-incubated with protein (with or without glucose) in the donor side of the cell to minimize subsequent lag times. The diffusion rate obtained as a function of glucose concentration are shown in Figure 3.

These experiments were repeated with two progressively

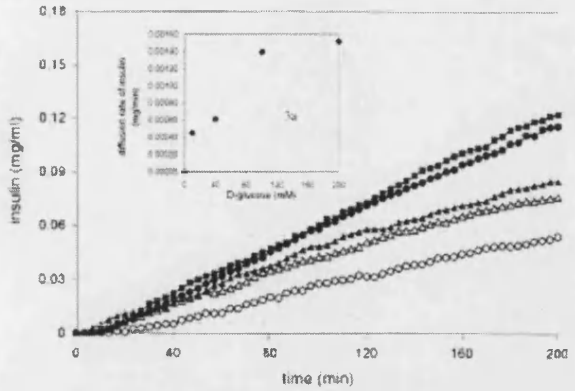

Figure 3. Insulin (2 mg/mL) diffusion in response to D-glucose concentration: 0 m*M* (control, ○), 10 m*M* (△), 40 m*M* (▲), 100 m*M* (●) or 200 m*M* (■). Glucose was added to the donor reservoir. Temperature 25°C. (a) The rate of insulin diffusion as a function of D-glucose concentration.

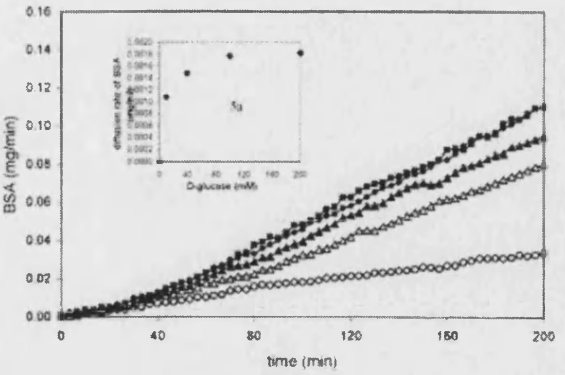

Figure 5. BSA (2.0 mg/mL) diffusion in response to D-glucose. Symbols as for Figure 5. Glucose was added to the donor reservoir. Temperature 25°C. (a) The rate of BSA diffusion as a function of glucose concentration.

larger proteins. Studies with lysozyme gave essentially similar results (Fig. 4). As might be expected from the higher molecular weight the diffusion in the absence of glucose was lower than that observed for insulin. However, glucose has a more pronounced effect on diffusion rates at low concentrations and shows a lower saturation value than that observed with insulin (Fig. 4). Results obtained with BSA are shown in Figure 5. Again, diffusion is sensitive to changes in glucose concentration with 100 m*M* glucose leading to a 3.5-fold increase in the rate of BSA diffusion. BSA diffusion in response to glucose is shown in Figure 5.

Reversibility of Glucose Effects

A series of experiments was conducted with each of the test proteins in which two reservoir solutions were used alternately: protein, and then protein containing 0.1*M* glucose. Results for insulin are shown in Figure 6. The donor solution was sequentially switched between glucose-containing and non-glucose-containing solutions as indicated by arrows on the plot. The response shows that, while there is a diffusion time lag between each solution change, the introduction and removal of glucose causes a reversible switch between lower and higher diffusion rates. Similar results obtained for lysozyme are shown in Figure 7, and for BSA in Figure 8. Again, the reversibility of the glucose effect on diffusion rate is clearly demonstrated.

Temperature, pH, and Membrane Thickness Effects

Diffusion experiments were conducted using a 0.4 mm membrane at 5°, 25°, and 37°C using lysozyme as the test

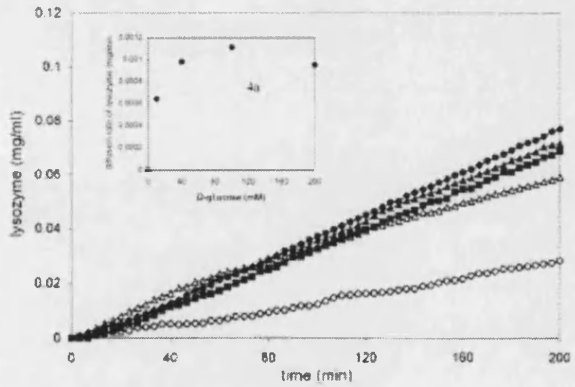

Figure 4. Lysozyme (2 mg/mL) diffusion in response to D-glucose. Symbols as for Figure 3. Glucose was added to the donor reservoir. Temperature 25°C. (a) The rate of lysozyme diffusion as a function of glucose concentration.

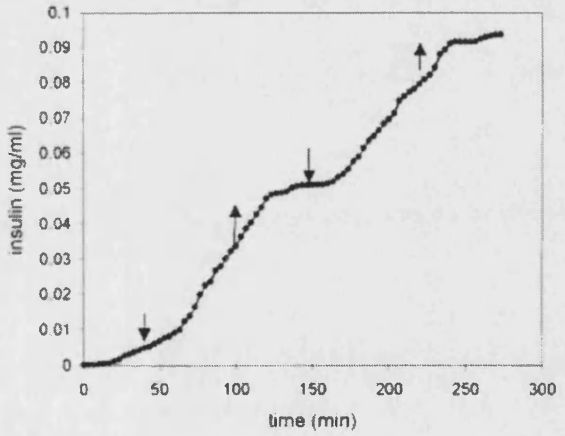

Figure 6. Reversibility of D-glucose effects on insulin diffusion. 0.1*M* glucose plus insulin (2.0 mg/mL) was added at (down-arrows): 42 min and 150 min. Insulin solutions without glucose were added at (up-arrows): 100 min and 225 min. Temperature 25°C.

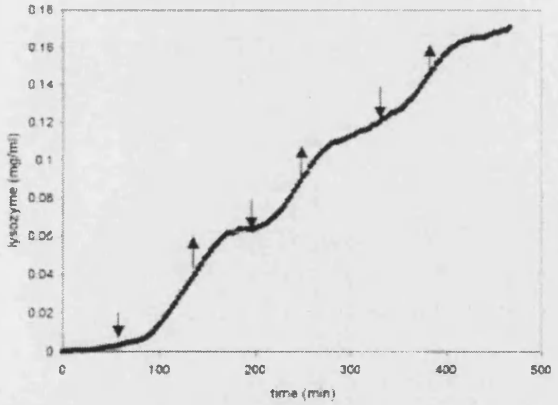

Figure 7. Reversibility of D-glucose effects on lysozyme diffusion. 0.1*M* glucose plus insulin (2.0 mg/mL) was added at (down-arrows): 65 min, 200 min, and 335 min. Lysozyme solutions without glucose were added at (up-arrows) 140 min, 250 min, and 383 min. Temperature 25°C.

protein. Glucose was introduced after 100 min. Results shown in Figure 9 confirm that diffusion rates increase with temperature between 5° and 25°, but that little additional increase is observed between 25–37°. It would appear that there is a slightly greater effect on specific transport compared with the nonspecific component.

Experiments with different gel thickness (Fig. 9b) show that diffusion rate decreases with increasing membrane thickness, as expected from Fick's law. More importantly, the fractional increase in diffusion rate obtained when glucose is introduced appears inversely proportional to membrane thickness.

Figure 9c shows pH effects over the range 5.4–8.4. This shows an optimum response at pH 7.4.

DISCUSSION

In undertaking this project, our goal was to produce a chemically and mechanically stable membrane capable of

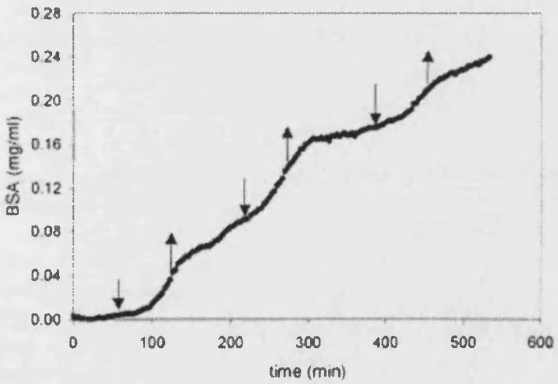

Figure 8. Reversibility of D-glucose effects on BSA diffusion. 0.1*M* glucose plus BSA (2.0 mg/mL) was added at (down-arrows): 67 min, 222 min, and 385 min. BSA solutions without glucose were added at (up-arrows): 125 min, 283 min, and 467 min. Temperature 25°C.

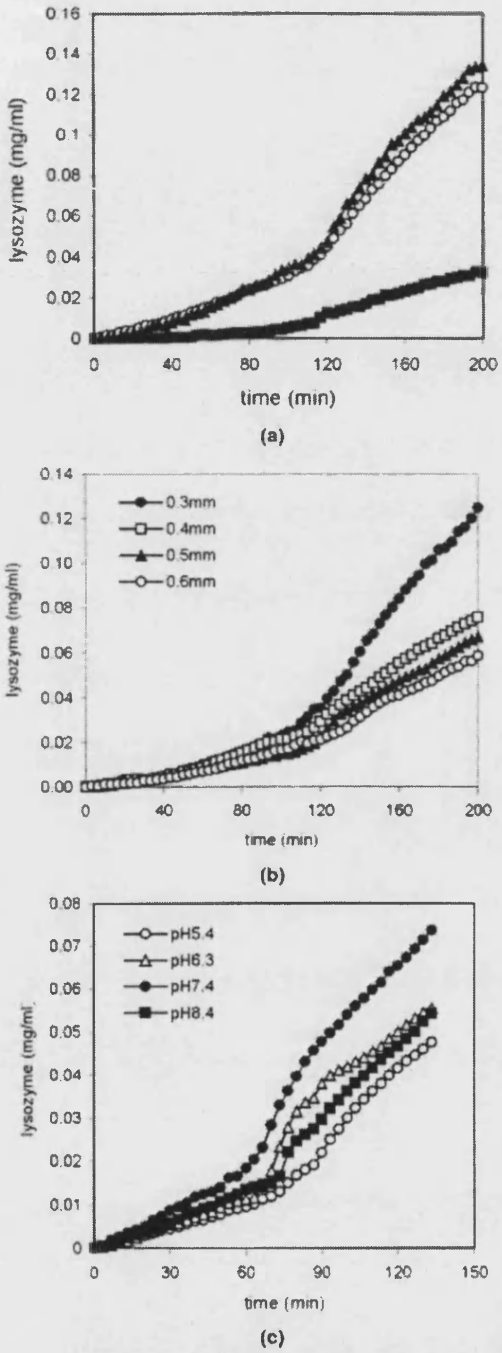

Figure 9. (a) Effects of temperature on the diffusion of lysozyme (2.0 mg/mL). 0.1*M* D-glucose was added to the donor reservoir 100 min. Temperatures 5°C (■), 25°C (○), and 37°C (▲). (b) Effects of membrane thickness on the diffusion rate of lysozyme (2 mg/mL). D-glucose (0.1*M*) was added to the donor reservoir at 100 min. Temperature 25°C. (c) Effects of pH on the diffusion rate of lysozyme (2 mg/mL). D-glucose (0.1*M*) was added to the donor reservoir at 50 min. Temperature 25°C.

specific permeability changes in response to concentration changes in external metabolites. While generic in scope, the initial application envisaged was the controlled release of insulin in response to D-glucose concentration.

Initial experiments to assess the mechanical stability of pre-cast membranes showed no evidence of dissolution over a 1-week incubation period in storage buffer. Assays of buffer composition showed no evidence of con A leakage during this period.

The first phase of characterization studies aimed to establish: (1) that permeability as evidenced by protein diffusion, could change in response to concentration changes in D-glucose concentration, and (2) that this effect was specific. The results presented in Figure 2 confirm that this is the case. While it is apparent that the porosity of the gel does not totally exclude insulin, the addition of D-glucose results in a threefold increase in diffusion rate. While there is a very slight increase observed with the addition of L-glucose and glycerol this probably results from a nonspecific chemical effect modifying the degree of gel swelling.

Similar experiments with a hydrogel membrane synthesized with BSA instead of con A failed to show any significant increase in diffusion when glucose was applied. This confirms that changes in the porosity of the gel membrane resulting from the dissociation of affinity crosslinks led to changes in protein diffusion. Previous reports (Ballerstadt and Schultz, 1998; Miyata et al., 1999), suggest the diffusion of glucose through hydrogels will be slower than the dissociation of con A/dextran affinity crosslinks. As proteins have lower diffusivities than sugars, the response will be determined by the diffusivity of the protein in the dissociated gel membrane. Similar specific increases in diffusion rate were observed with mannose, which is also known to bind to con A.

The effect of D-glucose concentration on the diffusion of three different-sized proteins is shown in Figures 3, 4, and 5. The inset figures show transport rate as a function of D-glucose concentration, and indicate a half-saturation constant between 40–60 m*M*. This is consistent with the displacement of a weak affinity interaction. As the size of the protein increases, the ratio of competitor induced to background diffusion also increases. This suggests that, in addition to optimizing the base level of affinity plus covalent crosslinks to ensure zero background diffusion, porosity should also be optimized with respect to maximizing competitor-induced transport.

As our goal is to make a responsive material suitable for drug delivery applications, reversibility of the selective response is an essential requirement. The results reported in Figures 6, 7, and 8, where D-glucose was sequentially added and removed, clearly show that the con-A/dextran membrane meets this requirement. Reversible responses were found with all three proteins tested.

The affinity displacement of an interaction between con A and an immobilized ligand is clearly attractive for an insulin delivery application, but it also has the specific advantage that the displaced ligand also forms part of the gel matrix. However, in the two-component synthesis protocol described here, the larger dextran might be regarded as acting as the matrix and the smaller, pendant, dextran as the ligand. In an analogous system, Miyata et al. (1999) report the synthesis of an antigen–antibody hydrogel membrane where goat anti-rabbit IgG and rabbit IgG were coupled to *N*-succinimidylacrylate separately, and then co-polymerized with acrylamide to form a hydrogel. This gel also showed a reversible response to the environmental addition of rabbit lgG, suggesting that it should be possible to develop responsive polymers for a range of solute delivery applications.

CONCLUSIONS

Dextran/con-A hydrogel membranes can be synthesized that are capable of releasing insulin in a dose-dependent response to changes in D-glucose concentrations. The response observed is selective to sugars that are bound by con A and is repeatably reversible. Data shown in Figures 6, 7, and 8 suggest a lag time of approximately 40 minutes between point of insulin introduction and increase in transport rate. While this could be improved if thinner membranes were used, it compares favorably with the 30–120 minutes reported by Lembert et al. (2001) for insulin release by free-floating islets. Unlike sol-gel systems, the membrane described here retains structural integrity in the presence of elevated D-glucose concentrations and needs no additional external membrane containment. The synthesis protocol we report can be extended to allow the attachment of ligands as well as receptors to an inert support. This would allow the formation of responsive gels based on a range of ligand-receptor interactions.

R. Zhang is supported by the University of Bath and an ORS award for which we are grateful.

References

Ballerstadt R, Schultz JS. 1998. Kinetics of dissolution of concanavalin A/dextran sols in response to glucose measured by surface plasma response. Sensors and Actuators B 46:50–55.

Brownlee M, Cerami A. 1979. A glucose-controlled insulin-delivery system: semisynthetic insulin bound to lectin. Science 206:1190–1191.

Galaev IY, Mattiasson B. 1999. 'Smart' polymers and what they could do in biotechnology and medicine. Trends Biotechnol 17:335–340.

Hinchclifffe M, Illum L. 1999. Intranasal insulin delivery and therapy. Adv Drug Delivery Rev 35:199–234.

Kim JJ, Park K. 2001. Glucose-binding property of pegylated concanavalin A. Pharmaceut Res 18:794–799.

Lembert N, Peterson P, Wesche J, Zschocke P, Ederle A, Doser M, Planck H, Becher HD, Ammon HPT. 2001. In vitro test of new biomaterials for the development of artificial pancreas. Ann NY Acad Sci 944: 271–276.

Loris R, Hamelryck T, Bouckaert J, Wyns L. 1998. Legume lectin structure. Biochim et Biophys Acta 1383:9–36.

Miyata T, Asami N, Uragami T. 1999. A reversibly antigen-responsive hydrogel. Nature 399:766–769.

Obaidat AA, Park K. 1997. Characterization of protein release through glucose-sensitive hydrogel membranes. Biomaterials 18:801–806.
Pitt CG. 1990. The controlled parentral delivery of polypeptides and proteins. Int J Pharm 59:173–196.
Qiu Y, Park K. 2001. Environment-sensitive hydrogels for drug delivery. Adv Drug Del Rev 53:321–339.
Sato S, Ebert CD, Kim SW. 1983. Prevention of insulin self association and surface adsorption. J Pharm Sci 72:228–232.
Singh RS, Tiwary AK, Kennedy JF. 1999. Lectins: sources, activities and applications. Crit Rev Biotechnol 19:145–178.
Tanna S, Taylor MJ, Adams G. 1999. Insulin delivery governed by covalently modified lectin-glucogen gels sensitive to glucose. J Pharm Pharmacol 51:1093–1098.
Taylor MJ, Tanna S, Taylor PM, Adams G. 1995. The delivery of insulin from aqueous and non-aqueous reservoirs governed by glucose sensitive gels. J Drug Targeting 3:209–216.

An NAD-sensitive Hydrogel for the Release of Macromolecules

M.Tang,[1] R.Zhang,[1] A.Bowyer,[2] R.Eisenthal,[3] J.Hubble [1]

[1] Department of Chemical Engineering, University of Bath, Claverton Down, Bath BA2 7AY, United Kingdom; telephone:+44 1225 386221; fax:+44 1225 386491; e-mail:j.hubble@bath.ac.uk
[2] Department of Mechanical Engineering, University of Bath, United Kingdom
[3] Department of Biology and Biochemistry, University of Bath, United Kingdom

Abstract: A hydrogel membrane containing immobilized ligands and receptors was synthesized and investigated for the controlled diffusion of test proteins (cytochrome C and hemoglobin). Both Cibacron blue (ligand) and lysozyme (receptor) were covalently linked to dextran molecules that were subsequently cross-linked to form a gel. The resulting stable hydrogels contained both covalent and affinity cross-links such that their intrinsic porosities were sensitive to competitive displacers of the affinity interaction between lysozyme and Cibacron blue. Transport experiments in a twin chamber diffusion cell showed that, as NAD was added to the donor side, the dissociation of the binding sites between the Cibacron blue and the lysozyme led to an increase in protein diffusion through the hydrogel. The results showed that addition of NAD caused a saturable concentration-dependent increase in the transport of both cytochrome C and hemoglobin. This effect was shown to be both specific and reversible.

(Key words: bio-affinity, responsive, hydrogel, smart)

INTRODUCTION

Recent developments in biotechnology and genetic engineering have meant that more and more bioactive peptides and proteins have been obtained for novel drug applications (Kikuchi and Okana, 2002). However, these bioactive molecules are often not suitable for oral delivery and are usually metabolized quickly in the body. Therefore, there is a requirement for effective delivery systems if these materials are to form the basis of successful therapies.

Conventional controlled drug delivery systems are based on constant slow-release mechanisms. These materials do not respond to metabolite changes in the patient's body in order to deliver the drug at an appropriate rate; i.e. there is no feedback to improve control. Smart drug delivery systems that do respond to metabolite changes offer the potential for developing much more effective dosing regimes that mimic natural functions. For example, insulin release from the pancreas is induced by an increase of blood glucose concentration (Pitt, 1990). Systems incorporating the functions of both biosensor and actuator are required to provide complete selective feedback-controlled drug delivery (Kikuchi and Okana, 2002, Qiu and Park, 2001, Miyata et al., 2002).

Hydrogels have been extensively used in attempts to develop smart drug delivery systems. The responses used include: pH-sensitivity (Kou et al., 1988, Akala et al., 1998), temperature-sensitivity (Dong and Hoffman, 1990, Bromberg and Ron, 1998), and glucose-sensitivity (Brownlee and Cerami, 1979, Ito et al., 1989, Kitano, et al., 1992, Taylor et al., 1995, Lee and Park, 1996, Miyata et al., 1996, Obaidat and Park, 1997, Hassan, et al., 1997, Tanna et al., 1999, Kim and Park, 2001).

In model systems using glucose-sensitive hydrogels, specific recognition based on lectin-carbohydrate interactions has been the most widely studied (Taylor et al., 1995, Lee and Park, 1996, Miyata et al., 1996, Kim and Park, 2001). In addition to the potential application for use in the treatment of diabetes, these systems have the advantage that the structural polymer component of the gel (dextran) also acts as the ligand for the receptor (concanavalin A).

To broaden the potential application base for responsive hydrogels it is necessary to develop systems where both ligand and receptor are specifically coupled to an inert support. Miyata et al. (1999) reported the synthesis of an antigen-antibody hydrogel membrane where goat anti-rabbit IgG and rabbit IgG were coupled to N-succinimidylacrylate separately, and then co-polymerized with acrylamide to form a hydrogel. This gel showed a reversible response to the environmental addition of

*Correspondence to:*John Hubble
Contract grant sponsor: BBSRC;University of Bath
Contract grant number:86/E12129

rabbit IgG, suggesting that it should be possible to develop responsive polymers for a range of solute delivery applications.

Here we investigate such a system aimed at producing a gel that responds to changes in concentrations of nicotinamide adenine dinucleotide (NAD). NAD is an important bio-molecule with a central role in oxidation and reduction reactions in metabolic processes (Berg et al., 2002),. However, the major purpose of this study is to demonstrate the generality of our approach, which is to construct a responsive membrane by incorporating into the polymeric structure a pendant ligand and pendant receptor in such a manner that the permeability properties of the membrane may be altered in the presence of a competitor of the receptor/ligand interaction within the polymeric structure.

In this study, we have used Cibacron blue as the ligand and lysozyme as the receptor. Cibacron blue has a molecular shape similar to that of NAD and has been widely used as a biomimetic ligand in affinity chromatography of dehydrogenase enzymes. It also binds specifically and with high affinity to lysozyme (Mayes et al., 1990). There are also reports that lysozyme has a binding affinity for NAD (Yu et al., 2001). Considerations of cost, stability and availability thus make the Cibacron blue/lysozyme pair a target for an NAD responsive material.

We previously synthesized a glucose responsive membrane where a change in the porosity of the membrane led to increased transport rates of a number of proteins of different sizes (insulin, lysozyme and bovine serum albumin, Tang et al., 2002). In the work described in this paper, Cibacron blue was covalently linked to a dextran chain; then a spacer arm was introduced to link lysozyme and to crosslink dextran chains, to form the hydrogel. The primary target was to demonstrate that NAD-sensitive hydrogel membranes can be produced that change their porosity in response to changes in environmental NAD concentration, and that this response can control the delivery of macromolecules though the membrane.

MATERIALS AND METHODS

Materials

All reagents were obtained from Sigma Chemicals, Poole, Dorset unless otherwise stated.

Preparation of Cibacron blue–dextran derivatives

The NAD-sensitive hydrogel membrane synthesis protocol is shown in Figure 1.

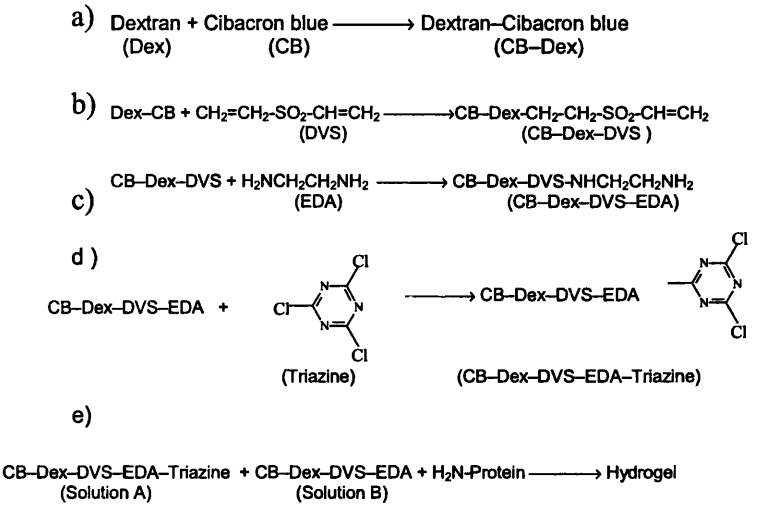

Figure 1. Synthetic scheme for Cibacron-blue–lysozyme hydrogel. Abbreviations are as defined in Materials and Methods

The synthesis proceeds as follows:

1) Conjugation of Cibacron blue (CB) to dextran

This was based on the methodology described by Dean et al. (1985). 5g Dextran 500kDa was dissolved in 100 ml water, followed by the addition of solid Na2CO3 (0.1 M final). CB (55% dye content) was added in five separate aliquots (total addition 4.3g) over 24 hours at room temperature. The solution was then maintained at 40°C for 24 hours to form a dextran–Cibacron blue conjugate (CB–Dex). The conjugate was precipitated with ethanol (50% v/v) and redissolved in distilled water; this procedure was repeated twice to remove most of the unreacted dye. The conjugate was then extensively dialysed against distilled water and finally freeze-dried.

2) Coupling of CB–Dex to divinyl sulfone (DVS)

This was based on the method of Porath et al. (1975), 4.0 g CB–Dex was dissolved in 40 ml distilled water, and solid Na2CO3 was added to a final concentration of 0.1 M. 0.46 ml 97% divinyl sulfone added slowly with continuous stirring. The reaction was allowed to proceed at 18°C for 80 minutes, and was then stopped by the addition of concentrated HCl to lower the pH to below 4 (the result will be referred to as CB–Dex–DVS).

3) Attachment of triazine to CB–Dex–DVS

2.5 g ethylenediamine dihydrochloride was added to the above mixture, followed by the addition of 10 M ethylenediamine (EDA) to

adjust the pH to 8-9; the reaction was allowed to proceed at room temperature for the next 48 h. The solution was then dialysed extensively and freeze-dried to concentrate to a volume of 28 ml. The ethylenediamine conjugate will be termed CB–Dex–DVS–DEA. To this solution, 0.30g cyanuric chloride (triazine) was added and the reaction kept at room temperature for the next 24 h. The solution was centrifuged at 4000g for 20 minute at 4°C and the supernatant used for the preparation of the hydrogel membranes; the dextran–triazine conjugate preparation will be referred to as solution A.

A similar procedure was followed to make a CB–dextran–DVS–EDA derivative using dextran of 43kDa; the final solution will be referred to as solution B.

4) Formulation of the hydrogels

Gels were produced using the method described by Tang et al. (2003), 1.0 g of solution A was mixed with 1.0 g of solution B, followed by 0.6 ml 0.8 M $NaHCO_3$, and stirred at room temperature for 10 minutes. 80 mg lysozyme in 1.4 ml water was added, and the mixture stirred for a further 15 minutes before vacuum degassing. This solution was poured into a mould containing a nylon gauze, pore size 0.1mm, to add mechanical strength. The mixture was allowed to gel at 25°C for 16 hours resulting in a 0.5mm membrane. The membrane was removed from the mould, washed with 20 mM Tris buffer, pH 7.4, containing 0.1 M NaCl and 0.01% NaN_3, and stored in this buffer at 4°C until used.

Protein transport experiments

The trans-membrane transport of protein was studied using a diffusion cell consisting of donor and receptor chambers of equal volumes of 4.4 ml. Gel membranes with a surface area of 4.6 cm2 were mounted between the two chambers. The proteins used for transport studies were cytochrome C and hemoglobin with molecular weights of 12kDa and 60kDa respectively. Once the membranes were mounted, both chambers were filled with 20 mM pH 7.4 Tris buffer as above. The donor chamber was connected to the protein reservoir via a pump. The receptor chamber was connected to a UV-Visible spectrophotometer (Shimadzu), to allow protein diffusion across the membrane to be automatically monitored and logged from optical density changes. The amount of protein diffusing across to the receptor chamber was calculated using calibration data for each of the proteins at the chosen wavelength. The effect of NAD was investigated by varying NAD levels in the protein solution feed to the donor chamber and following the resultant changes in transport rate.

For diffusion experiments with cytochrome C, the protein (1.0 mg/ml) was dissolved in 20 mM pH 7.4 Tris buffer containing 0.1 M NaCl and 0.01% NaN_3. Transport was monitored at 25°C in a water bath. The cytochrome-C concentration on the receptor side was determined at 410 nm. For diffusion experiments with hemoglobin (1.0 mg/ml), absorbance was monitored at 418 nm.

RESULTS

Specificity of membrane response

The specificity of the response characteristics of the Cibacron blue/lysozyme hydrogel membranes was explored using NAD as a specific competitor, and oxidized glutathione (GSSG) as a control. GSSG shows no affinity binding to lysozyme, but has a similar molecular weight to NAD. Figure 2 shows the diffusion curves for cytochrome C in the presence of buffer and buffer containing NAD or GSSG, through a 0.5 mm membrane.

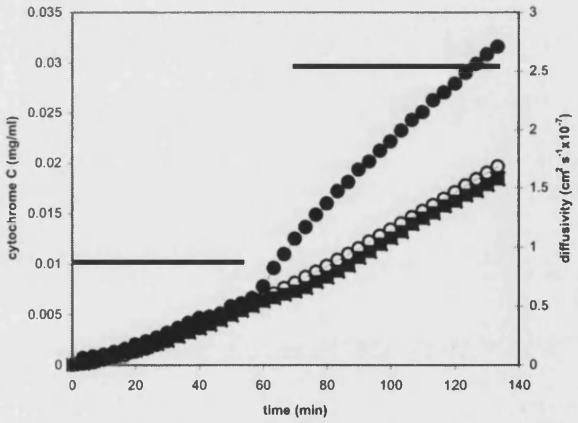

Figure 2. Diffusion curves of cytochrome C through Cibacron blue–lysozyme hydrogel, Response to 20 mM NAD and 20 mM GSSG. NAD or GSSG was added to the reservoir of the diffusion cell at 40 minutes. (No effector ○, NAD,●,CSSG ■,solid line shows diffusivity with and without NAD as an effector).

In control experiments, protein buffer solution was used without NAD or GSSG. In initial experiments with cytochrome C there was little background diffusion in the control system. Addition of 20 mM GSSG to the donor side of the diffusion cell caused only a small increase in the rate of diffusion. However, when 20 mM NAD was used a substantial increase in the cytochrome-C diffusion rate was observed (Figure 2). The lag time observed between addition of NAD and increased diffusion was approximately 20 minutes. This includes 4.0 minutes for the cytochrome C solution to be pumped from the reservoir into the diffusion cell followed by a mixing equilibration in the donor

reservoir during which the NAD concentration was increasing. Therefore, the response time for the membrane is substantially less than 15 minutes.

In order to confirm the specificity of the hydrogel membrane, a second, larger, protein, hemoglobin, was used. The molecular mass of hemoglobin is about five times that of cytochrome C. Therefore, larger gel pores are required for diffusion. Figure 3 shows the release of hemoglobin in response to NAD and GSSG in the hydrogel membrane. As with cytochrome C, GSSG did not significantly influence the release of hemoglobin. However, NAD addition again resulted in a significant increase in the rate of protein diffusion across the hydrogel membrane.

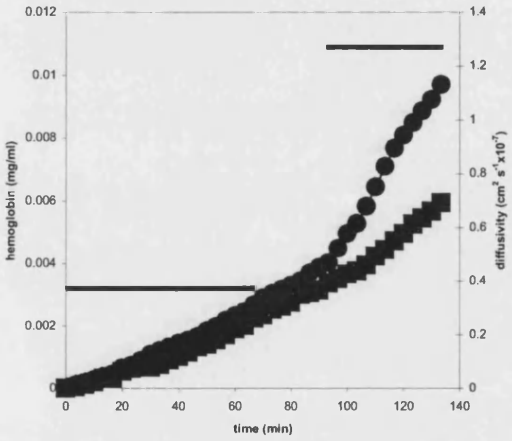

Figure 3. Diffusion curves of hemoglobin through the Cibacron blue–lysozyme hydrogel membrane , Response to 20 mM NAD and 20 mM GSSG respectively. NAD or GSSG was added to the reservoir of the diffusion cell at 70 minutes. (NAD,●,CSSG ■,solid line shows diffusivity with and without NAD as an effector)

These results demonstrate that the principle of a responsive membrane based on the competitive displacement of affinity cross-links is effective, and that the membrane response is specific to the anticipated competitor (NAD). The longer response times observed with hemoglobin compared with cytochrome C are consistent with differences in their respective molecular weights.

Effect of NAD concentration on transport rate

Cytochrome C and hemoglobin were used to examine diffusion across the hydrogel membrane in response to changes in NAD concentration. Figure 4 shows cytochrome C transport through the membrane, when NAD concentrations were varied between 0 to 100 mM.

To avoid artefacts arising from diffusion lags after solution changes, a pre-incubation period was allowed before data collection took place. In the experiments without NAD, there was only a low diffusion rate through the membrane (0.012 µg cm-2min-1). However, when NAD was added to the protein reservoir there was an obvious increase in the concentration time profiles obtained up to a concentration of 100mM (Figure 4). The rate of diffusion in response to NAD concentration is shown in Figure 4a indicating a half saturation constant around 20 mM

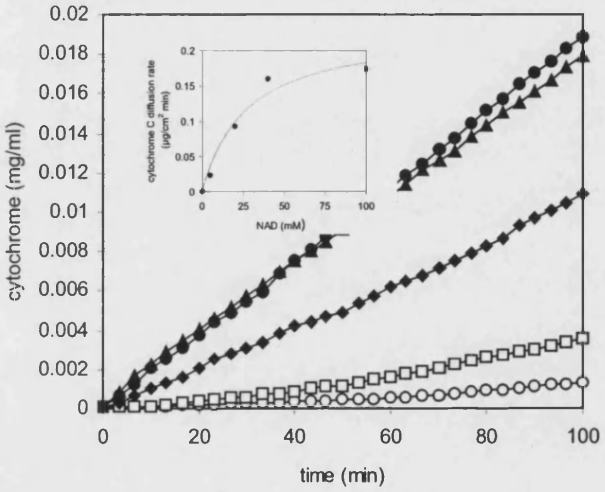

Figure 4. Diffusion curves of cytochrome C in response to NAD concentration. 0 mM (○), 5 mM (□), 20 mM (♦), 50 mM (▲) and 100 mM (●). The cytochrome C concentration was 1.0 mg/ml. Inset: Plot of Cytochrome C diffusion rates (corrected for background diffusion) against NAD concentration; the curve is a least squares fit to the Langmuir equation (maximum rate = 0.23 µg cm-2 min-1, half saturation constant = 26.5mM)

When the larger hemoglobin was used for protein diffusion experiments, similar results were obtained (Figure 5). As expected, the diffusion rates of the control experiment with hemoglobin and the maximum rate observed in the presence of NAD were both lower than those obtained with cytochrome C. The response of diffusion rate to change in NAD concentration also follows a saturation curve (Figure 5a). It is noteworthy that the value of the half-saturation constant for NAD is similar to that when cytochrome C is the diffusate – this demonstrates the specificity of the membrane response to NAD.

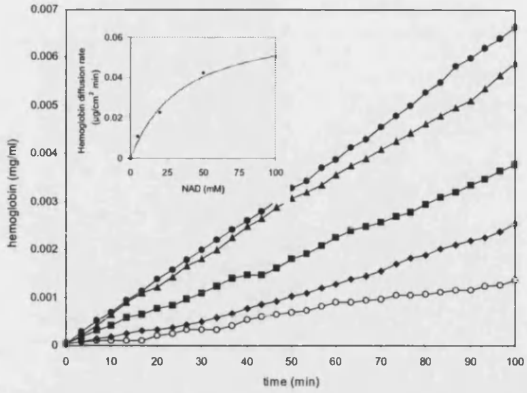

Figure 5. Diffusion curves of hemoglobin in response to NAD concentration. 0 mM (○), 5 mM (♦), 20 mM (■), 50 mM (▲) and 100 mM (●). The hemoglobin concentration was 1.0 mg/ml. Inset: Plot of hemoglobin diffusion rate (corrected for background diffusion) against NAD concentration; the curve is a least squares fit to the Langmuir equation (maximum rate = 0.068 µg cm-2 min-1, half saturation constant = 34.5mM).

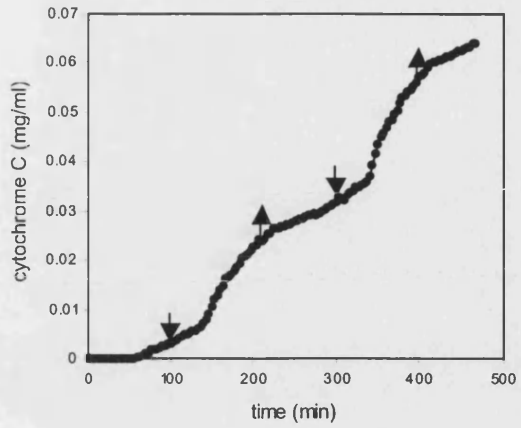

Figure 6. Reversibility of diffusion of cytochrome C through a hydrogel membrane. Diffusion curves for cytochrome C. NAD was added at 100 minutes and 300minutes (down arrows), and removed at 210 minutes and 400 minutes (up arrows).

Reversibility of the NAD response

The reversibility of the NAD effect was studied by switching between protein solutions with and without NAD at the half saturation concentration (20 mM). In experiments with cytochrome C (Figure 6), protein (1.0 mg/ml in the reservoir, 100 ml) was first used for the first 42 minutes, providing the baseline diffusion curve. At 100 minutes, the protein solution was replaced with one containing 20 mM NAD. The cell was flushed with 6.0 ml the new solution before recirculation was resumed to ensure no dilution of NAD. As the total amounts of cytochrome C and NAD in the reservoir were much higher than the corresponding amounts in the receptor side of diffusion cell the effective driving concentration can be assumed constant throughout the run. A resultant increase in the rate of cytochrome C diffusion occurred about 30 minutes after the switch to an NAD containing solution. This cycle was repeated: at 210 minutes, pure protein solution replaced that containing 20 mM NAD and at 300 minutes, protein solution containing 20 mM NAD was reintroduced.

At each solution change there is a clear diffusion lag before the transport rate responds to the NAD concentration, but the effect is the same for both cycles: addition of NAD increases the rate, removal reduces it.
These experiments were again repeated with hemoglobin following a similar procedure (Figure 7). After free diffusion of hemoglobin for 60 minutes, a hemoglobin solution containing NAD was used to replace the pure hemoglobin solution in the donor side of the cell. After a lag of 25 minutes an increased rate of diffusion was reached. At 180 minutes, pure hemoglobin

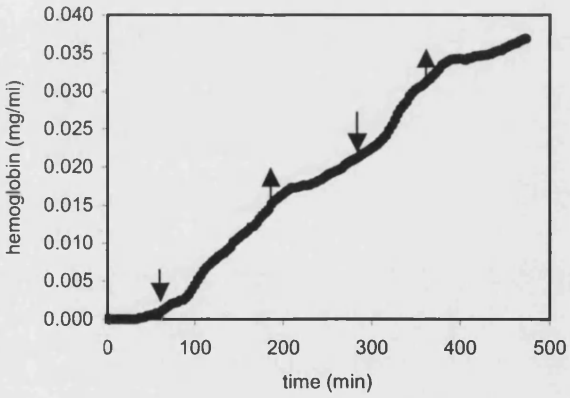

Figure 7. Reversibility of diffusion of hemoglobin through a hydrogel membrane. NAD was added at 90 minutes and 280 minutes (down arrows), and removed at 180 minutes and 367 minutes (up arrows) (Temperature 25°C).

solution was used to replace the NAD-containing hemoglobin solution in the donor side. Again, after a lag period the rate of diffusion decreased as the NAD was eluted from the donor chamber. A repeat of this procedure was executed and a similar response observed. The results obtained with both proteins show that the NAD-sensitive membrane exhibits a reversible response in protein diffusion in response to changes in competitor concentration.

DISCUSSION

The goal of this study was to demonstrate the feasibility of synthesising affinity-based responsive membranes where both ligand and receptor are attached to an inert polymer backbone.

The first stage aimed to establish (i) that permeability as evidenced by protein diffusion changed in response to concentration changes of specific affinity competitors, and (ii) that this effect was specific. The results presented in Figures 2 and 3 confirm this to be the case. However, it is apparent that the porosity of the gel in the absence of competitor does not totally exclude the protein in the control experiments, suggesting that a higher degree of covalent cross-linking is desirable. There was also a slight increase in diffusion observed with the addition of the GSSG control, which may result from non-specific interactions (e.g. charge effects).

The effect of NAD concentration on the diffusion of the different-sized proteins is shown in Figures 4 and 5. The inset figures show transport rate as a function of NAD concentration, and indicate a half-saturation constant around 20 mM. This is consistent with the displacement of a weak affinity interaction. As the size of the protein increases, the ratio of selective to intrinsic diffusion also increases. This suggests that, in addition to optimising the base level of affinity plus covalent cross-links to ensure zero intrinsic diffusion, porosity should also be optimized with respect to maximizing the selective transport.

The final objective was to assess the reversibility of the membrane response. The results described in Figures 6 and 7 confirm that membranes show a reversible response to stepwise changes in NAD concentration. Although a significant lag time (>20 minutes) was observed in these responses, at least 50% of this is attributable to system dead time and mixing effects. Ignoring extraneous effects, response times will be a function of a number of parameters. The diffusivities of effector and transported solute coupled with intrinsic porosity, and membrane thickness will all influence response times. However, a potentially more significant effect result from the chain relaxation time, where the rate of change in gel properties is essentially limited by the effective diffusivity of the polymer chains within the hydrogel matrix. Hassan et al, (1997) demonstrated these effects in both glucose and pH sensitive gels finding that relaxation times were similar in both systems despite significant differences in effector diffusivity. In their study there was between a 2-5 fold difference in the opening and closing rates of the gel. However, the results presented here for reversibility experiments in figures 6 and 7 do not show such a marked difference in response to addition and removal of effector, possibly as a result of a higher cross-linking density. For any given application the degree of cross-linking will be constrained by the need eliminate background diffusion hence the sole adjustable variable will be membrane thickness. The reported thickness of 0.5mm was constrained by mechanical properties. However, alternative support polymers with improved strength should allow this to be reduced.

CONCLUSIONS

Lysozyme/Cibacron blue coupled hydrogel membranes have been synthesized that are capable of releasing protein in a dose-dependent manner to changes in NAD concentration. Unlike gel-sol diffusion systems, where solute release occurs because of a phase transfer of a gel to a liquid (Qiu and Park, 2001, Obaidat and Park, 1997, Tanna et al., 1999), the membranes described here retain structural integrity even in the presence of elevated competitor concentrations and do not need external support membranes.

(Acknowledgements: The authors gratefully acknowledge financial support from the UK BBSRC under grant No E12129 and the University of Bath and Universities UK for financial support for RZ.)

REFERENCES

Akala EO, Kopeckova P, Kopecek J. 1998. Novel pH-sensitive hydrogel with adjustable swelling kinetics. Biomaterials, 19:1037-1047.

Berg JM., Timoczko JL, Stryer L. Biochemistry, 5th edition, W. H. Freeman and Company, New York, (2002) Part II.

Bromberg LE, Ron ES. 1998. Temperature-responsive gels and thermogelling polymer matrices for protein and peptide delivery. Advanced Drug Delivery Reviews, 31:197-221.

Brownlee M, Cerami A. 1979. A glucose-controlled insulin-delivery system: semisynthetic insulin bound to lectin. Science, 206:1190-1191.

Dean PDG, Johnson WS, Middle FA, Affinity Chromatography: a practical approach, IRL Press, Oxford, (1985).

Dong LC, Hoffman AS. 1990. Synthesis and application of thermally reversible heterogels for drug delivery. Journal of Controlled Release, 13:21-31.

Hassan CM, Doyle FJI, Peppas NA. 1997.Dynamic Behavior of Glucose-Responsive Poly(methacrylicacid-g-ethylene

glycol) Hydrogels. Macromolecules, 30:6166-6173.

Ito Y, Casolaro M, Kono K, Yukio I. 1989. An insulin-releasing system that is responsive to glucose. Journal of Controlled Release, 10:195-203.

Kikuchi A, Okana T. 2002. Pulsatile drug release control using hydrogels. Advanced Drug Delivery Reviews, 54:53-77.

Kim JJ, Park K. 2001. Modulated insulin delivery from glucose-sensitive hydrogel dosage forms. Journal of Controlled Release, 77:39-47.

Kitano S, Koyama Y, Kataoka K, Okana T, Sakurai Y. 1992 A novel drug delivery system utilizing a glucose responsive polymer complex between poly(vinyl alcohol) and poly(N-vinyl-2-pyrrolidone) with a phenyl boronic acid moiety. Journal of Controlled Release, 19: 162-170.

Kou JH, Amidon GL, Lee PI. 1988. pH-dependent swelling and solute diffusion characteristics of poly(hydroxyethyl methacrylate-co-methacrylic acid) hydrogels. Pharm Res, 5:592-597.

Lee SJ, Park K. 1996. Synthesis and characterization of sol-gel phase-reversible hydrogel sensitive to glucose. Journal of Molecular recognition, 9:549-557.

Mayes AG, Moore JD, Eisenthal R, Hubble J. 1990. Investigation of binding site density: effects on the interaction between Cibacron blue-dextran conjugates and lysozyme. Biotechnology and Bioengineering, 36:1090-1096.

Miyata T, Asami N. Uragami T. 1999. A reversibly antigen-responsive hydrogel, Nature 399: 766-769.

Miyata T, Jikihara A, Nakamae K, Hoffman AS. 1996. Preparation of poly(2-glucosyloxyethyl methacrylate)-concanavalin A complex hydrogel and its glucose-sensitivity. Macromolecular Chemistry and Physics, 197:1135-1146.

Miyata T, Uragami T, Nakamae K. 2002. Biomolecule-sensitive hydrogels. Advanced Drug Delivery Reviews, 54:79-98.

Obaidat AA, Park K. 1997. Characterization of protein release through glucose-sensitive hydrogel membranes. Biomaterials, 18:801-806.

Pitt CG. The controlled delivery of polypeptides and proteins. Int. J. Pharm., 59:173:196.

Porath J, Låås T, Janson J.-C. 1975. Agar derivatives for chromatography, electrophoresis and gel bound enzymes. III. Rigid agarose gels cross-linked with divinyl sulfone (DVS). J. Chromatogr. 103: 49-62.

Qiu Y, Park K. 2001. Environment-sensitive hydrogels for drug delivery. Advanced Drug Delivery Reviews, 53:321-339.

Tang M, Zhang R, Bowyer A. Eisenthal R. Hubble J. Smart membranes for delivery of macromolecules, ICOM Toulouse (2002) Abstract 131.

Tang M, Zhang R, Bowyer A, Eisenthal R. Hubble J. 2003 A reversible hydrogel membrane for controlling the delivery of macromolecules. Biotechnology & Bioengineering, 82: 47-53.

Tanna S, Taylor MJ, Adams G. 1999. Insulin delivery governed by covalently modified lectin-glucogen gels sensitive to glucose. J Pharm.Pharmacol 51:1093-1098.

Taylor MJ, Tanna S, Taylor PM, Adams G. 1995. The delivery of insulin from aqueous and non-aqueous reservoirs governed by glucose sensitive gels. J Drug Targeting 3:209-216.

Yu YH, Xue B, Sun Y. 2001. Dye-ligand poly(GMA-TAIC-DVB) affinity adsorbent for protein adsorption. Bioprocess and Biosystems Engineering, 24:25-31.